

# **Optimisation of congenital adrenal hyperplasia therapy in paediatric and foetal populations by leveraging pharmacometrics**

Inaugural-Dissertation

to obtain the academic degree  
Doctor rerum naturalium (Dr. rer. nat.)

submitted to the Department of Biology, Chemistry, Pharmacy  
of Freie Universität Berlin

by  
Viktoria Stachanow

2023



## **Declaration of Authorship**

Except where reference is made in the text, this thesis contains no material published elsewhere or extracted in whole or in part from a thesis presented by me for another degree or diploma. No other person's work has been used without due acknowledgment in the main text of the thesis. This thesis has not been submitted for the award of any other degree or diploma in any other tertiary institution.

Viktoria Stachanow

The present thesis was conducted from 2017 to 2023 under the supervision of Prof. Dr. Charlotte Kloft at the Institute of Pharmacy, Freie Universität Berlin.

1<sup>st</sup> reviewer: Prof. Dr. Charlotte Kloft

2<sup>nd</sup> reviewer: Prof. Dr. Ulrich Jaehde

Date of disputation: 31 October 2023

## Abstract

Congenital adrenal hyperplasia (CAH) is a rare form of adrenal insufficiency causing deficiency of the highly regulated hormone cortisol and accumulation of its precursors such as 17 $\alpha$ -hydroxyprogesterone (17-OHP) and subsequent androgen overproduction. Symptoms associated with CAH are premature pseudo puberty, earlier ending of longitudinal growth, and in female patients, virilisation and hirsutism. CAH patients require life-long cortisol replacement therapy, and dose optimisation through therapy monitoring is crucial to avoid potentially serious adverse events due to cortisol over- or underexposure. Paediatric CAH patients receive hydrocortisone (HC, synthetic cortisol) for cortisol replacement due to its lower risk for adverse effects whereas adult patients receive more potent glucocorticoids, e.g., dexamethasone (Dex). Especially in paediatrics, dried blood spot (DBS) sampling represents a highly advantageous alternative to plasma sampling. The major advantages include minimal invasiveness, low required blood volumes, stability of the analyte and easy storage of the matrix. Thus, DBS sampling has a high potential for facilitating CAH therapy monitoring routine. However, target concentrations of CAH biomarkers such as 17-OHP indicating a successful cortisol replacement are still unknown in DBS.

To prevent *in utero* virilisation of female foetuses with CAH, prenatal therapy with Dex, administered to the pregnant women, has been conducted for decades. Yet, prenatal CAH therapy is still considered experimental since the traditionally administered Dex dose of 20  $\mu\text{g}/\text{kg}/\text{day}$  is not based on a scientific rationale and is assumed to be too high, causing potential harm to the mother and foetus. In this regard, quantitative approaches such as pharmacometric modelling and simulation are powerful tools to provide a better understanding on pharmacokinetic (PK) and pharmacodynamic (PD) processes and to contribute to the optimisation of drug therapies.

This work aimed at paving the way towards an optimised CAH therapy in paediatric and foetal populations by (1) providing insights into the quantitative relationship between cortisol concentrations measured in plasma and in DBS, (2) identifying paediatric target DBS concentrations for the commonly used biomarker 17-OHP and (3) suggesting a rational Dex dose in prenatal CAH therapy.

To quantitatively link plasma and DBS cortisol concentrations, a semi-mechanistic nonlinear mixed-effects (NLME) PK model was developed based on data from paediatric CAH patients. The model characterised a nonlinear relationship between cortisol in plasma and DBS with plasma/DBS concentration ratios decreasing from approximately 8 to 2 with increasing DBS cortisol concentrations up to 800 nmol/L. These ratios decreased due to saturation of cortisol binding to corticosteroid-binding globulin and thus higher cortisol fraction associated with red blood cells. In future, more data from neonates and infants can be used to investigate a possible age effect, on the nonlinearity between plasma and DBS cortisol, in addition to the observed concentration effect.

For the first time, a target morning DBS 17-OHP concentration range was determined for monitoring paediatric CAH patients. The DBS target range of 2.1-8.3 nmol/L was derived from simulations by applying a developed PK/PD model linking cortisol in plasma to 17-OHP in DBS and by leveraging healthy paediatric cortisol profiles. By extending the PK/PD model, and using the same simulation approach, circadian target concentration profiles, providing DBS biomarker targets for any time of the day, can be derived in future. Furthermore, in Bland-Altman and Passing-Bablok analyses, it was shown that capillary and venous DBS concentrations, which are both commonly obtained in clinical practice, are comparable to each other for cortisol and 17-OHP in paediatric CAH patients.

For determining a reduced Dex dose which simultaneously decreases the risk for adverse events in prenatal CAH therapy and still shows sufficient efficacy in the foetus, a target Dex concentration range was identified from literature and a NLME model describing maternal Dex PK was developed. The Dex PK model was used to simulate maternal Dex concentration-time profiles following traditional or reduced Dex doses and to evaluate the tested dosing regimens with regard to the lowest effective dose. Based on the simulation results, a Dex dose of 7.5 µg/kg/day was suggested as a rational dose for prenatal CAH therapy, representing approximately a third of the traditional Dex dose. The suggested rational Dex dose should be evaluated in future clinical trials.

In summary, this work provides quantitative insights into DBS measurements for CAH therapy monitoring, presents first target DBS concentrations for the biomarker 17-OHP in paediatrics, and suggests a first model-based dose rationale for Dex in prenatal CAH therapy. Ultimately, this work can help to improve CAH treatment with HC and Dex and therapy monitoring in the highly vulnerable paediatric and foetal populations.

## Zusammenfassung

Das Adrenogenitale Syndrom (AGS) ist eine seltene Form der Nebenniereninsuffizienz, die sich durch einen Mangel an dem stark regulierten Hormon Cortisol und einer Anhäufung seiner Vorstufen wie 17 $\alpha$ -Hydroxyprogesteron (17-OHP) sowie eine daraus resultierende Androgenüberproduktion auszeichnet. Zu den mit AGS einhergehenden Symptomen gehören eine vorzeitige Pseudopubertät, ein frühes Ende des Längenwachstums und bei weiblichen Patienten Virilisierung und Hirsutismus. AGS-Patienten benötigen eine lebenslange Cortisol-Ersatztherapie und die Optimierung der Dosis durch Therapieüberwachung ist von entscheidender Bedeutung, um potenziell schwerwiegende unerwünschte Ereignisse aufgrund einer Über- oder Unterexposition mit Cortisol zu vermeiden. Pädiatrische AGS-Patienten erhalten Hydrocortison (HC, synthetisches Cortisol) als Cortisolersatz, da es ein geringeres Risiko für unerwünschte Wirkungen hat, während erwachsene Patienten stärkere Glucocorticoide, z. B. Dexamethason (Dex) erhalten. Insbesondere in der Pädiatrie stellt die Entnahme von „Dried Blood Spots“ (DBS), bei der Blut auf Filterpapier getropft und getrocknet wird, eine äußerst vorteilhafte Alternative zur Plasmaentnahme dar. Zu den wichtigsten Vorteilen gehören die minimale Invasivität, das geringe erforderliche Blutvolumen, die Stabilität der Analyten und die einfache Lagerung der Matrix, wodurch die Routineüberwachung der AGS-Therapie erheblich erleichtert werden kann. Allerdings sind die Zielkonzentrationen von AGS-Biomarkern, die einen erfolgreichen Cortisolersatz anzeigen, in DBS noch nicht bekannt.

Um die Virilisierung von weiblichen Föten mit AGS *in utero* zu verhindern, wird seit Jahrzehnten eine pränatale Therapie mit Dex durchgeführt, die den schwangeren Frauen verabreicht wird. Die pränatale AGS-Therapie gilt heute noch als experimentell, da die üblicherweise verabreichte Dex-Dosis von 20  $\mu\text{g}/\text{kg}/\text{Tag}$  nicht evidenzbasiert ist und zunehmend als zu hoch sowie potenziell schädlich für Mutter und Fötus angesehen wird. Quantitative Ansätze wie pharmakometrische Modellierung und Simulationen sind hilfreiche Instrumente, um ein besseres Verständnis über pharmakokinetische (PK) und pharmakodynamische (PD) Prozesse zu ermöglichen und zur Optimierung von Arzneimitteltherapien beizutragen.

Diese Arbeit hatte zum Ziel, den Weg zu einer optimierten AGS-Therapie in pädiatrischen und fötalen Populationen zu ebnen, indem sie (1) Erkenntnisse über die quantitative Beziehung zwischen in Plasma und DBS gemessenen Cortisolkonzentrationen erzielt, (2) pädiatrische DBS-Zielkonzentrationen für den häufig verwendeten Biomarker 17-OHP ermittelt und (3) eine evidenzbasierte Dex-Dosis für die pränatale AGS-Therapie empfiehlt.

Um einen quantitativen Zusammenhang zwischen Plasma- und DBS-Cortisol Konzentrationen herzustellen, wurde ein semi-mechanistisches „nonlinear mixed-effects“ (NLME) PK Modell auf der Grundlage von pädiatrischen AGS-Patientendaten entwickelt. Das Modell beschreibt eine nichtlineare

Beziehung zwischen Cortisol in Plasma und in DBS, wobei das Verhältnis zwischen Plasma- und DBS-Konzentrationen mit zunehmenden DBS-Cortisolkonzentrationen bis zu 800 nmol/L von etwa 8 auf 2 abnahm. Das Cortisol-Verhältnis zwischen Plasma und DBS verringerte sich aufgrund einer Sättigung der Cortisolbindung an das Corticosteroid-bindende Globulin und damit einer höheren Cortisol-Assoziation an Erythrozyten. In Zukunft können zusätzliche Daten von Neugeborenen und Kleinkindern verwendet werden, um einen möglichen Alterseffekt auf die beobachtete Nichtlinearität zwischen Plasma- und DBS-Cortisol zu untersuchen.

Zum ersten Mal wurde für DBS ein Zielbereich für die morgendliche 17-OHP-Konzentration zur Überwachung pädiatrischer AGS-Patienten ermittelt. Der DBS-Zielbereich von 2-8 nmol/L wurde aus Simulationen abgeleitet, indem ein PK/PD-Modell angewandt wurde, das Plasma-Cortisol mit 17-OHP in DBS verknüpft, und gesunde pädiatrische Cortisolprofile genutzt wurden. Durch die Erweiterung des PK/PD-Modells und die Anwendung desselben Simulationsansatzes können in Zukunft z. B. zirkadiane Zielkonzentrationsprofile abgeleitet werden, um DBS-Biomarker-Zielwerte für jede Tageszeit zur Verfügung zu stellen. Darüber hinaus wurde in Bland-Altman- und Passing-Bablok-Analysen gezeigt, dass kapilläre und venöse DBS-Konzentrationen, die beide in der klinischen Praxis üblicherweise gewonnen werden, von Cortisol und 17-OHP bei pädiatrischen AGS-Patienten miteinander vergleichbar sind.

Zur Bestimmung einer reduzierten Dex-Dosis, die gleichzeitig das Risiko für unerwünschte Ereignisse bei der pränatalen AGS-Therapie verringert und eine ausreichende Wirksamkeit im Fötus aufweist, wurde aus der Literatur ein Zielbereich für Dex-Konzentrationen ermittelt und ein NLME-Modell zur Beschreibung der mütterlichen Dex-PK entwickelt. Das Dex-PK-Modell wurde für Simulationen von mütterlichen Dex-Konzentrationsprofilen infolge der herkömmlichen oder reduzierter Dex-Dosen verwendet, um die getesteten Dosierungsschemata im Hinblick auf die niedrigste wirksame Dosis zu bewerten. Auf der Grundlage der Simulationsergebnisse wurde eine Dex-Dosis von 7,5 µg/kg/Tag als rationale Dosis für die pränatale AGS-Therapie vorgeschlagen, die etwa einem Drittel der herkömmlichen Dex-Dosis entspricht. Die vorgeschlagene rationale Dex-Dosis sollte in zukünftigen klinischen Studien erprobt werden.

Zusammengefasst bietet diese Arbeit quantitative Einblicke in DBS-Messungen für die AGS-Therapieüberwachung, stellt erste DBS-Zielkonzentrationen für den Biomarker 17-OHP in der Pädiatrie vor und schlägt eine erste modellgestützte, evidenzbasierte Dosis für Dex in der pränatalen AGS-Therapie vor. Letztendlich kann diese Arbeit dazu beitragen, die AGS-Behandlung mit HC und Dex sowie die Therapieüberwachung in der hochgefährdeten pädiatrischen und fötalen Population zu optimieren.

## Table of Content

<b>Abstract</b> .....	iv
<b>Zusammenfassung</b> .....	vi
<b>Table of Content</b> .....	viii
<b>Abbreviations</b> .....	xi
<b>Relevant publications</b> .....	xiv
<b>1 Introduction</b> .....	1
<b>1.1 Pharmacokinetics and pharmacotherapy in paediatric and foetal patients</b> .....	1
<b>1.2 Congenital adrenal hyperplasia</b> .....	2
<b>1.2.1 Healthy physiology of cortisol and 17<math>\alpha</math>-hydroxyprogesterone</b> .....	2
<b>1.2.2 Pathophysiology of congenital adrenal hyperplasia</b> .....	4
<b>1.2.3 Congenital adrenal hyperplasia pharmacotherapy</b> .....	5
<b>1.2.3.1 Cortisol replacement therapy in paediatric patients</b> .....	5
<b>1.2.3.2 Prenatal therapy with dexamethasone</b> .....	6
<b>1.3 Pharmacokinetics of hydrocortisone and dexamethasone</b> .....	6
<b>1.4 Pharmacodynamics of hydrocortisone and dexamethasone</b> .....	7
<b>1.5 Dried blood spot sampling</b> .....	8
<b>1.6 Pharmacometrics</b> .....	9
<b>1.6.1 Nonlinear mixed-effects modelling</b> .....	9
<b>1.6.2 Use of pharmacometrics in drug development and drug therapy</b> .....	9
<b>1.7 Objectives</b> .....	11
<b>2 Methods</b> .....	12
<b>2.1 Clinical data</b> .....	12
<b>2.1.1 Healthy adult data</b> .....	14
<b>2.1.1.1 Plasma cortisol data</b> .....	14
<b>2.1.1.2 Plasma dexamethasone data</b> .....	14
<b>2.1.2 Healthy paediatric plasma cortisol data</b> .....	15

---

2.1.3	Paediatric adrenal insufficiency patient data.....	15
2.1.3.1	Plasma cortisol data.....	15
2.1.3.2	Dried blood spot cortisol and 17 $\alpha$ -hydroxyprogesterone data.....	15
2.1.3.3	Capillary and venous dried blood spot cortisol and 17 $\alpha$ -hydroxyprogesterone data.....	16
2.2	Nonlinear mixed-effects modelling and simulation.....	17
2.2.1	General workflow of a pharmacometric analysis.....	17
2.2.2	Nonlinear mixed-effects model components.....	18
2.2.3	Parameter estimation.....	20
2.2.4	Modelling data below the lower limit of quantification.....	21
2.2.5	Modelling baseline data.....	21
2.2.6	Model evaluation.....	22
2.3	Relationship between plasma and dried blood spot cortisol concentrations (Paper I)....	23
2.4	Target morning dried blood spot 17 $\alpha$ -hydroxyprogesterone concentrations for paediatric congenital adrenal hyperplasia patients (Paper II).....	24
2.5	Rational dexamethasone dose in prenatal congenital adrenal hyperplasia therapy (Paper III).....	26
2.6	Software.....	28
3	Research articles.....	29
3.1	Paper I: Exploring dried blood spot cortisol concentrations as an alternative for monitoring pediatric adrenal insufficiency patients: A model-based analysis.....	29
3.2	Paper II: Model-informed target morning 17 $\alpha$ -hydroxyprogesterone concentrations in dried blood spots for pediatric congenital adrenal hyperplasia patients.....	48
3.3	Paper III: Rationale of a lower dexamethasone dose in prenatal congenital adrenal hyperplasia therapy based on pharmacokinetic modelling.....	72
4	Results and discussion.....	90
4.1	Relationship between plasma and dried blood spot cortisol concentrations (Paper I)....	90
4.2	Target morning dried blood spot 17 $\alpha$ -hydroxyprogesterone concentrations for paediatric congenital adrenal hyperplasia patients (Paper II).....	98
4.3	Rational dexamethasone dose in prenatal congenital adrenal hyperplasia therapy (Paper III).....	107

## Table of Content

---

<b>5</b>	<b>Conclusions and perspectives.....</b>	<b>113</b>
<b>6</b>	<b>Bibliography .....</b>	<b>116</b>
<b>7</b>	<b>Acknowledgements .....</b>	<b>125</b>
<b>8</b>	<b>Publications .....</b>	<b>127</b>
<b>9</b>	<b>Curriculum vitae.....</b>	<b>130</b>

## Abbreviations

11 $\beta$ -HSD1/2	11 $\beta$ -hydroxysteroid dehydrogenase type 1 or type 2
17-OHP	17 $\alpha$ -hydroxyprogesterone
A <sub>b</sub> :Alb	Cortisol amount bound to albumin
A <sub>b</sub> :CBG	Cortisol amount bound to corticosteroid-binding globulin
A <sub>b</sub> :RBC	Cortisol amount associated with red blood cells
ACTH	Adrenocorticotrophic hormone
A <sub>depot</sub>	Amount in depot compartment
AI	Adrenal insufficiency
AIC	Akaike information criterion
A <sub>pla</sub>	Total amount in plasma
A <sub>u</sub>	Unbound amount
BASE <sub>adult, pla</sub>	Adult plasma cortisol baseline
BASE <sub>child, DBS</sub>	Paediatric dried blood spot cortisol baseline
BASE <sub>child, pla</sub>	Paediatric plasma cortisol baseline
BASE <sub>child, RBC</sub>	Paediatric cortisol associated with red blood cells at baseline
B <sub>max</sub>	Maximum binding capacity
CAH	Congenital adrenal hyperplasia
CBG	Corticosteroid-binding globulin or transcortin
CI	Confidence interval
CL	Clearance
C <sub>max</sub>	Maximum concentration
C <sub>pla,child</sub>	Paediatric plasma cortisol concentration
CRH	Corticotropin releasing hormone
CV	Coefficient of variation
DBS	Dried blood spots

## Abbreviations

---

Dex	Dexamethasone
EBE	Empirical Bayes estimate
EM	Expectation-maximisation
EMA	European Medicines Agency
F	Bioavailability
FDA	U.S Food and Drug Administration
FOCE-I	First-order condition estimation method with interaction
GOF	Goodness of fit
HC	Hydrocortisone
HPA	Hypothalamus-pituitary-adrenal
HPLC-UV	High-performance liquid chromatography with ultraviolet detection
$I_{\max}$	Maximum inhibitory effect
$IC_{50}$	Concentration inhibiting 50% of the maximum inhibitory effect
IMP	Importance sampling
IMPMAP	Importance sampling assisted by mode a posteriori
IIV	Interindividual variability
$k_a$	First-order absorption rate constant
$k_{aRBC}$	Linear association constant for association with red blood cells
$k_d$	Equilibrium dissociation constant
$k_{deg}$	First-order degradation rate constant
$K_m$	Amount in depot compartment resulting in 50% of $V_{\max}$
$k_{syn}$	First-order synthesis rate constant
LC-MS/MS	Liquid chromatography with tandem mass spectrometry
LLOQ	Lower limit of quantification
NLME(M)	Nonlinear mixed-effects (modelling)
$NS_{Alb}$	Linear non-specific parameter for albumin binding
OFV	Objective function value
$OHP_{BASE}$	Dried blood spot $17\alpha$ -hydroxyprogesterone concentration at baseline

## Abbreviations

---

PBPK(M)	Physiologically-based pharmacokinetic (modelling)
PD	Pharmacodynamic(s)
PK	Pharmacokinetic(s)
p.o.	peroral (per os)
Q	Intercompartmental clearance
QSP	Quantitative systems pharmacology
RBC	Red blood cells (erythrocytes)
RSE	Relative standard error
RUV	Residual unexplained variability
SAEM	Stochastic approximation expectation maximisation
SD	Standard deviation
SIR	Sampling importance resampling
$V_{c(en)}$	Central volume of distribution
$V_{\text{delta}}$	Volume of the red blood cell compartment
$V_{\text{max}}$	maximum absorption rate
VPC	Visual predictive check
$V_{p(er)}$	Peripheral volume of distribution

## Relevant publications

This thesis is a cumulative work based on the following papers, which are referred to in the text by their Roman numerals:

- I. Exploring dried blood spot cortisol concentrations as an alternative for monitoring pediatric adrenal insufficiency patients: A model-based analysis. *Frontiers in Pharmacology*. doi: 10.3389/fphar.2022.819590 (2022).
- II. Model-informed target morning  $17\alpha$ -hydroxyprogesterone concentrations in dried blood spots for pediatric congenital adrenal hyperplasia patients. *Pharmaceuticals*. doi: 10.3390/ph16030464 (2023).
- III. Rationale of a lower dexamethasone dose in prenatal congenital adrenal hyperplasia therapy based on pharmacokinetic modelling. *European Journal of Endocrinology*. doi: 10.1530/EJE-21-0395 (2021).

Reprints were made with permission from the respective publishers.

# 1 Introduction

## 1.1 Pharmacokinetics and pharmacotherapy in paediatric and foetal patients

Paediatric patients are defined as children and adolescents from 0-18 years and can be further classified according to their age [1,2]. The age groups relevant for this work are defined as neonates (<28 days), infants ( $\geq$ 28 days-2 years), and young children ( $\geq$ 2-6 years), according to the classification in the clinical study in *Paper I* and *Paper II* (see section 2.1.3.1). Paediatric patients are viewed as a vulnerable population due to differences in their maturing physiology compared to adults as well as their underrepresentation in drug research, development and available medicines on the market.

Pharmacokinetics (PK) is describing ‘what the body does to the drug’ and comprises the absorption, distribution, metabolism and excretion processes of the drug. Especially in neonates and young infants, these processes differ relevantly from the better studied PK processes in adults [3]. For instance, the higher stomach pH in neonates can lead to altered absorption of perorally administered drugs, the different body composition in young children due to a higher body water proportion can affect the distribution of certain drugs or the not fully developed glomerular function in the neonatal kidneys can limit drug excretion. Most importantly, numerous drug metabolism processes underlie maturation processes [4]. Although it was often stated that children cannot be simply viewed as ‘small adults’, Anderson and Holford concluded that ‘children are small adults, neonates are immature children’ [4]. Since growth and maturation are no linear processes, predicting paediatric PK and adequate drug dosing is challenging. In drug research and development, allometric scaling using mathematical power relations with empirical exponents is often applied to translate PK parameters such as volume of distribution or clearance, i.e., metabolism and excretion, from adults to children [5,6]. Also, for pharmacodynamics (PD), i.e., ‘what the drug does to the body’ or the drug effect, children show different responses which are however less well studied in paediatrics.

The vast majority of pharmacotherapeutic treatments are off-label in children, especially in neonates, due to a lack of available drugs licensed for paediatric use and pharmaceutical forms specifically tailored to the needs of paediatric patients [1,7,8]. Initiatives by the U.S. Food and Drug Administration (FDA) and the European Medicines Agency (EMA), e.g., the Paediatric Regulation by the European Commission [9], were introduced to improve the development and availability of such drugs.

Prenatal pharmacotherapies aiming at treating the unborn child face similar challenges with not only immature physiology of the foetus but also pregnancy-related PK changes in the mother [10,11] making therapy outcomes difficult to predict. Since pregnant women are usually not enrolled in clinical studies, knowledge on PK and PD during pregnancy is scattered [11]. Moreover, information on PK processes in the human foetus is rare due to limited possibilities for investigation.

## 1.2 Congenital adrenal hyperplasia

To understand the pathophysiology (1.2.2) of congenital adrenal hyperplasia (CAH), it is important to know the physiological role as well as biosynthesis of the endogenous cortisol. The healthy physiology is shortly described in section 1.2.1.

### 1.2.1 Healthy physiology of cortisol and 17 $\alpha$ -hydroxyprogesterone

Cortisol is an endogenous glucocorticoid and plays a relevant role in numerous physiological processes such as metabolism, growth and the immune system [12]. The cortisol biosynthesis is centrally regulated via the hypothalamus-pituitary-adrenal (HPA) axis where corticotropin releasing hormone (CRH) is released from the hypothalamus and promotes the release of adrenocorticotrophic hormone (ACTH) from the pituitary gland (Figure 1.1).

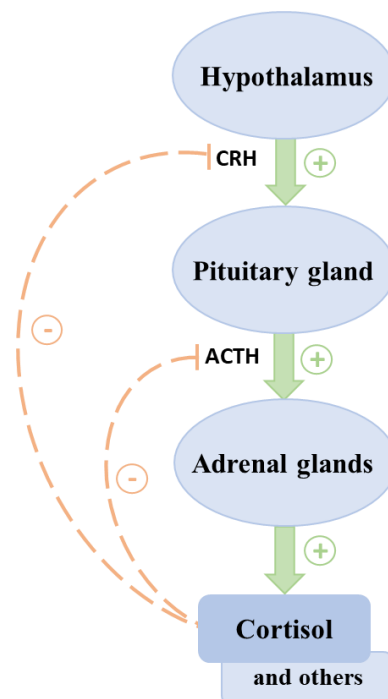


**Figure 1.1** Regulation of cortisol biosynthesis via the hypothalamic-pituitary-adrenal axis. Corticotropin releasing hormone (CRH), adrenocorticotrophic hormone (ACTH).

ACTH then stimulates the synthesis of glucocorticoids, mineralocorticoids and androgens in the adrenal glands. The biosynthesis pathways of these three groups of steroids are shown in detail in Figure 1.2.A. Cortisol, among other glucocorticoids, exerts negative feedback on the CRH and ACTH release, thereby regulating its own biosynthesis through inhibition of the HPA axis [13-16]. Moreover, the cortisol biosynthesis shows a circadian rhythm, where the cortisol concentration reaches its maximum in the morning and decreases over the course of the day (Figure 1.3) [13].

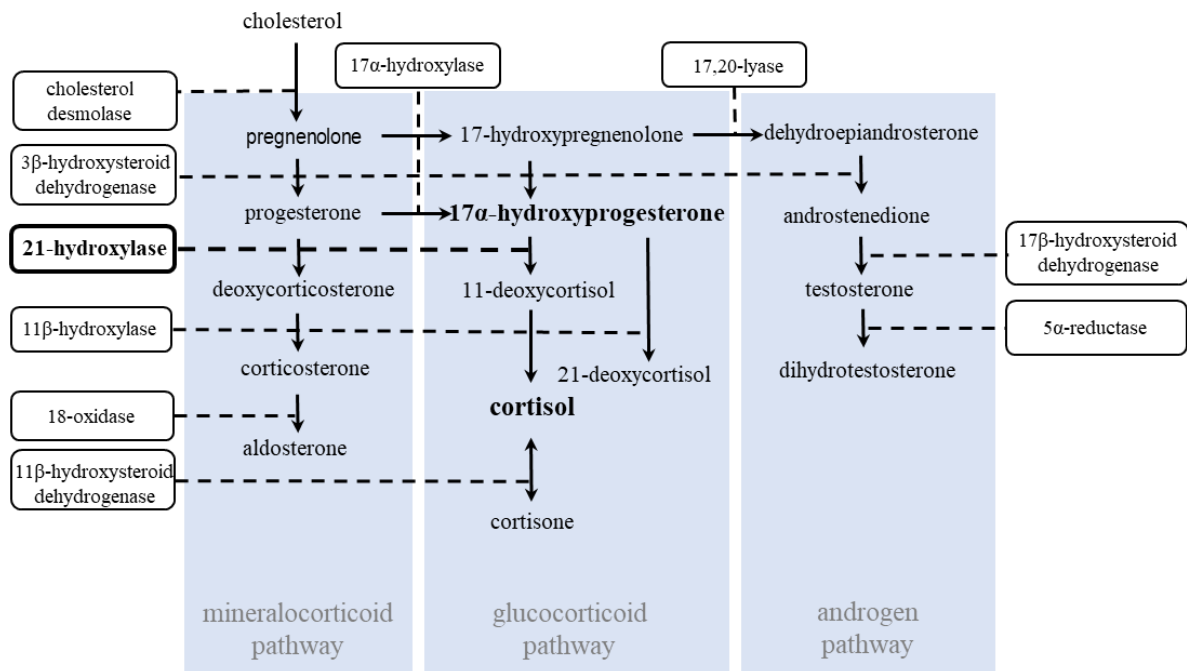


**Figure 1.2.A** Biosynthesis pathways of mineralocorticoids, glucocorticoids and androgens in the adrenal glands of healthy individuals. Boxes indicate enzymes. This image was adapted from J.S.E. Melin. Pharmacometric approaches to assess hydrocortisone therapy in paediatric patients with adrenal insufficiency. Freie Universität Berlin. (2017) [17].

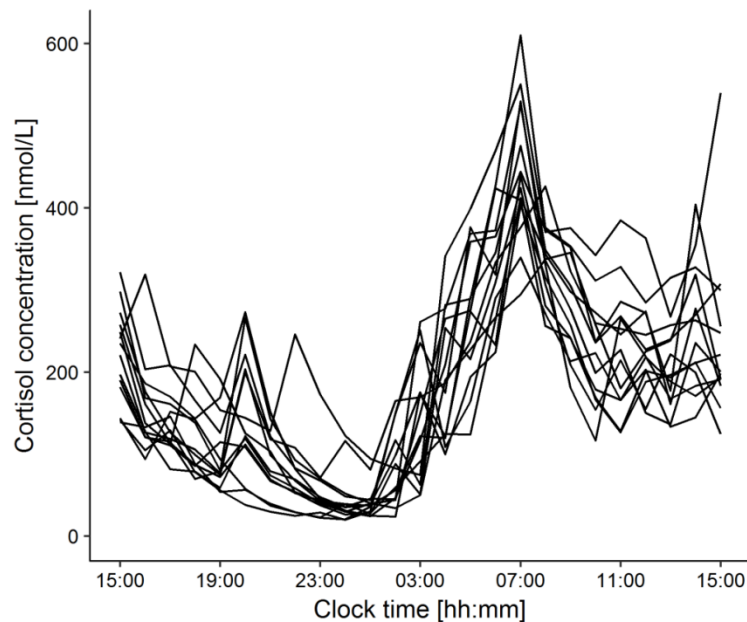


**Figure 1.3** Circadian cortisol concentration-time profiles of 14 healthy adults in the clinical study described in 2.1.1, before suppression of the hypothalamic-pituitary-adrenal axis with dexamethasone.

This image was taken from J.S.E. Melin. Pharmacometric approaches to assess hydrocortisone therapy in paediatric patients with adrenal insufficiency. Freie Universität Berlin. (2017) [17].

## 1.2.2 Pathophysiology of congenital adrenal hyperplasia

CAH is the most common primary adrenal insufficiency (AI) in paediatric patients with a prevalence of 1:15000-16000 in Europe and in the USA [18]. In brief, it is a group of rare autosomal recessively inherited metabolic diseases characterised by a largely decreased or absent cortisol biosynthesis. In 90%-95% of cases, the disorder of adrenal steroidogenesis is due to a deficiency of the enzyme steroid 21-hydroxylase, also known as cytochrome P450c21 (see Figure 1.2.B) [19,20]. A major complication of CAH is adrenal crisis which can be lethal [13]. Due to the cortisol deficiency and thus a lacking feedback mechanism on the steroidogenesis, the hypothalamic-pituitary-adrenal (HPA) axis is activated, leading to an accumulation of cortisol precursors such as progesterone and 17 $\alpha$ -hydroxyprogesterone. As these steroids are also androgen precursors, the cortisol biosynthesis pathway is shifted towards androgen production [21] (Figure 1.2.B). The overproduction of androgens, e.g., of testosterone, is leading to corresponding symptoms such as premature pseudo puberty and ending of longitudinal growth, and virilisation and hirsutism in female patients [13,14,20]. The accumulating cortisol and androgen precursors as well as androgens are therefore useful biomarkers to assess the disease progression and treatment success.

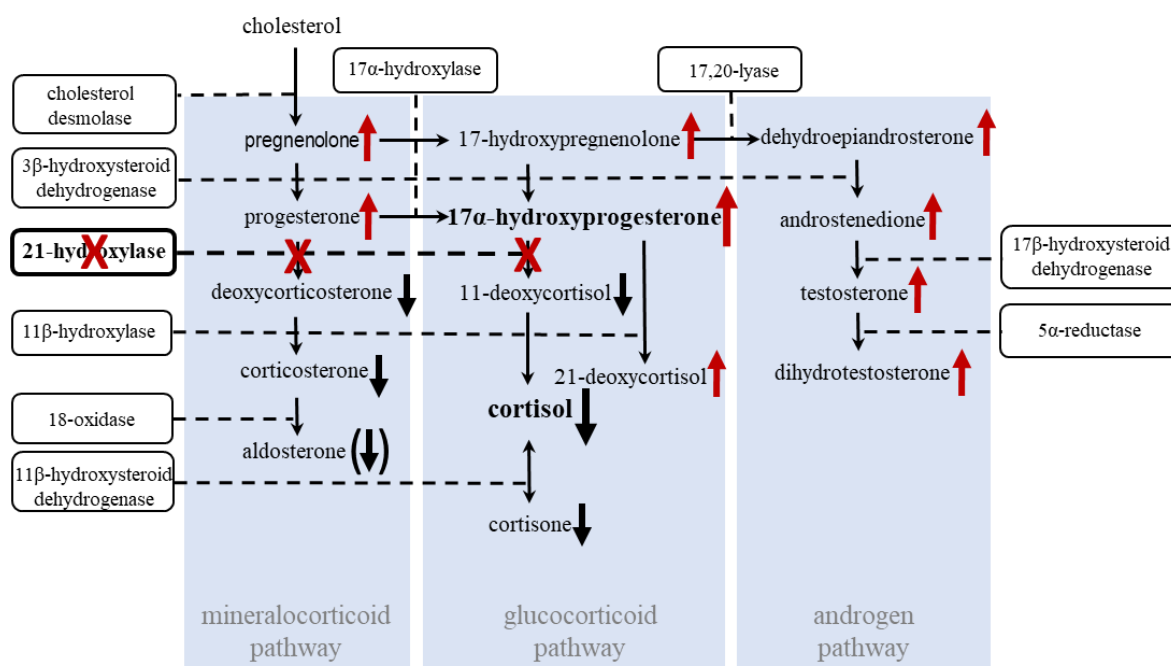


**Figure 1.2.B** Biosynthesis pathways of mineralocorticoids, glucocorticoids and androgens. Boxes indicate enzymes. The bold black and red arrows indicate the pathophysiological steroid concentration changes due to 21-hydroxylase deficiency in untreated CAH patients. This image was adapted from

J.S.E. Melin. Pharmacometric approaches to assess hydrocortisone therapy in paediatric patients with adrenal insufficiency. Freie Universität Berlin. (2017) [17].

CAH can occur in a non-classical form which is less severe and, in many cases, asymptomatic, whereas classical form patients can be distinguished into salt wasters and simple virilisers. The simple virilisers require a lifelong replacement of cortisol. The salt wasters make up 75% of the classical patients, showing an aldosterone deficiency, in addition to the cortisol deficiency. These patients face a possible life-threatening electrolyte imbalance due to the underproduction of mineralocorticoids [21] and need an additional aldosterone replacement which is given by fludrocortisone. The work in this thesis focuses on cortisol replacement therapy (see 1.2.3.1).

Furthermore, the adrenal excess is already taking place in foetal CAH patients resulting in female patients born with virilised external genitalia who, in certain severe cases, undergo reconstructive surgery [21]. The prenatal CAH therapy to prevent this virilisation is addressed in section 1.2.3.2.

### **1.2.3 Congenital adrenal hyperplasia pharmacotherapy**

#### **1.2.3.1 Cortisol replacement therapy in paediatric patients**

CAH patients require a life-long cortisol replacement therapy. For paediatric patients, hydrocortisone (HC), a synthetic drug substance identical to cortisol, is the recommended glucocorticoid since its short half-life of 1.5 hours and low potency decrease the risk for adverse events related to cortisol overexposure [21,22]. Compared to cortisol, dexamethasone (Dex) is assumed to have a 50-80 fold higher potency [23] and is given to adult CAH patients. Typical adverse events of cortisol replacement therapy can be Cushing's syndrome, reduced final height, hypertension, dyslipidaemia, obesity, decreased glucose tolerance or osteoporosis [13]. Moreover, too low cortisol exposure can result in disease progression and adrenal crisis [21]. Therefore, dosing of HC requires special consideration to result in drug concentrations mimicking the physiological conditions and the circadian rhythm of cortisol [13] which represents a challenge in CAH therapy. The recommended daily HC dose for children is 10-15 mg/m<sup>2</sup> given three times per day, with the highest dose in the morning [21,24,25]. The single doses are adjusted according to the patients' individual needs, laboratory parameters and symptoms evaluation [26].

Since no paediatric HC formulation was available for decades, either manually broken or crushed HC tablets approved for adults or capsules containing paediatric doses manufactured in pharmacies were administered to children with CAH. These off-label administrations had the risk of inaccurate doses as well as adherence concerns due to the bitter taste of cortisol [27,28]. Also HC suspensions represent a suboptimal pharmaceutical formulation due to an inhomogeneous distribution of the drug and a short shelf-life [29]. Therefore, Alkindi<sup>®</sup>, a formulation of oral HC granules with taste masking, was developed and licensed for use in the EU for children from birth to 18 years in 2018 [28,30,31]. Data

from Alkindi® clinical trials was used in this work and is introduced in section 2.1. Moreover, sustained-release oral HC formulations [32,33] as well as formulations for subcutaneous use [34,35] are currently in development.

### 1.2.3.2 Prenatal therapy with dexamethasone

To prevent the virilisation of female CAH patients *in utero*, Dex is used in prenatal CAH pharmacotherapy as it has the ability to cross the placenta and suppress the foetal HPA axis. Since the first description of prenatal CAH therapy with Dex in 1984 [36,37], a Dex dose of 20 µg/kg/d, to a maximum of 1.5 mg/d given in 2-3 daily doses, is administered to pregnant women expecting a child with CAH. There is evidence from case studies that prenatal therapy with Dex significantly reduces virilisation in female foetuses with CAH, given the therapy was started before the window of sexual differentiation, i.e., week 7 to 12 post conception [38,39]. Prenatal CAH therapy with Dex is considered experimental due to a lack of clinical evidence for the Dex dose [23,40-42]. This experimental Dex dose which has been traditionally given for decades is assumed to be associated to safety risks for both the mother and the unborn child. Prenatal glucocorticoid overexposure was found to result in postnatal hypertension, impact on glucose homeostasis, decreased glomerular filtration, fatty liver disease and multiple negative effects on brain development [23,43]. Additionally, clinical studies showed potentially negative impacts on neuropsychological and behavioural outcome in foetuses at risk for CAH who were treated prenatally with Dex [42-51]. These studies however showed conflicting results and included very low numbers of patients. Furthermore, in animal studies, high Dex doses showed teratogenic effects [43]. In treated mothers, possible adverse events included oedema, increased mean weight gain, mood swings, and a slightly increased occurrence of hypertension, pre-eclampsia and gestational diabetes [23,39,41]. Since Dex is assumed to be 50-80 times more potent than cortisol, Miller concluded in his review that the traditional prenatal Dex therapy provides the mother with about 6-fold her physiological need for glucocorticoids, i.e., the traditional Dex dose is approximately 6-fold too high [23].

## 1.3 Pharmacokinetics of hydrocortisone and dexamethasone

HC, or its endogenous equivalent cortisol, is known to show complex PK as it binds to corticosteroid-binding globulin (CBG, also known as transcortin) with high affinity and to albumin and erythrocytes with a lower affinity [54]. The binding to CBG is saturated within therapeutic drug concentrations causing nonlinear cortisol PK [55,56]. Poor solubility at higher oral HC doses can lead to a saturable absorption [57,58]. Cortisol is transformed into numerous metabolites which are renally excreted. The enzymes 5 $\alpha$ -reductase, 5 $\beta$ -reductase and 3 $\alpha$ -hydroxysteroid dehydrogenase sequentially metabolise cortisol to allo-tetrahydrocortisol, tetrahydrocortisol and tetrahydrocortisone, respectively. Furthermore, approximately 1% of cortisol is metabolised to 6 $\beta$ -hydroxycortisol by the enzyme 6 $\beta$ -

hydroxylase, also known as cytochrome P450(CYP)3A4 [59]. In the kidney, cortisol is transformed via the enzyme 11 $\beta$ -hydroxysteroid dehydrogenase type 2 (11 $\beta$ -HSD2) to the biologically less active cortisone, which has the same binding partners as cortisol [60]. This process is bidirectional with 11 $\beta$ -hydroxysteroid dehydrogenase type 1 (11 $\beta$ -HSD1) transforming cortisone back to cortisol in the liver and adipose tissue.

Several PK processes for cortisol undergo maturation in early childhood. In neonates and in infants 5 $\alpha$ -reductase activity was observed to be lower and higher compared to adults, respectively, with an activity peak at 3 months [61]. The activity then declined until the age of 12 months [62]. Moreover, 11 $\beta$ -HSD1 was found to have undetectable activity during the first 3 months of life, and reached adult activity at 12 months [63]. Also for CBG maturation was observed during the first year of life [64]. Pharmacokinetic analyses concluded that HC PK including binding kinetics can be assumed to be similar in adolescents (12-18 years) and in adults [65].

Dex is known as a highly potent glucocorticoid and its PK has been studied for many decades. Dex binds to albumin and shows little or no binding to CBG [66]. Dex PK was found to be dose-dependent, i.e., Dex exposure did not increase linearly with oral doses [67]. Moreover, PK parameters often showed a high variability in pre-clinical as well as clinical populations [66-68]. Dex PK was often described with a two-compartment model, a first-order absorption and a fast elimination [69,70]. In contrast to cortisol, Dex is only minimally inactivated by placental 11 $\beta$ -HSD2 [71]. Despite the broad use of Dex in adults and children [68], only little is known about Dex PK in pregnant women. In near-term pregnant women, the terminal half-life of Dex and plasma protein binding to Dex was not affected by pregnancy [72,73]. No Dex target concentrations are known for CAH therapy in the foetus due to a lack of knowledge on foetal Dex PK.

### **1.4 Pharmacodynamics of hydrocortisone and dexamethasone**

The administration of glucocorticoids, such as HC and Dex, leads to a downregulation of CRH and ACTH via negative feedback on the HPA axis [12-14]. Consequently, concentrations of cortisol precursors which are accumulating in CAH decrease. Among them is 17-OHP which is the most conventionally used biomarker in CAH monitoring as it is the precursor of cortisol as well as of androgens. Other important biomarkers include androstenedione, testosterone, progesterone, cortisone and the 17-OHP metabolite 21-deoxycortisol [13,21] (see Figure 1.2 B). As previously mentioned, Dex has a 50-80 times higher potency compared to HC, i.e., cortisol [23].

## 1.5 Dried blood spot sampling

Dried blood spot (DBS) sampling is a minimally invasive sampling technique where whole blood volumes of 20-100  $\mu\text{L}$  are obtained via a prick in the fingertip or heel and dropped on cellulose-based sampling paper. Dropping whole blood on these sampling cards allows storage at room temperature as well as easy transportation [74,75]. Discs of a certain diameter, representing a fixed volume, are subsequently punched out of the DBS spots, extracted and subjected to bioanalysis (see Figure 1.4) [74-76].

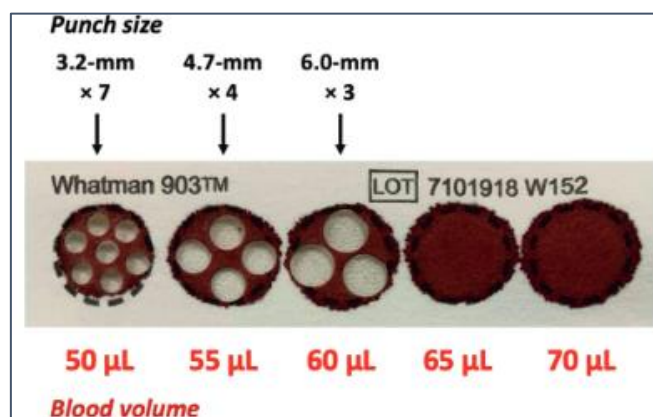


**Figure 1.4** Collection card with dried blood spots of blood volumes from 50  $\mu\text{L}$  to 70  $\mu\text{L}$  and punches of commonly used disc sizes shown on the first three spots. This image was taken from T.A. Jacobson *et al.*, *J. Expo. Sci. Environ.* (2022) [77].

The low blood volumes required for DBS sampling pose an advantage for the vulnerable paediatric population, compared to traditional plasma sampling [76]. Therefore, DBS have been used since the 1960s to perform newborn screenings for diseases such as phenylketonuria [78,79] and are also commonly used for neonatal CAH screening [18]. Long-term stability at room temperature and feasibility of quantification following DBS sampling has been widely investigated for CAH-relevant steroids [78-80]. In paediatric CAH therapy monitoring, besides DBS sampling of capillary blood from the fingertip, also venous blood from an existing venous access is commonly used. The quantitative relationship between concentrations obtained by DBS and plasma sampling is specific to the analyte [75] and had not been fully investigated for cortisol or CAH biomarkers yet. Since DBS sampling involves whole blood and cortisol is known to be associated to red blood cells (RBCs) [54], understanding the relationship between plasma and DBS cortisol is crucial for a correct interpretation of DBS measurements. The target morning concentration for the biomarker 17-OHP has been suggested to be 12-36 nmol/L in plasma [13], but is still unknown for concentrations collected by DBS sampling.

## 1.6 Pharmacometrics

Pharmacometrics is a young, interdisciplinary science field where the interplay between the drug behaviour and (patho-)physiology is quantitatively characterised in mathematical models which are developed to be applied to answer specific research questions [83]. Such models are then often used in simulations to, e.g., further elucidate processes in drug behaviour or therapy or to investigate drug dosing scenarios [84,85]. Thus, pharmacometrics represents a powerful approach to close knowledge gaps in drug development and therapy and has therefore gained growing recognition and relevance in the past few decades. Commonly used so-called ‘bottom-up approaches’ are physiologically-based pharmacokinetic (PBPK) and quantitative systems pharmacology (QSP) modelling, where PK, PD and disease processes are mechanistically described on the physiological organ and cell level, respectively. In this thesis, population PK/PD modelling [84-86], more specifically nonlinear mixed-effects (NLME) modelling (see section 1.6.1), was applied as a ‘top-down approach’, i.e., modelling based on, e.g., clinical data.

### 1.6.1 Nonlinear mixed-effects modelling

In population modelling approaches such as NLME modelling [85,89], individual data of populations is leveraged to build models where e.g., drug PK is characterised by concentration data over time and addition of biomarker data enables the development of PK/PD models describing drug effect over time. Population models usually consist of so-called compartments, in which the drug is homogeneously distributed and shows a distinct uniform PK behaviour, e.g., a central and a peripheral compartment, lumping organs which are well and poorly perfused, respectively. In NLME modelling, all available data is analysed at the same time which enables the estimation of fixed effects, i.e., model parameters of a typical individual within the population, as well as of random effects, i.e., model parameters quantifying interindividual and residual variabilities. These variabilities can be explained by quantitatively linking them to so-called covariates which can be patient-, disease- or treatment-specific characteristics, e.g., age, body weight, disease severity or drug dose. More details on the applied NLME modelling methods are covered in section 2.2.

### 1.6.2 Use of pharmacometrics in drug development and drug therapy

Pharmacometrics has become an established part of drug research and development [90] and is encouraged and regulated by authorities such as the EMA and the FDA [82,91-94]. The use of pharmacometric analyses increases efficiency in drug development by reducing cost and time resources. Pharmacometric models are e.g., applied to translate drug PK and PD from animals to humans, to extrapolate PK and PD to specific populations such as paediatrics or to predict and suggest dosing regimens for clinical studies. Moreover, pharmacometrics is widely used in academic and clinical research to foster the rational use of licensed drugs by e.g., identifying individualised doses for special

populations and optimising therapeutic drug monitoring [95]. Especially in the field of paediatrics where data is often scarce, pharmacometrics modelling offers a great potential for answering drug dosing and therapy monitoring related questions [96,97].

Whereas no pharmacometric analyses have been applied to suggest a rational Dex dose for prenatal CAH therapy, several modelling analyses on CAH therapy in paediatric patients have been published: A semi-mechanistic PK model capturing the complex cortisol PK including binding to CBG and albumin has been previously developed at our department, based on adult phase 1 study data for the paediatric HC formulation Alkindi<sup>®</sup>. The model was used to predict Alkindi<sup>®</sup> PK in paediatrics, finding a high variability in drug exposure related to body weight, especially in younger children (<20 kg) which confirmed the high need for dose optimisation in these patients [58]. In a subsequent analysis, phase 3 Alkindi<sup>®</sup> data was leveraged together with the adult data to develop a paediatric HC PK model which was then applied to simulate dosing regimens for paediatric CAH patients [98]. The outcome was that with none of the tested dosing regimens, administering an immediate release HC formulation, it is possible to capture the physiological circadian cortisol time-profiles, highlighting the importance of developing sustained-release formulations. In addition to PK models, PK/PD models were developed describing the relationship between cortisol and the biomarkers 17-OHP and androstenedione in plasma [99,100]. Moreover, the circadian rhythm of CBG [101,102] was modelled and found not to have a clinical relevance for HC dosing in paediatric CAH patients [103]. As shortly discussed in section 1.5, no pharmacometrics models have been developed based on DBS data to further quantitatively investigate DBS steroid measurements, and no biomarker target concentrations have been identified for monitoring CAH patients with DBS sampling.

## 1.7 Objectives

Cortisol replacement therapy for treating CAH, a rare form of adrenal insufficiency, requires special monitoring due to the risk of adverse effects such as Cushing's syndrome or disease progression caused by cortisol over- or underexposure, respectively. Especially paediatric patients can highly profit from the minimally invasive DBS sampling technique during therapy monitoring. However, there is little knowledge on cortisol concentrations in whole blood samples such as DBS compared to traditionally sampled blood plasma. Thus, there are no known DBS target concentrations for cortisol or CAH biomarkers and the feasibility of DBS sampling for CAH therapy monitoring needs to be evaluated. Furthermore, DBS sampling is usually conducted with either capillary or venous blood and the comparability of cortisol and CAH biomarker concentrations in these two matrices is still to be investigated. To prevent *in utero* virilisation of female fetuses with CAH, prenatal CAH therapy has been conducted since decades by orally administering Dex to the pregnant mother. The traditionally used dose of 20 µg/kg/d is however assumed to be too high and to potentially cause adverse effects for both the mother and the foetus. No alternative evidence-based Dex dose has been established or suggested to this day.

The overall objective of this doctoral work was to generate new insights into the PK and PD characteristics of the CAH compounds hydrocortisone and dexamethasone by applying pharmacometric methods, and thereby to contribute to the optimisation of CAH therapy and therapy monitoring in the vulnerable paediatric and foetal patient population.

The specific objectives of the three projects presented in this dissertation were:

### *Paper I*

- Quantitative exploration and interpretation of DBS cortisol concentrations in paediatric CAH patients and characterising association of cortisol with red blood cells

### *Paper II*

- Derivation of a target morning concentration range in DBS for the important disease biomarker 17-OHP in paediatric CAH patients by performance of PK/PD modelling and simulation
- Assessment of the comparability of capillary and venous DBS concentrations for cortisol and 17-OHP in paediatric CAH patients

### *Paper III*

- Determining a model-based rationale of a lower, efficacious dexamethasone dose to reduce adverse effects in prenatal CAH therapy

## 2 Methods

### 2.1 Clinical data

A comprehensive overview of all clinical data used in this work is presented in Table 2.1. The different datasets are described in more detail in the following subsections of 2.1.

**Table 2.1** Overview of all clinical data analysed in this work with details given in the specified subsections of 2.1 in the table header row.

Study characteristic	2.1.1 Healthy adult data		2.1.2 Healthy paediatric plasma cortisol data	2.1.3 Paediatric AI patient data		
	2.1.1.1 Plasma cortisol data	2.1.1.2 Plasma Dex data		2.1.3.1 Plasma cortisol data	2.1.3.2 DBS cortisol and 17-OHP data	2.1.3.3 Capillary and venous DBS cortisol and 17-OHP data
<i>Paper</i>	<i>I</i>	<i>III</i>	<i>II</i>	<i>I, II</i>	<i>I, II</i>	<i>II</i>
Study type	Phase 1 clinical study (two crossover studies)	Part of a clinical bioavailability study	Part of a randomised controlled study	Phase 3 clinical study	Clinical routine monitoring	Clinical routine monitoring
Population	Healthy male adults	Healthy adults, female and male	Healthy children, 5-9 years	Paediatric AI patients (CAH, 1 hypopituitarism patient), 0-6 years		Paediatric CAH patients, 2 months–11 years
Number of individuals	n=30	n=24	n=28	n=24 in <i>Paper I</i> Young children, $\geq 2$ –6 years, n=12 Infants, $\geq 28$ days–2 years, n=6 Neonates, <28 days, n=6  n=18 in <i>Paper II</i> (Young children and infants)		n=15

## Methods

Drug dosing	0.5, 2, 5, 10 or 20 mg single morning dose of Alkindi® (HC) <i>p.o.</i>	2 mg Dex <i>p.o.</i> , immediate-release tablet in the morning	NA	1-4 mg individual single morning dose of Alkindi® (HC) <i>p.o.</i>	0.5-7 mg individual doses of HC	
Sampling times	Crossover study 1: 0.5, 1, 1.5, 2.5, 3, 3.5, 4, 4.5, 5, 5.5, 6, 6.5, 7, 7.5, 8, 9, 10, 11 and 12 h post-dose  Crossover study 2: pre-dose, 0.25, 0.5, 0.75, 1, 1.25, 1.5, 2, 2.5, 3, 4, 5, 6, 8, 10 and 12 h post-dose	Pre-dose and 0.25, 0.5, 0.75, 1, 1.25, 1.5, 1.75, 2, 2.5, 3, 4, 5, 6, 8, 12, 16, and 24 h post-dose	20-min intervals over 24 h	All patients: Pre-dose, 1 and 4 h post-dosing  Young children: Three additional sampling points each (two between 30, 45, 90, 120, 150 and/or 180 min post-dose, one at time of C <sub>min</sub> )	1-9 h after last HC administration	
Number of samples	n=1482	n=432	n=2016	n=106 (88 in <i>Paper II</i> , excluding neonates)	n=15	
Sampling matrix	Total plasma	Total plasma	Total plasma	Total plasma	Total DBS	Total DBS
Analyte(s)	Cortisol	Dex	Cortisol	Cortisol	Cortisol 17-OHP	Cortisol 17-OHP

17-OHP: 17 $\alpha$ -hydroxyprogesterone, AI: Adrenal insufficiency, CAH: Congenital adrenal hyperplasia, DBS: Dried blood spots, Dex: Dexamethasone, HC: Hydrocortisone, NA: Not applicable.

## 2.1.1 Healthy adult data

### 2.1.1.1 Plasma cortisol data

In *Paper I*, data from a clinical phase 1 trial on the paediatric HC formulation Alkindi® (hydrocortisone granules in capsules, Diurnal Europe B.V., Netherlands) was leveraged. The trial consisted of two independent crossover studies (ClinicalTrials.gov identifiers: NCT02777268, NCT01960530) [104] and were conducted at the Institute of Experimental Paediatric Endocrinology at Charité-Universitätsmedizin Berlin, CVK, Berlin. A single oral Alkindi® morning dose of 0.5-20 mg was administered to 30 healthy male volunteers in total after they received a single dose of Dex to suppress the endogenous cortisol biosynthesis. Total cortisol was densely sampled pre-dose and from 0.5 to 12 hours post-dose, resulting in a total of 1482 PK samples. Bioanalysis was performed at Simbec Research Ltd (Merthyr Tydfil, UK) by a validated liquid chromatography with tandem mass spectrometry detection (LC-MS/MS).

### 2.1.1.2 Plasma dexamethasone data

In *Paper III*, data from the reference treatment arm of a published bioavailability study in 24 healthy individuals receiving Dex (EudraCT number: 2008-001389-10) [68] was leveraged to develop a Dex PK model describing maternal Dex concentrations during prenatal CAH therapy (see 2.5). The study individuals were 15 female and 9 male healthy subjects receiving a single dose of 2 mg of Dex as an orally administered immediate-release tablet. More detailed population characteristics are shown in Table 2.2. Plasma was sampled 18 times per individual, up to 24 h post-dose, resulting in a total of 432 plasma samples. Total plasma Dex concentrations were quantified in plasma using a high-performance liquid chromatography with ultraviolet detection (HPLC-UV) assay.

**Table 2.2** Population characteristics of the healthy adult plasma dexamethasone data (median (range)).

Characteristic	Unit	Female (n=15)	Male (n=9)	Total (n=24)
Age	[years]	30.0 (22.0-54.0)	38.0 (25.0-54.0)	32.0 (22.0-54.0)
Body weight	[kg]	65.0 (60.0-77.5)	79.0 (73.0-90.0)	70.0 (60.0-90.0)
Height	[m]	1.66 (1.63-1.76)	1.84 (1.72-1.88)	1.71 (1.63-1.88)
Body mass index	[kg/m <sup>2</sup> ]	23.2 (21.0-26.9)	25.5 (20.7-27.0)	23.7 (20.7-27.0)

---

Dexamethasone concentrations*	[nmol/L]	15.4 (1.12-39.0)	10.1 (1.9-29.3)	12.61 (1.12-39.0)
-------------------------------	----------	---------------------	--------------------	----------------------

---

\*After peroral administration of a 2 mg dexamethasone immediate release tablet

## 2.1.2 Healthy paediatric plasma cortisol data

In *Paper II*, physiological (=healthy) plasma cortisol concentration-time profiles from non-CAH children were leveraged for simulations [105,106]. The study was approved by the University College London Hospitals Committee on Ethics in Human Research [106]. Plasma samples were taken from 28 non-CAH children, aged from 5 to 9 years, at 20-minute intervals over 24 hours through an in-dwelling cannula. This dense sampling resulted in 2016 total plasma cortisol concentrations. The cortisol concentrations were measured using the Coat-A-Count radioimmunoassay (Coat-A-Count, DPC, Los Angeles, CA, USA).

## 2.1.3 Paediatric adrenal insufficiency patient data

### 2.1.3.1 Plasma cortisol data

In *Paper I and II*, data from the phase 3 trial (EudraCT number: 2014-002265-30, ClinicalTrials.gov Identifier: NCT02720952) [28], following the phase 1 trial described in 2.1.1.1, was used. The study was conducted at the Institute of Experimental Paediatric Endocrinology at Charité-Universitätsmedizin Berlin, CVK, Berlin, with 24 paediatric AI patients (23 patients with CAH, 1 patient with hypopituitarism) receiving an individualised oral Alkindi® morning dose of 1-4 mg. The patients were divided into three cohorts according to their age group (12 young children of  $\geq 2$ -6 years, 6 infants of  $\geq 28$  days-2 years, neonates of  $< 28$  days). A total of 106 plasma samples were collected pre-dose, 1 and 4 hours post-dose, and at 3 additional time points in young children (see Table 2.1). All measured total plasma cortisol concentrations (n=106) were used in *Paper I* whereas only data from the young children and infant cohorts (n=88 cortisol concentrations) was used in *Paper II*. Bioanalysis was conducted as described in 2.1.1.1.

### 2.1.3.2 Dried blood spot cortisol and 17 $\alpha$ -hydroxyprogesterone data

Besides the plasma samples described in 2.1.3.1, DBS samples were taken from the venous access in the same 24 paediatric AI patients and at the same sampling times. The DBS sampling was conducted as routine clinical sampling in accordance with the study protocol (ClinicalTrials.gov Identifier: NCT02720952). A multi-steroid analysis was then conducted in which cortisol and 17-OHP were measured by LC-MS/MS. Linearity, accuracy, and precision were tested for DBS steroid quantification with the respective acceptance criteria being met according to the guideline on bioanalytical method validation of the European Medicines Agency (European Medicines Agency, 2012) [107]. The DBS sampling as well as the bioanalysis were conducted at Charité-Universitätsmedizin Berlin, CVK, Berlin.

Analogously to the plasma cortisol data from the Alkindi® phase 3 study, 106 and 88 simultaneously sampled DBS cortisol concentrations of the three and two age cohorts were used for the PK model development in *Paper I* and *Paper II*, respectively. Additionally, 88 DBS 17-OHP concentrations were used in the model analysis in *Paper II*.

### **2.1.3.3 Capillary and venous dried blood spot cortisol and 17 $\alpha$ -hydroxyprogesterone data**

A dataset containing venous and capillary DBS concentrations was created during clinical routine sampling for CAH therapy monitoring at Charité-Universitätsmedizin Berlin and was used in *Paper II*. One venous and one capillary DBS sample each was obtained in parallel from 15 paediatric CAH patients, aged from 2 months to 11 years (median: 8 years). The multi-steroid analysis described in 2.1.3.2 was conducted, quantifying concentrations for cortisol and for 17-OHP. Sampling times were between the morning and late afternoon, and between one to nine hours after the last HC administration.

## 2.2 Nonlinear mixed-effects modelling and simulation

### 2.2.1 General workflow of a pharmacometric analysis

All pharmacometric analyses presented in this dissertation followed a general workflow which is depicted in Figure 2.1.

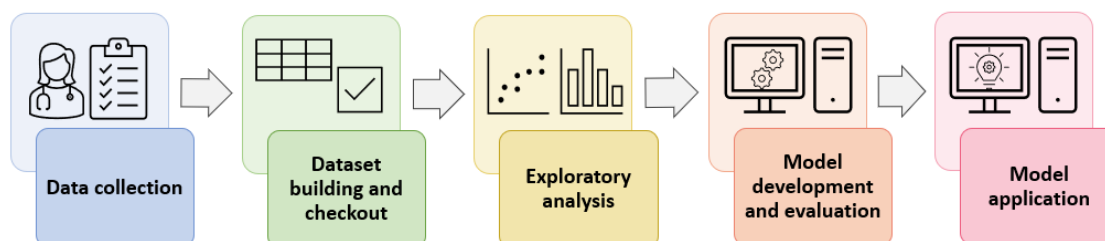


**Figure 2.1** General workflow of a pharmacometric analysis

First, PK and/or biomarker data relevant to the research questions of the projects was collected. Sources of data were e.g., clinical studies and clinical routine monitoring performed by project collaboration partners or literature research.

The collected data, also referred to as ‘raw data’ was then formatted to obtain datasets compatible with the NLME parameter estimation software NONMEM<sup>®</sup> (Icon Development Solutions, Ellicott City, MD, USA) [108] which was used throughout all modelling activities as well as for simulations. For this purpose, datasets in a comma separated values (csv) format were built in R/RStudio, containing table columns required for NONMEM<sup>®</sup>, such as subject identifier (ID), TIME, administered amount of the drug (AMT), dependent variable (DV), missing dependent variable (MDV), event (EVID) and event compartment (CMT). The dataset building was followed by a dataset checkout in which the datasets were controlled and if needed adjusted for the desired NONMEM-compatible structure, dataset management errors, inconsistencies and missing data.

In all projects, the final datasets were graphically and statistically analysed prior to be used for modelling and simulation. The graphical investigation of the data commonly comprised the exploration of PK concentration-time profiles as well as PK/PD relationships, PK/covariate relationships and correlations between covariates.

The quality-checked and appropriately formatted datasets were finally used to develop NLME PK or PK/PD models (see 2.2.2–2.2.5). The models were continuously evaluated during their development in order to assess if the data was adequately described (see 2.2.6). The final models which were judged as appropriate were then applied in simulations to address the research questions.

## 2.2.2 Nonlinear mixed-effects model components

After the graphical analysis of the formatted datasets, the NLME models were developed. The NLME model development consisted of three main steps: (1) The development of a structural submodel describing the behaviour of the PK or PD data originating from a typical individual, using population parameters, i.e., the fixed effects, (2) the addition of a statistical submodel including interindividual variability (IIV) and residual unexplained variability (RUV), i.e., the random effects, and finally, (3) the addition of a covariate submodel to explain parts of the random effects using individual characteristics [89].

### 2.2.2.1 Structural submodel

The structural submodel described the typical individual within the population, with their typical population parameters.

$$Y_{ij} = f(\phi_i, x_{ij}) \quad (\text{Eq. 2.1})$$

In Eq. 2.1,  $Y_{ij}$  was the observed dependent variable of the  $i^{\text{th}}$  individual corresponding at the  $j^{\text{th}}$  observation. The structural submodel was represented by the function ( $f$ ),  $\phi_i$  was the vector of model parameters (e.g., clearance) and  $x_{ij}$  describes known independent study design variables such as time or the administered dose.

### 2.2.2.2 Statistical submodel

The statistical submodel characterised different levels of variability around the typical model parameters.

#### *Interindividual variability*

IIV quantified the deviations of the best-fitting individual parameter values (i.e., empirical Bayes estimates EBEs) from the typical population parameter value. IIV was implemented using an exponential relationship (Eq. 2.2), assuming the model parameters to follow a log-normal distribution and thereby preventing them from taking negative, i.e., physiologically implausible values [89]. Eq. 2.2 shows  $\theta_{i,k}$ , which is the  $k^{\text{th}}$  model parameter of the  $i^{\text{th}}$  individual.  $\theta_k$  denotes the typical population value of the  $k^{\text{th}}$  parameter and  $\eta_{ik}$  is the individual random-effect parameter value which was assumed to follow a normal distribution with a mean of zero and the variance  $\omega_k^2$  of the random-effects parameter.

$$\theta_{ik} = \theta_k \cdot e^{\eta_{ik}} \quad \eta_{ik} \sim N(0, \omega_k^2) \quad (\text{Eq. 2.2})$$

For an easier interpretation, the interindividual variability was converted to the coefficient of variation (CV%), as shown in Eq. 2.3 [85,89].

$$CV, \% = \sqrt{e^{\omega_k^2} - 1} \cdot 100 \quad (\text{Eq. 2.3})$$

### ***Residual unexplained variability***

RUV describes the deviation of the observed dependent variable from the individual model predictions and can originate from e.g., (1) imprecision of the bioanalytical assay used to measure the dependent variable, (2) erroneous documentation of the independent variable (e.g., sampling time points) or (3) model misspecification.

The RUV models implemented in this work included the additive (*Paper I and II*) and the proportional (*Paper III*) model, depicted in Eq. 2.4 and Eq. 2.5, respectively.

$$Y_{ij} = f(\phi_i, x_{ij}) + \varepsilon_{add,ij} \quad \varepsilon \sim N(0, \sigma^2) \quad (\text{Eq. 2.4})$$

$$Y_{ij} = f(\phi_i, x_{ij}) \cdot (1 + \varepsilon_{prop,ij}) \quad \varepsilon \sim N(0, \sigma^2) \quad (\text{Eq. 2.5})$$

In both equations,  $\varepsilon_{ij}$  describes the discrepancy between the  $j^{\text{th}}$  observation of the  $i^{\text{th}}$  individual ( $Y_{ij}$ ) and the model prediction  $f(\phi_i, x_{ij})$ .  $\varepsilon_{ij}$  is assumed to be normally distributed, with a mean of zero and variance  $\sigma^2$ . In the additive RUV model (Eq. 2.4) the variance is assumed to be constant over the full range of model predictions. The proportional RUV model (Eq. 2.5) assumes a variance which is proportional to the magnitude of the model prediction, i.e., the variance increases with higher model predictions.

### **Covariate submodel**

As the final main step of the NLME model development, patient-, disease- or treatment-specific characteristics influencing the model parameters were assessed. First, correlations between individual parameters and covariates of interest were graphically evaluated. After the graphical evaluation, different relationships between the characteristics and PK parameters were tested and kept in the model as covariates if they led to a substantial reduction of unexplained IIV [89]. Tested covariates were continuous covariates, such as body weight (all papers), age, CBG and albumin (*Paper I and Paper II*) as well as age group as a dichotomous categorical covariate (*Paper I*).

For the continuous covariates, a power relationship between the covariate effect and the parameter was assessed, as depicted in Eq. 2.6.  $\theta_{k,cov}$  describes the value for parameter  $k$  for a specific value of the continuous covariate  $cont\_cov$ . The relative impact was centred to the median covariate value  $cont\_cov_{med}$ , and the power exponent  $\theta_{cov}$ . The power exponent was either estimated or fixed to 0.75 and 1 for quantifying the body weight effect on clearance and on volume of distribution parameters,

respectively. These fixed power exponents are commonly applied in theory-based allometric scaling which aims at relating body function (here: model parameter) to body size [5].

Another covariate relationship evaluated for continuous covariates was a fractional change of the parameter in question from the median covariate value (Eq. 2.7).

For the two values of the dichotomous categorical covariate (*cat\_cov1* and *cat\_cov2*) two different parameter values  $\theta_{k,cov}$  were estimated (Eq. 2.8 and Eq. 2.9).

$$\theta_{k,cov} = \theta_k \cdot \left( \frac{cont\_cov}{cont\_cov_{med}} \right)^{\theta_{cov}} \quad (\text{Eq. 2.6})$$

$$\theta_{k,cov} = \theta_k \cdot (1 + \theta_{cov} \cdot (cont\_cov - cont\_cov_{med})) \quad (\text{Eq. 2.7})$$

$$\theta_{k,cov1} = \theta_{k,cat\_cov1} \quad (\text{Eq. 2.8})$$

$$\theta_{k,cov2} = \theta_{k,cat\_cov2} \quad (\text{Eq. 2.9})$$

### 2.2.3 Parameter estimation

For all NLME models developed in this work, maximum likelihood estimation was used to estimate the most likely set of model parameters ( $\theta, \omega^2, \sigma^2$ ), both on the population and individual level, given the observed data  $Y_{obs,ij}$  (Eq. 2.10). The variable  $p$  denotes the corresponding probability density function. The objective function value (OFV) is defined as minus twice the natural logarithm of the likelihood  $\mathcal{L}$  (Eq. 2.11). During the estimation process the parameters were changed towards a maximised log-likelihood and thus a minimised OFV. A lower OFV therefore served as one of the criteria to determine the most adequate models.

$$\mathcal{L}(\theta, \omega^2, \sigma^2 | Y_{obs,ij}) = p(Y_{obs,ij} | \theta, \omega^2, \sigma^2) \quad (\text{Eq. 2.10})$$

$$OFV = -2\mathcal{L}\mathcal{L} = -2 \cdot \log(\mathcal{L}(\theta, \omega^2, \sigma^2 | Y)) \quad (\text{Eq. 2.11})$$

Since the analytical computation of the likelihood is not possible for most NLME models, the OFV is approximated using numerical methods. NONMEM<sup>®</sup> offers various estimation methods for this purpose [109,110]. One commonly used method is the first-order conditional estimation with interaction (FOCE-I) which was applied in *Paper I* and *Paper III*. FOCE-I uses first-order Taylor series approximation to linearise the model by conditioning on  $\eta$ , and delivers population parameter estimates as well as individual parameter estimates, also referred to as EBEs, in a single step [89]. The interaction in FOCE-I accounts for dependencies between interindividual random-effects ( $\eta$ ) and residual random-effects ( $\varepsilon$ ) which usually occur when proportional RUV models are applied [111,112].

The Laplacian method is another conditional estimation method which uses second derivatives with respect to  $\eta$  [109,113,114]. Since this estimation method can be used for categorical data [115], it was evaluated in *Paper II* to consider observations below the LLOQ (see section 2.2.4).

Furthermore, so-called expectation-maximisation (EM) algorithms, such as stochastic approximation expectation maximisation (SAEM) or importance sampling (IMP), can be applied for complex PK/PD models [113,116]. EM methods are characterised by exact likelihood maximisation achieved by calculating the expected likelihood given the current parameter estimates (E-step) and a subsequent computation of new parameter estimates maximising the likelihood, given the expected likelihood from the E-step (M-step). These two steps are repeated until a stable OFV is obtained [113]. In the E-step of the IMP method, the conditional mean and variance of  $\eta$  are evaluated by Monte Carlo sampling. The parameter estimates are then updated from the individuals' conditional parameters by a single iteration in the M-step [113]. In *Paper II*, the importance sampling assisted by mode *a posteriori* (IMPMPAP) estimation was evaluated. Here, conditional modes and conditional first order variances were evaluated, as in the FOCE-I method, called mode *a posteriori* (MAP) estimation [109]. These were then used as parameters to the proposal density for the Monte Carlo IMP sampling step [109,116].

#### **2.2.4 Modelling data below the lower limit of quantification**

For handling observations below the lower limit of quantification (LLOQ), two commonly applied approaches were used: The so-called M1 method used in *Paper I* and in *Paper III* and the M3 method in *Paper II*.

Using the M1 method, all observations below the LLOQ (BLQ) are censored, i.e., they are not included in the maximum likelihood estimation [117,118]. This simple approach is usually applied when a low fraction of observations is below the LLOQ. The disadvantage of the M1 method is an overprediction of concentrations close to or below the LLOQ and a potential bias of parameter estimates [119]. It is therefore recommended to choose an approach which also considers BLQ concentrations if the BLQ fraction exceeds 10%.

By applying the M3 method, all observations, including the ones below the LLOQ, are considered in the estimation process, with the likelihood for the BLQ observations being assessed [117]. Therefore, using the M3 method results in more accurate parameter estimation, compared to M1.

#### **2.2.5 Modelling baseline data**

In *Paper I*, a cortisol PK model was developed. To account for the endogenous cortisol baseline concentrations before and after the hydrocortisone administration, a baseline modelling approach was applied. In *Paper II*, baseline models were evaluated to account for the endogenous concentrations of

the biomarker 17-OHP. In Dansirikul *et al.* [120], four different baseline modelling approaches (B1-B4) are presented of which the B1 and the B2 method were evaluated in both papers.

$$baseline_i = baseline \cdot e^{\eta_i} \quad (\text{Eq. 2.12})$$

$$baseline_i = baseline_{i,obs} \cdot e^{\eta_i^{RUV}} \quad (\text{Eq. 2.13})$$

Using the B1 method, which is considered the gold standard, a population baseline (*baseline*, Eq. 2.12) was estimated. The individual baseline (*baseline<sub>i</sub>*) was then derived considering IIV ( $\eta_i$ ) in an exponential IIV model, thereby assuming a log-normal distribution of the baseline [120].

In the B2 method, the individual *baseline<sub>i</sub>* is informed by the individual baseline observations (*baseline<sub>i,obs</sub>*) and the IIV corresponding to the RUV ( $\eta_i^{RUV}$ , Eq. 2.13). An initialisation of the cortisol and 17-OHP compartments with *baseline<sub>i</sub>* was evaluated [120].

### 2.2.6 Model evaluation

The model evaluation was iteratively performed during model development to identify the model best describing the data. The main diagnostic criteria used in this work were OFV (for nested models) or Akaike Information Criterion (AIC), parameter plausibility and parameter precision, determined by relative standard errors (RSE) or confidence intervals (CI). In *Paper I*, the CIs were obtained by performing sampling importance resampling (SIR), an evaluation technique which, opposed to the ‘gold standard’ bootstrapping technique [121], does not require time-consuming estimation and is suitable for models based on heterogeneous, unbalanced or small datasets [122,123].

Applied graphical model evaluations were goodness-of-fit (GOF) plots and visual predictive checks (VPCs). In the basic GOF [85,89] plots, population predictions as well as individual predictions were graphically compared to the observations and conditional weighted residuals were investigated versus time and population predictions to evaluate the models for biases hinting at e.g., an inadequate number of compartments or an inappropriate RUV model. The VPCs [124] were based on stochastic simulations (n=1000) of the model predictions which were, together with the observations, plotted versus time. The simulated predictions and the observations were then compared by investigating their lower (e.g., 5<sup>th</sup>), median and upper (e.g., 95<sup>th</sup>) percentiles as well as the 95% CIs around the simulated percentiles.

---

## 2.3 Relationship between plasma and dried blood spot cortisol concentrations (Paper I)

In *Paper I*, the aim was to understand the quantitative relationship between cortisol concentrations in plasma and in DBS as DBS sampling represents a promising alternative to plasma sampling in CAH monitoring. Thus, this relationship was graphically explored and subsequently leveraged in a NLME modelling and simulation analysis to fully characterise the binding behaviour of cortisol, including association with RBCs.

### *Graphical exploration of plasma versus DBS cortisol concentrations*

The relationship between plasma cortisol concentrations (n=106) obtained during the phase III Alkindi<sup>®</sup> study (see 2.1.3.1) and simultaneously sampled DBS cortisol concentrations (see 2.1.3.2) was graphically explored. Concentration–time profiles of the data, plasma versus DBS cortisol concentrations, and the plasma/DBS concentration ratio as a function of the cortisol concentrations were evaluated.

### *Cortisol PK model development*

A co-authored, previously published semi-mechanistic cortisol PK model [98], based on healthy adult (cortisol biosynthesis suppressed by Dex) and paediatric patient data from the Alkindi<sup>®</sup> studies and describing saturable cortisol binding to CBG and linear binding to albumin, was used as a starting point for the modelling analysis. The published model included a constant cortisol baseline estimate for the adult data, whereas for the paediatric cortisol data, the B2 method for modelling baseline data was applied (see 2.2.5) using the individual measured pre-dose concentration [98]. Body weight was included as a covariate using theory-based allometric scaling with fixed exponents of 0.75 and 1 on the clearance parameters (CL and Q) and on the volumes of distribution ( $V_c$  and  $V_p$ ), respectively, to account for body size differences within the dataset pooling adults and paediatrics. The dataset of this published model was then further extended with the DBS cortisol concentrations corresponding to the already included plasma cortisol concentrations. The implemented cortisol binding processes were extended by an assumed linear association of cortisol with RBCs.

### *Simulations of cortisol binding in whole blood*

The extended cortisol PK model, characterising the binding behaviour of cortisol in full blood, was then applied in deterministic simulations, i.e., simulations excluding the IIV estimated in the model [84]. The aim of these simulations was to determine the typical fractions of free cortisol as well as of all cortisol binding species, i.e., fraction bound to CBG, to albumin and associated with RBCs, in paediatric CAH patients. The fractions were simulated separately for the two age groups of young children/infants

and neonates, over the respective total cortisol blood concentration ranges which were observed in the Alkindi® study. The typical simulated individuals representing the two age groups were virtually dosed with 7 mg HC and the concentrations of the cortisol binding species and whole blood cortisol concentrations were simulated over 6 h.

## 2.4 Target morning dried blood spot 17 $\alpha$ -hydroxyprogesterone concentrations for paediatric congenital adrenal hyperplasia patients (Paper II)

The aim of *Paper II* was to derive a target morning DBS 17-OHP concentration range for paediatric CAH patients by developing a PK/PD model linking plasma cortisol concentrations to DBS 17-OHP concentrations and applying the model in simulations. The different steps of the modelling and simulation analysis framework are depicted in Figure 2.2 and described in the sections below.

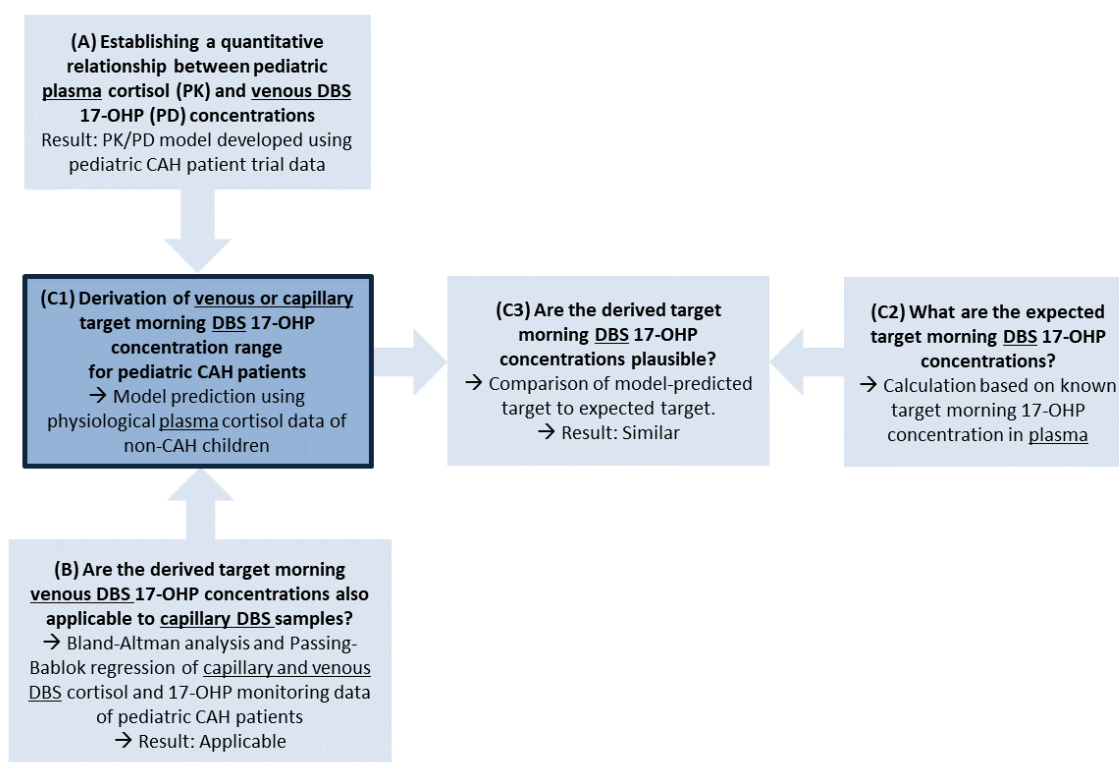


**Figure 2.2** Modelling and simulation framework to derive target morning concentration range for the biomarker 17 $\alpha$ -hydroxyprogesterone (17-OHP) sampled from dried blood spots (DBS) in paediatric congenital adrenal hyperplasia (CAH) patients, in clinical routine.

For the goal of this analysis, the derivation of the target range (dark blue box C1), a pharmacokinetic/pharmacodynamic (PK/PD) model, quantitatively linking plasma cortisol and venous DBS 17-OHP, was developed (A). The applicability of the derived target range, which was based on

venous DBS data, to capillary DBS sampling was shown in a Bland-Altman analysis and Passing-Bablok regression (B). To check for plausibility (C3), the derived target range was compared to a calculated expected target range (C2).

### ***Exploratory graphical analysis and PK/PD model development***

To determine the relationship between paediatric plasma cortisol and venous DBS 17-OHP concentrations (Figure 2.2 A), young children and infant data from the phase 3 trial for the paediatric hydrocortisone formulation Alkindi® (see 2.1.3.1) was used as well as the additionally sampled venous DBS cortisol and 17-OHP concentrations of the same patients (see 2.1.3.2). The DBS 17-OHP concentrations were evaluated as a function of time and of plasma cortisol concentrations.

The PK/PD model development was based on the paediatric cortisol PK model developed in *Paper I* and was performed with a so-called sequential approach [125,126], i.e., the individual PK model parameters of the PK model were included into the model dataset and only the PD parameters were estimated. Since 22 (25%; 22.5% in young children and 35.3% in infants) out of 88 venous DBS 17-OHP concentrations were below the LLOQ (1.3 nmol/L), the M3 method (see 2.2.4) was applied.

### ***Deriving target morning DBS 17-OHP concentrations in simulations***

Stochastic simulations (n = 1000), i.e., simulations including the IIV [84], were performed applying the developed PK/PD model (Figure 2.2 C1). Physiological, i.e., healthy, circadian cortisol concentration-time profiles from 28 children (see 2.1.2) were thereby used as the PK input in the model dataset to simulate corresponding physiological DBS 17-OHP concentrations over 48 hours. The simulation output of interest was the physiological DBS 17-OHP concentrations simulated between 6 and 8 a.m. in the morning, representing the monitoring time range of interest, corresponding to the time before the morning dose. The 17-OHP compartment was initialised with the median 17-OHP baseline, i.e., morning concentrations observed in the young children and infants from the Alkindi® trial.

In general, target 17-OHP concentrations are recommended to be approximately 3-5 times higher than physiological 17-OHP concentrations since the suppression of 17-OHP down to physiological concentrations leads to an increased risk for adverse events caused by the administered glucocorticoid [14,21]. Thus, as a next step, the simulated physiological morning concentrations of 17-OHP in DBS were multiplied by 3 to 5 to approximate a DBS 17-OHP target morning concentration range.

### ***Plausibility check of the derived target morning DBS 17-OHP concentration range***

The plausibility of the simulation-derived DBS 17-OHP target morning concentration range was assessed (Figure 2.2 C3) by a simple calculation of an expected DBS 17-OHP target morning range (Figure 2.2 C2). Apart from DBS 17-OHP concentrations in young children and infants (see 2.1.3.2), also plasma 17-OHP concentrations at baseline (n=12) were quantified in parallel. The plasma/DBS ratio from these 17-OHP samples, together with the plasma 17-OHP target morning concentration range

known from literature [13], was used for the calculation of the expected morning DBS 17-OHP target range, to which the simulation-derived target was then compared.

### ***Investigating the agreement between capillary and venous DBS measurements***

During CAH therapy monitoring, either venous or capillary DBS samples can be obtained in paediatric patients, whereas the DBS data used for the PK/PD analysis was venous DBS data only. Therefore, the comparability between capillary and venous cortisol and 17-OHP DBS concentrations, obtained in clinical routine at the Charité-Universitätsmedizin Berlin (see 2.1.3.3), was assessed in two kinds of analyses which are commonly applied to investigate the agreement between two measurement methods, i.e., in a (1) Bland-Altman analysis [127] and (2) Passing-Bablok regression analysis [128] (Figure 2.2 B).

In the Bland-Altman analysis, the differences between the capillary and venous concentrations were plotted versus the concentration mean of the two measurement methods. Since the concentrations in the investigated dataset showed a large range, the relative method differences, i.e., differences divided by mean in %, were presented. The relative difference range, in which agreement between the two methods is determined, was defined as the mean difference  $\pm 1.96$ \*standard deviation (SD) [127,129].

In the Passing-Bablok regression, venous versus capillary DBS concentrations were visualised in scatter plots, which included a regression line, a 95% confidence interval (CI) of its intercept and slope as well as a regression function. If the intercept and slope of the line of identity lay within the CI of the regression, no relevant constant and proportional difference was concluded between the two examined methods, respectively [128,130].

## **2.5 Rational dexamethasone dose in prenatal congenital adrenal hyperplasia therapy (Paper III)**

The aim of the modelling and simulation analysis in *Paper III* was to suggest a lower, rational Dex dose in prenatal CAH therapy which reduces the risk for adverse events for the pregnant women as well as their unborn children with CAH, while maintaining efficacy. The different steps of the modelling and simulation analysis workflow are depicted in Figure 2.3.

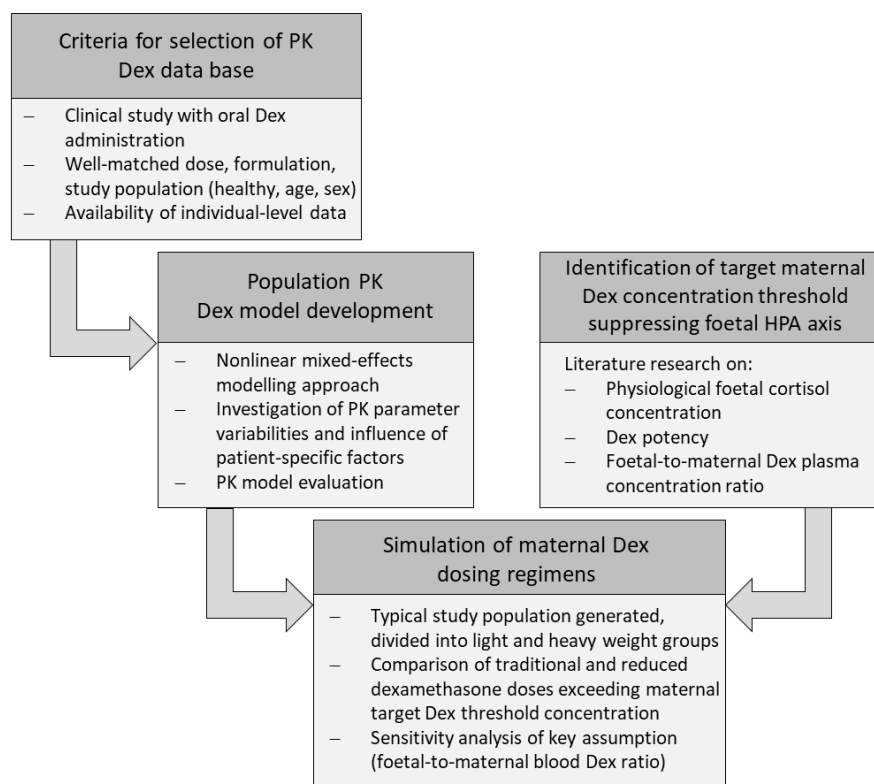


**Figure 2.3** Modelling and simulation analysis workflow in *Paper III*. PK: Pharmacokinetic(s), Dex: Dexamethasone.

### ***Data selection and Dex PK model development***

First, data for the development of a PK model needed to be selected. Literature research was conducted to find a matching clinical study with perorally administrated Dex. Selection criteria were Dex doses in a similar range as administered in prenatal CAH therapy, a healthy adult study population, preferably including women, within an age range which is realistic for pregnancy as well as the availability of data on an individual level. Next, a NLME model including IIV, RUV and covariates was developed and evaluated based on the selected data.

### ***Identification of target Dex concentration threshold***

Moreover, an extensive literature search was performed to identify the foetal target Dex concentration threshold leading to suppression of the foetal HPA axis. Since no such target was known, the concentration threshold was calculated from physiological foetal cortisol concentrations and the Dex/cortisol potency ratio retrieved in literature. The modelled Dex PK concentrations were assumed to correspond to maternal Dex concentrations during prenatal CAH therapy. Thus, literature was searched for foetal-to-maternal plasma Dex concentration ratios to calculate the corresponding maternal target Dex concentration threshold.

### ***Simulation of Dex dosing regimens***

Finally, the developed Dex PK model and the results from the literature search on the target threshold were applied in stochastic simulations (n=1000), including the estimated IIV, of maternal Dex dosing regimens. A typical study population representing pregnant women (n=124) was generated, including a ‘light’ weight group of 50-72 kg and a ‘heavy’ weight group of 73-95 kg. In the simulations, half of both weight groups received the traditional dose of 20 µg/kg/day whereas the other half received reduced doses of 5, 6, 7.5, 9 or 10 µg/kg/day, divided into three single doses every 8 h. The subjects were dosed according to the group’s median body weight (61 and 84 kg, respectively). The dosing regimen with the lowest Dex dose and with the 10<sup>th</sup> percentile of the maternal concentration-time profiles exceeding the maternal target threshold at steady state was judged as rational and effective. Furthermore, a sensitivity analysis was conducted to assess the impact of the assumed foetal-to-maternal plasma Dex concentration ratio.

## **2.6 Software**

Throughout all projects R (version 3.6.0 in *Paper I* and *Paper III* and version 4.0.2 in *Paper II*) and RStudio (version 1.3.1056) were used for dataset formatting, graphical analysis, generation of model diagnostic plots (GOF, VPC) and for generating figures presenting modelling and simulation results. Moreover, the deterministic simulation in *Paper I* was conducted in R. The NLME model development in all projects as well as the stochastic simulations in *Paper II* and *Paper III* were conducted with NONMEM® (version 7.4.3), using Perl speaks NONMEM (Uppsala University, Sweden, version 3.4.2 in *Paper I* and *Paper III* and version 4.7.0 in *Paper II*) [131] and the workbench Pirana (version 2.9.6) [132]. Parts of the model estimations, evaluations and simulations in all projects were performed on the high-performance computing cluster ‘Curta’ [133].

## **3 Research articles**

### **3.1 Paper I: Exploring dried blood spot cortisol concentrations as an alternative for monitoring pediatric adrenal insufficiency patients: A model-based analysis**

## Equity Ratio Statement

### Paper I

**Title of the manuscript:**

“Exploring dried blood spot cortisol concentrations as an alternative for monitoring pediatric adrenal insufficiency patients: A model-based analysis.”

**Journal**           Frontiers in Pharmacology  
Volume 13, Pages 1-8 (2022)

**Authorship**     First author

**Status**           Published

DOI: <https://doi.org/10.3389/fphar.2022.819590>

*Reprinted with permission from Frontiers in Pharmacology.*

**Own contribution**

- Data set modification and checkouts
- All modelling and simulation activities, including PK model development, model evaluation, and simulations
- Interpretation of the results, including literature research related to interpretation of the results
- Drafting of all parts of the manuscript
- Creation of all figures and tables
- Adaptation of the manuscript according to the reviewers’ and editor’s comments



# Exploring Dried Blood Spot Cortisol Concentrations as an Alternative for Monitoring Pediatric Adrenal Insufficiency Patients: A Model-Based Analysis

Viktoria Stachanow<sup>1,2</sup>, Uta Neumann<sup>3</sup>, Oliver Blankenstein<sup>3,4</sup>, Davide Bindellini<sup>1,2</sup>, Johanna Melin<sup>1,2</sup>, Richard Ross<sup>5</sup>, Martin J. Whitaker<sup>5</sup>, Wilhelm Huisinga<sup>6</sup>, Robin Michelet<sup>1\*†</sup> and Charlotte Kloft<sup>1†</sup>

## OPEN ACCESS

### Edited by:

Catherine M. T. Sherwin,  
Wright State University, United States

### Reviewed by:

Gregory Thomas Knipp,  
Purdue University, United States  
Kit Wun Kathy Cheung,  
Genentech, Inc., United States

### \*Correspondence:

Robin Michelet  
robin.michelet@fu-berlin.de

<sup>†</sup>These authors share senior  
authorship

### Specialty section:

This article was submitted to  
Obstetric and Pediatric Pharmacology,  
a section of the journal  
Frontiers in Pharmacology

**Received:** 21 November 2021

**Accepted:** 26 January 2022

**Published:** 17 March 2022

### Citation:

Stachanow V, Neumann U,  
Blankenstein O, Bindellini D, Melin J,  
Ross R, Whitaker MJ, Huisinga W,  
Michelet R and Kloft C (2022) Exploring  
Dried Blood Spot Cortisol  
Concentrations as an Alternative for  
Monitoring Pediatric Adrenal  
Insufficiency Patients: A Model-  
Based Analysis.  
*Front. Pharmacol.* 13:819590.  
doi: 10.3389/fphar.2022.819590

<sup>1</sup>Department of Clinical Pharmacy and Biochemistry, Institute of Pharmacy, Freie Universität Berlin, Berlin, Germany, <sup>2</sup>Graduate Research Training Program PharMetriX, Berlin, Germany, <sup>3</sup>Pediatric Endocrinology, Charité-Universitätsmedizin, Berlin, Germany, <sup>4</sup>Labor Berlin, Charité Vivantes GmbH, Berlin, Germany, <sup>5</sup>Diurnal Limited, Cardiff, United Kingdom, <sup>6</sup>Institute of Mathematics, Universität Potsdam, Potsdam, Germany

Congenital adrenal hyperplasia (CAH) is the most common form of adrenal insufficiency in childhood; it requires cortisol replacement therapy with hydrocortisone (HC, synthetic cortisol) from birth and therapy monitoring for successful treatment. In children, the less invasive dried blood spot (DBS) sampling with whole blood including red blood cells (RBCs) provides an advantageous alternative to plasma sampling. Potential differences in binding/association processes between plasma and DBS however need to be considered to correctly interpret DBS measurements for therapy monitoring. While capillary DBS samples would be used in clinical practice, venous cortisol DBS samples from children with adrenal insufficiency were analyzed due to data availability and to directly compare and thus understand potential differences between venous DBS and plasma. A previously published HC plasma pharmacokinetic (PK) model was extended by leveraging these DBS concentrations. In addition to previously characterized binding of cortisol to albumin (linear process) and corticosteroid-binding globulin (CBG; saturable process), DBS data enabled the characterization of a linear cortisol association with RBCs, and thereby providing a quantitative link between DBS and plasma cortisol concentrations. The ratio between the observed cortisol plasma and DBS concentrations varies highly from 2 to 8. Deterministic simulations of the different cortisol binding/association fractions demonstrated that with higher blood cortisol concentrations, saturation of cortisol binding to CBG was observed, leading to an increase in all other cortisol binding fractions. In conclusion, a mathematical PK model was developed which links DBS measurements to plasma exposure and thus allows for quantitative interpretation of measurements of DBS samples.

**Keywords:** adrenal insufficiency, cortisol, dried blood spots, pediatrics, pharmacokinetics, binding, association, red blood cells

## INTRODUCTION

Congenital adrenal hyperplasia (CAH) is a group of rare autosomal recessive diseases, which are characterized by largely decreased or absent cortisol biosynthesis. In 90–95% of cases, a deficiency of the 21-hydroxylase enzyme is the cause for CAH (Podgórski et al., 2018; Balsamo et al., 2020). A major complication in patients is an adrenal crisis which may even lead to death. Other symptoms of CAH include virilization, hirsutism, premature adrenarche, and premature ending of longitudinal growth due to an overproduction of androgens and possible life-threatening electrolyte imbalance due to the underproduction of mineralocorticoids (Merke and Bornstein, 2005).

The treatment of CAH requires life-long cortisol replacement therapy. The recommended glucocorticoid for pediatric CAH patients is hydrocortisone (HC, name of synthetic cortisol) due to its short half-life and lower risk for adverse events (Oprea et al., 2019). To mimic the circadian rhythm of cortisol biosynthesis, oral administration of 10–15 mg/m<sup>2</sup> hydrocortisone daily is recommended, divided into two to three doses, and with the highest dose in the morning (Kamoun et al., 2013; Khattab and Marshall, 2019; Dabas et al., 2020). It is essential to monitor cortisol replacement in CAH patients frequently and adjust dosages according to the patients' individual needs, based on the body surface area, laboratory parameters, and symptoms evaluation (Bornstein et al., 2016) as too high or too low cortisol exposure can cause adverse events, such as Cushing's syndrome, and or lead to an adrenal crisis (Merke and Bornstein, 2005).

Dried blood spot (DBS) samples have been used since the 1960s to perform newborn screenings for diseases such as phenylketonuria (Moat et al., 2020). Currently, because of technological development allowing for more specific and sensitive specimen analysis, DBS has been exploited to monitor CAH patients (Moat et al., 2020). DBS sampling consists of dropping small volumes of whole blood drops (approximately 20 µl) collected via a fingerpick on a cellulose-based sampling paper. Therefore, this sampling procedure is simpler and less invasive than traditional plasma sampling. It is thus of great advantage for the pediatric population because of their vulnerability and limited blood volume (Qasrawi et al., 2021). DBS sampling provides additional benefits such as higher analyte stability, allowing storage at room temperature, and easy transportation (Edelbroek et al., 2009; Wilhelm et al., 2014).

To evaluate the applicability of DBS sampling, it is essential to understand the relationship between cortisol DBS concentrations, and plasma concentrations. Cortisol has complex PK with saturable binding to corticosteroid-binding globulin (CBG) and linear binding to albumin which previously has been identified using a nonlinear mixed-effects (NLME) HC PK model [(Melin et al., 2017; Michelet et al., 2020)]. Moreover, cortisol is known to associate with RBCs (Lentjes and Romijn, 1999). This is of special interest for interpreting DBS samples as these are whole blood samples containing RBCs. The aim of this analysis was to explore and quantify the relationship between venous DBS cortisol concentrations and plasma cortisol

concentrations by characterizing the association of cortisol with RBCs; which is the first step towards the use and interpretation of DBS samples for monitoring pediatric CAH patients.

## METHODS

### Data

A previously published NLME HC PK model based on cortisol plasma data from healthy adults and pediatric patients (Melin et al., 2017; Michelet et al., 2020) served as the starting point for our analysis. The model leveraged data from 1) rich plasma sampling ( $n = 1,482$  total cortisol concentrations) in a phase 1 study (Whitaker et al., 2015) with 30 healthy adult subjects, whose cortisol biosynthesis was suppressed with dexamethasone, and who received a single dose of 0.5 mg up to 20 mg of the pediatric HC formulation Alkindi<sup>®</sup> (hydrocortisone granules in capsules for opening) (Diurnal Europe B.V., Netherlands).

Additionally, the model leveraged 2) sparse phase 3 cortisol plasma data from 24 pediatric adrenal insufficiency (AI) patients receiving their regular HC-morning dose of Alkindi<sup>®</sup>, ranging from 1 to 4 mg (Neumann et al., 2018; Melin et al., 2020; Michelet et al., 2020). The pediatric patients were divided into three different cohorts according to their age groups: Young children ( $n = 12$ , 2–6 years), infants ( $n = 6$ , 28 days–2 years), and term neonates ( $n = 6$ : 0–28 days). The pediatric total cortisol plasma concentrations were measured prior to dose and 1 and 4 h post-dose in all cohorts. In neonates and infants, the sampling was ethically limited to these 3 times due to the lower total blood volume, whereas in the children cohort, blood sampling at 2 additional times between 30 and 90 h post-dose was allowed as well as at time to  $C_{\min}$  ( $t_{\min}$ ).

To expand this model, simultaneously collected venous total cortisol DBS samples, obtained from the pediatric patients in the phase 3 study, were included. Both total cortisol concentrations in plasma (Whitaker et al., 2015; Melin et al., 2017; Michelet et al., 2020) and in DBS ( $n = 106$  each) were quantified by liquid chromatography with tandem mass spectrometry detection (LC-MS/MS). Linearity, accuracy, and precision were tested for DBS cortisol quantification with the respective acceptance criteria being met according to the guideline on bioanalytical method validation of the European Medicines Agency (European Medicines Agency, 2012).

### Graphical Evaluation of Plasma Versus DBS Cortisol Concentrations

The relationship between the pediatric total cortisol concentrations in plasma and DBS was graphically evaluated based on concentration–time profiles, plotting plasma versus DBS cortisol concentrations and graphically investigating the plasma/DBS ratio as a function of the cortisol concentration, and the cortisol concentration dependency of the plasma/DBS cortisol concentration ratio. The graphical analysis was performed using R (3.6.0) and R Studio (1.3.1056) (R Core Team, 2019; RStudio Team, 2020).

## Pharmacokinetic Model Development and Evaluation

The previously published NLME HC PK model, based on adult and pediatric plasma cortisol data, was a two-compartment PK model describing saturable absorption (Michaelis–Menten type) and a plasma protein binding model considering both nonlinear binding to CBG and linear binding to albumin. An underlying constant cortisol baseline was estimated for the adult data, whereas for the pediatric cortisol data, the baseline was modeled using the individual measured pre-dose concentration. For baseline cortisol concentrations below the lower limit of quantification (LLOQ), a baseline concentration was estimated with the same interindividual variability as the observed pre-dose concentrations above LLOQ (Melin et al., 2020; Michelet et al., 2020).

Body weight was included as an influential factor using theory-based allometric scaling with fixed exponents of 0.75 and 1 on the clearance parameters (CL and Q) and on the volumes of distribution ( $V_c$  and  $V_p$ ), respectively, to account for differences in the body size within the pooled dataset. No other covariates besides body weight were evaluated in the structural plasma PK model. Interindividual variability (IIV) was modeled, assuming the structural model parameters to follow a log-normal distribution, and residual unexplained variability (RUV) was modeled following a proportional residual error model (Melin et al., 2020; Michelet et al., 2020).

Based on this PK model structure and modeling approach, the published HC PK model was further developed by extending the underlying data with the pediatric DBS cortisol concentrations. Implemented cortisol binding processes were extended by the association of cortisol with RBCs which were all assumed to contain hemoglobin. For the model development, NONMEM (7.4.3, ICON, Dublin, Ireland, Development Solutions, Ellicott City, MD, United States) and Perl-speaks-NONMEM (3.4.2, Uppsala University, Uppsala, Sweden), embedded in the workbench Pirana (version 2.9.6), were used (Bauer, 2010; Keizer et al., 2013). The appropriateness of the PK model was evaluated based on standard model diagnostics, for example, the difference of the objective function value (dOFV, best fit = maximum likelihood = minimum OFV) and goodness-of-fit (GOF) plots (Mould and Upton, 2012, 2013). Model performance was evaluated using visual predictive checks (VPCs,  $n = 1,000$  simulations) (Bergstrand et al., 2011) (see the **Supplementary Material**) and sampling importance resampling (SIR, with 1,000, 1,000, 1,000, 2,000, and 2,000 samples and 200, 400, 500, 1,000, and 1,000 resamples) (Dosne et al., 2017).

## Simulation of Cortisol Binding Species

The final and evaluated PK model allowed simulating the fractions of the three different binding/association species of cortisol (specific binding to CBG, non-specific binding to albumin, and non-specific association with RBCs) and the unbound cortisol fraction. One individual representing the children/infants age group and one individual representing neonates were virtually dosed with 7 mg HC each; the concentrations of the binding species and cortisol whole blood concentrations were simulated over 6 h [deterministic simulations using NONMEM (7.4.3)].

## RESULTS

### Data

Of the pediatric plasma and DBS concentrations, 17.9% ( $n = 19$  of 106, LLOQ = 14.1 nmol/L) and 0.94% ( $n = 1$  of 106, LLOQ = 1.8 nmol/L) were below the LLOQ, respectively. All adult total cortisol plasma concentrations were above the LLOQ. As in the previously published model, all BLQ observations were discarded so that 87 pediatric plasma samples and 105 pediatric DBS samples remained for the subsequent graphical analysis, modeling, and simulation analysis.

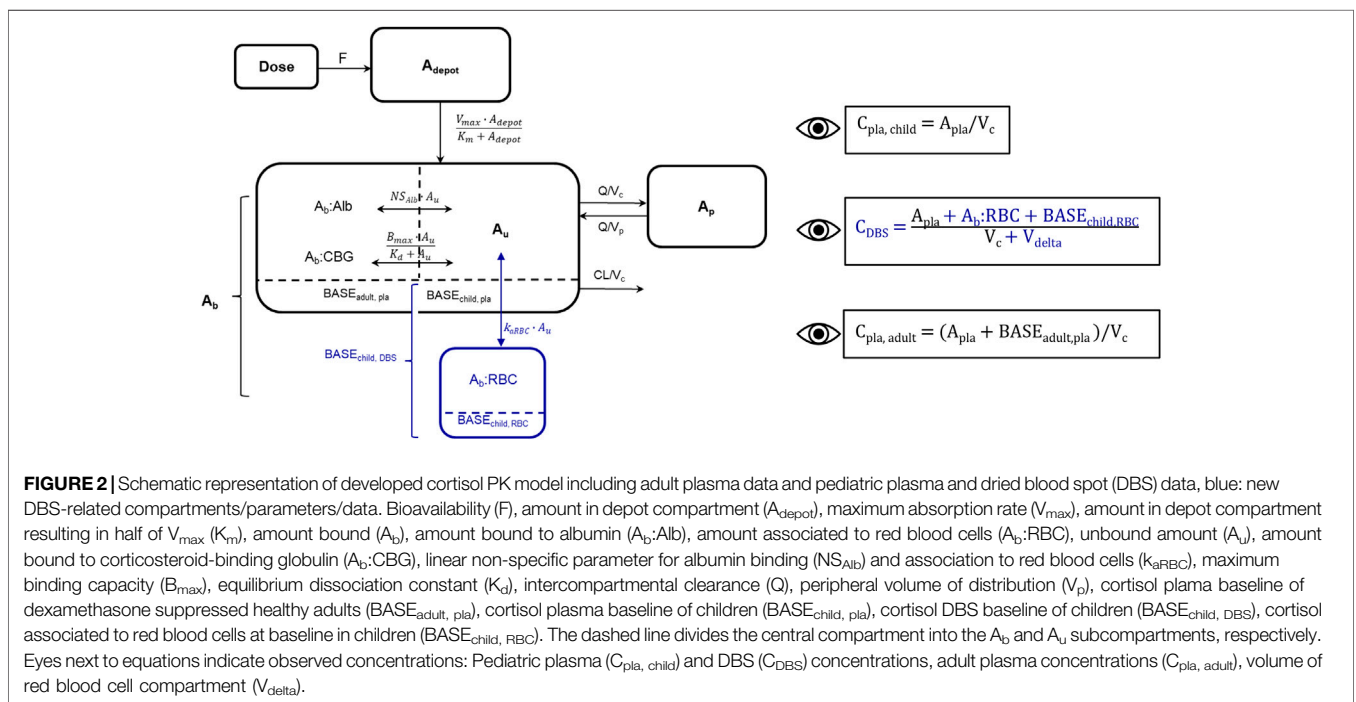
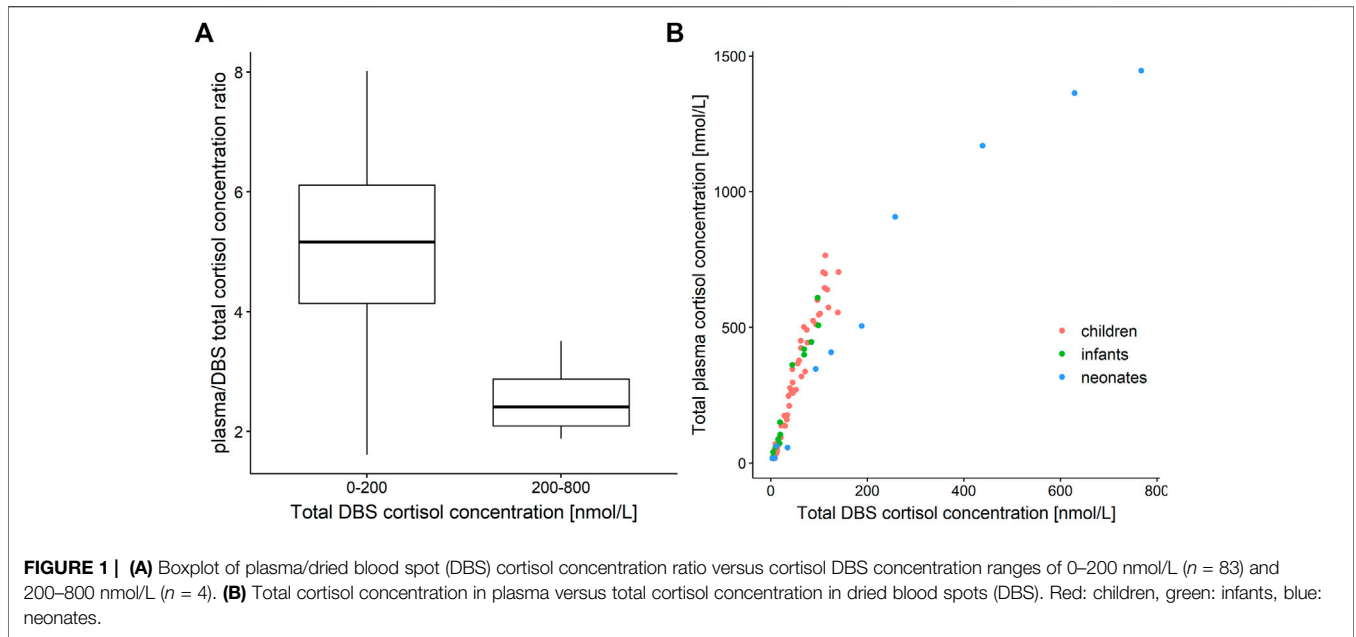
### Graphical Evaluation of Plasma Versus DBS Cortisol Concentrations

Measured plasma cortisol concentrations were considerably higher than DBS cortisol concentrations with ratios with a very high variability, ranging from approximately 2 to 8 (**Figure 1A**). The relationship between total cortisol concentrations in plasma and DBS was nonlinear (**Figure 1B**), where the plasma/DBS cortisol concentration ratio decreased with higher cortisol concentrations, reaching the lowest ratio at the highest concentrations. Regarding the ratio and slope, the data shown in **Figure 1B** could be divided into 2 groups, with DBS concentrations ranging from 0 to 200 nmol/L and from 200 to 800 nmol/L. When observing cortisol DBS concentrations from 0 to 200 nmol/L ( $n = 83$ , **Figure 1A**), the plasma/DBS cortisol concentration ratio ranges widely from 1.62 up to 8.01, with a median of 5.17. With higher concentrations ( $n = 4$ ), which were only observed in the neonatal age group, the concentration ratio decreases to a median value of 2.41 (range 1.88–3.51). The comparison of DBS concentration ranges from 0 to 100 nmol/L and from 100 to 200 nmol/L showed no significant difference in plasma/DBS cortisol concentration ratios.

### Pharmacokinetic Model Development and Evaluation

Since the association of cortisol with RBCs is described as a linear process in the literature (Lentjes and Romijn, 1999), a linear association constant  $K_{aRBC}$  was estimated. An additional compartment describing cortisol bound to RBCs was implemented, and an additional apparent volume ( $V_{\text{delta}}$ ) was estimated, with the whole blood volume being defined as the sum of  $V_c$  and  $V_{\text{delta}}$ . Similarly, to the pediatric plasma cortisol baseline ( $\text{BASE}_{\text{child, pla}}$ ), a pediatric DBS cortisol baseline ( $\text{BASE}_{\text{child, DBS}}$ ) was implemented, and based on pre-dose observations or was estimated if no observation was present.  $\text{BASE}_{\text{child, pla}}$  was used as an initial value of the central plasma concentration, whereas  $\text{BASE}_{\text{child, RBC}}$  represented cortisol bound to RBCs at baseline and was described in amounts (nmol) as  $A_{\text{BASERBC}} = A_{\text{BASEchild, DBS}} - A_{\text{BASEchild, pla}}$  (**Figure 2**). The underlying model equations can be found in the **Supplementary Material**.

Since higher cortisol concentrations, leading to relatively higher cortisol DBS concentrations, were only observed in the neonatal cohort, “age group” was evaluated as a dichotomous categorical covariate, that is, the influential factor (“children/infants” and “neonates”) on the estimated  $V_{\text{delta}}$ . The inclusion of this



covariate resulted in  $-47.06$  dOFV and explained more than two-thirds (69.1%) of the interindividual variability (IIV) of  $V_{\text{delta}}$  (before: 196% CV, after: 60.6% CV). Age was tested as a covariate on  $V_{\text{delta}}$ , with exponential and fractional changes from the median age, and resulted in an OFV drop of  $-23.0$  and of  $-6.3$ , explaining 20 and 27% of the  $V_{\text{delta}}$  IIV, respectively. Given the higher reduction of IIV and the limited neonatal data, the two age groups were chosen and

kept in the model as the simplest and thus most appropriate covariate.

**Table 1** shows the parameter estimates and the SIR medians and 95% confidence intervals (CI) of the final PK model including adult plasma cortisol data and pediatric plasma and DBS cortisol data. The resulting  $V_{\text{delta}}$  for children/infants was 11.1 L compared to 1.05 L in neonates, corresponding to 0.82 L/kg and 0.29 L/kg for children + infants and for neonates, respectively. The linear binding/association

**TABLE 1 |** Parameter estimates with sampling importance resampling (SIR) median and 95% confidence intervals (CI) of developed cortisol pharmacokinetic (PK) model including adult plasma data and pediatric plasma and dried blood spot (DBS) data.

Parameter	SIR median [95% CI]
<b>Structural model</b>	
CL [L/h]	400 [289–549]
$V_c$ [L]	10.6 [7.99–14.0]
$Q$ [L/h]	160 [90.4–268]
$V_p$ [L]	124 [80.7–178]
$K_m$ [nmol]	4,810*
$V_{max}$ [nmol/h]	21,388 [13,888–31,463]
$F$ [-]	1*
$K_d$ [nM]	9.71*
$NS_{Alb}$ [-]	4.15*
$K_{aRBC}$ [-]	6.62 [1.95–13.4]
$V_{\Delta}$ , children+infants [L]	11.1 [7.05–18.8]
$V_{\Delta}$ , neonates [L]	1.05 [0.50–1.80]
$BASE_{adult, pla}$ [nM]	15.2 [11.1–20.7]
$BASE_{child, pla}$ [nM]	9.41 [3.32–16.7]
$BASE_{child, DBS}$ [nM]	4.22 [1.10–7.60]
<b>Interindividual variability</b>	
$\omega_{CL}$ , %CV	25.8 [14.9–35.8]
$\omega_{K_m}$ , %CV	55.7 [31.1–75.5]
$\omega_{V_{max}}$ , %CV	46.5 [30.1–65.5]
$\omega_F$ , %CV	36.1 [20.4–49.4]
$\omega_{V_{\Delta}}$ , %CV	43.4 [27.5–62.2]
$\omega_{BASE_{adult, pla}}$ , %CV	35.3 [23.5–47.4]
$\omega_{BASE_{child, pla}}$ and $DBS$ , %CV	131.1*
<b>Residual variability</b>	
$\sigma_{exp}$ [CV%]	14.4 [13.2–16.0]

Clearance (CL), central volume of distribution ( $V_c$ ), intercompartmental clearance (Q), peripheral volume of distribution ( $V_p$ ), amount in depot compartment resulting in half of  $V_{max}$  ( $K_m$ ), maximum absorption rate ( $V_{max}$ ), bioavailability (F), equilibrium dissociation constant ( $K_d$ ), linear non-specific parameter for albumin binding and association to red blood cells ( $NS_{Alb}$  and  $k_{aRBC}$ ), volume of red blood cell compartment ( $V_{\Delta}$ ), plasma cortisol baseline in adults ( $BASE_{adult, pla}$ ), plasma cortisol baseline in children ( $BASE_{child, pla}$ ), dried blood spot cortisol baseline in children ( $BASE_{child, DBS}$ ). For  $BASE_{child, pla}$  and  $BASE_{child, DBS}$  a common interindividual variability was fixed, residual variability was estimated as an additive error on a logarithmic scale.

\*fixed parameter.

parameters of cortisol to albumin ( $NS_{Alb}$ ) and RBCs ( $K_{aRBC}$ ) resulted in 4.15 and 6.62, respectively. The predominant binding partner was CBG, with a fixed  $K_d$  of 9.71 nmol/L, indicating the unbound cortisol concentration at 50% of  $B_{max}$ . The estimates for the pediatric plasma and DBS cortisol baselines were 9.41 nmol/L and 4.22 nmol/L, respectively.

The 95% CIs for the parameter estimates resulting from the SIR show good precision of the parameter estimates. Standard model evaluations, that is, GOF plots and VPCs showed that the adult and pediatric plasma and the pediatric DBS concentrations were adequately described by the final PK model (see the **Supplementary Material**).

## Simulation of Cortisol Binding Species

Simulated whole blood cortisol concentrations of children/infants (**Figure 3A**) and of neonates (**Figure 3B**) were based on the PK model with the two different  $V_{\Delta}$ s of the respective age groups based on a dose of 7 mg HC. The fractions of the simulated cortisol species (%) against the whole blood concentration demonstrated the substantial decrease in the cortisol fraction bound to CBG with

higher total cortisol concentrations due to the saturation of the binding process. The fraction bound to CBG decreased from approximately 90% at 1.8 nmol/L (LLOQ; i.e., shortly after drug intake) to 45 and 22% at the highest simulated whole blood cortisol concentrations for children/infants (180 nmol/L =  $C_{max}$ , maximum concentration) and neonates (820 nmol/L =  $C_{max}$ ), respectively. Consequently, a substantial increase was observed for the fraction unbound (children/infants: from 1.7 to 9.0%; neonates: from 1.6 to 13%), the fraction bound to albumin (children/infants: from 7.0 to 37%; neonates: from 6.8 to 53%), and the fraction associated with RBCs (children/infants: from 1.9 to 8.3%; neonates: from 1.9 to 12%).

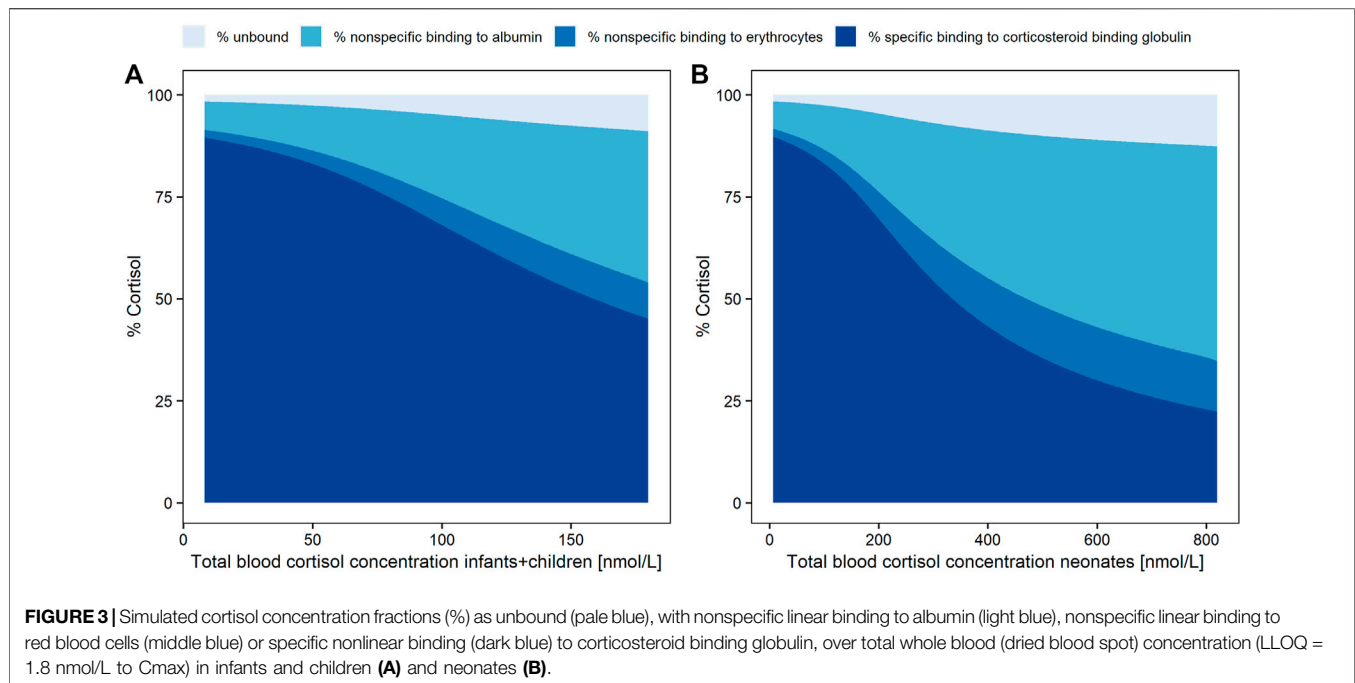
## DISCUSSION

Leveraging cortisol concentrations from adult plasma data and pediatric plasma and DBS data, we successfully established a quantitative link between pediatric total plasma cortisol concentrations and pediatric total DBS cortisol concentrations by extending a published NLME HC PK model based on adult and pediatric plasma cortisol data with pediatric DBS concentrations.

The inclusion of the whole blood DBS cortisol data into the model allowed to quantitatively characterize cortisol association with RBCs by a linear, non-specific association process, in addition to cortisol binding to CBG, and to albumin. Since the linear association of cortisol with RBCs was only described in adults (Lentjes and Romijn, 1999) and generally a saturation of this process should not be expected due to the abundance of RBCs in all age groups, we assumed that these findings also apply to children. A corresponding RBC-associated cortisol compartment was added to the PK model and RBC volumes were successfully estimated for the neonatal age group and for children/infants. With the age group implemented as a covariate on  $V_{\Delta}$ , the  $V_{\Delta}$  estimate (1.05 L) for neonates was considerably lower than the estimated  $V_{\Delta}$  for children/infants (11.1 L) (**Table 1**) and thereby, as an apparent volume of distribution, accounting for the lower plasma/DBS concentration ratio which was observed for neonates.

The estimates for the pediatric baselines in plasma and DBS were reasonably low and close to respective LLOQs. Overall, the inclusion of the pediatric cortisol DBS data barely changed the plasma-related parameter estimates, which were taken from the previous model, whereas the additional DBS-related parameters resulted in plausible estimates.

For a better comparison of  $K_{aRBC}$  (6.62) with the other two binding parameters  $K_d$  (9.71 nmol/L) and  $NS_{Alb}$  (4.15), the PK model was applied to simulate the fractions of cortisol bound to CBG, to albumin, and associated with RBCs. As already expected from the graphical analysis, with increasing cortisol concentrations the ratio between cortisol plasma and DBS concentrations decreased. The simulation results supported this finding, due to the saturation of the nonlinear binding between cortisol and CBG and thus higher availability of unbound cortisol to be associated with RBCs. The simulated fraction of cortisol bound to CBG decreased by 75% in neonates (from 90 to 22%) compared to a decrease of 50% in children/infants (from 90 to 45%). Consequently, a considerably higher



amount of free cortisol became available for binding to albumin or association with RBCs. At the highest simulated whole blood cortisol concentrations, 45% more cortisol is associated with RBCs in neonates (12% at 820 nmol/L Cmax) compared to children/infants (8.3% at 180 nmol/L Cmax). These considerably different simulated fractions of cortisol associated with RBCs could partly explain the highly variable plasma/DBS concentration ratios which were observed in the graphical analysis for the two age groups. The higher cortisol concentrations were only observed in neonates due to a higher dose relative to body weight in the phase 3 trial, which was mimicked in the simulations by dosing both age groups with the same HC dose. Since the simulations were deterministic, that is, did not include interindividual variability, simulations with 4 mg (Supplementary Figure S3), which was the maximum single dose given in the phase 3 study, resulted in maximum concentrations lower than the ones observed in the phase 3 study (767.5 nmol/L and 141 nmol/L for neonates and children + infants, respectively). Thus, to ensure simulated total blood cortisol concentrations representing the full range of observed concentrations, the simulation dose was increased to 7 mg. It was assumed that the plasma/DBS concentration ratio depends on the overall cortisol concentration. The high cortisol concentrations observed in neonates were the result of a relatively higher HC dose given in the phase 3 study to avoid underdosing in this highly vulnerable cohort. To further explain the high variability observed in the plasma/DBS concentration ratio, more data are required to investigate whether, besides the concentration dependency, there is also, for example, an age dependency for the ratio.

The graphical investigation of the plasma/DBS cortisol concentration ratio leads to the conclusion that with the observed DBS cortisol concentrations ranging from 0 to

200 nmol/L and from 200 to 800 nmol/L, the corresponding plasma cortisol concentrations are higher than DBS concentrations by a factor of 5 and 2.5, respectively. However, this finding should be confirmed with a richer dataset, especially in the higher concentration range where only four neonatal samples were available, before being considered as a rule of thumb when DBS cortisol sampling is used for clinical monitoring in pediatric adrenal insufficiency patients.

As the cortisol concentration data from the pediatric population were sparse in general, the PK model should be re-evaluated with more plasma and DBS cortisol data to confirm the conclusions of our current analysis. A regression equation based on simulations from the updated PK model could then be identified to enable the calculation of plasma cortisol concentrations from measured DBS cortisol concentrations, opening the opportunity to routinely use and interpret DBS sampling for monitoring this vulnerable patient population. As this analysis is based on data from patients aged from 0 to 6 years, the applicability of the PK model to children older than 6 years can be investigated in future with respective available data. The PK in adolescents aged 12 to 18 years can be assumed to be similar to adult HC PK and binding kinetics as it was found in published pharmacokinetic analyses (Bonner et al., 2021).

Furthermore, the DBS data used in this analysis were venous whole blood concentrations, whereas in clinical practice capillary whole blood is obtained for DBS sampling. It is therefore important to re-evaluate the comparability of venous and capillary whole blood cortisol concentrations. Moreover, the underlying mechanism behind cortisol being associated with RBCs is still unknown, and it should be investigated if cortisol associated with RBCs is biologically active due to its low affinity to RBCs (Lentjes and Romijn, 1999). Thus, further *in vitro* studies are needed to elucidate the underlying mechanisms of

the RBC-associated processes (e.g., adsorption and uptake) qualitatively and quantitatively.

## DATA AVAILABILITY STATEMENT

The original contributions presented in the study are included in the article/**Supplementary Material**; further inquiries can be directed to the corresponding author.

## ETHICS STATEMENT

The studies involving human participants were reviewed and approved by the Local Ethics Committee at Charite Berlin (study nr 15/0375-EK 15). Written informed consent to participate in this study was provided by the participants' legal guardian/next of kin.

## AUTHOR CONTRIBUTIONS

Conceptualization: VS, RM, and CK; formal analysis: VS; data collection: UN, OB, RR, and MW; writing—original draft preparation: VS and DB; writing—review and editing: all authors; and visualization: VS; supervision: RM and CK.

## REFERENCES

- Balsamo, A., Baronio, F., Ortolano, R., Menabo, S., Baldazzi, L., di Natale, V., et al. (2020). Congenital Adrenal Hyperplasias Presenting in the Newborn and Young Infant. *Front. Pediatr.* 8, 864. doi:10.3389/fped.2020.593315/BIBTEX
- Bauer, R. (2010). *NONMEM Users Guide: Introduction to NONMEM 7*. Ellicott City, MD: ICON Development Solutions Ellicott City, MD, 1–61. Available at: [ftp://nonmem.iconplc.com/Public/nonmem7/Release\\_Notes\\_Plus/nm720.pdf](ftp://nonmem.iconplc.com/Public/nonmem7/Release_Notes_Plus/nm720.pdf).
- Bergstrand, M., Hooker, A. C., Wallin, J. E., and Karlsson, M. O. (2011). Prediction-Corrected Visual Predictive Checks for Diagnosing Nonlinear Mixed-Effects Models. *AAPS J.* 13, 143–151. doi:10.1208/s12248-011-9255-z
- Bonner, J. J., Burt, H., Johnson, T. N., Whitaker, M. J., Porter, J., and Ross, R. J. (2021). Development and Verification of an Endogenous PBPK Model to Inform Hydrocortisone Replacement Dosing in Children and Adults with Cortisol Deficiency. *Eur. J. Pharm. Sci.* 165, 105913. doi:10.1016/j.ejps.2021.105913
- Bornstein, S. R., Allolio, B., Arlt, W., Barthel, A., Don-Wauchope, A., Hammer, G. D., et al. (2016). Diagnosis and Treatment of Primary Adrenal Insufficiency: An Endocrine Society Clinical Practice Guideline. *J. Clin. Endocrinol. Metab.* 101, 364–389. doi:10.1210/JC.2015-1710
- Dabas, A., Vats, P., Sharma, R., Singh, P., Seth, A., Jain, V., et al. (2020). Management of Infants with Congenital Adrenal Hyperplasia. *Indian Pediatr.* 57, 159–164. doi:10.1007/s13312-020-1735-8
- Dosne, A. G., Bergstrand, M., and Karlsson, M. O. (2017). An Automated Sampling Importance Resampling Procedure for Estimating Parameter Uncertainty. *J. Pharmacokinet. Pharmacodyn.* 44, 509–520. doi:10.1007/s10928-017-9542-0
- Edelbroek, P. M., van der Heijden, J., and Stolk, L. M. (2009). Dried Blood Spot Methods in Therapeutic Drug Monitoring: Methods, Assays, and Pitfalls. *Ther. Drug Monit.* 31, 327–336. doi:10.1097/FTD.0B013E31819E91CE
- European Medicines Agency (2012). *Guideline on Bioanalytical Method Validation*.

All authors have read and approved final version for publication.

## FUNDING

The modeling and simulation work described here was carried out under a Cooperation Agreement between Freie Universitaet and Diurnal funded by Diurnal Lt, based on a clinical trial designed by Diurnal and Charite Berlin.

## ACKNOWLEDGMENTS

The authors acknowledge the High-Performance Computing Service of ZEDAT at Freie Universitaet Berlin (<https://www.zedat.fu-berlin.de/HPC/Home>) for computing time. We acknowledge the support by the Open Access Publication Initiative of Freie Universität Berlin.

## SUPPLEMENTARY MATERIAL

The Supplementary Material for this article can be found online at: <https://www.frontiersin.org/articles/10.3389/fphar.2022.819590/full#supplementary-material>

- Kamoun, M., Feki, M. M., Sfar, M. H., and Abid, M. (2013). Congenital Adrenal Hyperplasia: Treatment and Outcomes. *Indian J. Endocrinol. Metab.* 17, S14–S17. doi:10.4103/2230-8210.119491
- Keizer, R. J., Karlsson, M. O., and Hooker, A. (2013). Modeling and Simulation Workbench for NONMEM: Tutorial on Pirana, PsN, and Xpose. *CPT Pharmacometrics Syst. Pharmacol.* 2, e50. doi:10.1038/psp.2013.24
- Khatab, A., and Marshall, I. (2019). Management of Congenital Adrenal Hyperplasia: beyond Conventional Glucocorticoid Therapy. *Curr. Opin. Pediatr.* 31, 550–554. doi:10.1097/MOP.0000000000000780
- Lentjes, E. G., and Romijn, F. H. (1999). Temperature-dependent Cortisol Distribution Among the Blood Compartments in Man. *J. Clin. Endocrinol. Metab.* 84, 682–687. doi:10.1210/jcem.84.2.5461
- Melin, J., Parra-Guillen, Z. P., Michelet, R., Truong, T., Huisinga, W., Hartung, N., et al. (2020). Pharmacokinetic/Pharmacodynamic Evaluation of Hydrocortisone Therapy in Pediatric Patients with Congenital Adrenal Hyperplasia. *J. Clin. Endocrinol. Metab.* 105. doi:10.1210/clinem/dgaa071
- Melin, J., Parra-Guillen, Z. P., Hartung, N., Huisinga, W., Ross, R. J., Whitaker, M. J., et al. (2017). Predicting Cortisol Exposure from Paediatric Hydrocortisone Formulation Using a Semi-mechanistic Pharmacokinetic Model Established in Healthy Adults. *Clin. Pharmacokinet.* 57, 515–527. doi:10.1007/s40262-017-0575-8
- Merke, D. P., and Bornstein, S. R. (2005). Congenital Adrenal Hyperplasia. *Lancet* 365, 2125–2136. doi:10.1016/S0140-6736(05)66736-0
- Michelet, R., Melin, J., Parra-Guillen, Z. P., Neumann, U., Whitaker, J. M., Stachanow, V., et al. (2020). Paediatric Population Pharmacokinetic Modelling to Assess Hydrocortisone Replacement Dosing Regimens in Young Children. *Eur. J. Endocrinol.* 183, 357–368. doi:10.1530/EJE-20-0231
- Moat, S. J., George, R. S., and Carling, R. S. (20202020). Use of Dried Blood Spot Specimens to Monitor Patients with Inherited Metabolic Disorders. *Int. J. Neonatal. Screen.* 6, 26. doi:10.3390/IJNS6020026
- Mould, D. R., and Upton, R. N. (2012). Basic Concepts in Population Modeling, Simulation, and Model-Based Drug Development. *CPT Pharmacometrics Syst. Pharmacol.* 1, e6. doi:10.1038/psp.2012.4

- Mould, D. R., and Upton, R. N. (2013). Basic Concepts in Population Modeling, Simulation, and Model-Based Drug Development-Part 2: Introduction to Pharmacokinetic Modeling Methods. *CPT Pharmacometrics Syst. Pharmacol.* 2, e38. doi:10.1038/psp.2013.14
- Neumann, U., Whitaker, M. J., Wiegand, S., Krude, H., Porter, J., Davies, M., et al. (2018). Absorption and Tolerability of Taste-Masked Hydrocortisone Granules in Neonates, Infants and Children under 6 Years of Age with Adrenal Insufficiency. *Clin. Endocrinol. (Oxf)* 88, 21–29. doi:10.1111/cen.13447
- Oprea, A., Bonnet, N. C. G., Pollé, O., and Lysy, P. A. (2019). Novel Insights into Glucocorticoid Replacement Therapy for Pediatric and Adult Adrenal Insufficiency. *Ther. Adv. Endocrinol. Metab.* 10, 2042018818821294. doi:10.1177/2042018818821294
- Podgórski, R., Aebischer, D., Stompor, M., Podgórska, D., and Mazur, A. (2018). Congenital Adrenal Hyperplasia: Clinical Symptoms and Diagnostic Methods. *Acta Biochim. Pol.* 65, 25–33. doi:10.18388/ABP.2017\_2343
- Qasrawi, D. O., Boyd, J. M., and Sadrzadeh, S. M. H. (2021). Measuring Steroids from Dried Blood Spots Using Tandem Mass Spectrometry to Diagnose Congenital Adrenal Hyperplasia. *Clin. Chim. Acta* 520, 202–207. doi:10.1016/J.CCA.2021.06.005
- R Core Team (2019). R: A Language and Environment for Statistical Computing. Available at: <https://www.R-project.org/> (Accessed November 21, 2021).
- RStudio Team (2020). *RStudio*. Boston, MA: Integrated Development Environment for R.
- Whitaker, M. J., Spielmann, S., Digweed, D., Huatan, H., Eckland, D., Johnson, T. N., et al. (2015). Development and Testing in Healthy Adults of Oral Hydrocortisone Granules with Taste Masking for the Treatment of Neonates and Infants with Adrenal Insufficiency. *J. Clin. Endocrinol. Metab.* 100, 1681–1688. doi:10.1210/jc.2014-4060
- Wilhelm, A. J., den Burger, J. C., and Swart, E. L. (2014). Therapeutic Drug Monitoring by Dried Blood Spot: Progress to Date and Future Directions. *Clin. Pharmacokinet.* 53, 961–973. doi:10.1007/S40262-014-0177-7/TABLES/2

**Conflict of Interest:** The modeling and simulation work described here was carried out under a Cooperation Agreement between Freie Universitaet and Diurnal funded by Diurnal Lt, based on a clinical trial designed by Diurnal and Charite Berlin. The manuscript writing was done by all involved parties, that is, Freie Universitaet Berlin, Diurnal Lt, University of Potsdam and Charite Berlin.

The remaining authors declare that the research was conducted in the absence of any commercial or financial relationships that could be construed as a potential conflict of interest.

**Publisher's Note:** All claims expressed in this article are solely those of the authors and do not necessarily represent those of their affiliated organizations, or those of the publisher, the editors, and the reviewers. Any product that may be evaluated in this article, or claim that may be made by its manufacturer, is not guaranteed or endorsed by the publisher.

Copyright © 2022 Stachanow, Neumann, Blankenstein, Bindellini, Melin, Ross, Whitaker, Huisinga, Michelet and Kloft. This is an open-access article distributed under the terms of the Creative Commons Attribution License (CC BY). The use, distribution or reproduction in other forums is permitted, provided the original author(s) and the copyright owner(s) are credited and that the original publication in this journal is cited, in accordance with accepted academic practice. No use, distribution or reproduction is permitted which does not comply with these terms.

# Supplementary Material

## 1 Supplementary Data

### Final model structure:

#### Initial conditions

$$A_{depot,0} = F * DOSE$$

$$A_{pla,0,adult} = 0$$

$$A_{pla,0,child} = BASE_{child,pla} * V_c$$

$$A_{DBS,0,child} = 0$$

$$A_{p,0} = 0$$

#### State variables and outputs

$$A_{pla,adult}(t) = A_{pla}(t) + BASE_{adult} * V_c$$

$$A_{pla,child,pla}(t) = A_{pla}(t)$$

$$A_{ABASERBC} = A_{ABASEchild,DBS} - A_{ABASEchild,pla}$$

$$A_{DBS,child}(t) = A_{pla}(t) + A_{RBC}(t) + A_{ABASERBC}$$

$$K_{dA} = K_d * V_c$$

$$A_{max} = B_{max} * V_c$$

$$A_u$$

$$= \frac{A_{pla} - K_{dA} \cdot (1 + NS_{Alb}) - A_{max} + \sqrt{(A_{pla} - K_{dA} \cdot (1 + NS_{Alb}) - A_{max})^2 + 4 \cdot A_{pla} \cdot K_{dA} \cdot (1 + NS_{Alb})}}{2 \cdot (1 + NS_{Alb})}$$

$$A_p(t) = A_p(t)$$

$$C(t) = \frac{A_{pla}(t)}{V_c}$$

$$V_{wholeblood} = V_c + V_{delta}$$

$$C_{DBS,child}(t) = \frac{(A_{pla}(t) + A_{RBC}(t) + A_{ABASERBC})}{V_{wholeblood}}$$

**Differential equations**

$$dA_{depot}/dt = -\frac{V_{abs,max} \cdot A_{depot}}{K_{abs,50} + A_{depot}}$$

$$dA_{pla}/dt = \frac{V_{abs,max} \cdot A_{depot}}{K_{abs,50} + A_{depot}} - CL/V_c \cdot A_u - Q/V_c \cdot A_u + Q/V_p \cdot A_p$$

$$dA_p/dt = Q/V_c \cdot A_u - Q/V_p \cdot A_p$$

$$dA_{RBC}/dt = K_{aRBC} \cdot A_u - K_{aRBC} \cdot A_{RBC}$$

**Estimated model parameters**

$$CL_{ind} = CL_{pop} \cdot (BW/70)^{0.75} \cdot e^{\eta_{CL,ind}} \quad \eta_{CL} \sim N(0, \omega_{CL})$$

$$V_{c,ind} = V_{c,pop} \cdot (BW/70)$$

$$Q_{ind} = Q_{pop} \cdot (BW/70)^{0.75}$$

$$V_{p,ind} = V_{p,pop} \cdot (BW/70)$$

$$V_{abs,max} = V_{abs,max,pop} \cdot e^{\eta_{V_{abs,max},ind}} \quad \eta_{V_{abs,max}} \sim N(0, \omega_{V_{abs,max}})$$

$$F_{ind} = F_{pop} \cdot e^{\eta_{F,ind}} \quad \eta_{F,ind} \sim N(0, \omega_F)$$

$$K_{aRBC,ind} = K_{aRBC,pop} \cdot e^{\eta_{K_{aRBC},ind}} \quad \eta_{K_{aRBC},ind} \sim N(0, \omega_{K_{aRBC}})$$

$$V_{delta,children+infants,ind} = V_{delta,children+infants,pop} \cdot e^{\eta_{V_{delta},ind}}$$

$$V_{delta,neonates,ind} = V_{delta,neonates,pop} \cdot e^{\eta_{V_{delta},ind}} \quad \eta_{V_{delta},ind} \sim N(0, \omega_{V_{delta}})$$

$$BASE_{adult,ind} = BASE_{adult,pop} \cdot e^{\eta_{BASE_{adult},ind}} \quad \eta_{BASE_{adult}} \sim N(0, \omega_{BASE_{adult}})$$

for  $BASE_{child,pla}$  and  $BASE_{child,DBS}$  :

$$BASE_{child,pop} = BASE_{observed} \text{ OR } BASE_{pop,estimate}$$

$$BASE_{child,ind} = BASE_{child,pop} \cdot e^{\epsilon_{ind}} \quad \epsilon_{ind} \sim N(0, \sigma^2)$$

**Fixed model parameters**

$$K_{abs,50} = 4810 \text{ nmol/L}$$

$$F_{pop} = 1 (-)$$

$$K_d = 9.71 \text{ nmol/L}$$

$$NS_{Alb} = 4.15 (-)$$

$$B_{max} = \text{CBG concentration } \left[ \frac{\text{nmol}}{\text{L}} \right] = 22.4 \frac{\text{ug}}{\text{mL}} * \frac{1000}{52 \frac{\text{g}}{\text{nmol}}} \left[ \frac{\text{nmol}}{\text{L}} \right] \text{ when not measured}$$

## NONMEM model code

\$PROBLEM

pediatric plasma and DBS cortisol PK model

\$INPUT

ID COHORT DROP=DAT2 DROP=TIME2 TIME AMT DROP=RATE DROP=DVX DROP=LDVX  
 DROP=DV2 DROP=LDV2 DROP=DV3 DV ODV DROP=MDVX DROP=MDV2 MDV EVID BLQ CMT  
 FLAG FLAGM FLAGB HCT HCTF AGE BW HT BMI BSA SEX CBG ALB DOSE TAFO  
 \$DATA dataset.csv IGNORE=@ IGNORE(BLQ,EQ.1)  
 \$SUBROUTINE ADVAN13 TOL=9

\$MODEL

COMP = (DEPOT DEFDOSE) ;dose compartment  
 COMP = (CENTRAL DEFOBSERVATION) ;central plasma compartment  
 COMP = (PERIPH) ;peripheral plasma compartment  
 COMP = (OUTPUT1) ;compartment with cortisol associated to RBCs

\$PK

;allometric scaling applied to CL and Q (exponent 0.75) and to V1 and V2 (exponent 1),  
 ;referring to 70 kg as normal adult BW

TVCL = THETA(1)\*((BW/70)\*\*0.75)  
 CL = TVCL\*EXP(ETA(1))

TVV1 = THETA(2)\*(BW/70)  
 V1 = TVV1\*EXP(ETA(2))

TVQ = THETA(3)\*(BW/70)\*\*0.75  
 Q = TVQ\*EXP(ETA(3))

TVV2 = THETA(4)\*(BW/70)  
 V2 = TVV2\*EXP(ETA(4))

TVKM = THETA(5)  
 KM = TVKM\*EXP(ETA(5))

;number of CBG binding sites fixed to 1  
 TVBS = THETA(6)  
 BS = TVBS\*EXP(ETA(6))

TVKD = THETA(7)  
 KD = TVKD\*EXP(ETA(7))

;converting concentration to amount  
 KDa = KD\*V1

```

TVNSALB = THETA(8)
NSALB = TVNSALB*EXP(ETA(8))

TVVM = THETA(9)
VM = TVVM*EXP(ETA(9))

;CBG given in dataset for adult study 2 and for pediatric data
CBG2 = CBG
IF(CBG.EQ.-99) THEN
CBG2 = THETA(15)
ENDIF

;converting CBG from ug/mL to nmol/L. MW=52000g/mol
CBGmol = CBG2*1000/52

BMAX = CBGmol*BS
;converting concentration to amount
AMAX = BMAX*V1

TVF1 = THETA(10)
F1 = TVF1*EXP(ETA(10))

TVKaRBC = THETA(11)
KaRBC = TVKaRBC*EXP(ETA(11))

;adult (COHORT 4) baseline
IF (COHORT.EQ.4) THEN
TVABASE = THETA(12)
ABASE = TVABASE*EXP(ETA(12))
ELSE
ABASE = 0
ENDIF

;Vdelta for neonates (COHORT 3) and children+infants (COHORT 1+2)
IF(COHORT.LT.3) THEN
TVV3 = THETA(13)
ENDIF
IF(COHORT.EQ.3) THEN
TVV3 = THETA(16)
ENDIF
V3 = TVV3*EXP(ETA(14))

IF(COHORT.EQ.4) THEN
IBASE = 0
IBASEB = 0
ENDIF

;pediatric baseline observations in plasma (FLAGM=0)
IF(COHORT.LT.4.AND.FLAGM.EQ.0) THEN
OBASE = ODV
ENDIF
;pediatric baseline observations in DBS (FLAGM=1)

```

```
IF(COHORT.LT.4.AND.FLAGM.EQ.1) THEN
OBASEB = ODV
ENDIF
```

```
;pediatric baseline in plasma if no baseline observation given
IF(OBASE.EQ.0) THEN
IBASE = THETA(17)*EXP(ETA(13)*THETA(14))
ENDIF
```

```
;pediatric baseline in plasma if baseline observation given
IF(OBASE.GT.0) THEN
IBASE = OBASE*EXP(ETA(13)*THETA(14))
ENDIF
```

```
IF(COHORT.EQ.4) THEN
IBASE = 0
ENDIF
```

```
;pediatric baseline in DBS if no baseline observation given
IF(OBASEB.EQ.0) THEN
IBASEB = THETA(18)*EXP(ETA(13)*THETA(14))
ENDIF
```

```
;pediatric baseline in DBS if baseline observation given
IF(OBASEB.GT.0) THEN
IBASEB = OBASEB*EXP(ETA(13)*THETA(14))
ENDIF
```

```
IF(COHORT.EQ.4) THEN
IBASEB = 0
ENDIF
```

```
; Time after dose
TAD = 0
IF (AMT.GT.0) THEN
TDOS = TIME
TAD = 0.0
ENDIF
IF (AMT.EQ.0) TAD = TIME-TDOS
IF (TAD.LT.0) TAD = 0
```

```
S1 = V1
k10 = CL/V1
k12 = Q/V1
k21 = Q/V2
```

```
;amount at timepoint 0 in central plasma compartment, IBASE is 0 for adults
A_0(2) = IBASE*V1
```

```
;baseline amounts
AIBASE = IBASE*V1
AIBASEB = IBASEB*(V1+V3)
```

```
ABASERBC = AIBASEB-AIBASE
```

```
IF(ABASERBC.LT.0) THEN
ABASERBC = 0.1
ENDIF
```

```
$DES
```

```
;calculating unbound amount in plasma with binding model from Melin et al., 2017
```

```
AUP = (A(2)-KDa*(1+NSALB)-AMAX+SQRT(((A(2)-KDa*(1+NSALB)-
AMAX)**2)+4*KDa*A(2)*(1+NSALB)))/(2*(1+NSALB))
```

```
DADT(1) = -(VM*A(1)/(KM+A(1))) ;saturable absorption from dose compartment
```

```
DADT(2) = (VM*A(1)/(KM+A(1))) - k10*AUP - k12*AUP + k21*A(3) ;central compartment
```

```
DADT(3) = -k21*A(3)+k12*AUP ;peripheral compartment
```

```
DADT(4) = AUP*KaRBC-A(4)*KaRBC ;compartment with cortisol associated to RBCs
```

```
$ERROR
```

```
A1 = A(1)
```

```
A2 = A(2)
```

```
AUP2 = (A(2)-KDa*(1+NSALB)-AMAX+SQRT(((A(2)-KDa*(1+NSALB)-
AMAX)**2)+4*KDa*A(2)*(1+NSALB)))/(2*(1+NSALB))
```

```
A3 = A(3)
```

```
A4 = A(4)
```

```
C1 = A1/V1
```

```
C2 = A2/V1
```

```
BASEB = 0
```

```
BASEP = 0
```

```
IPRED = 0
```

```
;TAFO = time at baseline observation
```

```
IF(TAFO.EQ.0) THEN
```

```
BASEB = IBASEB
```

```
BASEP = IBASEP
```

```
ENDIF
```

```
;pediatric DBS concentrations
```

```
IF (FLAGM.EQ.1.AND.COHORT.LT.4) THEN
```

```
IPRED = (A2+A4+ABASERBC)/(V1+V3)
```

```
ENDIF
```

```
;pediatric plasma concentrations
```

```
IF (FLAGM.EQ.0.AND.COHORT.LT.4) THEN
```

```
IPRED = A2/V1
```

```
ENDIF
```

```
;adult plasma concentrations
```

```
IF(COHORT.EQ.4) THEN
```

```
IPRED = A2/V1 + ABASE
```

```
ENDIF
```

```
IF(IPRED.GT.0) THEN
```

```

IPRED = LOG(IPRED)
ELSE
IPRED = LOG(IPRED+0.01)
ENDIF
W = THETA(14)
Y = IPRED+W*EPS(1)
IRES = DV-IPRED
IWRES = IRES/W

```

\$THETA

```

(0.001,478.556342893741) ; 1. CL [L/h]
(0.001,10.7708078998368) ; 2. V1 [L]
(0.001,297.932200383505) ; 3. Q [L/h]
(0.001,154.39641074985) ; 4. V2 [L]
4810 FIX ; 5. Km [nmol] fixed to final model estimate from Michelet et al.,
2020
1 FIX ; 6. BS [-], from binding model in Melin et al., 2017
9.71 FIX ; 7. KD [nmol/L], from binding model in Melin et al., 2017
4.15 FIX ; 8. NSALB [-], from binding model in Melin et al., 2017
(0.001,18048.2801258582) ; 9. Vmax [nmol/h]
1 FIX ; 10. Bioavailability [-]
(0.001,3.36024393996957) ; 11. KaRBC [-], association constant for red blood cells
(0.001,14.1273301672484,100) ; 12. adult baseline [nmol/L]
(0.001,0.518880215219603) ; 13. Vdelta children+infants [L]
(0.001,0.143723649120103) ; 14. additive error on a logarithmic scale [sd]
22.4 FIX ; 15. CBG Baseline [ug/mL]
(0.001,0.547320889482403) ; 16. Vdelta neonates [L]
(0.001,14.2481176260859) ; 17. pediatric plasma baseline [nmol/L]
(0.001,20.2496941719316) ; 18. pediatric DBS baseline [nmol/L]

```

\$OMEGA

```

0.0564712567464341 ;1. CL
0 FIX ;2. V1
0 FIX ;3. Q
0 FIX ;4. V2
0.208 ;5. KM
0.049 FIX ;6. BS
0 FIX ;7. KD
0 FIX ;8. NSALB
0.351586646476232 ;9. Vmax
0.149665511339003 ;10. Bioavailability
0 FIX ;11. KaRBC
0.115109316120945 ;12. adult baseline
1 FIX ;13. pediatric baselines
0.183683503993367 ;14. Vdelta

```

\$SIGMA 1 FIX

```

$ESTIMATION MAXEVAL=10000 METHOD=1 INTER SIG=2 NOABORT
$COVARIANCE UNCONDITIONAL PRINT=E

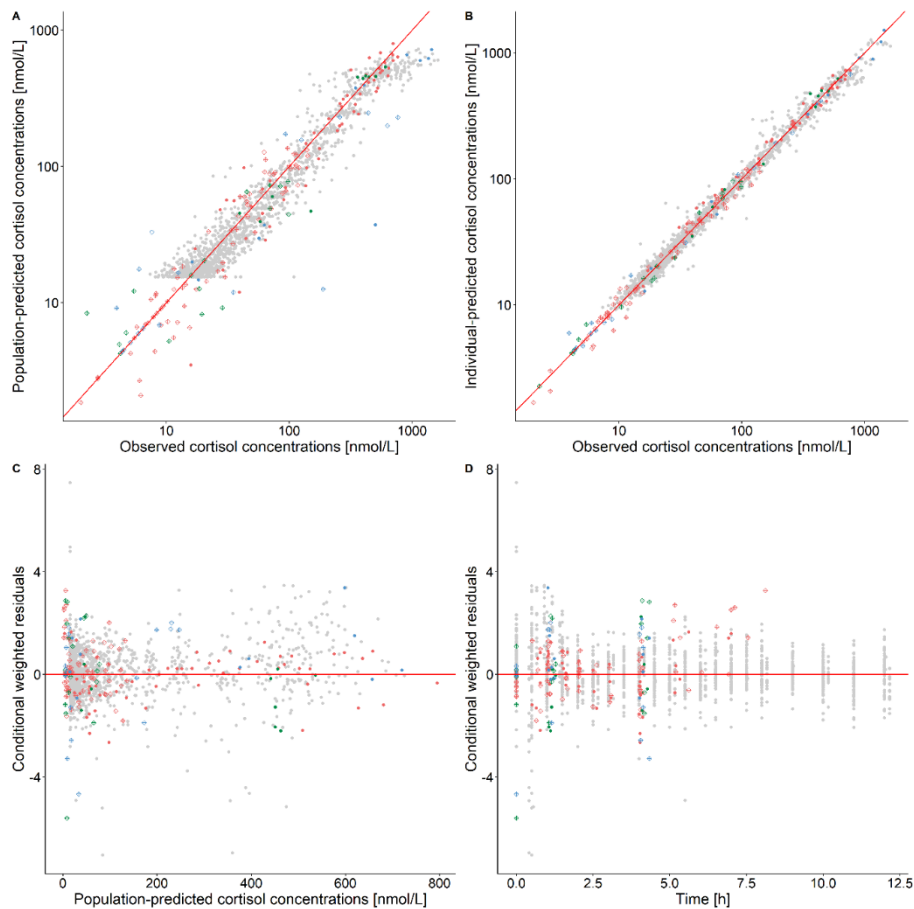
```

```
$TABLE ID TIME TAD TAFO DV PRED IPRED WRES IWRES CWRES COHORT MDV A1 A2 A3 A4
AUP C1 C2 FLAGM FLAGB ONEHEADER NOPRINT FILE=sdtab230
```

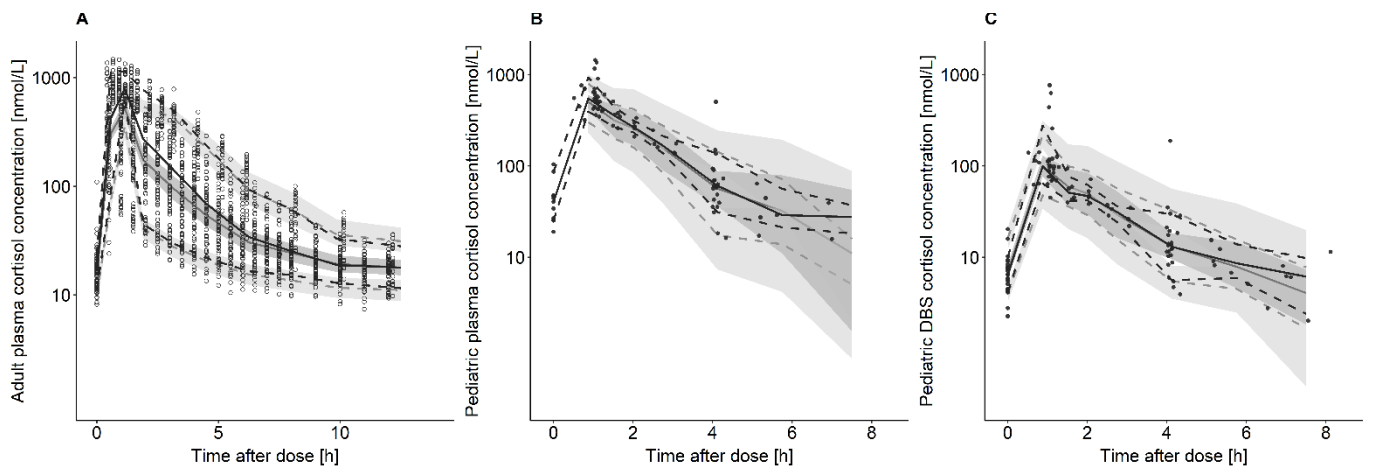
```
$TABLE ID TIME DV CL V1 Q V2 V3 KaRBC IBASE IBASEB BMAX KD NSALB VM KM OBASE
OBASE ABASE COHORT F1 CBG BW HT ALB AGE ODV FLAGM FLAGB ETA1 ETA2 ETA3 ETA4
ETA5 ETA6 ETA7 ETA8 ETA9 ETA10 ETA11 ETA12 ETA13 ETA14 NOAPPEND ONEHEADER
NOPRINT FILE=patab230
```

```
$TABLE DV PRED IPRED WRES IWRES CWRES MDV NPDE ESAMPLE=1000 SEED=1234567
ONEHEADER NOPRINT FILE=NPDEtab_230
```

## 2 Supplementary Figures

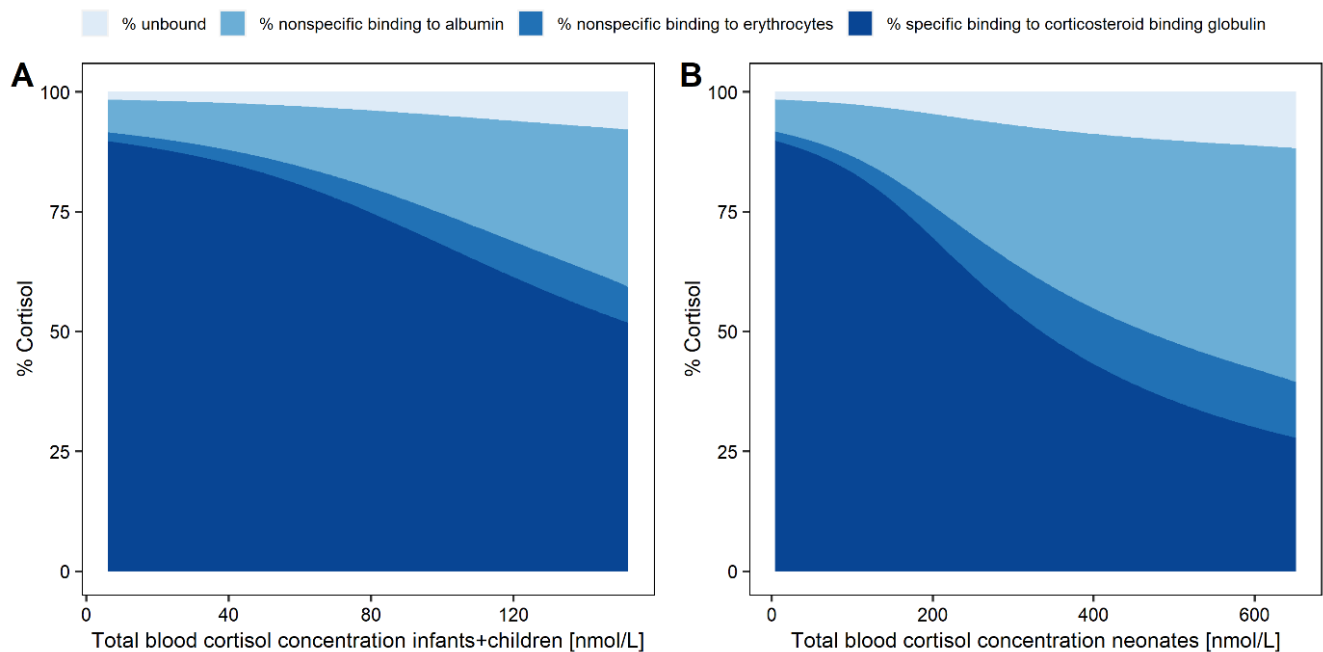


**Supplementary Figure 1.** Goodness-of-fit plots of the developed cortisol pharmacokinetic (PK) model. **(A)** Population-predicted cortisol concentrations versus observed cortisol concentrations, **(B)** Individual cortisol predictions versus observed cortisol concentrations, **(C)** Conditional weighted residuals versus population-predicted cortisol concentrations, **(D)** Conditional weighted residuals versus time. Red: children, green: infants, blue: neonates, gray: adult observations, filled circles: plasma concentrations, diamonds: dried blood spot concentrations, red line: line of identity (A, B), line  $y=0$  (C, D).



**Supplementary Figure 2.** Visual predictive check (n=1000 simulations) for developed cortisol PK model. Adult total cortisol plasma concentrations (**A**), pediatric total cortisol plasma concentrations (**B**), pediatric total cortisol dried blood spot (DBS) concentrations (**C**).

Circles: cortisol observations, black/gray solid line: 50th percentile of observed/simulated concentrations, black/gray dashed lines: 10th and 90th percentiles of observed/simulated concentrations, gray shaded areas: 95 % confidence intervals for the percentiles of the simulated data.



**Supplementary Figure 3.** Simulated cortisol concentration fractions (%) after dosing with 4 mg hydrocortisone over total whole blood (dried blood spot) concentration (LLOQ=1.8 nmol/L to C<sub>max</sub>) in infants and children (**A**) and neonates (**B**). Unbound (pale blue), with nonspecific linear binding to albumin (light blue), nonspecific linear binding to red blood cells (middle blue) and specific nonlinear binding (dark blue) to corticosteroid binding globulin.

### **3.2 Paper II: Model-informed target morning $17\alpha$ -hydroxyprogesterone concentrations in dried blood spots for pediatric congenital adrenal hyperplasia patients**

## Equity Ratio Statement

### Paper II

**Title of the manuscript:**

“Model-informed target morning  $17\alpha$ -hydroxyprogesterone concentrations in dried blood spots for pediatric congenital adrenal hyperplasia patients”

**Journal**            Pharmaceuticals  
                          Volume 16, Issue 464, Pages 1-13 (2023)

**Authorship**      First author

**Status**             Published

                          DOI: <https://doi.org/10.3390/ph16030464>

*Reprinted with permission from Pharmaceuticals.*

**Own contribution**

- Data set modification and checkouts
- All modelling and simulation activities, including PK/PD model development, model evaluation, and simulations
- Interpretation of the results, including literature research related to interpretation of the results
- Drafting of all parts of the manuscript
- Creation of all figures and tables
- Adaptation of the manuscript according to the reviewers' and editor's comments

## Article

# Model-Informed Target Morning $17\alpha$ -Hydroxyprogesterone Concentrations in Dried Blood Spots for Pediatric Congenital Adrenal Hyperplasia Patients

Viktoria Stachanow<sup>1,2</sup>, Uta Neumann<sup>3</sup>, Oliver Blankenstein<sup>3,4</sup>, Nele Alder-Baerens<sup>4</sup>, Davide Bindellini<sup>1,2</sup>, Peter Hindmarsh<sup>5</sup>, Richard J. Ross<sup>6</sup>, Martin J. Whitaker<sup>6</sup>, Johanna Melin<sup>1,2</sup>, Wilhelm Huisinga<sup>7</sup>, Robin Michelet<sup>1,\*</sup> and Charlotte Kloft<sup>1</sup>

- <sup>1</sup> Department of Clinical Pharmacy and Biochemistry, Institute of Pharmacy, Freie Universitaet Berlin, Kelchstr 31, 12169 Berlin, Germany; viktoria.stachanow@fu-berlin.de (V.S.); davide.bindellini@fu-berlin.de (D.B.); charlotte.kloft@fu-berlin.de (C.K.)
- <sup>2</sup> Graduate Research Training Program, PharMetrx, 12169 Berlin, Germany
- <sup>3</sup> Charité-Universitätsmedizin, Freie Universität Berlin, 13353 Berlin, Germany; uta.neumann@charite.de (U.N.)
- <sup>4</sup> Labor Berlin, Charité Vivantes GmbH, 13353 Berlin, Germany; nele.alder-baerens@charite.de
- <sup>5</sup> Developmental Endocrinology Research Group, UCL Institute of Child Health, London WC1E 6BT, UK
- <sup>6</sup> Department of Oncology and Metabolism, University of Sheffield, Sheffield S10 2TN, UK; r.j.ross@sheffield.ac.uk (R.J.R.); martin.whitaker@sheffield.ac.uk (M.J.W.)
- <sup>7</sup> Institute of Mathematics, Universität Potsdam, 14476 Potsdam, Germany; huisinga@uni-potsdam.de
- \* Correspondence: robin.michelet@fu-berlin.de

**Abstract:** Monitoring cortisol replacement therapy in congenital adrenal hyperplasia (CAH) patients is vital to avoid serious adverse events such as adrenal crises due to cortisol underexposure or metabolic consequences due to cortisol overexposure. The less invasive dried blood spot (DBS) sampling is an advantageous alternative to traditional plasma sampling, especially in pediatric patients. However, target concentrations for important disease biomarkers such as  $17\alpha$ -hydroxyprogesterone (17-OHP) are unknown using DBS. Therefore, a modeling and simulation framework, including a pharmacokinetic/pharmacodynamic model linking plasma cortisol concentrations to DBS 17-OHP concentrations, was used to derive a target morning DBS 17-OHP concentration range of 2–8 nmol/L in pediatric CAH patients. Since either capillary or venous DBS sampling is becoming more common in the clinics, the clinical applicability of this work was shown by demonstrating the comparability of capillary and venous cortisol and 17-OHP concentrations collected by DBS sampling, using a Bland-Altman and Passing-Bablok analysis. The derived target morning DBS 17-OHP concentration range is a first step towards providing improved therapy monitoring using DBS sampling and adjusting hydrocortisone (synthetic cortisol) dosing in children with CAH. In the future, this framework can be used to assess further research questions, e.g., target replacement ranges for the entire day.

**Keywords:** congenital adrenal hyperplasia;  $17\alpha$ -hydroxyprogesterone; dried blood spots; target concentration range; pediatrics; pharmacometrics



**Citation:** Stachanow, V.; Neumann, U.; Blankenstein, O.; Alder-Baerens, N.; Bindellini, D.; Hindmarsh, P.; Ross, R.J.; Whitaker, M.J.; Melin, J.; Huisinga, W.; et al. Model-Informed Target Morning  $17\alpha$ -Hydroxyprogesterone Concentrations in Dried Blood Spots for Pediatric Congenital Adrenal Hyperplasia Patients. *Pharmaceuticals* **2023**, *16*, 464. <https://doi.org/10.3390/ph16030464>

Academic Editor: Guendalina Zuccari

Received: 15 February 2023

Revised: 16 March 2023

Accepted: 17 March 2023

Published: 21 March 2023



**Copyright:** © 2023 by the authors. Licensee MDPI, Basel, Switzerland. This article is an open access article distributed under the terms and conditions of the Creative Commons Attribution (CC BY) license (<https://creativecommons.org/licenses/by/4.0/>).

## 1. Introduction

Congenital adrenal hyperplasia (CAH) is a form of adrenal insufficiency most commonly leading to a lack of the enzyme P450c21 and, therefore, to cortisol deficiency. The accumulation of cortisol precursors, including dehydroepiandrosterone and androstenedione (adrenal androgens), often results in clinical signs of virilization or hirsutism in female patients and acceleration of skeletal age in both sexes [1–3]. Cortisol deficiency in CAH requires life-long hormone replacement therapy with hydrocortisone (synthetic cortisol) in a daily dose of 10–15 mg/m<sup>2</sup> given three times per day to the growing patient [4]. Cortisol replacement needs to be carefully monitored to avoid adverse events such as adrenal crisis (cortisol underexposure) or Cushing’s syndrome (cortisol overexposure) [2,4].

Dried blood spot (DBS) sampling, when compared to plasma blood sampling, is a less invasive option to monitor cortisol and further steroid marker concentrations. DBS sampling only requires full blood volumes of approximately 20  $\mu\text{L}$ , obtained via a finger prick and dropped on filter paper [5–7]. The feasibility of DBS sampling, as well as long-term stability at room temperature, was investigated and confirmed for CAH-relevant steroids in DBS in previous literature [8–10]. Therefore, DBS sampling can facilitate therapeutic monitoring for pediatric CAH patients. However, therapeutic monitoring using DBS measurements remains a challenge since no target blood biomarker concentrations are currently established for the DBS methodology. Analyte concentrations collected by DBS relate linearly to plasma or serum concentrations, differing by a factor specific to the analyte [7] or nonlinearly, as is observed for cortisol [11].

Knowing target morning biomarker concentrations is vital for successful CAH therapy monitoring. A key biomarker for guiding replacement therapy in CAH is 17 $\alpha$ -hydroxyprogesterone (17-OHP), a precursor of cortisol and adrenal androgens, which accumulates in CAH patients. The administration of hydrocortisone downregulates adrenocorticotropic hormone (ACTH) and sequentially the 17-OHP concentration by negative feedback [1,2,12]. The target morning 17-OHP concentration range in traditionally measured plasma has been suggested to be 12–36 nmol/L (dependent on body surface area) in CAH patients [2] but is still unknown for concentrations collected by DBS sampling. The aim of this analysis was to derive a DBS 17-OHP morning target concentration range using nonlinear mixed effects (NLME) modeling, a pharmacometric modeling and simulation approach. In contrast to classical regression methods, NLME modeling enables the quantification of the relationship between, e.g., plasma and DBS concentrations by considering all available data simultaneously, thereby quantifying within- and between-subject-variability and explaining this variability using subject-specific characteristics [13]. The modeling and simulation-derived target range can pave the way for guidance for clinicians when investigating biomarker concentrations using DBS sampling and could have the potential to improve therapy monitoring in pediatric CAH patients.

## 2. Methods

To derive a target morning 17-OHP concentration range using DBS sampling, a modeling and simulation framework was developed, leveraging different sources of drug pharmacokinetics (PK, i.e., cortisol concentrations) and biomarker pharmacodynamics (PD, i.e., 17-OHP concentrations), and exploring their relationships. This framework approach was chosen because of the limited availability of data from clinical studies or routine clinical data collection, i.e., clinical study data including plasma cortisol concentrations in pediatric CAH patients, venous 17-OHP concentrations from simultaneous DBS measurements, endogenous plasma cortisol concentrations in healthy children and 17-OHP target morning concentrations only known in plasma (Figure 1). An overview of the population characteristics in all used datasets can be found in the Supplementary Material (Supplementary Table S1).

The following sections describe the different steps of this framework in detail, namely: (A) the development of a PK/PD model linking plasma cortisol concentrations and venous DBS 17-OHP concentrations based on a pediatric CAH patient study, (B) a Bland-Altman and Passing-Bablok regression analysis to investigate the comparability of simultaneously measured venous and capillary 17-OHP concentrations, because in clinical practice both matrices can be used for DBS sampling in pediatric CAH patients; and finally, (C1) the derivation of a DBS 17-OHP target morning range by leveraging the developed PK/PD model and plasma cortisol data of non-CAH children and (C2 and C3) assessing the plausibility of the derived 17-OHP target morning concentration from DBS sampling by comparing to an expected target range, based on 17-OHP target morning concentration range in plasma, known from the literature.

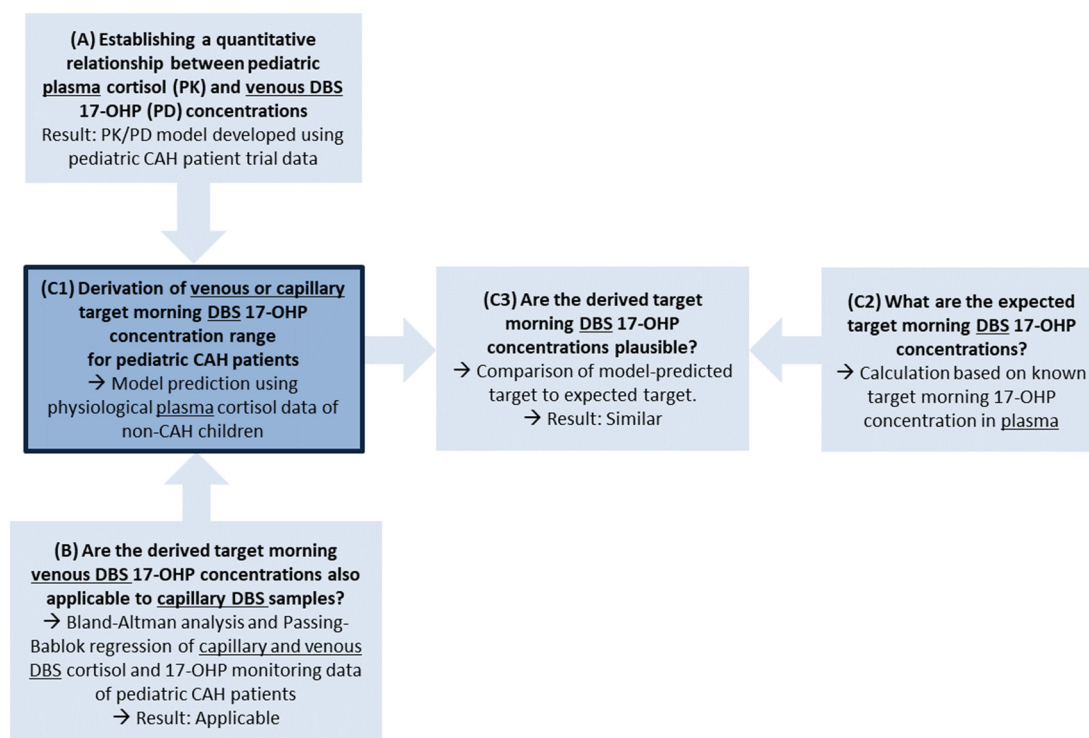


**Figure 1.** Modeling and simulation framework to derive target morning concentration range for the biomarker 17 $\alpha$ -hydroxyprogesterone (17-OHP) sampled from dried blood spots (DBS) in pediatric congenital adrenal hyperplasia (CAH) patients in clinical routine. For the goal of this analysis, the derivation of the target range (dark blue box C1), a pharmacokinetic/pharmacodynamic (PK/PD) model, quantitatively linking plasma cortisol and venous DBS 17-OHP, was developed (A). The applicability of the derived target range, which was based on venous DBS data, to capillary DBS sampling was shown in a Bland–Altman analysis and Passing–Bablok regression (B). To check for plausibility (C3), the derived target range was compared to a calculated expected DBS 17-OHP target range (C2).

### 2.1. Step A: Establishing a Quantitative Relationship between Plasma Cortisol (PK) and Venous DBS 17-OHP (PD) Concentrations in Pediatric CAH Patients: PK/PD Clinical Trial Data and Model Development

#### 2.1.1. Data and Graphical Evaluation

To determine a relationship between pediatric plasma cortisol and venous DBS 17-OHP concentrations, data from a phase 3 trial for the pediatric hydrocortisone formulation Alkindi<sup>®</sup> (Cardiff Medicentre, Cardiff, UK) (ClinicalTrials.gov Identifier: NCT02720952) [14,15] was used (Figure 1, Box A). In this study, 24 pediatric adrenal insufficiency patients (23 CAH patients, 1 hypopituitarism patient) received an individualized morning dose of Alkindi<sup>®</sup> (Cardiff Medicentre, Cardiff, UK). For the PK/PD model development, the data of 12 young children, aged 2–6 years and of 6 infants, aged 28 days–2 years old, was used. Total plasma cortisol concentrations were available prior to dosing, 1 h and 4 h post-dose and in the young children cohort at 2 additional time points. Further details on the clinical trial data are described in Michelet et al. [16]. Additionally, venous DBS cortisol and 17-OHP concentrations were measured in the same patients [11]. The data used for PK/PD modeling were graphically analyzed, investigating the DBS 17-OHP concentrations as a function of time and of plasma cortisol concentrations (R (4.0.2) and R Studio (1.3.1056) [17,18]).

#### 2.1.2. PK/PD Modeling

For the development of the PK/PD model characterizing the relationship between cortisol in plasma and 17-OHP in venous DBS, NLME modeling was applied [13]. The model development was based on a previously published pediatric hydrocortisone PK

model [11,16]. A sequential approach was used [19] in which the individual PK model parameters from this previously published PK model [11] were included in the model dataset, and the PD parameters were estimated.

Since 22 (25%) out of 88 venous DBS 17-OHP concentrations were below the lower limit of quantification (LLOQ, <1.3 nmol/L: 22.5% in young children and 35.3% in infants), the so-called M3 method [20] was applied (for more details see Supplementary Material).

For the PK/PD model development, the software packages NONMEM (7.4.3, ICON, Dublin, Ireland) and Perl speaks NONMEM 4.7.0 (Uppsala University, Uppsala, Sweden) were used, embedded in the workbench Pirana (version 2.9.6) [21,22]. Model evaluation and selection were performed using standard diagnostics such as the objective function value (OFV), parameter plausibility, relative standard errors (RSE), goodness-of-fit (GOF) plots and visual predictive checks (VPC,  $n = 1000$ ).

### *2.2. Step B: Comparison of Capillary and Venous DBS Cortisol and 17-OHP Concentrations from Routine Monitoring in Pediatric CAH Patients: Bland-Altman and Passing-Bablok Regression Analysis*

In clinical practice, either venous or capillary DBS samples are usually obtained in pediatric CAH patients. However, the trial data used for the PK model [11] and PK/PD model development in step (A) included, besides plasma cortisol concentrations, venous (not capillary) DBS cortisol and 17-OHP concentrations only. To assess the comparability between capillary and venous DBS cortisol and 17-OHP concentrations, a Bland–Altman analysis as well as a Passing–Bablok regression were conducted (Figure 1, Box B) [23,24]. CAH monitoring data obtained from routine clinical sampling at the Charité–University Hospital Berlin was used for the analysis, including DBS cortisol and 17-OHP concentrations from venous and capillary blood, simultaneously measured in 15 pediatric patients aged from 2 months to 11 years (median: 8 years). One parallel venous and capillary DBS sample was obtained from each patient between the morning and late afternoon and between 1–9 h after the last HC administration.

In the Bland-Altman analysis, the differences in the measurements in the two matrices were plotted versus the mean of the capillary and venous concentrations. Due to the large concentration range, the relative method differences were presented. The agreement interval was defined as within the mean difference  $\pm 1.96$ \*standard deviation (SD) [23,25].

For the Passing-Bablok regression, scatter plots of venous versus capillary DBS concentrations were generated, including a regression line, a 95% confidence interval (CI) of its intercept and slope, as well as a regression function. The intercept and slope of the line of identity laying within the CI of the regression were used to demonstrate whether there was no constant and proportional difference between the two examined methods [24,26].

### *2.3. Step C: Derivation and Evaluation of Venous and Capillary DBS 17-OHP Target Morning Concentration Range for Pediatric CAH Patients: PK/PD Model Predictions*

The developed PK/PD model (Figure 1, Box A) was applied to derive a DBS 17-OHP target morning concentration range in simulations ( $n = 1000$ ; Figure 1, Box C1). To predict physiological (=healthy) DBS 17-OHP concentrations, physiological plasma cortisol concentrations, densely sampled over 24 h from 28 non-CAH children aged from 5 to 9 years (Figure 2) [27,28], were used as the PK (plasma cortisol) input, inhibiting the synthesis of 17-OHP. The 17-OHP compartment was initialized with the median 17-OHP baseline, i.e., morning concentrations observed in the young children and infants in the Alkindi® (Cardiff Medicentre, Cardiff, UK) trial (=14.4 nmol/L). The prediction focused on physiological DBS 17-OHP concentrations simulated between 6 and 8 a.m. in order to cover the monitoring time range of interest, corresponding to the time before the morning dose.

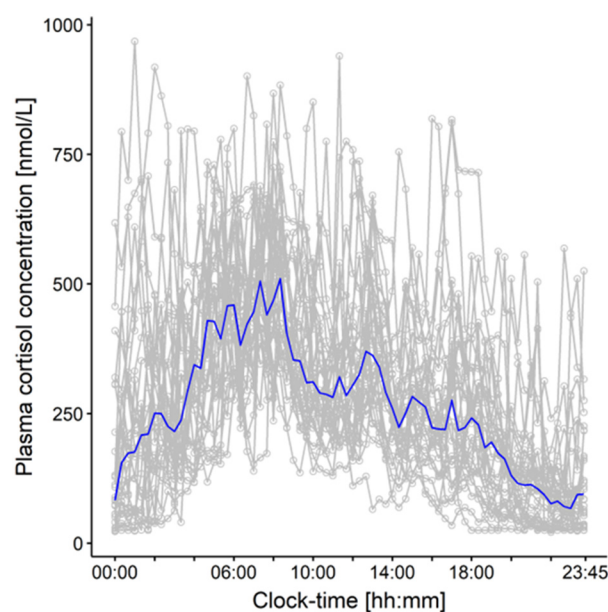


**Figure 2.** Individual plasma cortisol concentration-time profiles (gray) and median plasma cortisol concentration-time profiles (blue) obtained over 24 h from 28 healthy children aged 5–9 years.

To avoid a higher risk for adverse events, it is advised not to let the 17-OHP concentrations decrease to physiological ranges in CAH therapy [1]. Indeed, among clinical experts, the target 17-OHP concentrations are assumed to be approximately 3–5 times higher than physiological 17-OHP concentrations. Thus, the simulated physiological DBS 17-OHP morning concentrations were multiplied by 3 and by 5 to approximate the DBS 17-OHP target morning concentration range.

To assess the plausibility of the simulation-derived DBS 17-OHP target morning concentration range, a simple calculation of an expected DBS 17-OHP target morning range was performed (Figure 1, Box C2). The calculation of the expected range was based on baseline 17-OHP concentrations which were simultaneously measured in plasma and in DBS in the same young children and infants who were investigated during the Alkindi® (Cardiff Medicentre, Cardiff, UK) study. The ratio of these plasma and DBS 17-OHP baseline concentrations observed in the two age groups as well as the (adult) plasma 17-OHP target morning concentration range known from the literature [2], were used for determining the expected target morning range to which the model-based derived target morning range was then compared (Figure 1, Box C3).

### 3. Results

#### 3.1. Step A: Establishing a Quantitative Relationship between Plasma Cortisol (PK) and Venous DBS 17-OHP (PD) Concentrations in Pediatric CAH Patients: PK/PD Clinical Trial Data and Model Development

##### 3.1.1. Data and Graphical Evaluation

The observed concentration-time profiles of DBS 17-OHP (Figure 3A) indicated a trend towards a u-shape relationship, which was more pronounced in the young children patient cohort due to the longer sampling interval. This u-shape trend indicated an initial decrease of 17-OHP, likely due to the hydrocortisone treatment-mediated inhibition of 17-OHP synthesis, followed by a subsequent increase of 17-OHP due to decreasing plasma cortisol concentrations after hydrocortisone administration. The result of these mechanisms/processes was also visible in DBS 17-OHP versus plasma cortisol concentrations (Figure 3B), revealing 17-OHP decreasing with increasing cortisol concentrations, except the highest cortisol concentrations measured right after hydrocortisone administration, i.e., before the feedback mechanism set in (gray box in Figure 3B). The DBS 17-OHP concentra-

tions, including the concentrations at baseline, had similar ranges in young children and infants.

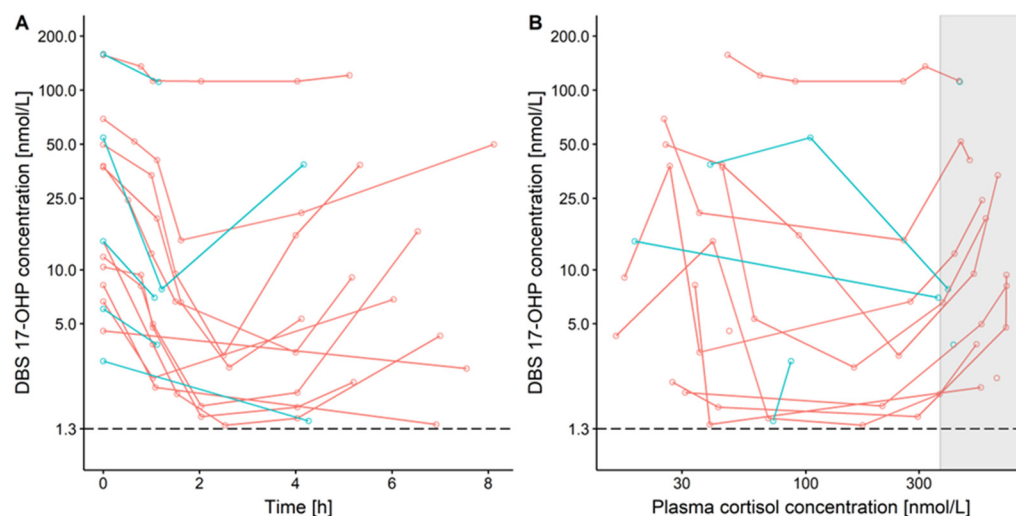


**Figure 3.**  $17\alpha$ -hydroxyprogesterone (17-OHP) concentrations measured in venous dried blood spots (DBS) over time after first (baseline) observation, semi-log scale (A) and versus plasma cortisol concentration, log scales (B), in pediatric CAH patients receiving hydrocortisone single morning dose. Red: young children, blue: infants, dashed line: lower limit of quantification = 1.3 nmol/L, gray box: highest plasma cortisol concentrations directly after hydrocortisone administration.

### 3.1.2. PK/PD Modeling

Based on the exploratory graphical analysis, the PK/PD model was developed to describe a cortisol-mediated inhibition of the 17-OHP synthesis, concretely on its synthesis rate  $k_{syn}$  (indirect response model; Figure 4). The full PK/PD model scheme (Supplementary Figure S1), information on the estimated pediatric individual parameters from Stachanow et al. [11], which were part of the dataset, corresponding model equations and the NONMEM model code can be found in Supplementary Materials.

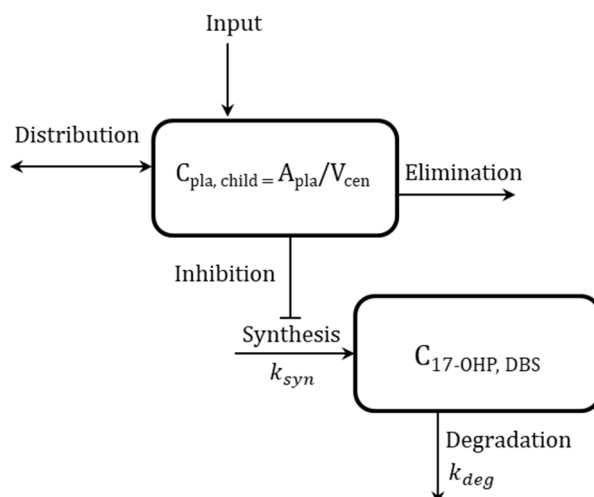


**Figure 4.** Simplified schematic representation of developed pharmacokinetic/pharmacodynamic (PK/PD) model for cortisol (top box)-mediated inhibition of synthesis of  $17\alpha$ -hydroxyprogesterone (17-OHP; bottom box). Pediatric cortisol concentration in plasma ( $C_{pla, child}$ ), pediatric cortisol amount ( $A_{pla}$ ), central volume of distribution ( $V_{cen}$ ), 17-OHP concentration in dried blood spots ( $C_{17-OHP, DBS}$ ), synthesis rate constant of 17-OHP ( $k_{syn}$ ), and first-order degradation rate constant of 17-OHP ( $k_{deg}$ ). For the full model scheme of the developed PK/PD model, see Supplementary Material.

The maximum inhibitory effect ( $I_{\max}$ ) was pre-defined as 1 (=100% inhibition), and the Hill Factor (Hill) was fixed to 1 after obtaining estimates close to 1 (Table 1). The synthesis rate constant  $k_{\text{syn}}$  was defined as the product of the estimated first-order degradation rate constant ( $k_{\text{deg}}$ ) and the DBS 17-OHP concentration at baseline ( $17\text{-OHP}_{\text{BASE}}$ ). The cortisol concentration inhibiting 50% of the maximum inhibitory effect ( $IC_{50}$ ) was estimated to be 21 nmol/L with a high estimated interindividual variability (IIV on  $IC_{50}$  = 104 %CV), which was not explained by any covariate present in the dataset, such as body weight, corticosteroid-binding globulin (CBG) or albumin. Relative standard errors of the estimated model parameters were low, except for IIV on  $IC_{50}$  (53%).

**Table 1.** Parameter estimates of developed pharmacokinetic/pharmacodynamic (PK/PD) model for cortisol (drug) and  $17\alpha$ -hydroxyprogesterone (biomarker) concentrations in young children and infants.

Parameter	Estimate (RSE, %)
<b>Structural model</b>	
$k_{\text{deg}}$ [1/h]	1.22 (7.0)
$IC_{50}$ [nmol/L]	21.0 (27)
$I_{\max}$ [-]	1 *
Hill [-]	1 *
<b>Interindividual variability (IIV)</b>	
IIV on $k_{\text{deg}}$ , %CV	5.0*
IIV on $IC_{50}$ , %CV	104 (53)
IIV on $17\text{-OHP}_{\text{BASE}}$ , %CV	131 *
<b>Residual unexplained variability (RUV)</b>	
RUV [%CV]	38.1 (15)

\* Fixed parameter. Residual variability was estimated by an additive model on a logarithmic scale.  $17\text{-OHP}_{\text{BASE}}$ :  $17\alpha$ -hydroxyprogesterone (17-OHP) dried blood spot concentration at baseline, Hill: Hill coefficient,  $IC_{50}$ : Cortisol concentration inhibiting 50% of the maximum inhibitory effect  $I_{\max}$ ,  $k_{\text{deg}}$ : first-order degradation rate constant of 17-OHP, RSE: Relative standard error.

The GOF plots and the VPC indicated that the venous DBS 17-OHP observations were appropriately described by the PK/PD model (Supplementary Materials, Figures S2 and S3).

### 3.2. Step B: Comparison of Capillary and Venous DBS Cortisol and 17-OHP Concentrations from Routine Monitoring in Pediatric CAH Patients: Bland-Altman and Passing-Bablok Regression Analysis

To investigate whether venous DBS concentrations (as in step (A)) are comparable to capillary DBS concentrations, which can be obtained in clinical practice as well, the Bland-Altman and Passing-Bablok regression analyses were conducted (Figure 1, Box B). The Bland-Altman analysis (Figure 5A,B) did not show any substantial bias between capillary and venous DBS measurements for the drug (cortisol mean difference: +3.13%) and 17-OHP (mean difference: +3.73%). Almost all data points except one each (93% of both cortisol and 17-OHP measurements) were within the range of the mean difference  $\pm 1.96 \times \text{SD}$ . Moreover, the Passing-Bablok regression also showed an agreement between the venous and capillary DBS concentrations since, for both cortisol and 17-OHP, the lines of identity lay within the CIs of the regression lines (Figure 5C,D). The slopes of the regression lines for cortisol and 17-OHP were close to 1 (1.0 and 0.7, respectively), and the y-intercept for cortisol was close to 0 (0.8), indicating a high similarity between capillary and venous DBS concentrations.

Thus, the capillary and venous DBS concentrations were considered comparable for cortisol and 17-OHP. This finding allowed us to use the developed PK/PD model for deriving a 17-OHP target morning range for DBS sampling, which is applicable for both venous and capillary DBS 17-OHP concentrations (Figure 1, Box C1).

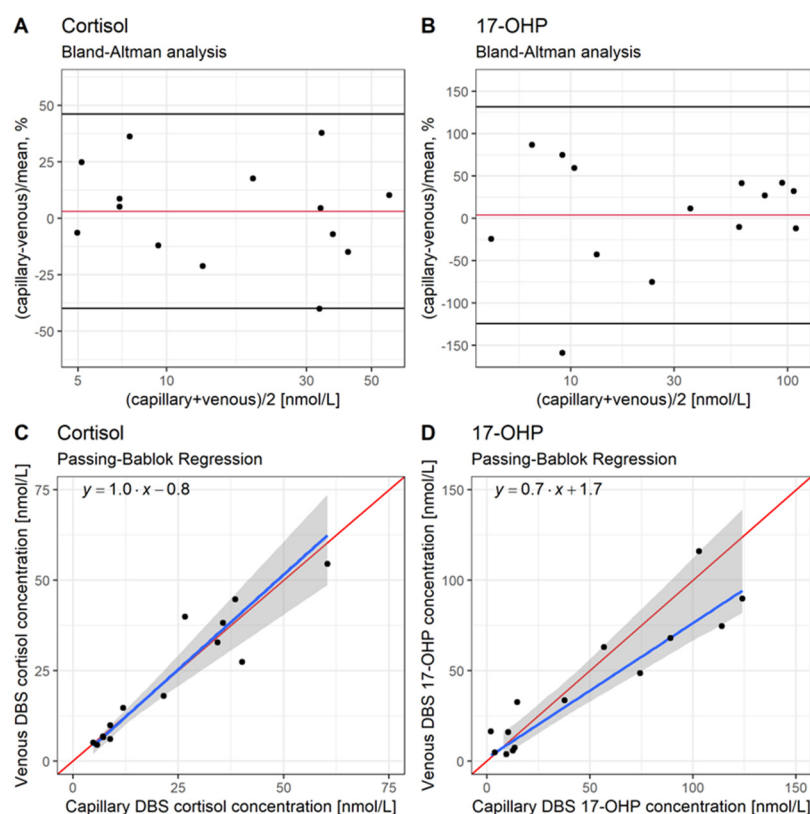


**Figure 5.** Comparison between capillary and venous cortisol (A,C) and  $17\alpha$ -hydroxyprogesterone (17-OHP, A,D) dried blood spot (DBS) concentrations, obtained from 15 pediatric congenital adrenal hyperplasia (CAH) patients. (A,B): Bland–Altman analysis. Capillary-venous/mean of difference [%] versus the mean of capillary venous cortisol and DBS 17-OHP concentrations. Red line: Mean difference [%], black lines: Mean difference  $-1.96 \times \text{SD}$  (standard deviation) and mean difference  $+1.96 \times \text{SD}$  [%]. (C,D): Passing–Bablok regression. Red line: line of identity, blue line: regression line, gray area: 95% confidence interval for the regression line.

### 3.3. Step C: Derivation and Evaluation of Venous and Capillary DBS 17-OHP Target Morning Concentration Range for Pediatric CAH Patients: PK/PD Model Predictions

The PK/PD model-based derivation of the DBS 17-OHP morning target concentration range for pediatric CAH patients resulted in a range of 2.1–8.3 nmol/L (Figure 6, median: 4.4 nmol/L) after multiplying simulated physiological (=healthy) concentrations by factors 3 and 5 as assumed ratios for the target-to-physiological 17-OHP concentrations (see Section 2.3). The derived target range (interquartile range) excluded 25% of the lowest and 25% of the highest concentrations of all simulated physiological DBS 17-OHP morning (6–8 a.m.) concentrations due to the very high variability in the prediction.

To assess the plausibility of the derived target range (Figure 1, box C3), an approximately expected DBS 17-OHP target morning range was calculated (Figure 1, box C2) based on the known (adult) 17-OHP target morning concentration range in plasma (12–36 nmol/L) [2], divided by the median plasma/DBS 17-OHP morning concentration ratio of 9.29 which was observed in young children and infants ( $n = 18$ ) during the Alkindi<sup>®</sup> (Cardiff Medicentre, Cardiff, UK) trial (Supplementary Materials, Figure S4).

Since the DBS 17-OHP target morning range (2.1–8.3 nmol/L), derived from the modeling and simulation framework analysis, was in the same order of magnitude as the approximately expected range (1.3–3.9 nmol/L), indicated by the red horizontal lines (Figure 6), the results were judged as plausible.

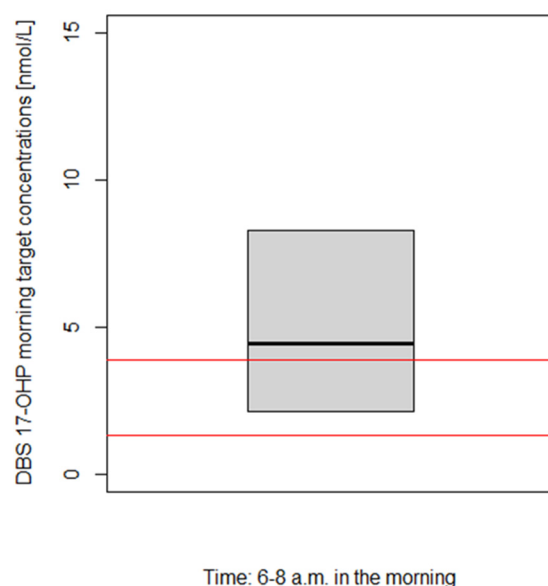


**Figure 6.** Derived dried blood spot (DBS) 17 $\alpha$ -hydroxyprogesterone (17-OHP) target morning concentration range (=model-predicted physiological range multiplied by 3 to 5). Interquartile range (gray box) and median (black line) of the derived DBS 17-OHP target morning concentrations (see step (C1) in text). Red lines: Calculated expected target DBS 17-OHP concentration range in the morning (see step (C2) in text).

#### 4. Discussion

We developed a modeling and simulation framework based on data from different matrices (i.e., plasma, venous and capillary DBS samples) and different sources (i.e., clinical trials, clinical routine and literature data) due to the limited availability of data. The framework included a PK/PD model which successfully linked DBS 17-OHP to plasma cortisol concentrations in pediatric CAH patients. By leveraging this framework, we were able to derive a plausible target morning concentration range for the clinically important biomarker 17-OHP, for DBS sampling in pediatric CAH patients, in the range of 2–8 nmol/L, which is applicable for both venous or capillary DBS samples.

The PK/PD model captured the known mechanism of administered hydrocortisone inhibiting 17-OHP biosynthesis via the suppression of the HPA-axis by a negative feedback mechanism [1,2,12]. This mechanism was implemented in an indirect response model with 17-OHP synthesis inhibition, well characterizing the u-shape trend observed in the 17-OHP concentration-time profiles. A main limitation of *in silico* approaches such as PK/PD modeling is that the purpose and validity of the model depend on the data it is based on. The development of the PK/PD model was based on sparse pediatric clinical trial data and therefore did not allow for a more complex model structure, e.g., including covariate relationships. Despite the limited available data, as typical for trials in this vulnerable patient population, the model resulted in plausible parameter estimates with satisfactory precision. The estimated  $IC_{50}$  of 21.0 nmol/L (=plasma cortisol concentration leading to 50% of maximum inhibitory effect  $I_{max}$  on 17-OHP synthesis) was in the same order of magnitude as previously determined  $IC_{50}$  values, e.g., 40.3 nmol/L by Al-Kofahi et al. [29] and 48.6 nmol/L by Melin et al. [30]. The current lower estimate of  $IC_{50}$  can be explained by the difference in matrices between the former studies and our analysis. As in the current study, plasma cortisol PK was linked to PD in full blood obtained via DBS, where DBS cortisol concentrations are substantially lower than plasma concentrations, an approximately 2-fold lower  $IC_{50}$  value, in line with reported plasma/DBS cortisol ratio ranges [11], was expected.

For the derivation of a DBS 17-OHP target morning concentration range, published physiological plasma cortisol concentrations from healthy children aged between 5 and

9 were applied [27,28]. This age range was also covered in the young children cohort in the Alkindi<sup>®</sup> (Cardiff Medicentre, Cardiff, UK) trial (2–6 years). Besides the young children data, infant data (28 days–2 years) was also included due to the very similar 17-OHP concentrations between these two age groups in the current study. To support this inclusion, we also developed a PK/PD model based on young children only. No significant differences were found in the estimated model parameters, their imprecisions, and the derived DBS 17-OHP concentrations using this further reduced model dataset. The presented model for infants and young children can serve as a basis to obtain DBS 17-OHP target concentrations in, e.g., neonates or older children in the future when corresponding data becomes available.

Bland-Altman and Passing-Bablok regression analyses were conducted to translate the modeling and simulation results which are based on venous DBS 17-OHP concentrations to clinical routine where, besides venous, also capillary DBS 17-OHP concentrations can be sampled. The analyses demonstrated that capillary and venous DBS measurements of cortisol and 17-OHP are comparable. Thus, the results from our previously published PK model [11], as well as from this PK/PD analysis (both based on venous DBS data), can be applied to capillary DBS samples.

The plausibility of the derived DBS 17-OHP morning concentration range was assessed by comparing the results to an expected concentration range which was based on the 17-OHP target morning concentration range in plasma, reported in Merke et al. [2]. This expected target range is to be viewed as a simple plausibility check only since the underlying plasma 17-OHP target range applies to adults. To the best of our knowledge, no further 17-OHP target concentrations have been reported.

Whereas a target range is established for plasma 17-OHP concentrations [2], there are no cortisol target concentrations suggested except for mimicking the physiological circadian rhythm [1]. 17-OHP is a commonly used biomarker as it is a precursor of cortisol and androgens, of which elevated concentrations are closely linked to the clinical signs of CAH. DBS sampling can facilitate regular and less invasive measurement of cortisol and numerous biomarkers [5]. Therefore, besides in plasma, it is also needed to identify biomarker target concentrations in DBS.

Despite its advantages and high potential, especially for pediatric patients, DBS sampling is not fully established yet in drug and biomarker monitoring. The techniques used for DBS sampling and measurements can vary between laboratories [6,31,32], and therefore further research, the establishment of standardization of DBS sampling and of the corresponding bioanalysis is needed. Furthermore, taking the patients' hematocrit values into consideration is vital to ensure accurate quantification of the analyte, as the hematocrit influences the spreading of the sampled blood on the DBS filter paper [5,7,33]. Since hematocrit values are known to be higher in neonates [33], these are potentially valuable covariates to be investigated in future analyses, once available. Target biomarker concentrations for alternative child-friendly sampling techniques, such as mouth swabs to measure steroids in saliva, are to be investigated in the future, for which the developed modeling and simulation framework could serve as a starting point.

Since the cortisol-mediated inhibition of the 17-OHP synthesis, which is incorporated into the PK/PD model, does not suffice to characterize the circadian rhythm of 17-OHP during the day, we focused on the most relevant target concentrations in the morning only. Circadian rhythms of 17-OHP and other CAH-relevant analytes, e.g., corticosteroid-binding globulin, have already been quantified within PK model analyses [30,34]. In the future, the presented PK/PD model can be expanded with the impact of ACTH on the circadian rhythm of 17-OHP to suggest target DBS 17-OHP concentration-time profiles indicating the target ranges for any time of the day.

## 5. Conclusions

Within the modeling and simulation framework described here, we obtained a plausible 17-OHP concentrations target range to be measured before the morning hydrocortisone

dose for the first time using DBS sampling methodology. This derived target morning range has the potential to develop further and could provide guidance for monitoring young children suffering from CAH in the future.

Further model development is suggested to derive circadian DBS-derived target 17-OHP concentration-time profiles over 24 h to contribute meaningful target concentrations which clinicians can refer to for the treatment of CAH in children.

**Supplementary Materials:** The supporting information can be downloaded at: <https://www.mdpi.com/article/10.3390/ph16030464/s1>. Figure S1. Schematic representation of developed pharmacokinetic/pharmacodynamic (PK/PD) model. PK parameters of which the pediatric individual estimates from the previous PK model (Stachanow et al.) [2] were used as part of the dataset are marked in orange. Pharmacokinetics: Bioavailability (F), amount in depot compartment (Adepot), maximum absorption rate (Vmax), amount in depot compartment resulting in half of Vmax (Km), amount bound (Ab), amount bound to albumin (Ab:Alb), amount associated to red blood cells (Ab:RBC), unbound amount (Au), amount bound to corticosteroid-binding globulin (Ab:CBG), linear non-specific parameter for albumin binding (NSAlb) and association to red blood cells (kaRBC), maximum binding capacity (Bmax), equilibrium dissociation constant (Kd), intercompartmental clearance (Q), central volume of distribution (Vcen), peripheral volume of distribution (Vper), cortisol plasma baseline of children (BASEchild, pla). The dashed line divides the central compartment into the Ab and Au subcompartments, respectively. Pharmacodynamics: 17- $\alpha$ -hydroxyprogesterone (17-OHP) concentration in dried blood spots (C17-OHP, DBS), synthesis rate constant of 17-OHP (ksyn), first-order elimination rate constant of 17-OHP (kdeg). Figure S2. Goodness-of-fit plots for developed pharmacokinetic/pharmacodynamic (PK/PD) model. A: Population-predicted dried blood spot (DBS) 17- $\alpha$ -hydroxyprogesterone (17-OHP) concentrations versus observed DBS 17-OHP concentrations, B: Individual DBS 17-OHP predictions versus observed DBS 17-OHP concentrations, C: Conditional weighted residuals versus population-predicted DBS 17-OHP concentrations, D: Conditional weighted residuals versus time. Red dots: children (cohort 1, age: 2–6 years), green dots: infants (cohort 2, age: 28 days–2 years), red line: line of identity (A, B), line  $y = 0$  (C, D), vertical dashed line: lower limit of quantification (LLOQ) = 1.3 nmol/L. Figure S3. Visual predictive check ( $n = 1000$ ) for developed pharmacokinetic/pharmacodynamic (PK/PD) model. A: Circles: 17- $\alpha$ -hydroxyprogesterone (17-OHP) dried blood spot (DBS) observations, solid line: 50th percentile of observed (black) and simulated (gray) DBS 17-OHP concentrations, dashed lines: 10th and 90th percentiles of observed (black) and simulated (gray) DBS 17-OHP concentrations, shaded areas: 95% confidence intervals for the percentiles of the simulated data. B: Black line: Observed probability of DBS 17-OHP concentrations below lower limit of quantification (LLOQ), gray area: 95% confidence interval for simulated probability of 17-OHP concentrations below LLOQ. Figure S4. Plasma to dried blood spot (DBS) 17- $\alpha$ -hydroxyprogesterone (17-OHP) concentration ratio, measured at baseline in the morning, in young children and infants. Table S1. Summary of population characteristics in all datasets leveraged in the modeling and simulation analysis, by framework step as described in Figure 1.

**Author Contributions:** Conceptualization, V.S., R.M. and C.K.; formal analysis, V.S.; data collection, U.N., O.B., N.A.-B., P.H., R.J.R. and M.J.W.; writing—original draft preparation, V.S.; writing—review and editing, all authors; visualization, V.S.; supervision, R.M. and C.K. All authors have read and agreed to the published version of the manuscript.

**Funding:** The work was carried out under a Cooperation Agreement between Freie Universitaet and Diurnal, funded by Diurnal Ltd, Cardiff, CF14 4UJ, United Kingdom.

**Institutional Review Board Statement:** Not applicable.

**Informed Consent Statement:** Not applicable.

**Data Availability Statement:** Data is contained within the article and Supplementary Material.

**Acknowledgments:** The authors acknowledge the High-Performance Computing Service of ZEDAT at Freie Universitaet Berlin (<https://www.zedat.fu-berlin.de/HPC/Home>, accessed on 1 March 2023) for computing time. We acknowledge support from the Open Access Publication Initiative of Freie Universität Berlin for funding the publication of this article.

**Conflicts of Interest:** R.M., D.B., N.A., M.J.W. and P.H. have nothing to declare. V.S. is currently working at Sanofi in Ghent, Belgium. J.M. is currently working at AstraZeneca in Gothenburg, Sweden. C.K. and W.H. report grants from an industry consortium (AbbVie Deutschland GmbH & Co. K.G., AstraZeneca, Boehringer Ingelheim Pharma GmbH & Co. K.G., Grünenthal GmbH, F. Hoffmann-La Roche Ltd., Novo Nordisk, Merck KGaA and SANOFI) for the PharMetrX Ph.D. program. C.K. reports an additional grant from the Innovative Medicines Initiative-Joint Undertaking ('DDMoRe'), grants from the Federal Ministry of Education and Research within the Joint Programming Initiative on Antimicrobial Resistance Initiative (JPIAMR) and from the European Commission within the Horizon 2020 framework program ("FAIR"), all outside the submitted work. C.K. reports a grant from Diurnal Ltd. U.N. and O.B. report a fee for presentation, and U.N. reports grants from Diurnal Ltd. R.R. is the Director of Diurnal Limited.

## References

1. Van der Grinten, H.L.C.; Speiser, P.W.; Faisal Ahmed, S.; Arlt, W.; Auchus, R.J.; Falhammar, H.; Flück, C.E.; Guasti, L.; Huebner, A.; Kortmann, B.B.M.; et al. Congenital Adrenal Hyperplasia—Current Insights in Pathophysiology, Diagnostics, and Management. *Endocr. Rev.* **2022**, *43*, 91–159. [[CrossRef](#)] [[PubMed](#)]
2. Merke, D.P.; Bornstein, S.R. Congenital Adrenal Hyperplasia. *Lancet* **2005**, *365*, 2125–2136. [[CrossRef](#)] [[PubMed](#)]
3. Balsamo, A.; Baronio, F.; Ortolano, R.; Menabo, S.; Baldazzi, L.; Di Natale, V.; Vissani, S.; Cassio, A. Congenital Adrenal Hyperplasias Presenting in the Newborn and Young Infant. *Front. Pediatr.* **2020**, *8*, 593315. [[CrossRef](#)] [[PubMed](#)]
4. Speiser, P.W.; Arlt, W.; Auchus, R.J.; Baskin, L.S.; Conway, G.S.; Merke, D.P.; Meyer-Bahlburg, H.F.L.; Miller, W.L.; Hassan Murad, M.; Oberfield, S.E.; et al. Congenital Adrenal Hyperplasia Due to Steroid 21-Hydroxylase Deficiency: An Endocrine Society\* Clinical Practice Guideline. *J. Clin. Endocrinol. Metab.* **2018**, *103*, 4043–4088. [[CrossRef](#)] [[PubMed](#)]
5. Qasrawi, D.O.; Boyd, J.M.; Sadrzadeh, S.M.H. Measuring Steroids from Dried Blood Spots Using Tandem Mass Spectrometry to Diagnose Congenital Adrenal Hyperplasia. *Clin. Chim. Acta* **2021**, *520*, 202–207. [[CrossRef](#)] [[PubMed](#)]
6. Edelbroek, P.M.; Van Der Heijden, J.; Stolk, L.M.L. Dried Blood Spot Methods in Therapeutic Drug Monitoring: Methods, Assays, and Pitfalls. *Ther. Drug Monit.* **2009**, *31*, 327–336. [[CrossRef](#)] [[PubMed](#)]
7. Wilhelm, A.J.; den Burger, J.C.G.; Swart, E.L. Therapeutic Drug Monitoring by Dried Blood Spot: Progress to Date and Future Directions. *Clin. Pharmacokinet.* **2014**, *53*, 961–973. [[CrossRef](#)]
8. Grecsó, N.; Zádori, A.; Szécsi, I.; Baráth, Á.; Galla, Z.; Bereczki, C.; Monostori, P. Storage Stability of Five Steroids and in Dried Blood Spots for Newborn Screening and Retrospective Diagnosis of Congenital Adrenal Hyperplasia. *PLoS ONE* **2020**, *15*, e0233724. [[CrossRef](#)]
9. Lando, V.S.; Batista, M.C.; Nakamura, I.T.; Mazi, C.R.; Mendonca, B.B.; Brito, V.N. Effects of Long-Term Storage of Filter Paper Blood Samples on Neonatal Thyroid Stimulating Hormone, Thyroxin and 17-Alpha-Hydroxyprogesterone Measurements. *J. Med. Screen.* **2008**, *15*, 109–111. [[CrossRef](#)]
10. Boelen, A.; Ruiters, A.F.C.; Claahsen-Van Der Grinten, H.L.; Endert, E.; Ackermans, M.T. Determination of a Steroid Profile in Heel Prick Blood Using LC-MS/MS. *Bioanalysis* **2016**, *8*, 375–384. [[CrossRef](#)]
11. Stachanow, V.; Neumann, U.; Blankenstein, O.; Bindellini, D.; Melin, J.; Ross, R.; Whitaker, M.J.; Huisinga, W.; Michelet, R.; Kloft, C. Exploring Dried Blood Spot Cortisol Concentrations as an Alternative for Monitoring Pediatric Adrenal Insufficiency Patients: A Model-Based Analysis. *Front. Pharmacol.* **2022**, *13*, 819590. [[CrossRef](#)] [[PubMed](#)]
12. Nella, A.A.; Mallappa, A.; Perritt, A.F.; Gounden, V.; Kumar, P.; Sinaii, N.; Daley, L.-A.; Ling, A.; Liu, C.-Y.; Soldin, S.J.; et al. A Phase 2 Study of Continuous Subcutaneous Hydrocortisone Infusion in Adults With Congenital Adrenal Hyperplasia. *J. Clin. Endocrinol. Metab.* **2016**, *101*, 4690–4698. [[CrossRef](#)] [[PubMed](#)]
13. Mould, D.R.; Upton, R.N. Basic Concepts in Population Modeling, Simulation, and Model-Based Drug Development. *CPT Pharmacomet. Syst. Pharmacol.* **2012**, *1*, e6. [[CrossRef](#)]
14. Neumann, U.; Whitaker, M.J.; Wiegand, S.; Krude, H.; Porter, J.; Davies, M.; Digweed, D.; Voet, B.; Ross, R.J.; Blankenstein, O. Absorption and Tolerability of Taste-Masked Hydrocortisone Granules in Neonates, Infants and Children under 6 Years of Age with Adrenal Insufficiency. *Clin. Endocrinol.* **2018**, *88*, 21–29. [[CrossRef](#)]
15. Neumann, U.; Burau, D.; Spielmann, S.; Whitaker, M.J.; Ross, R.J.; Kloft, C.; Blankenstein, O. Quality of Compounded Hydrocortisone Capsules Used in the Treatment of Children. *Eur. J. Endocrinol.* **2017**, *177*, 239–242. [[CrossRef](#)] [[PubMed](#)]
16. Michelet, R.; Melin, J.; Parra-Guillen, Z.P.; Neumann, U.; Whitaker, M.J.; Stachanow, V.; Huisinga, W.; Porter, J.; Blankenstein, O.; Ross, R.J.; et al. Paediatric Population Pharmacokinetic Modelling to Assess Hydrocortisone Replacement Dosing Regimens in Young Children. *Eur. J. Endocrinol.* **2020**, *183*, 357–368. [[CrossRef](#)]
17. R Core Team. *R: A Language and Environment for Statistical Computing*; R Foundation for Statistical Computing: Vienna, Austria, 2019. Available online: <https://www.R-Project.org/> (accessed on 1 March 2023).
18. RStudio Team. *RStudio: Integrated Development Environment for R*; RStudio, PBC: Boston, MA, USA, 2020; Available online: <http://www.Rstudio.com/> (accessed on 1 March 2023).
19. Zhang, L.; Beal, S.L.; Sheiner, L.B. Simultaneous vs. Sequential Analysis for Population PK/PD Data I: Best-Case Performance. *J. Pharmacokinet. Pharmacodyn.* **2003**, *30*, 387–404. [[CrossRef](#)] [[PubMed](#)]

20. Beal, S.L. Ways to Fit a PK Model with Some Data below the Quantification Limit. *J. Pharmacokinet. Pharmacodyn.* **2001**, *28*, 481–504. [[CrossRef](#)] [[PubMed](#)]
21. Beal, S.; Sheiner, L.B.; Boeckmann, A.; Bauer, R.J. *NONMEM User's Guides 1989–2009*; Icon Development Solutions: Ellicott City, MD, USA, 2009.
22. Keizer, R.J.; Karlsson, M.O.; Hooker, A. Modeling and Simulation Workbench for NONMEM: Tutorial on Pirana, PsN, and Xpose. *CPT Pharmacometrics Syst. Pharmacol.* **2013**, *2*, e50. [[CrossRef](#)]
23. Bland, J.M.; Altman, D.G. Statistical Methods for Assessing Agreement between Two Methods of Clinical Measurement. *Lancet* **1986**, *1*, 307–310. [[CrossRef](#)]
24. Bablok, W.; Passing, H. Application of Statistical Procedures Analytical Instrument Testing. *J. Automat. Chem.* **1985**, *7*, 74–79. [[CrossRef](#)] [[PubMed](#)]
25. Giavarina, D. Understanding Bland Altman Analysis. *Biochem. Med.* **2015**, *25*, 141–151. [[CrossRef](#)] [[PubMed](#)]
26. Bilic-Zulle, L. Lessons in Biostatistics Comparison of Methods: Passing and Bablok Regression. *Biochem. Med.* **2011**, *21*, 49–52. [[CrossRef](#)] [[PubMed](#)]
27. Barton, J.S.; Gardiner, H.M.; Cullen, S.; Hindmarsh, P.C.; Brook, C.G.D.; Preece, M.A. The Growth and Cardiovascular Effects of High Dose Growth Hormone Therapy in Idiopathic Short Stature. *Clin. Endocrinol.* **1995**, *42*, 619–626. [[CrossRef](#)]
28. Peters, C.J.; Hill, N.; Dattani, M.T.; Charmandari, E.; Matthews, D.R.; Hindmarsh, P.C. Deconvolution Analysis of 24-h Serum Cortisol Profiles Informs the Amount and Distribution of Hydrocortisone Replacement Therapy. *Clin. Endocrinol.* **2013**, *78*, 347–351. [[CrossRef](#)]
29. Al-Kofahi, M.; Ahmed, M.A.; Jaber, M.M.; Tran, T.N.; Willis, B.A.; Zimmerman, C.L.; Gonzalez-Bolanos, M.T.; Brundage, R.C.; Sarafoglou, K. An Integrated PK-PD Model for Cortisol and the 17-Hydroxyprogesterone and Androstenedione Biomarkers in Children with Congenital Adrenal Hyperplasia. *Br. J. Clin. Pharmacol.* **2021**, *87*, 1098–1110. [[CrossRef](#)]
30. Melin, J.; Parra-Guillen, Z.P.; Michelet, R.; Truong, T.; Huisinga, W.; Hartung, N.; Hindmarsh, P.; Kloft, C. Pharmacokinetic/Pharmacodynamic Evaluation of Hydrocortisone Therapy in Pediatric Patients with Congenital Adrenal Hyperplasia. *J. Clin. Endocrinol. Metab.* **2020**, *105*, E1729–E1740. [[CrossRef](#)]
31. Wagner, M.; Tonoli, D.; Varesio, E.; Hopfgartner, G. The Use of Mass Spectrometry to Analyze Dried Blood Spots. *Mass Spectrom. Rev.* **2016**, *35*, 361–438. [[CrossRef](#)]
32. Enderle, Y.; Foerster, K.; Burhenne, J. Clinical Feasibility of Dried Blood Spots: Analytics, Validation, and Applications. *J. Pharm. Biomed. Anal.* **2016**, *130*, 231–243. [[CrossRef](#)]
33. De Kesel, P.M.M.; Sadones, N.; Capiou, S.; Lambert, W.E.; Stove, C.P. Hemato-Critical Issues in Quantitative Analysis of Dried Blood Spots: Challenges and Solutions. *Bioanalysis* **2013**, *5*, 2023–2041. [[CrossRef](#)]
34. Melin, J.; Hartung, N.; Parra-Guillen, Z.P.; Whitaker, M.J.; Ross, R.J.; Kloft, C. The Circadian Rhythm of Corticosteroid-Binding Globulin Has Little Impact on Cortisol Exposure after Hydrocortisone Dosing. *Clin. Endocrinol.* **2019**, *91*, 33–40. [[CrossRef](#)] [[PubMed](#)]

**Disclaimer/Publisher's Note:** The statements, opinions and data contained in all publications are solely those of the individual author(s) and contributor(s) and not of MDPI and/or the editor(s). MDPI and/or the editor(s) disclaim responsibility for any injury to people or property resulting from any ideas, methods, instructions or products referred to in the content.

# Deriving target morning $17\alpha$ -hydroxyprogesterone concentrations in dried blood spots for pediatric congenital adrenal hyperplasia patients

Viktoria Stachanow <sup>1,2</sup>, Uta Neumann <sup>3</sup>, Oliver Blankenstein <sup>3,4</sup>, Nele Alder-Baerens <sup>4</sup>, Davide Bindellini <sup>1,2</sup>, Peter Hindmarsh <sup>5</sup>, Richard Ross <sup>6</sup>, Martin J Whitaker <sup>6</sup>, Johanna Melin <sup>1,2</sup>, Wilhelm Huisinga <sup>7</sup>, Robin Michelet <sup>1,\*</sup> and Charlotte Kloft <sup>1</sup>

<sup>1</sup> Department of Clinical Pharmacy and Biochemistry, Institute of Pharmacy, Freie Universitaet Berlin, Kelchstr 31, 12169 Berlin, Germany

<sup>2</sup> Graduate Research Training Program, PharMetrx, Berlin, Germany

<sup>3</sup> Charité-Universitätsmedizin, Berlin, Germany

<sup>4</sup> Labor Berlin, Charité Vivantes GmbH, Berlin, Germany

<sup>5</sup> Developmental Endocrinology Research Group, UCL Institute of Child Health, London, UK

<sup>6</sup> University of Sheffield, UK

<sup>7</sup> Institute of Mathematics, Universität Potsdam, Germany

\* Correspondence: [robin.michelet@fu-berlin.de](mailto:robin.michelet@fu-berlin.de)

## 1 Pharmacokinetic/Pharmacodynamic model structure

### Differential equations

$$dA_{depot}/dt = -\frac{V_{abs,max} \cdot A_{depot}}{K_{abs,50} + A_{depot}}$$

$$dA_{pla,child}/dt = \frac{V_{abs,max} \cdot A_{depot}}{K_{abs,50} + A_{depot}} - CL/V_{cen} \cdot A_u - Q/V_{cen} \cdot A_u + Q/V_{per} \cdot A_{per}$$

$$dA_{per}/dt = Q/V_{cen} \cdot A_u - Q/V_{per} \cdot A_{per}$$

$$dA_{RBC}/dt = K_{aRBC} \cdot A_u - K_{aRBC} \cdot A_{RBC}$$

$$dC_{17-OHP,DBS}/dt = k_{syn} \cdot I - k_{deg} \cdot C_{17-OHP,DBS}$$

### Initial conditions

$$A_{depot,0} = F \cdot DOSE$$

$$A_{pla,child,0} = BASE_{child,pla} \cdot V_{cen}$$

$$A_{per,0} = 0$$

$$A_{RBC,0} = 0$$

$$C_{17-OHP,DBS,0} = OHP_{BASE}$$

### State variables and outputs

$$k_{syn} = OHP_{BASE} \cdot k_{deg}$$

$$I = 1 - \frac{I_{max} \cdot C_{pla,child}^{Hill}}{IC_{50}^{Hill} + C_{pla,child}^{Hill}}$$

$$K_{dA} = K_d \cdot V_{cen}$$

$$A_{max} = B_{max} \cdot V_{cen}$$

$$A_u$$

$$= \frac{A_{pla,child} - K_{dA} \cdot (1 + NS_{Alb}) - A_{max} + \sqrt{(A_{pla,child} - K_{dA} \cdot (1 + NS_{Alb}) - A_{max})^2 + 4 \cdot A_{pla,child} \cdot K_{dA} \cdot (1 + NS_{Alb})}}{2 \cdot (1 + NS_{Alb})}$$

$$C_{pla,child}(t) = A_{pla,child}(t) / V_{cen}$$

### Estimated model parameters

$$k_{deg,ind} = k_{deg,pop} \cdot e^{\eta_{kdeg,ind}}$$

$$\eta_{kdeg} \sim N(0, \omega_{kdeg})$$

$$IC_{50,ind} = IC_{50,pop} \cdot e^{\eta_{IC50,ind}}$$

$$\eta_{IC50} \sim N(0, \omega_{IC50})$$

### Fixed model parameters\*

$$Hill = 1$$

$$OHP_{BASE,pop} = OHP_{BASE,observed} \text{ OR } 1/2 \text{ LLOQ}$$

$$OHP_{BASE,ind} = OHP_{BASE,pop} \cdot e^{\eta_{OHPBASE,ind}} \cdot RUV$$

$$\eta_{OHPBASE} \sim N(0, \omega_{OHPBASE})$$

$$\eta_{OHPBASE} = 1$$

\*2 out of 18 17-OHP baseline DBS observations were below the lower limit of quantification (LLOQ) and were replaced by the LLOQ divided by two (= 1.3/2 nmol/L).

## Handling data below the lower limit of quantification

25% (22/88) of all venous DBS 17-OHP concentrations were below the LLOQ (22.5% in young children and 35.3% in infants). Thus, the M3 method [1] was applied where all observations were fitted to the model, including the concentrations below the LLOQ which were treated as censored observations for which the likelihood of an observation being below the LLOQ given the model parameters is maximized.

### 2 NONMEM model code

\$PROBLEM

PKPD indirect response model, cortisol plasma and 17-OHP in DBS, pediatric model

\$INPUT

ID TIME AMT DROP=RATE MDV ODV EVID BLQ CMT FLAG ICL IV1 IQ IV2 IKaRBC IIBASE  
IBMAX IKD INSALB IVM IKM IF1

\$DATA Data\_PKPD.csv IGNORE=@

\$SUBROUTINE ADVAN13 TOL=15

\$MODEL

NCOMPARTMENTS=5 NPARAMETERS=3

COMP = (DEPOT DEFDOSE) ;dose compartment

COMP = (CENTRAL DEFOBSERVATION) ;central plasma concentration

COMP = (PERIPH) ;peripheral plasma compartment

COMP = (OUTPUT1) ;compartment with cortisol bound to erythrocytes

COMP = (EFFECT) ;compartment with indirect response, inhibition of synthesis

\$PK

;; individual PK parameter estimates from previous PK model (Stachanow et al., 2022) [2]

CL = ICL ;clearance (CL)

V1 = IV1 ;central volume of distribution (V<sub>cen</sub>)

Q = IQ ;intercompartmental clearance (Q)

V2 = IV2 ;peripheral volume of distribution (V<sub>per</sub>)

KaRBC = IKaRBC ;association constant for red blood cells (kaRBC)

IIBASE = IIBASE ;pediatric plasma cortisol baseline (BASE<sub>child,pla</sub>)

BMAX = IBMAX ;maximum binding capacity for CBG binding (B<sub>max</sub>)

KD = IKD ;equilibrium dissociation constant for CBG binding (K<sub>d</sub>)

NSALB = INSALB ;linear non-specific parameter for albumin binding (NSAlb)

VM = IVM ;maximum absorption rate (V<sub>max</sub>)

KM = IKM ;amount in depot compartment resulting in half of V<sub>max</sub> (K<sub>m</sub>)

F1 = IF1 ;bioavailability (F)

```

;; PD Parameters
IMAX = 1                ;maximum inhibitory effect (Imax)
GAM = 1                 ;Hill coefficient (Hill)

TVKDEG = THETA(1)      ;first-order degradation rate constant of 17-OHP (kdeg)
TVIC50 = THETA(2)      ;cortisol conc. leading to 50% of the maximum inhibitory effect (IC50)
MU_1 = TVKDEG
MU_2 = TVIC50

KDEG = EXP(MU_1 + ETA(1))
IC50 = EXP(MU_2 + ETA(2))

;17-OHP baseline observations in DBS
BASEDV = ODV
;17-OHP baseline observations in DBS if no baseline observation given
IF(ODV.LT.1.3) THEN
BASEDV = 0.65          ;BLQ baselines replaced by 1/2 LLOQ
ENDIF

OHPBASE = BASEDV*EXP(ETA(3)*THETA(3))
KSYN = OHPBASE*KDEG   ;17-OHP synthesis rate (ksyn)

;converting concentrations to amounts
KDa = KD*V1
AMAX = BMAX*V1

;amount at timepoint 0 in central plasma compartment and in 17-OHP DBS compartment
A_0(2) = IBASE*V1
A_0(5) = OHPBASE

IF(IC50.EQ.0) THEN
IC50 = 0.001
ENDIF
IF(IC50.LT.0) THEN
IC50 = 0.001
ENDIF

k10 = CL/V1
k12 = Q/V1
k21 = Q/V2

; Time after dose
TAD = 0
IF (AMT.GT.0) THEN

```

```

TDOS = TIME
TAD = 0.0
ENDIF
IF (AMT.EQ.0) TAD = TIME-TDOS
IF (TAD.LT.0) TAD = 0

```

```

;;LLOQ of 17-OHP in DBS
LLOQ = LOG(1.3)

```

```

$DES

```

```

;;calculating unbound amount in plasma with binding model of previous model(s)
AUP = (A(2)-KDa*(1+NSALB) - AMAX + SQRT(((A(2) - KDa*(1 + NSALB) -AMAX)**2) +
4*KDa*A(2)*(1 + NSALB)))/(2*(1 + NSALB))

```

```

DADT(1) = -(VM*A(1)/(KM+A(1))) ;saturable absorption
DADT(2) = (VM*A(1)/(KM+A(1))) - k10*AUP - k12*AUP + k21*A(3) ;central compartment
DADT(3) = -k21*A(3)+k12*AUP ;peripheral compartment
DADT(4) = AUP* KaRBC -A(4)* KaRBC ;red blood cell compartment

```

```

CP = A(2)/V1
IF(CP.LT.0) THEN
CP=0.001
ENDIF

```

```

INH = 1-(IMAX*CP**GAM/(IC50**GAM+CP**GAM))
DADT(5) = KSYN*INH-KDEG*A(5) ;17-OHP compartment

```

```

$ERROR
IPRED = A(5)

```

```

IF(IPRED.GT.0) THEN
IPRED = IPRED
ELSE
IPRED = IPRED+0.0001
ENDIF

```

```

IPRED = LOG(IPRED)
W = THETA(3)
IRES= DV-IPRED
IWRES = IRES/W

```

```

IF(BLQ.EQ.0) THEN
F_FLAG = 0
Y = IPRED+W*EPS(1)

```

```

ELSE
F_FLAG = 1
DUM = (LLOQ-IPRED)/W
CUMD = PHI(DUM)
Y = CUMD
MDVRES = 1
ENDIF
$THETA
THETA(1:2) = DLOG(THETA(1:2))

```

```

$THETAR
THETAR(1:2) = EXP(THETA(1:2))

```

```

$THETA
(0, 1.22)      ;1. KDEG [1/h]
(0, 20)        ;2. IC50 [nmol/L]]
(0, 0.2)       ;3. RUV

```

```

$OMEGA
0.0025 FIX     ;KDEG
(0.0025, 0.5) ;IC50
1 FIX          ;OHPBASE

```

```

$SIGMA 1 FIX

```

```

$ESTIMATION METHOD=IMPMAP LAPLACE INTERACTION NITER=2000 ISAMPLE=300
SEED=987213 NOABORT NSIG=3 PRINT=1 NOABORT FILE=psn.ext
SIGL=9 GRD=DDDS
$ESTIMATION METHOD=IMPMAP LAPLACE INTERACTION NITER=200 ISAMPLE=3000
SEED=987213 NOABORT NSIG=3 PRINT=1 NOABORT FILE=psn.ext
SIGL=15 EONLY=1 GRD=DDDS
$COVARIANCE PRINT=E UNCONDITIONAL SIGL=9

```

```

$TABLE ID TIME TAD DV PRED IPRED WRES IWRES CWRES MDV BLQ AUP CP FLAG
ONEHEADER NOPRINT FILE=sdtab313_1_2

```

```

$TABLE ID TIME TAD DV CL V1 Q V2 KaRBC IBASE BMAX KD NSALB VM KM F1 ODV
FLAG ETA1 ETA2 ETA3 KSYN KDEG OHPBASE IMAX IC50 GAM NOAPPEND ONEHEADER
NOPRINT FILE=patab313_1_2

```

```

$TABLE ID TIME TAD DV FLAG NOAPPEND ONEHEADER NOPRINT FILE=catab313_1_2
$TABLE ID TIME TAD DV ODV FLAG NOAPPEND ONEHEADER NOPRINT FILE=cotab313_1_2

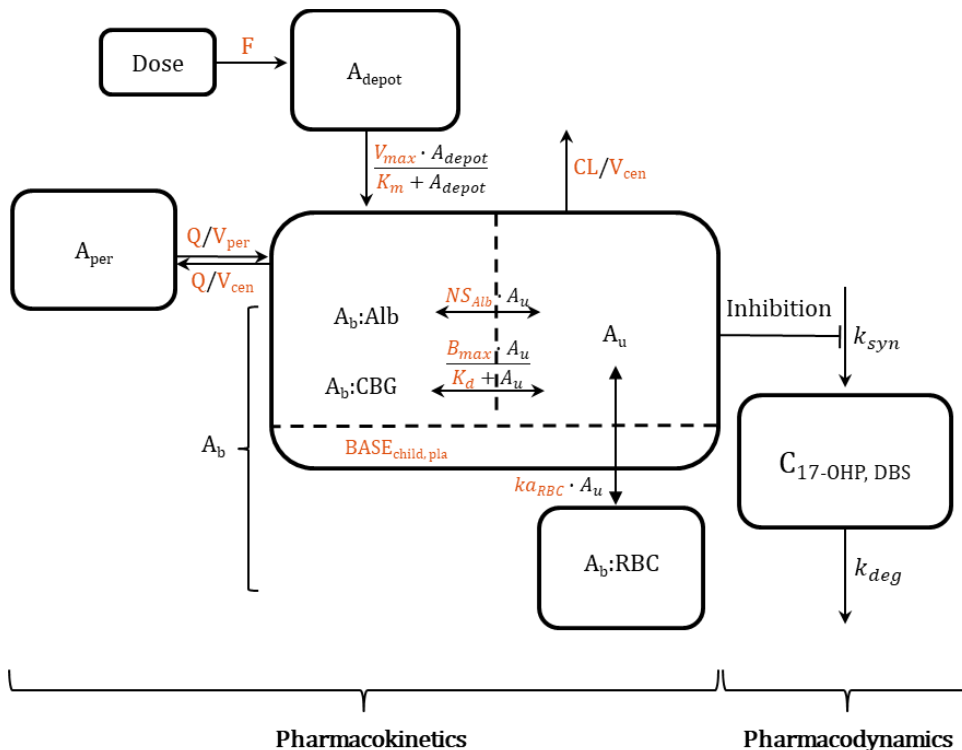
```

### 3 Supplementary Tables and Figures

**Supplementary Table 1.** Summary of population characteristics in all datasets leveraged in the modeling and simulation analysis, by framework step as described in Figure 1.

	<b>Step A: PK/PD modeling</b>	<b>Step B: Bland-Altman and Passing-Bablok analysis</b>	<b>Step C: Simulation of target range</b>
<b>Population</b>	Pediatric CAH patients (n=18), clinical study	Pediatric CAH patients (n=15), clinical routine monitoring	Non-CAH children (n=28)
<b>Analyte and matrix</b>	Cortisol in plasma 17-OHP in venous DBS	Cortisol and 17-OHP in capillary and venous DBS	Cortisol in plasma
<b>Number of samples</b>	88 (per matrix)	15	2016
<b>Age, median (range)</b>	2.5 years (4 months – 5 years)	8 years (2 months – 11 years)	(5-9) years
<b>Weight, median (range)</b>	15 (7-21) kg	-	-

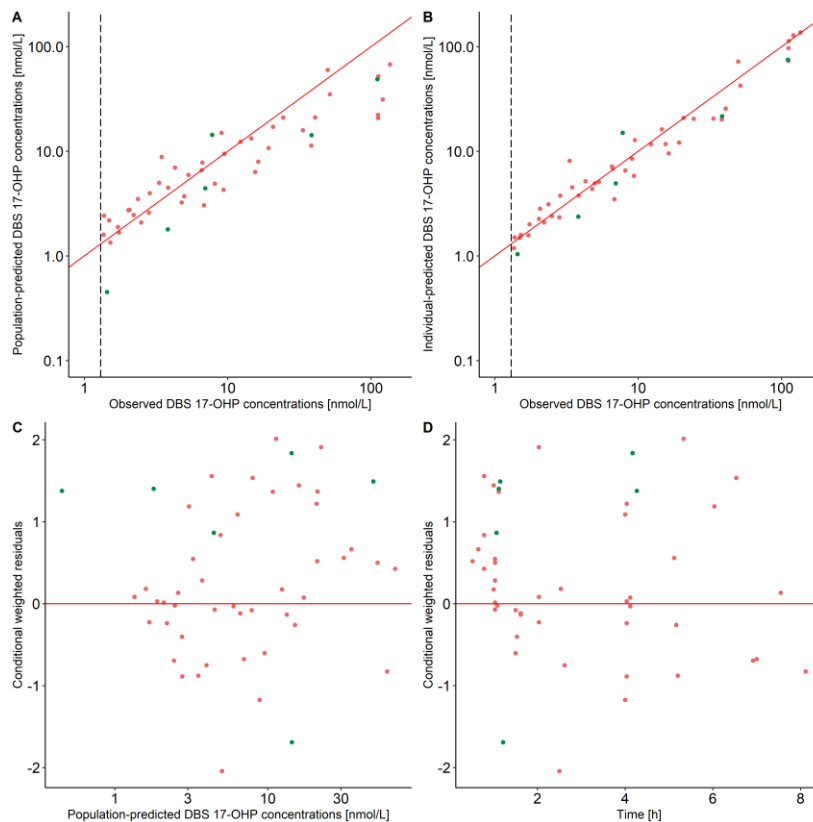
Congenital adrenal hyperplasia (CAH), 17 $\alpha$ -hydroxyprogesterone (17-OHP), dried blood spots (DBS)



**Supplementary Figure 1.** Schematic representation of developed pharmacokinetic/pharmacodynamic (PK/PD) model. PK parameters of which the pediatric individual estimates from the previous PK model (Stachanow et al.) [2] were used as part of the dataset are marked in orange.

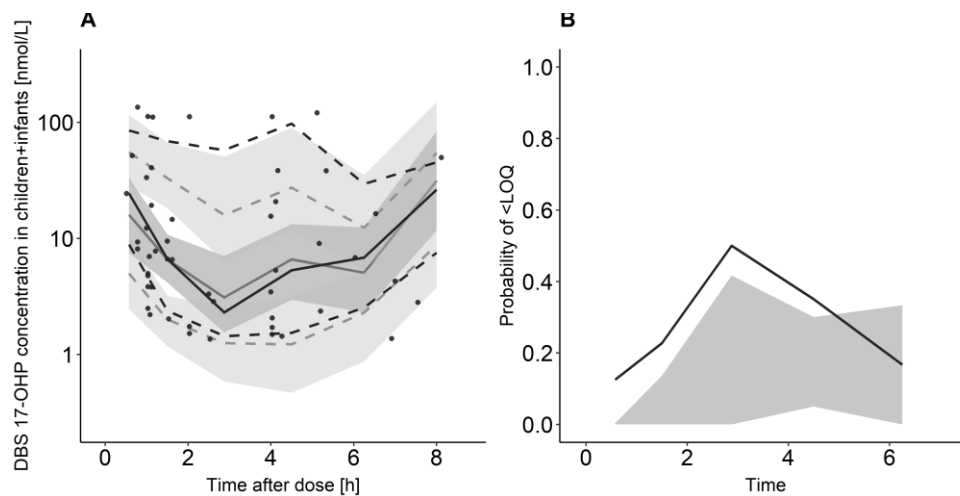
Pharmacokinetics: Bioavailability ( $F$ ), amount in depot compartment ( $A_{\text{depot}}$ ), maximum absorption rate ( $V_{\text{max}}$ ), amount in depot compartment resulting in half of  $V_{\text{max}}$  ( $K_m$ ), amount bound ( $A_b$ ), amount bound to albumin ( $A_b:\text{Alb}$ ), amount associated to red blood cells ( $A_b:\text{RBC}$ ), unbound amount ( $A_u$ ), amount bound to corticosteroid-binding globulin ( $A_b:\text{CBG}$ ), linear non-specific parameter for albumin binding ( $\text{NS}_{\text{Alb}}$ ) and association to red blood cells ( $k_{a\text{RBC}}$ ), maximum binding capacity ( $B_{\text{max}}$ ), equilibrium dissociation constant ( $K_d$ ), intercompartmental clearance ( $Q$ ), central volume of distribution ( $V_{\text{cen}}$ ), peripheral volume of distribution ( $V_{\text{per}}$ ), cortisol plasma baseline of children ( $\text{BASE}_{\text{child, pla}}$ ). The dashed line divides the central compartment into the  $A_b$  and  $A_u$  subcompartments, respectively.

Pharmacodynamics:  $17\alpha$ -hydroxyprogesterone (17-OHP) concentration in dried blood spots ( $C_{17\text{-OHP, DBS}}$ ), synthesis rate constant of 17-OHP ( $k_{\text{syn}}$ ), first-order elimination rate constant of 17-OHP ( $k_{\text{deg}}$ ).



**Supplementary Figure 2.** Goodness-of-fit plots for developed pharmacokinetic/pharmacodynamic (PK/PD) model.

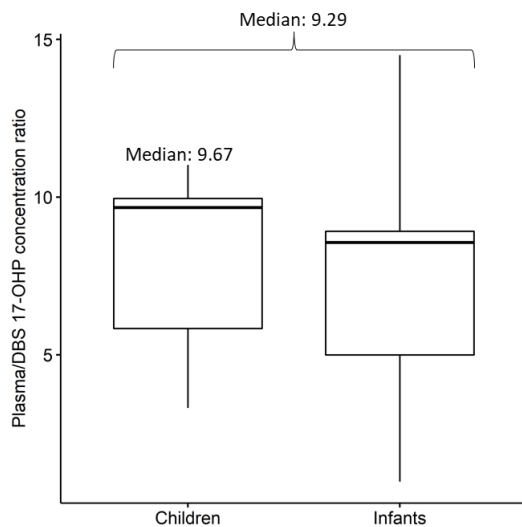
A: Population-predicted dried blood spot (DBS)  $17\alpha$ -hydroxyprogesterone (17-OHP) concentrations versus observed DBS 17-OHP concentrations, B: Individual DBS 17-OHP predictions versus observed DBS 17-OHP concentrations, C: Conditional weighted residuals versus population-predicted DBS 17-OHP concentrations, D: Conditional weighted residuals versus time. Red dots: children (cohort 1, age: 2-6 years), green dots: infants (cohort 2, age: 28 days-2 years), red line: line of identity (A, B), line  $y=0$  (C, D), vertical dashed line: lower limit of quantification (LLOQ) = 1.3 nmol/L.



**Supplementary Figure 3.** Visual predictive check (n=1000) for developed pharmacokinetic/pharmacodynamic (PK/PD) model.

A: Circles: 17 $\alpha$ -hydroxyprogesterone (17-OHP) dried blood spot (DBS) observations, solid line: 50<sup>th</sup> percentile of observed (black) and simulated (gray) DBS 17-OHP concentrations, dashed lines: 10<sup>th</sup> and 90<sup>th</sup> percentiles of observed (black) and simulated (gray) DBS 17-OHP concentrations, shaded areas: 95 % confidence intervals for the percentiles of the simulated data.

B: Black line: Observed probability of DBS 17-OHP concentrations below lower limit of quantification (LLOQ), gray area: 95 % confidence interval for simulated probability of 17-OHP concentrations below LLOQ.



**Supplementary Figure 4.** Plasma to dried blood spot (DBS) 17 $\alpha$ -hydroxyprogesterone (17-OHP) concentration ratio, measured at baseline in the morning, in young children and infants.

1. Beal, S.L. Ways to Fit a PK Model with Some Data below the Quantification Limit. *J. Pharmacokinet. Pharmacodyn.* **2001**, *28*, 481–504, doi:10.1023/A:1012299115260.
2. Stachanow, V.; Neumann, U.; Blankenstein, O.; Bindellini, D.; Melin, J.; Ross, R.; Whitaker, M.J.; Huisinga, W.; Michelet, R.; Kloft, C. Exploring Dried Blood Spot Cortisol Concentrations as an Alternative for Monitoring Pediatric Adrenal Insufficiency Patients: A Model-Based Analysis. *Front. Pharmacol.* **2022**, *13*, 1–8, doi:10.3389/fphar.2022.819590.

### **3.3 Paper III: Rationale of a lower dexamethasone dose in prenatal congenital adrenal hyperplasia therapy based on pharmacokinetic modelling**

## Equity Ratio Statement

### Paper III

**Title of the manuscript:**

“Rationale of a lower dexamethasone dose in prenatal congenital adrenal hyperplasia therapy based on pharmacokinetic modelling”

**Journal** European Journal of Endocrinology  
Volume 185, Issue 3, Pages 365–374 (2021)

**Authorship** First author

**Status** Published

DOI: <https://doi.org/10.1530/EJE-21-0395>

*Reprinted with permission from European Journal of Endocrinology.*

**Own contribution**

- Data set modification and checkouts
- All modelling and simulation activities, including PK model development, model evaluation, and simulations
- Interpretation of the results, including literature research related to interpretation of the results
- Drafting of all parts of the manuscript
- Creation of all figures and tables
- Adaptation of the manuscript according to the reviewers’ and editor’s comments

# Rationale of a lower dexamethasone dose in prenatal congenital adrenal hyperplasia therapy based on pharmacokinetic modelling

Viktoria Stachanow<sup>1,2</sup>, Uta Neumann<sup>3</sup>, Oliver Blankenstein<sup>3</sup>, Uwe Fuhr<sup>4</sup>, Wilhelm Huisinga<sup>5</sup>, Robin Michelet<sup>1</sup>, Nicole Reisch<sup>6</sup> and Charlotte Kloft<sup>1</sup>

<sup>1</sup>Department of Clinical Pharmacy and Biochemistry, Institute of Pharmacy, Freie Universitaet Berlin, Berlin, Germany,

<sup>2</sup>Graduate Research Training Program PharMetrX, Berlin, Germany, <sup>3</sup>Institute for Experimental Paediatric

Endocrinology, Charité-Universitätsmedizin, Berlin, Germany, <sup>4</sup>Department I of Pharmacology, Center for

Pharmacology, University of Cologne, Faculty of Medicine and University Hospital Cologne, Cologne, Germany, and

<sup>5</sup>Institute of Mathematics, Universität Potsdam, Gollm, Germany, and <sup>6</sup>Medizinische Klinik und Poliklinik IV, Klinikum der Universität München, Munich, Germany

\*(N Reisch and C Kloft contributed equally as senior authors)

Correspondence should be addressed to C Kloft

**Email**  
charlotte.kloft@fu-berlin.de

## Abstract

**Context:** Prenatal dexamethasone therapy is used in female fetuses with congenital adrenal hyperplasia to suppress androgen excess and prevent virilisation of the external genitalia. The traditional dexamethasone dose of 20 µg/kg/day has been used since decades without examination in clinical trials and is thus still considered experimental.

**Objective:** As the traditional dexamethasone dose potentially causes adverse effects in treated mothers and fetuses, we aimed to provide a rationale of a reduced dexamethasone dose in prenatal congenital adrenal hyperplasia therapy based on a pharmacokinetics-based modelling and simulation framework.

**Methods:** Based on a published dexamethasone dataset, a nonlinear mixed-effects model was developed describing maternal dexamethasone pharmacokinetics. In stochastic simulations ( $n = 1000$ ), a typical pregnant population ( $n = 124$ ) was split into two dosing arms receiving either the traditional 20 µg/kg/day dexamethasone dose or reduced doses between 5 and 10 µg/kg/day. Target maternal dexamethasone concentrations, identified from the literature, served as a threshold to be exceeded by 90% of mothers at a steady state to ensure foetal hypothalamic-pituitary-adrenal axis suppression.

**Results:** A two-compartment dexamethasone pharmacokinetic model was developed and subsequently evaluated to be fit for purpose. The simulations, including a sensitivity analysis regarding the assumed foetal:maternal dexamethasone concentration ratio, resulted in 7.5 µg/kg/day to be the minimum effective dose and thus our suggested dose.

**Conclusions:** We conclude that the traditional dexamethasone dose is three-fold higher than needed, possibly causing harm in treated fetuses and mothers. The clinical relevance and appropriateness of our recommended dose should be tested in a prospective clinical trial.

European Journal of  
Endocrinology  
(2021) **185**, 365–374

## Introduction

Congenital adrenal hyperplasia (CAH) due to 21-hydroxylase deficiency is a recessively inherited disorder of adrenal steroidogenesis resulting in cortisol deficiency and, due to the activation of the hypothalamic-

pituitary-adrenal (HPA) axis, in adrenal androgen excess (1). The latter is already present during foetal development resulting in virilisation of female fetuses and the current practice of urogenital reconstructive surgery in severe

cases (1). Prenatal therapy with dexamethasone (Dex) has been used since its first description by David and Forest in 1984 (2, 3) at risk pregnancies for classic CAH due to 21-hydroxylase deficiency. Dex is a potent glucocorticoid (GC) with a long half-life and the ability to traverse the placenta and suppress the foetal hypothalamic-pituitary-adrenal axis and thus can prevent virilisation of the external genitalia caused by foetal adrenal androgen excess. If started before the window of sexual differentiation (7–12 week post conception), there is evidence that prenatal Dex can significantly reduce virilisation in female fetuses with CAH (4, 5).

Dex therapy during pregnancy, however, is still considered an experimental therapy (6) and current guidelines do not recommend a specific treatment protocol (1). Its use is highly controversial for several reasons (6, 7, 8). One main reason is its unclear safety for treated mothers and fetuses. High doses of Dex administered to pregnant animals have teratogenic effects (9), and prenatal GC overexposure in animals has resulted in postnatal hypertension, programming effects on glucose homeostasis, decreased glomerular filtration, fatty liver disease and multiple negative effects on brain development (6, 9). Clinical outcome studies of fetuses treated with prenatal Dex at risk pregnancies for CAH show conflicting results with potentially negative neuropsychological and behavioural outcomes in Dex-treated children for CAH (10, 11, 12, 13, 14, 15, 16, 17, 18, 19). All studies, however, included very low numbers of patients and thus low power. Possible adverse effects described in treated mothers are more striae, oedema, increased mean weight gain, mood swings, and a slightly increased occurrence of hypertension, pre-eclampsia and gestational diabetes (4, 5, 6).

Since its first description, the same experimental (traditional) Dex dose of 20 µg/kg/day (pre-pregnancy maternal body weight), to a maximum of 1.5 mg/day given in 2–3 daily doses, is used (2). As Dex is 50–80 times more potent than cortisol, the traditional prenatal Dex treatment provides already the mother with about six-fold her physiologic GC, that is, cortisol, need (6). Additionally, Dex is minimal if at all inactivated by placental 11β-hydroxysteroid dehydrogenase (20). Investigations in non-CAH affected and untreated pregnancies showed that physiological foetal cortisol concentrations are low in early gestation and reach only a small fraction (approximately 10%) of maternal cortisol concentrations in midgestation (21). Consequently, the currently used Dex treatment during pregnancy bears the risk of a massively increased foetal exposure with Dex (6). As potential adverse effects

are dose-related, we asked ourselves if the currently used Dex dose can be reduced to minimise potential adverse events but still be efficacious with regard to the prevention of genital virilisation in female fetuses.

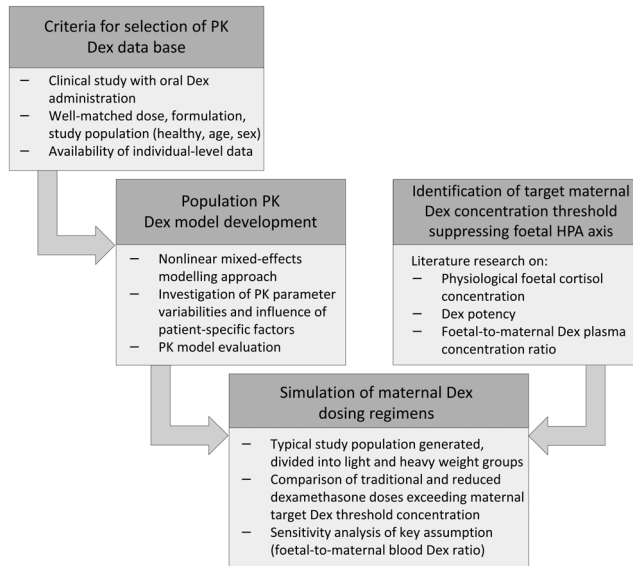
To investigate a rational dose recommendation, we developed a pharmacokinetic (PK)-based modelling and simulation framework. A key component is the availability of a PK model for Dex in prenatal CAH treatment. For its development, the nonlinear mixed-effects (NLME) modelling approach was applied. NLME modelling is a widely used and well-established gold standard approach for population PK analysis (22) and allows for simultaneous analysis of PK on the population as well as individual level. Characterising the PK of all individuals enables, for example, the determination of dosages that are adequate for the large majority of the population. Additionally, patient factors that can explain interindividual variability (IIV) in the PK can be identified. NLME modelling has been previously applied to assess CAH treatment with hydrocortisone in paediatric patients (23, 24, 25). PK models are structured in so-called compartments, representing kinetically homogenous regions of the body, such as well-perfused and poorly perfused organs (26). Finally, we applied the developed PK model to generate a rationale for the lowest possible but still effective Dex dose for successful HPA axis suppression in the foetus, with the ultimate aim to suggest a reduced dosing regimen for prenatal CAH therapy.

## Methods

A graphical overview of the stepwise pharmacokinetics-based modelling and simulation framework is depicted in Fig. 1.

### Selection of pharmacokinetic dexamethasone data base

The development of a PK model requires an underlying dataset including a population that is representative of the target population to be treated with DEX and thus is 'fit for purpose'. Therefore, literature research was conducted to identify clinical studies investigating Dex PK that could serve as a suitable database for the development of a Dex PK model. Criteria to be met were a study population that well-matched the pregnant target population with respect to health status, age, weight and sex. Further criteria were a well-matched Dex dose, administration of an oral-immediate release formulation and access to individual

**Figure 1**

Pharmacokinetics-based modelling and simulation framework. PK, pharmacokinetic; Dex, dexamethasone.

dosing and sampling data as well as PK and demographic data. The database preparation, the graphical analysis of the identified dataset and the plotting of the PK modelling and simulation results were performed using R (3.6.0) (27) and R Studio 1.3.1056 (28).

### Population pharmacokinetic dexamethasone model development

This data base retrieved from literature was used for the development of a comprehensive PK model by applying NLME modelling. Models were developed in NONMEM (7.4.3, ICON, Dublin, Ireland) Development Solutions, Ellicott City, MD, USA (29) using Perl speaks Nonmem (3.4.2, Uppsala University, Uppsala, Sweden) (30) embedded in the workbench Pirana (version 2.9.6) (31). One-, two- and three-compartment models were tested on the PK dataset and compared using the likelihood ratio test and the Akaike Information Criterion (AIC). Subsequently, interindividual variabilities (IIV) and covariate-parameter relations were investigated using the forward inclusion ( $P = 0.05$ ,  $df = 1$ )/backwards deletion ( $P = 0.01$ ,  $df = 1$ ) approach (32). The reliability of the models was evaluated using objective function value (OFV), a quality criterion defined as minus twice the natural logarithm of the likelihood of observing the data given the model indicating how well the model can predict the data (26), and standard model evaluation techniques such as goodness-of-fit (GOF) plots (33) and visual predictive checks (VPC,  $n(\text{simulations}) = 1000$ ) (34).

### Identification of target maternal Dex concentration suppressing foetal HPA axis

A literature search was performed to determine the minimum maternal Dex threshold concentration that leads to successful suppression of the foetal HPA axis as a decision criterion for an appropriate Dex dose. To this end and since no foetal Dex target concentrations for HPA axis suppression were found for prenatal CAH therapy, as a proxy, physiological foetal cortisol concentrations were identified first. Taking into account the higher potency of Dex compared to cortisol (hydrocortisone), the required foetal Dex target concentration was calculated. Finally, to obtain a maternal Dex target concentration, literature was searched for maternal-foetal Dex blood concentration ratios.

### Simulation of maternal dexamethasone dosing regimens reaching target

The developed PK model was then applied for identifying rational dosing regimens that suppress the foetal HPA axis by conducting stochastic simulations ( $n = 1000$ ) in NONMEM 7.4.3, randomly sampling individual PK parameters based on the estimated interindividual variability of the developed PK model. With these stochastic simulations, not only the Dex concentration-time profiles for typical patients were obtained but also variability in these profiles between patients was taken into account. First, a virtual but typical target population was generated with uniformly distributed body weights ranging from 50 to 95 kg. This virtual target population ( $n = 124$ ) was divided into a 'light' (50–72 kg) and 'heavy' (73–95 kg) group and the individuals were dosed according to the group's median body weight (61 and 84 kg, respectively). These two weight groups enabled the simulation of a realistic scenario for a clinical study in which pharmacies would only need to compound one dose strength per study arm. Two dosing arms were simulated with half of the patients receiving the traditional dose of 20  $\mu\text{g}/\text{kg}/\text{day}$  and the other half receiving reduced doses of 5, 6, 7.5, 9 or 10  $\mu\text{g}/\text{kg}/\text{day}$ , divided into three single doses given every 8 h. Regimens with reduced doses where the 10<sup>th</sup> percentiles of the maternal concentration-time profiles, that is, 90% of the patients, exceeded the minimum maternal target threshold at steady state (after the 5<sup>th</sup> Dex administration), were judged as rational and effective Dex dosings. We assume that for the remaining 10% of the patients, having the minimum below the assumed threshold for only several minutes, a successful suppression of the foetal HPA axis might be anticipated.

Furthermore, in order to assess the impact of the assumed foetal-maternal Dex concentration ratio, a sensitivity analysis was conducted by simulating the administration of the reduced doses with lower than reported foetal-maternal Dex concentration ratios as ‘worst-case scenarios’.

## Results

### Selection of pharmacokinetic dexamethasone data base

The retrieved clinical study best matching the pre-set criteria was a bioavailability study with 24 healthy volunteers receiving a dose of 2 mg Dex as an orally administered immediate-release tablet (EudraCT number: 2008-001389-10) (35). The study population had a median age of 32 years and 15 of 24 volunteers (63%) of the healthy volunteers were female. Body weights ranged from 60 to 90 kg and were overlapping between sexes (Table 1). Plasma was sampled up to 24 h post-dose, resulting in a total of 432 plasma samples and 18 samples per individual. Total Dex concentrations were determined in plasma using a HPLC-UV assay. Method validation was performed in accordance with current International Conference on Harmonisation Guideline recommendations (Center for Drug Evaluation and Research, Guidance for Industry: Bioanalytical Method Validation, 2001) and the conference report of Shah *et al.* (36). The lower limit of quantification (LLOQ) was 0.7 ng/mL (1.78 nmol/L). Dex concentrations reported below the LLOQ were discarded for the graphical analysis and the subsequent model development; thus, the Dex PK database comprised 349 Dex concentrations.

The individual Dex concentration-time profiles revealed a bi-phasic decline, that is, an initial phase with a steep concentration decline over time, followed by a phase with a less steep slope, in a semilogarithmic plot (Fig. 2), suggesting a two-compartment PK model structure (32). Moreover, the individual profiles suggested high interindividual variability between healthy volunteers.

**Table 1** Study characteristics (median (range)).

Characteristics	Female (n = 15)	Male (n = 9)	Total (n = 24)
Age, years	30.0 (22.0–54.0)	38.0 (25.0–54.0)	32.0 (22.0–54.0)
Body weight, kg	65.0 (60.0–77.5)	79.0 (73.0–90.0)	70.0 (60.0–90.0)
Height, m	1.66 (1.63–1.76)	1.84 (1.72–1.88)	1.71 (1.63–1.88)
BMI, kg/m <sup>2</sup>	23.2 (21.0–26.9)	25.5 (20.7–27.0)	23.7 (20.7–27.0)
Dexa*, nmol/L	15.4 (1.12–39.0)	10.1 (1.9–29.3)	12.61 (1.12–39.0)

\*After peroral administration of a 2 mg dexamethasone immediate release tablet. Dexa, dexamethasone concentration.

### Population pharmacokinetic dexamethasone model development

PK models with two compartments were superior to one and three-compartmental models according to all model diagnostics, for example, the OFV was 55.1 points better than for the one-compartment models, whereas a third compartment did not result in any significant model improvement (OFV non-significantly better (2.20 points); AICs: 1558.489, 1507.399, 1509.197 with one, two, three compartments, respectively). The final PK model contained the first-order absorption of Dex with an estimated lag-time of 12 min and a first-order elimination process (schematic depiction: Fig. 3). Residual variability was small (14.6% CV; proportional model). All PK parameter estimates were plausible and in line with the literature. IIV (assuming a log-normal distribution of individual parameters) was moderate to high: on clearance (33.1% CV), central volume of distribution (36.0% CV), intercompartmental clearance (98.7% CV), peripheral volume of distribution (42.9% CV), and absorption rate constant (116% CV). The identified effect of body weight on clearance and volume of distribution parameters was implemented using theory-based allometric scaling (37). Standard model evaluation techniques, such as GOF plot and VPCs, showed that the PK model adequately predicted the measured Dex concentrations and that standard criteria for a suitable and reliable model were fulfilled. More details about the model development and evaluation are presented in the Supplementary material (see section on [supplementary materials](#) given at the end of this article).

### Identification of target maternal Dex concentration suppressing foetal HPA axis

The minimum maternal Dex threshold concentration was derived as a target concentration to suppress the foetal HPA axis based on the following knowledge obtained in the literature research: in Goto *et al.* (38), a physiological foetal cortisol concentration of around 4 pmol/mg was

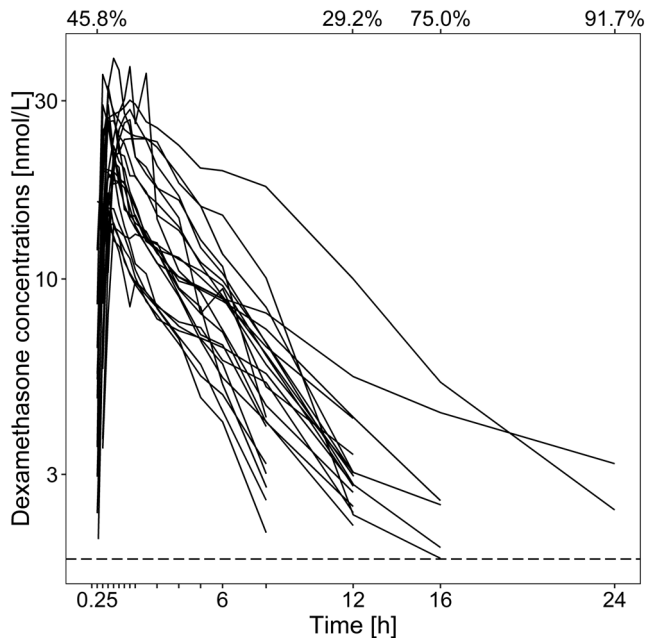


**Figure 2**

Individual profiles ( $n = 24$ ) of dexamethasone concentrations (nmol/L) over time (h) after administration of a 2 mg immediate-release tablet. Dashed line: Lower limit of quantification. Top: Percentage of concentrations below the lower limit of quantification at 0.25, 12, 16 and 24 h post-dose.

determined in adrenal tissue at 8 weeks post conception. Assuming a tissue density of  $1 \text{ g/cm}^3$ , the foetal target cortisol concentration was  $4 \text{ pmol/mL}$  or  $4 \text{ nmol/L}$ . Since Dex is reported to be between 50 and 80 times more potent than cortisol (39), the corresponding foetal target Dex concentration was derived to be  $0.05\text{--}0.08 \text{ nmol/L}$ . Considering the reported ratio of 0.45 for the foetal:maternal Dex concentration (40), the identified maternal plasma Dex threshold concentration was thereby calculated to be between  $0.11$  and  $0.18 \text{ nmol/L}$ .

### Simulation of maternal dexamethasone dosing regimens

The developed PK Dex model combined with the derived target maternal Dex concentration was employed to evaluate maternal Dex concentration-time profiles of the traditional compared to reduced maternal Dex doses (62 individuals per dose group). All reduced doses of 5, 6, 7.5, 9 and  $10 \text{ }\mu\text{g/kg/day}$  met the pre-set decision criterion of being above the target  $0.05\text{--}0.08 \text{ nmol/L}$  maternal Dex threshold concentration to successfully suppress the foetal HPA axis at steady state (Supplementary Fig. 3). As shown in Fig. 4A, with maternal Dex concentrations for the reduced dose of  $7.5 \text{ }\mu\text{g/kg/day}$ , in 90% of the patients

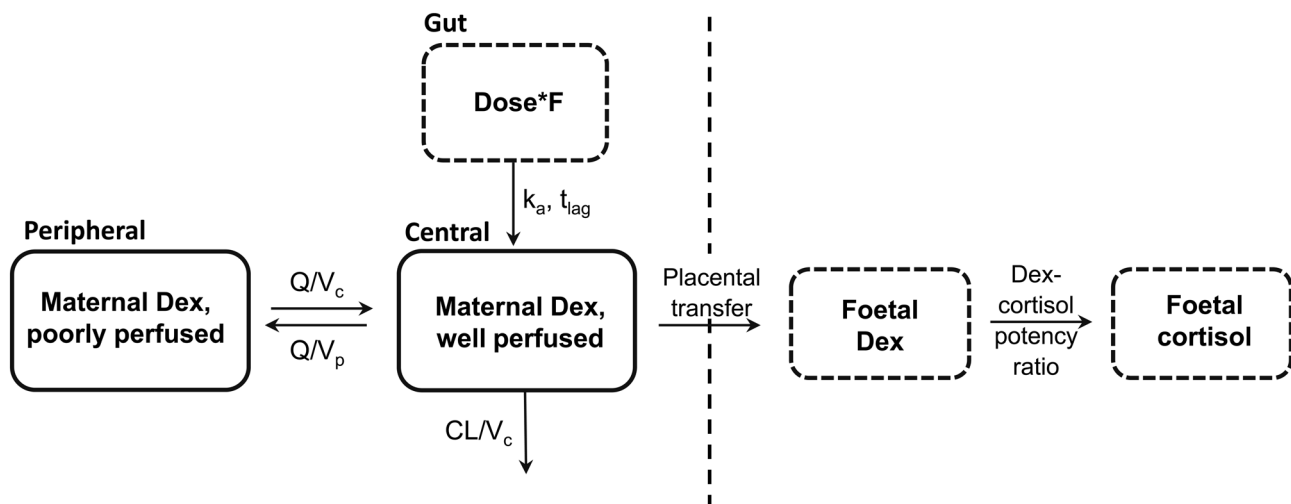


**Figure 3**

Left: structure of the developed two-compartment dexamethasone (Dex) pharmacokinetic (PK) model describing maternal Dex PK after intake of a 2 mg Dex immediate-release tablet. Solid line boxes: central and peripheral PK model compartments. Dashed line box: Dex dosing compartment. Right: calculated foetal Dex and cortisol concentrations (dashed line boxes), based on foetal-to-maternal Dex plasma concentration ratio and Dex-cortisol potency ratio retrieved from literature. Pharmacokinetic parameters: bioavailability ( $F$ , fixed to 1), absorption rate constant ( $k_a$ ), absorption lag time ( $t_{lag}$ ), clearance ( $CL$ ), volume of distribution of central maternal compartment ( $V_c$ ), intercompartmental clearance ( $Q$ ), volume of distribution of central maternal compartment ( $V_p$ ).

(i.e. 10<sup>th</sup> percentile), all Dex concentrations, including the minimum Dex concentration at a steady state (see grey box), were above the maternal Dex thresholds. Due to the dosing according to the group's median body weight, almost no difference was visible in the profiles of the light and heavy body weight group, with the concentrations of the lightweight group being slightly lower which was also the case for further analyses. Compared to the traditional dose of 20 µg/kg/day, the Dex exposure of the 7.5 µg/kg/day dose was considerably reduced over the entire time period with 63.1 % lower maximum (dashed box) and 62.7% lower minimum (grey box) Dex concentrations at steady state (Fig. 4B: 10<sup>th</sup> percentile concentration-time profiles).

### Sensitivity analysis

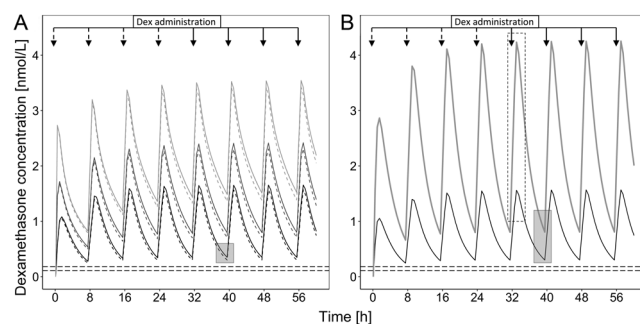
To test the sensitivity of our results to the assumed value of the foetal-to-maternal Dex plasma concentration ratio of 0.45 reported in the literature (40), the ratio was decreased to 0.3 and 0.25; For these decreased Dex transplacental transfer values, when 9 or 10 µg/kg/day was administered as a reduced dose respectively, for 90% of patients (10<sup>th</sup>

percentile) the Dex concentration-time profiles entirely exceeded the two maternal threshold Dex concentrations (Supplementary Fig. 4). With reduced doses of 5 or 6 µg/kg/day, and with both lower ratios and Dex being 50 times as potent as cortisol, the minimum concentrations of the 10<sup>th</sup> percentile (90% of patients) Dex profiles were not exceeding the upper maternal target threshold. Thus, these doses were considered too low for successful suppression of the foetal HPA axis (Fig. 5). After administration of 7.5 µg/kg/day with a ratio of 0.3, the 10<sup>th</sup> percentile Dex profiles were exceeding the upper maternal target threshold entirely. However, with a ratio of 0.25, the minimum concentrations of the 10<sup>th</sup> percentile Dex profiles were slightly below the upper maternal target threshold (Fig. 5C). Taking into account that in this 'worst-case-scenario' only 0.47% or 1.47% (with Dex being 80 or 50 times as potent as cortisol) of the total simulated Dex concentrations were below the target thresholds at steady state, we nevertheless selected 7.5 µg/kg/day as the lowest maternal dosage resulting in sufficient HPA axis suppression in the foetus.

### Discussion

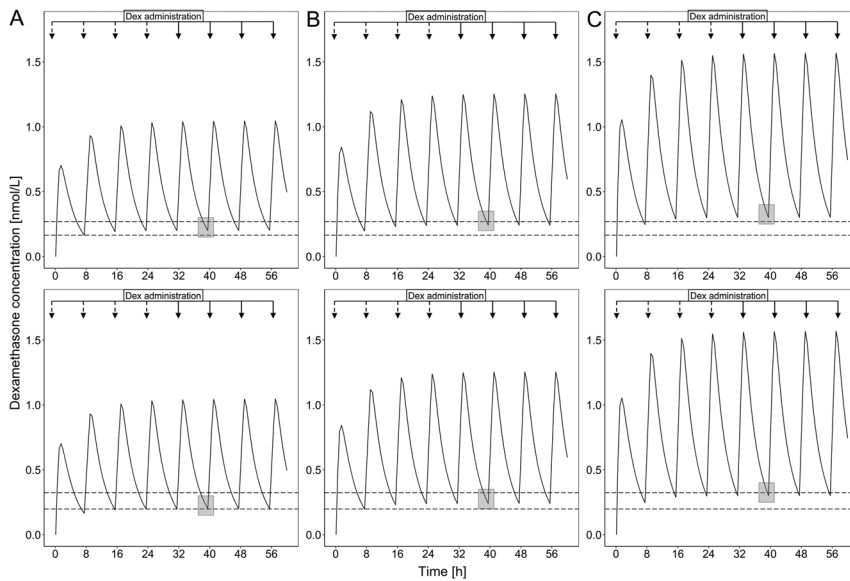
This study presents a scientific rationale for Dex dosing in prenatal CAH therapy. We successfully developed a pharmacokinetic NLME modelling and simulation framework in order to investigate different reduced Dex dosing regimens for prenatal therapy in CAH. Using simulations and sensitivity analysis, a suggested dose of 7.5 µg/kg/day was determined, which represents about a third of the traditional dose and judged as effective according to the identified target threshold for successful suppression of foetal HPA axis and thus prevention of foetal female virilisation.

The chosen PK database for the PK model development well-matched with the target population. As opposed to typical healthy volunteers, the majority (63%) of the subjects enrolled in the clinical study were female. The body weight range (60–90 kg) well-matched the expected weight of women in their early pregnancy and could be incorporated as a covariate on clearance and volume of distribution parameters. Moreover, with a median age of 32 (interquartile range: 27–46), the subjects had a well-matched age for representing pregnant women. The administered Dex dose of 2 mg in the model development dataset is approximately four times higher than the traditional dose in prenatal CAH therapy for a pregnant patient weighing 70 kg. Cummings *et al.* (41) observed a linear binding within a Dex concentration range of around 0.02–2 µg/L which is



**Figure 4**

Dexamethasone (Dex) concentration–time profiles after administration of (A) 7.5 µg/kg/day as reduced dose for light (50–72 kg, dashed lines) and heavy (73–95 kg, solid lines) body weight groups ( $n = 62$  patients per group with  $n = 1000$  simulations each) with 10<sup>th</sup> percentile (black lines), median (dark grey lines) and 90<sup>th</sup> percentile (light grey lines), (B) 7.5 µg/kg/day as reduced dose (black solid line of A) and traditional dose (20 µg/kg/day, grey line) of 10 percentiles and light body weight group only. Dashed horizontal lines: Dex threshold concentration if Dex is 50- (upper line) or 80-fold (lower line) more potent than cortisol, light grey filled boxes: minimum Dex concentration at steady state, dashed non-filled box: maximum Dex concentration at steady state. Arrows: Dex dose administrations before (dashed arrows) and after (solid line arrows) steady state.

**Figure 5**

Sensitivity analysis for foetal:maternal dexamethasone concentration ratio. Simulated 10<sup>th</sup> percentile dexamethasone concentration-time profiles of light (50–72 kg) body weight group ( $n = 62$  patients) after administration of reduced doses with 5 (A), 6 (B) and 7.5 (C)  $\mu\text{g}/\text{kg}/\text{day}$ , if foetal:maternal dexamethasone concentration ratio = 0.3 (top) or 0.25 (bottom) instead of 0.45 (ratio retrieved from literature). Dashed horizontal lines: dexamethasone threshold concentration if dexamethasone is 50- (upper line) or 80-fold (lower line) more potent than cortisol, light grey boxes: minimum dexamethasone concentration at steady state. Arrows: Dex dose administrations before (dashed arrows) and after (solid line arrows) steady state.

corresponding to the Dex concentrations in our analysis. Another publication described a nonlinear binding of Dex to albumin (42). However, the binding was investigated for substantially higher Dex concentrations up to 2 mg/L. Moreover, Loew *et al.* estimated very similar PK parameters after oral administration of 0.5, 0.75 and 1.5 mg Dex in healthy females (43), which are well in line with the doses investigated in our simulations. Given these findings, the PK of Dex was assumed to be linear within the range of the simulated doses and the dose administered in the retrieved clinical study.

One limitation of the database is the absence of pregnant individuals. In near-term pregnant women, Tsuei *et al.* stated that the Dex clearance is higher than in non-pregnant women whereas pregnancy did not affect the terminal half-life or plasma protein binding of Dex (40). Similar findings were described by Ke *et al.* in a physiologically based pharmacokinetic model (PBPK) for Dex in late pregnancy (44). Since sexual differentiation takes place at 7 to 12 weeks post conception (38), efficacy of the prenatal Dex administration is most important in this time period. Dex PK in early stage of pregnancy has not been characterised in a PK model yet as, in general, only few PK models exist for the first trimester of pregnancy (45). In pregnancy PBPK models, organ volumes are assumed to steadily increase with relatively little changes within the first trimester (46). It was, therefore, assumed that in this early period of pregnancy, being the sensitive phase of genital development, changes of Dex PK were negligible for

the analysis. Most important, from the retrieved clinical study, all relevant individual-level data were available.

The resulting parameter estimates from the final structural PK model were well in line with the knowledge on the PK of the well-studied drug Dex. The estimated typical clearance of 40.4 L/h was in accordance with the area under the curve (AUC) which was calculated in the publication presenting the PK model database (geometric mean of 48.1 ng/mL/h, corresponding to clearance of 41.6 L/h) (35). Moreover, the literature reports high variability in the PK of Dex (43) similar to the estimated interindividual variability parameters, as well as Dex PK models with a two-compartment structure and rapid first-order absorption (47, 48). In addition, the PK model adequately predicted the measured Dex concentrations (Supplementary Figs 1 and 2). The developed PK model was, therefore, judged well suitable for application in the subsequent stochastic simulations. These simulations showed that all reduced doses were effective according to the determined maternal Dex thresholds and underlying assumptions.

As the retrieved foetal-to-maternal Dex plasma concentration ratio was determined in near-term pregnant women (40), this ratio was identified as the most critical assumption. Thus, a sensitivity analysis was conducted by altering the ratio of 0.45 to 0.3 and, as a 'worst-case-scenario', to 0.25. In these investigated scenarios, 7.5  $\mu\text{g}/\text{kg}/\text{day}$  met the pre-defined criterion to be the lowest effective dose, with around 90% of pregnant women exceeding the pre-defined upper maternal Dex concentration

threshold at a steady state. For the assumed physiological foetal cortisol concentration, the cortisol concentration which was measured in adrenal tissue of human foetuses 8 weeks post-conception (38) was chosen as the only and, therefore, best information on human foetal cortisol concentrations during early pregnancy that could be found in the literature. Regarding the difference in potency between cortisol and Dex, the two factors of 50 and 80 (39) were used throughout the simulation-based evaluations, thereby assuming that the difference in potency between cortisol and Dex translates from adults and children to the foetus. By using both factors, the uncertainty on the target concentration was taken into account in the simulation study, as a difference in potency directly leads to required differences in target concentration. The recommended dose of 7.5 µg/kg/day corresponds to less than 1 mg/day (for body weights up to 130 kg), which is commonly regarded as a threshold Dex dose for iatrogenic Cushing's syndrome (49) and would thus substantially decrease the mother's risk for GC-related adverse events. In conclusion, a considerably, that is, about three-fold reduced recommended Dex dose for prenatal CAH therapy was identified based on NLME modelling and simulation and thereby based on a scientific rationale. These calculations can be the basis of a prospective research protocol which has been recommended for years (1, 4, 50, 51) to investigate the success of prenatal Dex therapy in CAH with regard to the prevention of virilisation in female foetuses and to prospectively monitor the adverse effects for the treated mother and child.

#### Supplementary materials

This is linked to the online version of the paper at <https://doi.org/10.1530/EJE-21-0395>.

#### Declaration of interest

V S and R M have nothing to declare. C K and W H report grants from an industry consortium (AbbVie Deutschland GmbH & Co. KG, AstraZeneca, Boehringer Ingelheim Pharma GmbH & Co. KG, Grünenthal GmbH, F. Hoffmann-La Roche Ltd, Merck KGaA and SANOFI) for the PharMetrX PhD program. C K, U N and O B report a grant from Diurnal Ltd. C K reports an additional grant from the Innovative Medicines Initiative-Joint Undertaking ('DDMoRe'), the Federal Ministry of Education and Research within the Joint Programming Initiative on Antimicrobial Resistance Initiative (JPIAMR) and from the European Commission within the Horizon 2020 framework programme ('FAIR'). U F report grants from InfectoPharm Arzneimittel und Consilium GmbH. All funding was outside the submitted work.

#### Funding

This work was supported by the Deutsche Forschungsgemeinschaft (Heisenberg Professorship 325768017 to N R and Projektnummer: 314061271-TRR205 to N R).

#### Acknowledgement

The authors acknowledge the High-Performance Computing Service of ZEDAT at Freie Universitaet Berlin (<https://www.zedat.fu-berlin.de/HPC/Home>) for computing time.

#### References

- Speiser PW, Arlt W, Auchus RJ, Baskin LS, Conway GS, Merke DP, Meyer-Bahlburg HFL, Miller WL, Hassan Murad MH, Oberfield SE *et al.* Congenital adrenal hyperplasia due to steroid 21-hydroxylase deficiency: an Endocrine Society clinical practice guideline. *Journal of Clinical Endocrinology and Metabolism* 2018 **103** 4043–4088. (<https://doi.org/10.1210/jc.2018-01865>)
- David M & Forest MG. Prenatal treatment of congenital adrenal hyperplasia resulting from 21-hydroxylase deficiency. *Journal of Pediatrics* 1984 **105** 799–803. ([https://doi.org/10.1016/s0022-3476\(84\)80310-8](https://doi.org/10.1016/s0022-3476(84)80310-8))
- Forest MG. Prenatal diagnosis, treatment, and outcome in infants with congenital adrenal hyperplasia. *Current Opinion in Endocrinology and Diabetes* 1997 **4** 209–217. (<https://doi.org/10.1097/00060793-199706000-00005>)
- Forest MG. Recent advances in the diagnosis and management of congenital adrenal hyperplasia due to 21-hydroxylase deficiency. *Human Reproduction Update* 2004 **10** 469–485. (<https://doi.org/10.1093/humupd/dmh047>)
- New MI, Carlson A, Obeid J, Marshall I, Cabrera MS, Goseco A, Lin-Su K, Putnam AS, Wei JQ & Wilson RC. Prenatal diagnosis for congenital adrenal hyperplasia in 532 pregnancies. *Journal of Clinical Endocrinology and Metabolism* 2001 **86** 5651–5657. (<https://doi.org/10.1210/jcem.86.12.8072>)
- Miller WL. Fetal endocrine therapy for congenital adrenal hyperplasia should not be done. *Best Practice and Research: Clinical Endocrinology and Metabolism* 2015 **29** 469–483. (<https://doi.org/10.1016/j.beem.2015.01.005>)
- Hirvikoski T, Nordenström A, Wedell A, Ritzén M & Lajic S. Prenatal dexamethasone treatment of children at risk for congenital adrenal hyperplasia: the Swedish experience and standpoint. *Journal of Clinical Endocrinology and Metabolism* 2012 **97** 1881–1883. (<https://doi.org/10.1210/jc.2012-1222>)
- New MI, Abraham M, Yuen T & Lekarev O. An update on prenatal diagnosis and treatment of congenital adrenal hyperplasia. *Seminars in Reproductive Medicine* 2012 **30** 396–399. (<https://doi.org/10.1055/s-0032-1324723>)
- Khulan B & Drake AJ. Glucocorticoids as mediators of developmental programming effects. *Best Practice and Research: Clinical Endocrinology and Metabolism* 2012 **26** 689–700. (<https://doi.org/10.1016/j.beem.2012.03.007>)
- Hirvikoski T, Lindholm T, Lajic S & Nordenström A. Gender role behaviour in prenatally dexamethasone-treated children at risk for congenital adrenal hyperplasia – a pilot study. *Acta Paediatrica* 2011 **100** e112–e119. (<https://doi.org/10.1111/j.1651-2227.2011.02260.x>)
- Hirvikoski T, Nordenström A, Lindholm T, Lindblad F, Ritzén EM & Lajic S. Long-term follow-up of prenatally treated children at risk for congenital adrenal hyperplasia: does dexamethasone cause behavioural problems? *European Journal of Endocrinology* 2008 **159** 309–316. (<https://doi.org/10.1530/EJE-08-0280>)
- Hirvikoski T, Nordenström A, Lindholm T, Lindblad F, Ritzén EM, Wedell A & Lajic S. Cognitive functions in children at risk for congenital adrenal hyperplasia treated prenatally with dexamethasone. *Journal of Clinical Endocrinology and Metabolism* 2007 **92** 542–548. (<https://doi.org/10.1210/jc.2006-1340>)
- Maryniak A, Ginalska-Malinowska M, Bielawska A & Ondruch A. Cognitive and social function in girls with congenital adrenal hyperplasia – influence of prenatally administered dexamethasone.

- Child Neuropsychology* 2014 **20** 60–70. (<https://doi.org/10.1080/09297049.2012.745495>)
- 14 Meyer-Bahlburg HFL, Dolezal C, Baker SW, Carlson AD, Obeid JS & New MI. Cognitive and motor development of children with and without congenital adrenal hyperplasia after early-prenatal dexamethasone. *Journal of Clinical Endocrinology and Metabolism* 2004 **89** 610–614. (<https://doi.org/10.1210/jc.2002-021129>)
  - 15 Meyer-Bahlburg HFL, Dolezal C, Haggerty R, Silverman M & New MI. Cognitive outcome of offspring from dexamethasone-treated pregnancies at risk for congenital adrenal hyperplasia due to 21-hydroxylase deficiency. *European Journal of Endocrinology* 2012 **167** 103–110. (<https://doi.org/10.1530/EJE-11-0789>)
  - 16 Trautman PD, Meyer-Bahlburg HFL, Postelnek J & New MI. Effects of early prenatal dexamethasone on the cognitive and behavioral development of young children: results of a pilot study. *Psychoneuroendocrinology* 1995 **20** 439–449. ([https://doi.org/10.1016/0306-4530\(94\)00070-0](https://doi.org/10.1016/0306-4530(94)00070-0))
  - 17 Van't Westeinde A, Karlsson L, Nordenström A, Padilla N & Lajic S. First-trimester prenatal dexamethasone treatment is associated with alterations in brain structure at adult age. *Journal of Clinical Endocrinology and Metabolism* 2020 **105** dgaa340. (<https://doi.org/10.1210/clinem/dgaa340>)
  - 18 Van't Westeinde A, Zimmermann M, Messina V, Karlsson L, Padilla N & Lajic S. First trimester DEX treatment is not associated with altered brain activity during working memory performance in adults. *Journal of Clinical Endocrinology and Metabolism* 2020 **105** e4074–e4082. (<https://doi.org/10.1210/clinem/dgaa611>)
  - 19 Karlsson L, Barbaro M, Ewing E, Gomez-Cabrero D & Lajic S. Epigenetic alterations associated with early prenatal dexamethasone treatment. *Journal of the Endocrine Society* 2019 **3** 250–263. (<https://doi.org/10.1210/js.2018-00377>)
  - 20 Seckl JR. Glucocorticoids, feto-placental 11 $\beta$ -hydroxysteroid dehydrogenase type 2, and the early life origins of adult disease. *Steroids* 1997 **62** 89–94. ([https://doi.org/10.1016/S0039-128X\(96\)00165-1](https://doi.org/10.1016/S0039-128X(96)00165-1))
  - 21 Kari MA, Raivio KO, Stenman UH & Voutilainen R. Serum cortisol, dehydroepiandrosterone sulfate, and steroid-binding globulins in preterm neonates: effect of gestational age and dexamethasone therapy. *Pediatric Research* 1996 **40** 319–324. (<https://doi.org/10.1203/00006450-199608000-00021>)
  - 22 Pillai GC, Mentré F & Steimer JL. Non-linear mixed effects modeling – from methodology and software development to driving implementation in drug development science. *Journal of Pharmacokinetics and Pharmacodynamics* 2005 **32** 161–183. (<https://doi.org/10.1007/s10928-005-0062-y>)
  - 23 Michelet R, Melin J, Parra-Guillen ZP, Neumann U, Whitaker JM, Stachanow V, Huisinga W, Porter J, Blankenstein O, Ross RJ *et al.* Paediatric population pharmacokinetic modelling to assess hydrocortisone replacement dosing regimens in young children. *European Journal of Endocrinology* 2020 **183** 357–368. (<https://doi.org/10.1530/EJE-20-0231>)
  - 24 Melin J, Parra-Guillen ZP, Michelet R, Truong T, Huisinga W, Hartung N, Hindmarsh P & Kloft C. Pharmacokinetic/ pharmacodynamic evaluation of hydrocortisone therapy in pediatric patients with congenital adrenal hyperplasia. *Journal of Clinical Endocrinology and Metabolism* 2020 **105** E1729–E1740. (<https://doi.org/10.1210/clinem/dgaa071>)
  - 25 Melin J, Parra-Guillen ZP, Hartung N, Huisinga W, Ross RJ, Whitaker MJ & Kloft C. Predicting cortisol exposure from paediatric hydrocortisone formulation using a semi-mechanistic pharmacokinetic model established in healthy adults. *Clinical Pharmacokinetics* 2018 **57** 515–527. (<https://doi.org/10.1007/s40262-017-0575-8>)
  - 26 Mould DR & Upton RN. Basic concepts in population modeling, simulation, and model-based drug development. *CPT: Pharmacometrics and Systems Pharmacology* 2012 **1** e6. (<https://doi.org/10.1038/psp.2012.4>)
  - 27 R Core Team. *R: A Language and Environment for Statistical Computing*. Vienna, Austria: R Foundation for Statistical Computing, 2019. (available at: <https://www.R-project.org/>)
  - 28 RStudio Team. *RStudio: Integrated Development Environment for R*. Boston, MA: Rstudio, PBC. 2020. (available at: <http://www.rstudio.com/>)
  - 29 Beal S, Sheiner LB, Boeckmann A & Bauer RJ. *NONMEM User's Guides 1989–2009*. Ellicott City, MD, USA: Icon Development Solutions, 2009.
  - 30 Lindbom L, Pihlgren P & Jonsson EN. PsN-Toolkit – a collection of computer intensive statistical methods for non-linear mixed effect modeling using NONMEM. *Computer Methods and Programs in Biomedicine* 2005 **79** 241–257. (<https://doi.org/10.1016/j.cmpb.2005.04.005>)
  - 31 Keizer RJ, Benten M, Beijnen JH, Schellens JH & Huitema AD. Piraña and PCluster: a modeling environment and cluster infrastructure for NONMEM. *Computer Methods and Programs in Biomedicine* 2011 **101** 72–79. (<https://doi.org/10.1016/j.cmpb.2010.04.018>)
  - 32 Mould DR & Upton RN. Basic concepts in population modeling, simulation, and model-based drug development-part 2: introduction to pharmacokinetic modeling methods. *CPT: Pharmacometrics and Systems Pharmacology* 2013 **2** e38. (<https://doi.org/10.1038/psp.2013.14>)
  - 33 Owen JS & Fielder-Kelly J. *Introduction to Population Pharmacokinetic/ Pharmacodynamic Analysis with Nonlinear Mixed Effect Models*. Hoboken, New Jersey: John Wiley & Sons, Inc., 2014.
  - 34 Bergstrand M, Hooker AC, Wallin JE & Karlsson MO. Prediction-corrected visual predictive checks for diagnosing nonlinear mixed-effects models. *AAPS Journal* 2011 **13** 143–151. (<https://doi.org/10.1208/s12248-011-9255-z>)
  - 35 Queckenberg C, Wachall B, Erlinghagen V, Di Gion P, Tomalik-Scharte D, Tawab M, Gerbeth K & Fuhr U. Pharmacokinetics, pharmacodynamics, and comparative bioavailability of single, oral 2-mg doses of dexamethasone liquid and tablet formulations: a randomized, controlled, crossover study in healthy adult volunteers. *Clinical Therapeutics* 2011 **33** 1831–1841. (<https://doi.org/10.1016/j.clinthera.2011.10.006>)
  - 36 Shah VP, Midha KK, Dighe S, McGilveray JJ, Skelly JP, Yacobi A, Layloff T, Viswanathan CT, Cook CE & McDowall RD. Analytical methods validation: bioavailability, bioequivalence and pharmacokinetic studies. Conference report. *European Journal of Drug Metabolism and Pharmacokinetics* 1991 **16** 249–255. (<https://doi.org/10.1007/BF03189968>)
  - 37 Holford NHG. A size standard for pharmacokinetics. *Clinical Pharmacokinetics* 1996 **30** 329–332. (<https://doi.org/10.2165/00003088-199630050-00001>)
  - 38 Goto M, Hanley KP, Marcos J, Wood PJ, Wright S, Postle AD, Cameron IT, Mason JI, Wilson DI & Hanley NA. In humans, early cortisol biosynthesis provides a mechanism to safeguard female sexual development. *Journal of Clinical Investigation* 2006 **116** 953–960. (<https://doi.org/10.1172/JCI25091>)
  - 39 Rivkees SA & Crawford JD. Dexamethasone treatment of virilizing congenital adrenal hyperplasia: the ability to achieve normal growth. *Pediatrics* 2000 **106** 767–773. (<https://doi.org/10.1542/peds.106.4.767>)
  - 40 Tsuei SE, Petersen MC, Ashley JJ, McBride WG & Moore RG. Disposition of synthetic glucocorticoids. *Clinical Pharmacology and Therapeutics* 1980 **28** 88–98. (<https://doi.org/10.1038/clpt.1980.136>)
  - 41 Cummings DM, Larijani GE, Conner DP, Ferguson RK & Rocci ML. Characterization of dexamethasone binding in normal and uremic human serum. *DICP: the Annals of Pharmacotherapy* 1990 **24** 229–231. (<https://doi.org/10.1177/106002809002400301>)
  - 42 Gonciarz A, Kus K, Szafarz M, Walczak M, Zakrzewska A & Szymura-Oleksiak J. Capillary electrophoresis/frontal analysis versus equilibrium dialysis in dexamethasone sodium phosphate-serum

- albumin binding studies. *Electrophoresis* 2012 **33** 3323–3330. (<https://doi.org/10.1002/elps.201200166>)
- 43 Loew D, Schuster O & Graul EH. Dose-dependent pharmacokinetics of dexamethasone. *European Journal of Clinical Pharmacology* 1986 **30** 225–230. (<https://doi.org/10.1007/BF00614309>)
- 44 Ke AB & Milad MA. Evaluation of maternal drug exposure following the administration of antenatal corticosteroids during late pregnancy using physiologically-based pharmacokinetic modeling. *Clinical Pharmacology and Therapeutics* 2019 **106** 164–173. (<https://doi.org/10.1002/cpt.1438>)
- 45 Dallmann A, Mian P, Anker J Van den & Allegaert K. Clinical pharmacokinetic studies in pregnant women and the relevance of pharmacometric tools. *Current Pharmaceutical Design* 2019 **25** 483–495. (<https://doi.org/10.2174/1381612825666190320135137>)
- 46 Dallmann A, Pfister M, van den Anker J & Eissing T. Physiologically based pharmacokinetic modeling in pregnancy: a systematic review of published models. *Clinical Pharmacology and Therapeutics* 2018 **104** 1110–1124. (<https://doi.org/10.1002/cpt.1084>)
- 47 Li J, Chen R, Yao QY, Liu SJ, Tian XY, Hao CY, Lu W & Zhou TY. Time-dependent pharmacokinetics of dexamethasone and its efficacy in human breast cancer xenograft mice: a semi-mechanism-based pharmacokinetic/pharmacodynamic model. *Acta Pharmacologica Sinica* 2018 **39** 472–481. (<https://doi.org/10.1038/aps.2017.153>)
- 48 Hochhaus G, Barth J, Al-Fayoumi S, Suarez S, Derendorf H, Hochhaus R & Möllmann H. Pharmacokinetics and pharmacodynamics of dexamethasone sodium-m-sulfobenzoate (DS) after intravenous and intramuscular administration: a comparison with dexamethasone phosphate (DP). *Journal of Clinical Pharmacology* 2001 **41** 425–434. (<https://doi.org/10.1177/00912700122010285>)
- 49 Ceccato F, Artusi C, Barbot M, Lizzul L, Pinelli S, Costantini G, Niero S, Antonelli G, Plebani M & Scaroni C. Dexamethasone measurement during low-dose suppression test for suspected hypercortisolism: threshold development with and validation. *Journal of Endocrinological Investigation* 2020 **43** 1105–1113. (<https://doi.org/10.1007/s40618-020-01197-6>)
- 50 Clayton PE, Oberfield SE, Martin Ritzén E, Sippell WG, Speiser PW, Hintz RL & Savage MO. Consensus: Consensus statement on 21-hydroxylase deficiency from the Lawson Wilkins Pediatric Endocrine Society and the European Society for Pediatric Endocrinology. *Journal of Clinical Endocrinology and Metabolism* 2002 **87** 4048–4053. (<https://doi.org/10.1210/jc.2002-020611>)
- 51 Technical Report: congenital adrenal hyperplasia. Section on Endocrinology and Committee on Genetics. *Pediatrics* 2000 **106** 1511–1518. (<https://doi.org/10.1542/peds.106.6.1511>)

---

Received 21 April 2021

Revised version received 28 June 2021

Accepted 6 July 2021

# Supplemental Information to: “Rationale of a lower dexamethasone dose in prenatal congenital adrenal hyperplasia therapy based on pharmacokinetic modelling”

Viktoria Stachanow<sup>1,2</sup>, Uta Neumann<sup>3</sup>, Oliver Blankenstein<sup>3</sup>, Uwe Fuhr<sup>5</sup>, Wilhelm Huisinga<sup>6</sup>, Robin Michelet<sup>1</sup>, Nicole Reisch<sup>4\*</sup>, Charlotte Kloft<sup>1\*</sup>

\*shared senior authorship

## Results: Final population pharmacokinetic model structure

For notation: see Figure 3 and Supplementary Table 1

### Initial conditions:

$$A_{c,0} = 0$$

$$A_{p,0} = 0$$

### State variables and outputs:

$$A_c(t) = A_c(t)$$

$$A_p(t) = A_p(t)$$

$$C(t) = A_c(t)/V_c$$

### System of ordinary differential equations:

$$dA_{gut}/dt = -k_a \cdot A_{gut}$$

$$dA_c/dt = k_a \cdot A_{gut} - CL/V_c \cdot A_c - Q/V_c \cdot A_c + Q/V_p \cdot A_p$$

$$dA_p/dt = Q/V_c \cdot A_c - Q/V_p \cdot A_p$$

### Estimated model parameters:

For individual (“ind.”) parameters

$$k_{a,ind} = k_a \cdot e^{\eta_{k_a,ind}} \quad \eta_{k_a} \sim N(0, \omega_{k_a})$$

$$CL_{ind} = CL \cdot (BW/70)^{\exp_{BW, CL}} \cdot e^{\eta_{CL,ind}} \quad \eta_{CL} \sim N(0, \omega_{CL})$$

$$V_{c,ind} = V_c \cdot (BW/70)^{\exp_{BW, V_c}} \cdot e^{\eta_{V_c,ind}} \quad \eta_{V_c} \sim N(0, \omega_{V_c})$$

$$Q_{ind} = Q \cdot (BW/70)^{\exp_{BW, Q}} \cdot e^{\eta_{Q,ind}} \quad \eta_Q \sim N(0, \omega_Q)$$

$$V_{p,ind} = V_p \cdot (BW/70)^{\exp BW, V_p} \cdot e^{\eta_{Vp,ind}} \quad \eta_{Vp} \sim N(0, \omega_{Vp})$$

## **PK model evaluation:**

### **Goodness-of-fit plots**

The PK model was evaluated with standard goodness-of-fit (GOF) plots indicating that the PK model structure captured the measured Dex concentrations well (Supplementary Figure 1). Figure S1A contained the population-predicted Dex concentrations and revealed the suitability of the structural PK model on the population level, whereas Figure S1B took the interindividual variabilities into account. As the model-predicted and the measured concentrations were close to the line of identity and randomly distributed on both sides of the line, the PK model well predicted the measured Dex concentrations of each individual. In Figure S1C and S1D the conditional weighted residuals (CWRES) were depicted over the Dex concentration range and over time, respectively. In these plots the good model fit was indicated by a symmetric distribution of points around CWRES=0.

### **Visual predictive check**

From the 1000 stochastic simulations performed with the PK model, the 5<sup>th</sup>, 50<sup>th</sup>, and 95<sup>th</sup> percentiles of the simulated Dex concentrations, as well as the 95% confidence intervals around the percentiles, were graphically compared with the measured Dex concentrations and corresponding measured percentiles in a visual predictive check (VPC, Supplementary Figure 2). The VPC revealed an adequate representation of the measured Dex data by the PK model and its predictive performance.

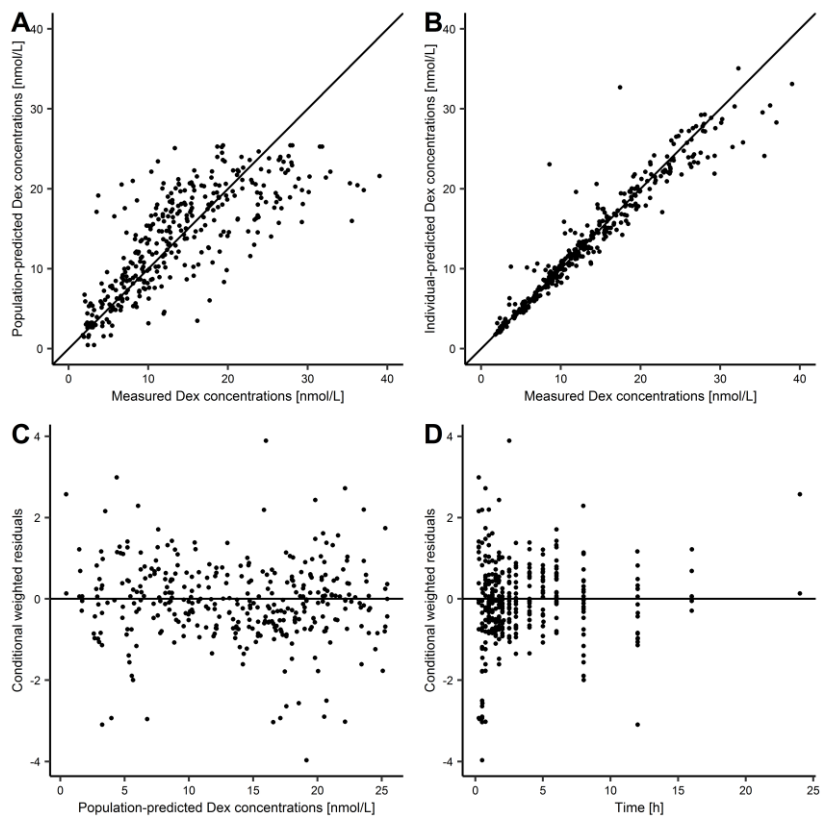
## Supplementary Tables and Figures

**Supplementary Table 1.** Pharmacokinetic parameter estimates of developed dexamethasone model.

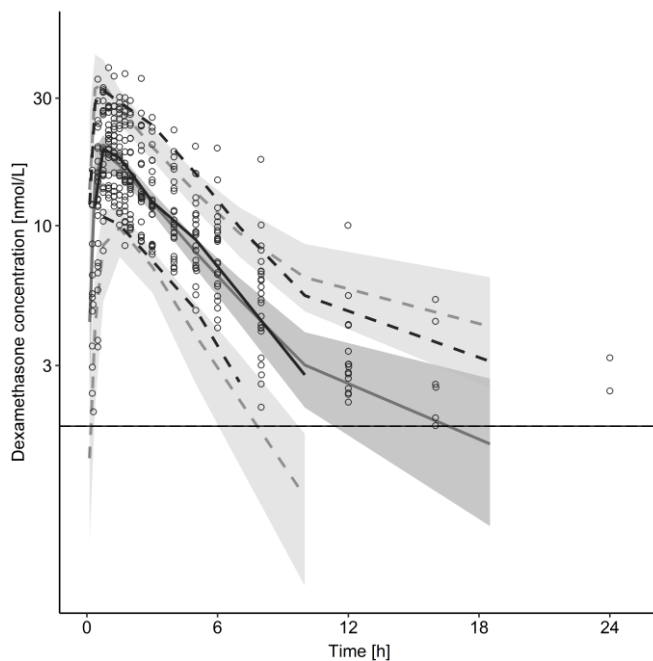
Parameter	Estimate (RSE, %) <sup>#</sup>
<b>Structural model</b>	
F [-]	1*
$k_a$ [ $h^{-1}$ ]	2.95 (20.6)
$t_{lag}$ [h]	0.20 (4.10)
$V_c$ [L]	148 (8.70)
expBW, $V_c$ [-]	1*
Q [L/h]	75.5 (26.6)
expBW, Q [-]	0.75*
$V_p$ [L]	88.9 (15.9)
expBW, $V_p$ [-]	1*
CL [L/h]	40.4 (6.80)
expBW, CL [-]	0.75*
<b>Interindividual variability</b>	
$\omega_{k_a}$ , %CV	110 (19.6)
$\omega_{V_c}$ , %CV	37.4 (14.2)
$\omega_Q$ , %CV	129 (17.5)
$\omega_{V_p}$ , %CV	29.9 (61.3)
$\omega_{CL}$ , %CV	33.6 (15.3)
<b>Residual variability</b>	
$\sigma_{prop}$ , %CV	14.6 (9.1)

Bioavailability (F), absorption rate constant ( $k_a$ ), absorption lag time ( $t_{lag}$ ), central volume of distribution ( $V_c$ ), body weight (BW), allometric scaling exponent for body weight (expBW), intercompartmental clearance (Q), peripheral volume of distribution ( $V_p$ ), clearance (CL), interindividual ( $\omega$ ) and residual ( $\sigma$ ) variability (proportional residual variability), \*: fixed parameters.

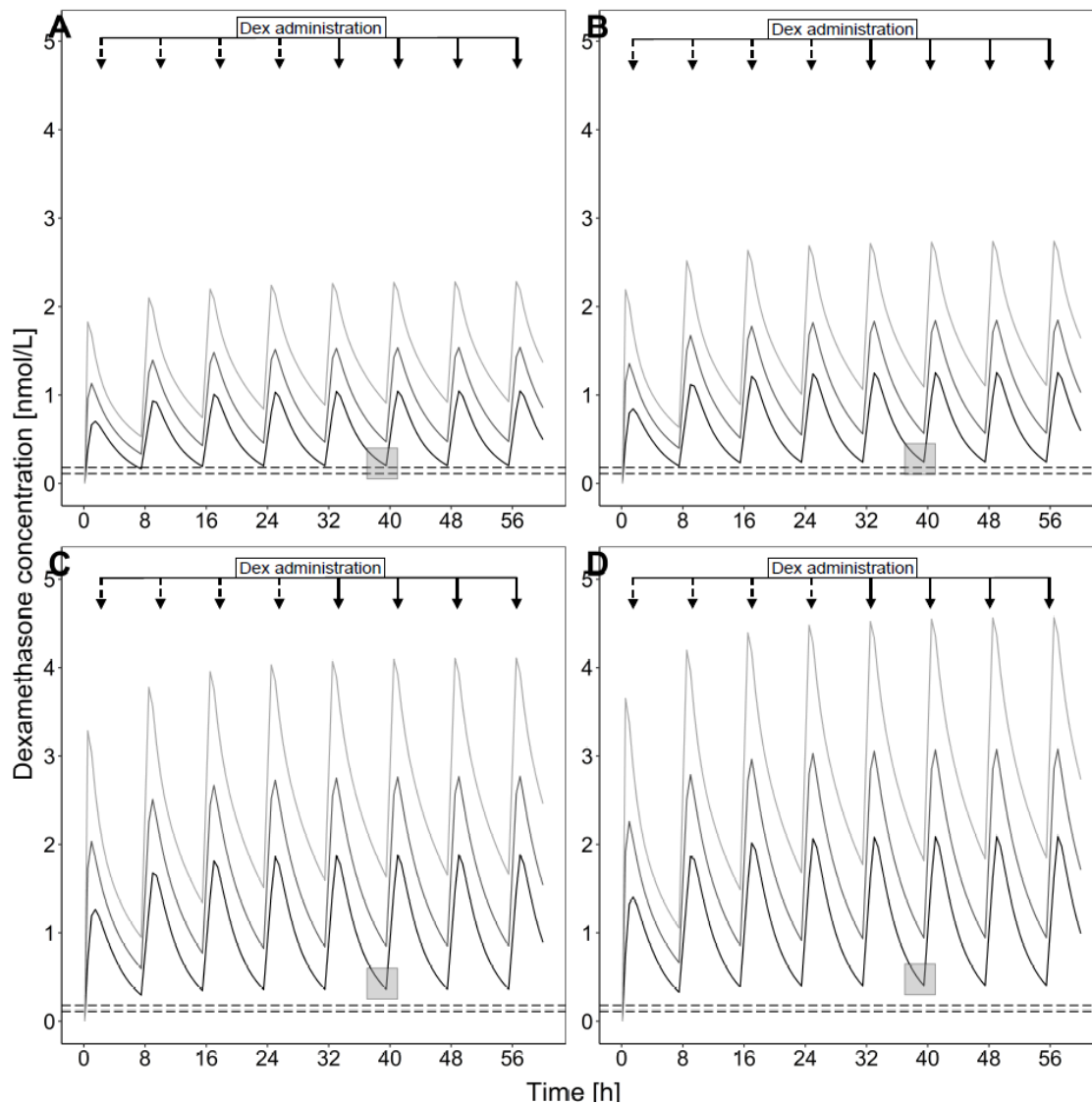
<sup>#</sup>Relative standard error (RSE, %): Standard error (SE) divided by the final parameter estimate times 100. SEs of the model parameters were derived by taking the square root of the diagonal elements of the variance-covariance matrix of the estimates.



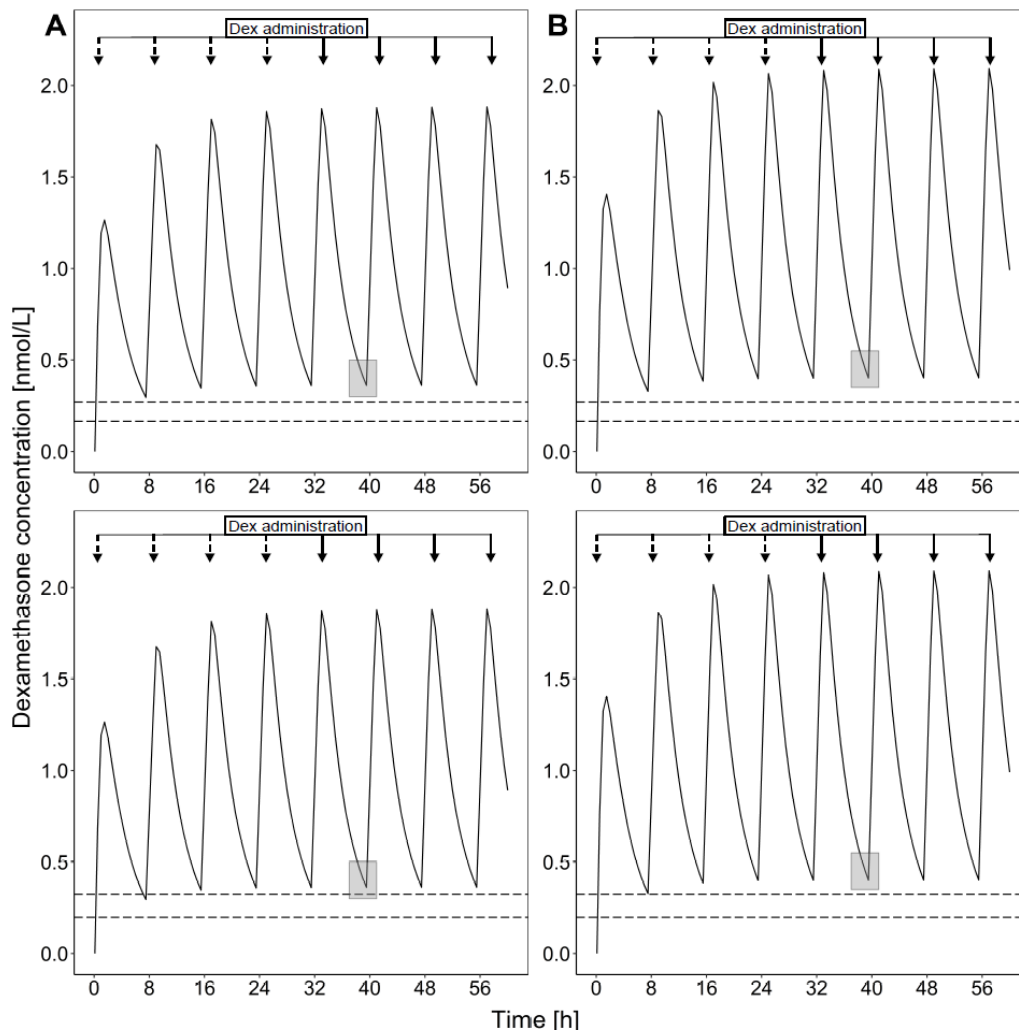
**Supplementary Figure 1.** Goodness-of-fit plots of the developed dexamethasone (Dex) pharmacokinetic model. A: Population-predicted Dex concentrations versus measured Dex concentrations, B: Individual Dex predictions versus measured Dex concentrations, C: Conditional weighted residuals (CWRES) versus population-predicted Dex concentrations, D: Conditional weighted residuals versus time. Solid line: Line of identity (A and B), CWRES=0 (C and D).



**Supplementary Figure 2.** Visual predictive check (n=1000 simulations) for the dexamethasone (Dex) pharmacokinetic model. Lines: the 5<sup>th</sup> (upper dashed), 50<sup>th</sup> (solid) and 95<sup>th</sup> (lower dashed) percentiles of measured (black) and simulated (grey) Dex concentrations; grey shaded areas: 95% confidence interval around the simulated percentiles. Circles: Measured Dex concentrations. Horizontal line: Lower limit of quantification.



**Supplementary Figure 3.** Dexamethasone (Dex) concentration–time profiles after administration of reduced doses with 5 (A), 6 (B), 9 (C) and 10 (D)  $\mu\text{g}/\text{kg}/\text{d}$  for light ( $n=62$ , 50–72 kg) body weight group with  $n=1000$  simulations. 10<sup>th</sup> percentiles (black lines), medians (dark grey lines) and 90<sup>th</sup> percentiles (light grey lines). Dashed horizontal lines: Dex threshold concentration if Dex is 50- (upper line) or 80- fold (lower line) more potent than cortisol, light grey boxes: Minimum Dex concentration at steady state. Arrows: Dex dose administrations before (dashed arrows) and after (solid line arrows) steady state.



**Supplementary Figure 4.** Sensitivity analysis for foetal:maternal dexamethasone concentration ratio. Simulated 10<sup>th</sup> percentile dexamethasone (Dex) profiles of light (n=62, 50-72 kg) body weight group after administration of reduced doses with 9 (A) and 10 (B) µg/kg/d, if foetal:maternal Dex concentration ratio was 0.3 (top) or 0.25 (bottom) instead of 0.45. Dashed horizontal lines: Dex threshold concentration if Dex is 50- (upper line) or 80-fold (lower line) more potent than cortisol, light grey boxes: Minimum Dex concentration at steady state. Arrows: Dex dose administrations before (dashed arrows) and after (solid line arrows) steady state.

## 4 Results and discussion

Pharmacometric analyses are a powerful tool to close knowledge gaps on drug PK and PD and therefore have a great potential to deepen the understanding on CAH therapeutics and to optimise CAH drug therapy with HC and Dex as well as the challenging CAH treatment monitoring in the most vulnerable patient populations. Throughout the work presented in this thesis, NLME modelling was applied to provide new quantitative insights into (1) DBS concentrations as a promising alternative for CAH monitoring in children, (3) a possible paediatric target morning 17-OHP concentration range in DBS and (2) a Dex dose suggestion for prenatal CAH therapy based on a scientific rationale.

### 4.1 Relationship between plasma and dried blood spot cortisol concentrations (Paper I)

In the project of *Paper I*, a quantitative link between plasma and DBS cortisol concentrations was successfully established by capitalising on DBS cortisol data to extend a published semi-mechanistic plasma cortisol PK model. The association of cortisol with RBCs was characterised in addition to CBG and albumin binding. The cortisol binding behaviour described in whole blood by the developed HC PK model was then further explored in simulations.

#### *Graphical exploration of plasma versus DBS cortisol concentrations*

In total, 19/106 (17.9%, LLOQ =14.1 nmol/L) of the plasma concentrations and 0.94% (n = 1 of 106, LLOQ =1.8 nmol/L) of the DBS concentrations from the paediatric CAH patients were below the LLOQ. All adult total cortisol plasma concentrations were above the LLOQ. The majority of paediatric plasma observations below LLOQ were pre-dose concentrations (13/18 in total, 6/6 in neonates, 3/6 in infants) which was expected as the circadian rhythm of cortisol becomes evident after an age of 2-3 months [134]. Therefore, and since only 6 out of 82 post-dose concentrations were below LLOQ (7.3%), all BLQ observations were discarded according to the M1 method (see 2.2.4) [15]. Thus, 87 paediatric plasma samples and 105 paediatric DBS samples remained for analysis.

The graphical analysis of the paediatric cortisol data revealed that plasma cortisol concentrations were considerably higher than DBS cortisol concentrations with highly variable ratios, ranging from approximately 2 to 8 (Figure 4.1 A). The relationship between total cortisol concentrations in plasma and DBS was nonlinear, as the plasma/DBS cortisol concentration ratio decreased with higher cortisol concentrations (Figure 4.1 B): Within DBS cortisol concentrations from 0 to 200 nmol/L (n = 83, Figure 4.1 A), the plasma/DBS cortisol concentration ratio ranges widely from 1.62 up to 8.01 (median 5.17) whereas with higher concentrations (n = 4), which were only observed in the neonatal age group, the

concentration ratio decreased to values of 1.88–3.51 (median: 2.41). Especially due to the limited number of observations in the higher concentration range, these ratios should be confirmed with a richer dataset, before they can be considered for interpreting DBS cortisol concentrations during clinical monitoring in paediatric adrenal insufficiency patients.

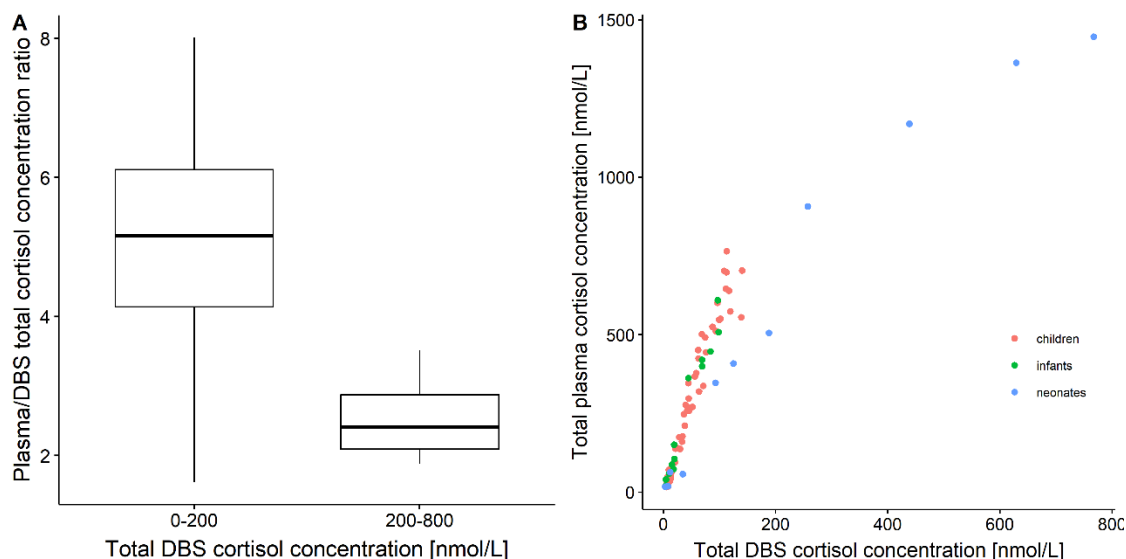


**Figure 4.1** (A) Boxplot of plasma to dried blood spot (DBS) cortisol concentration ratio versus cortisol DBS concentration ranges of 0-200 nmol/L ( $n=83$ ) and 200-800 nmol/L ( $n=4$ ). (B) Total cortisol concentration in plasma versus total cortisol concentration in DBS. Red: young children, green: infants, blue: neonates.

### *Cortisol PK model development*

By leveraging cortisol concentrations from adult plasma data ( $n=1482$ ) and paediatric plasma and DBS data ( $n=106$  each) a quantitative link between paediatric total plasma cortisol concentrations and paediatric total DBS cortisol concentrations was successfully established. This was achieved by extending a published NLME cortisol PK model [98], which was based on plasma cortisol data from healthy adults (cortisol biosynthesis suppressed by Dex) and paediatric CAH patients, with DBS concentrations from paediatric patients. As indicated in the model scheme in blue (Figure 4.2), the published cortisol PK model (black) [98] was extended by an additional compartment describing cortisol bound to RBCs with a linear first-order rate constant ( $k_{aRBC}$ ) describing cortisol association with RBCs, as well as with a corresponding estimated apparent volume ( $V_{\text{delta}}$ ) and a paediatric DBS cortisol baseline ( $\text{BASE}_{\text{child, DBS}}$ ).

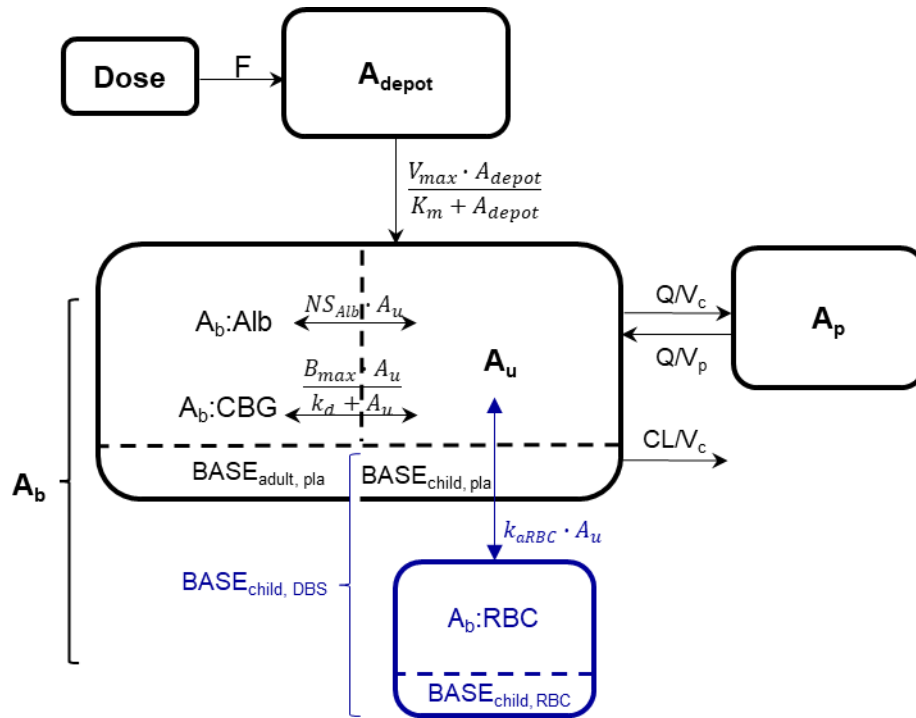


**Figure 4.2** Schematic representation of developed cortisol PK model including adult plasma data and paediatric plasma and dried blood spot (DBS) data, blue: new DBS-related compartments/parameters/data.

Bioavailability ( $F$ ), amount in depot compartment ( $A_{\text{depot}}$ ), maximum absorption rate ( $V_{\text{max}}$ ), amount in depot compartment resulting in half of  $V_{\text{max}}$  ( $K_m$ ), amount bound ( $A_b$ ), amount bound to albumin ( $A_b:\text{Alb}$ ), amount associated with red blood cells ( $A_b:\text{RBC}$ ), unbound amount ( $A_u$ ), amount bound to corticosteroid-binding globulin ( $A_b:\text{CBG}$ ), linear non-specific parameter for albumin binding ( $NS_{\text{Alb}}$ ) and linear association constant for association with red blood cells ( $k_{\text{aRBC}}$ ), maximum binding capacity ( $B_{\text{max}}$ ), equilibrium dissociation constant ( $k_d$ ), clearance ( $CL$ ), intercompartmental clearance ( $Q$ ), central volume of distribution ( $V_c$ ), peripheral volume of distribution ( $V_p$ ), cortisol plasma baseline of dexamethasone-suppressed healthy adults ( $\text{BASE}_{\text{adult, pla}}$ ), cortisol plasma baseline of children ( $\text{BASE}_{\text{child, pla}}$ ), cortisol DBS baseline of children ( $\text{BASE}_{\text{child, DBS}}$ ), cortisol associated with red blood cells at baseline in children ( $\text{BASE}_{\text{child, RBC}}$ ). The dashed line divides the central compartment into the subcompartments of bound and unbound cortisol amount ( $A_b$  and  $A_u$ ), respectively.

Equations 4.1-4.3 show how the three different kinds of observations in the dataset (paediatric plasma cortisol, paediatric DBS cortisol and adult plasma cortisol concentrations) were determined by the PK model.

$$C_{\text{pla,child}} = A_{\text{pla}} / V_c \quad (\text{Eq. 4.1})$$

$$C_{\text{DBS,child}} = (A_{\text{pla}} + A_b:\text{RBC} + \text{BASE}_{\text{child,RBC}}) / (V_c + V_{\text{delta}}) \quad (\text{Eq. 4.2})$$

$$C_{\text{pla,adult}} = (A_{\text{pla}} + \text{BASE}_{\text{adult,pla}}) / V_c \quad (\text{Eq. 4.3})$$

The paediatric plasma cortisol concentration ( $C_{pla,child}$ ) was defined as the total amount of cortisol in plasma ( $A_{pla}$ ) divided by the central volume of distribution ( $V_c$ ) (Eq. 4.1). The paediatric DBS cortisol concentration was the sum of  $A_{pla}$ , the amount of cortisol associated with RBCs ( $A_b:RBC$ ) and the amount of cortisol associated with RBCs at baseline ( $BASE_{child,RBC}$ ), divided by the whole blood volume which was the sum of  $V_c$  and the volume of the RBC compartment ( $V_{delta}$ ) (Eq. 4.2).  $BASE_{child,RBC}$  was thereby defined as the difference between the two parameter values of the paediatric plasma and DBS baselines ( $BASE_{child,pla}$  and  $BASE_{child,DBS}$ ). These two baselines were modelled according to the B2 method by using the baseline observations or were estimated (B1 method) if no observation was available (see 2.2.5). The central plasma compartment in paediatrics was initialised with the concentration value of  $BASE_{child,pla}$ , whereas the adult plasma baseline concentration was estimated as a constant value and was added to the adult cortisol amount (Eq. 4.3). Since the PK parameters were estimated using log-transformed data, the RUV was estimated by an additive model on a logarithmic scale, which approximated a proportional RUV model on a linear scale. GOF plots and VPCs indicated a good fit of the PK model to both the paediatric and adult data (Figures 4.3 and 4.4).

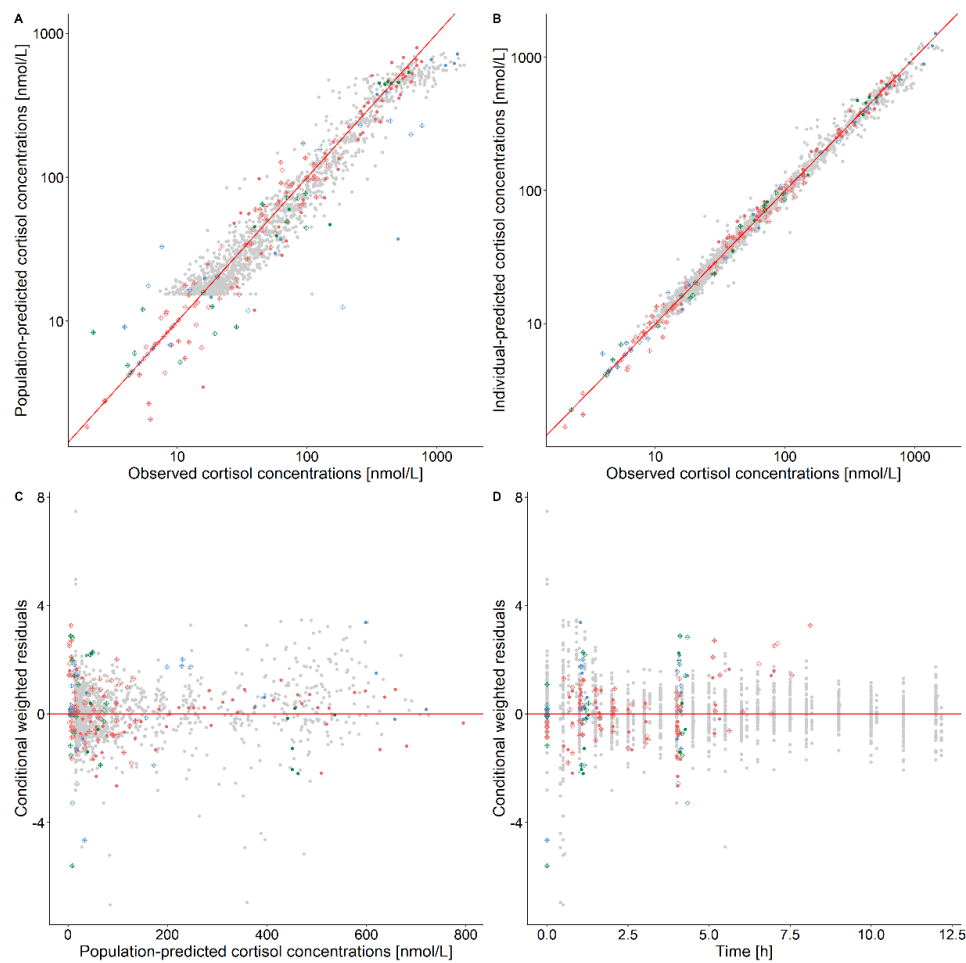


**Figure 4.3** Goodness-of-fit plots of the developed cortisol pharmacokinetic model including adult plasma data and paediatric plasma and dried blood spot data.

(A) Population-predicted cortisol concentrations versus observed cortisol concentrations, (B) Individual cortisol predictions versus observed cortisol concentrations, (C) Conditional weighted residuals versus population-predicted cortisol concentrations, (D) Conditional weighted residuals versus time. Red: young children, green: infants, blue: neonates, grey: adult observations, filled circles: plasma concentrations, diamonds: dried blood spot concentrations, red line: line of identity (A, B), line  $y=0$  (C, D).

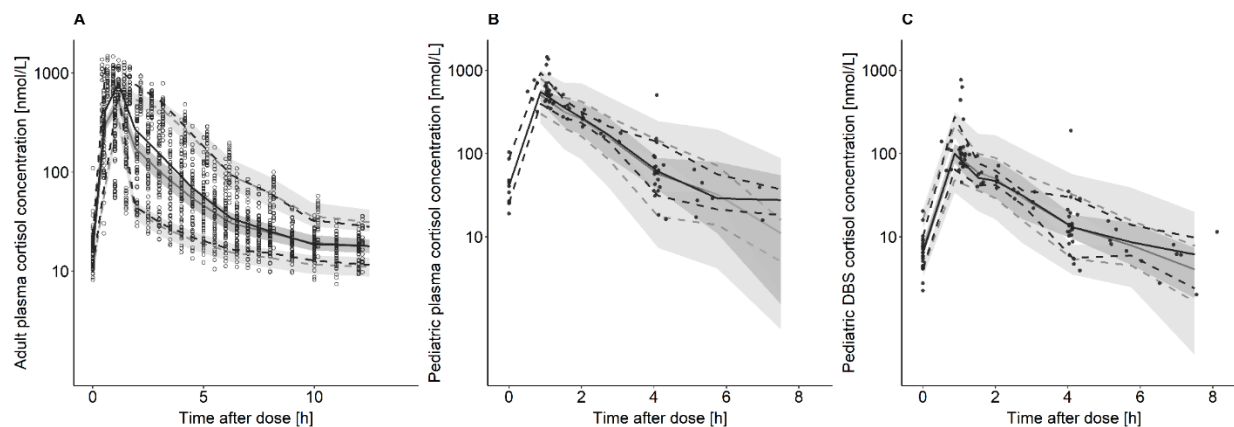


**Figure 4.4** Visual predictive check ( $n=1000$  simulations) for developed cortisol pharmacokinetic model including adult plasma data and paediatric plasma and dried blood spot (DBS) data.

Adult total cortisol plasma concentrations (A), paediatric total cortisol plasma concentrations (B), paediatric total cortisol DBS concentrations (C). Circles: cortisol observations, black/grey solid line: 50<sup>th</sup> percentile of observed/simulated concentrations, black/grey dashed lines: 10<sup>th</sup> and 90<sup>th</sup> percentiles of observed/simulated concentrations, grey shaded areas: 95 % confidence intervals for the percentiles of the simulated data.

The higher cortisol concentrations, which were leading to relatively higher cortisol DBS concentrations compared to cortisol concentrations in plasma, were for the most part observed in neonates. Therefore, ‘age group’, i.e., ‘children/infants’ and ‘neonates’, was evaluated as a dichotomous categorical covariate on  $V_{\text{delta}}$ . The age group explained more than two-thirds (69.1%) of the  $V_{\text{delta}}$  IIV (before: 196% CV, after: 60.6% CV). Moreover, age was tested as a continuous covariate on  $V_{\text{delta}}$ , with exponential and fractional changes from the median age (see 2.2.2), but explained only 20 and 27% of the  $V_{\text{delta}}$  IIV, respectively. The inclusion of the paediatric cortisol DBS data changed the plasma-related parameter estimates only minimally, compared to the estimates from the previous model, whereas the additional DBS-related parameter estimates were plausible. The estimated typical  $V_{\text{delta}}$  for children/infants was 11.1 L compared to 1.05 L in neonates, corresponding to 0.82 L/kg and 0.29 L/kg for children + infants and for neonates, respectively, and was thereby, as an apparent volume of distribution, accounting for the lower plasma/DBS concentration ratio observed in neonates (see Table 4.1). It was however assumed that these differences in plasma/DBS concentration ratios were observed due to the cortisol concentration, not due to an age effect. The high cortisol concentrations observed in neonates were the result of a relatively higher HC dose which was given to avoid underexposure in this highly vulnerable cohort.

**Table 4.1.** Parameter estimates with sampling importance resampling (SIR) median and 95% confidence intervals (CI) of developed cortisol pharmacokinetic (PK) model including adult plasma data and paediatric plasma and dried blood spot (DBS) data.

Parameter	SIR median [95% CI]
<b>Structural model</b>	
CL [L/h]	400 [289-549]
$V_c$ [L]	10.6 [7.99-14.0]
Q [L/h]	160 [90.4-268]
$V_p$ [L]	124 [80.7-178]
$K_m$ [nmol]	4810*
$V_{max}$ [nmol/h]	21388 [13888-31463]
F [-]	1*
$k_d$ [nM]	9.71*
$NS_{Alb}$ [-]	4.15*
$k_{aRBC}$ [-]	6.62 [1.95-13.4]
$V_{\Delta, children+infants}$ [L]	11.1 [7.05-18.8]
$V_{\Delta, neonates}$ [L]	1.05 [0.50-1.80]
$BASE_{adult, pla}$ [nM]	15.2 [11.1-20.7]
$BASE_{child, pla}$ [nM]	9.41 [3.32-16.7]
$BASE_{child, DBS}$ [nM]	4.22 [1.10-7.60]
<b>Interindividual variability</b>	
$\omega_{CL}$ , %CV	25.8 [14.9-35.8]
$\omega_{K_m}$ , %CV	55.7 [31.1-75.5]
$\omega_{V_{max}}$ , %CV	46.5 [30.1-65.5]
$\omega_F$ , %CV	36.1 [20.4-49.4]
$\omega_{V_{\Delta}}$ , %CV	43.4 [27.5-62.2]
$\omega_{BASE_{adult, pla}}$ , %CV	35.3 [23.5-47.4]
$\omega_{BASE_{child, pla \text{ and } DBS}}$ , %CV	131.1*
<b>Residual variability</b>	
$\sigma_{exp}$ [CV%]	14.4 [13.2-16.0]

Clearance (CL), central volume of distribution ( $V_c$ ), intercompartmental clearance (Q), peripheral volume of distribution ( $V_p$ ), amount in depot compartment resulting in half of  $V_{max}$  ( $K_m$ ), maximum absorption rate ( $V_{max}$ ), bioavailability (F), equilibrium dissociation constant ( $k_d$ ), linear non-specific binding parameter for albumin and association to red blood cells ( $NS_{Alb}$  and  $k_{aRBC}$ ), apparent volume of red blood cell compartment ( $V_{\Delta}$ ), plasma cortisol baseline in children ( $BASE_{child, pla}$ ), dried blood spot cortisol baseline in children ( $BASE_{child, DBS}$ ), cortisol bound to red blood cells at baseline in children ( $BASE_{child, RBC}$ ). For  $BASE_{child, pla}$  and  $BASE_{child, DBS}$  a common interindividual variability was fixed, interindividual ( $\omega$ ) and residual ( $\sigma$ ) variability (additive model on a logarithmic scale), \*fixed parameter.

More data is required to investigate whether there is an actual age impact on the highly variable plasma/DBS concentration ratio. A possible age effect could be e.g., due to CBG maturation during the first year of life [64] or due to haematocrit which is known to be higher in neonates, compared to older children and adults [135,136]. In general, the PK model should be re-evaluated with more profound paediatric plasma and DBS cortisol data to confirm the conclusions made in this analysis, since the used paediatric cortisol data was sparse, and the estimation was therefore also based on rich adult data.

Since the association of cortisol with RBCs has been described as a linear process [54],  $k_{aRBC}$  was defined and estimated as a linear association constant and allowed to quantitatively characterise cortisol association with RBCs, in addition to cortisol binding to CBG, and to albumin. The linear association described in literature referred to adults only. However, due to the general abundance of RBCs, a saturation of this process should not be expected and thus these findings were assumed to also apply to children. As the underlying mechanism of cortisol association with RBCs is still not fully elucidated (e.g., adsorption or uptake), it should be further investigated qualitatively and quantitatively in *in vitro* studies. The linear binding/association parameters of cortisol to albumin ( $NS_{Alb}$ ) and RBCs ( $k_{aRBC}$ ) resulted in 4.15 and 6.62, respectively. The predominant binding partner was, as expected, CBG, with a fixed  $k_d$  of 9.71 nmol/L. For a better comparison of these binding parameters, the fractions of cortisol bound to CBG, to albumin, and associated with RBCs were simulated.

### ***Simulations of cortisol binding in full blood***

The deterministically simulated whole blood cortisol concentrations of children/infants (Figure 4.5 A) and of neonates (Figure 4.5 B) were based on the estimated  $V_{\text{delta}}$  of the respective age group. Giving the same HC dose to both age groups mimicked the relatively higher exposure in neonates during the Alkindi® trial and thus the higher cortisol concentrations observed in neonates. The cortisol fraction (%) bound to CBG substantially decreased with increasing total cortisol concentrations (from 90 to 22% in neonates and from 90% to 45% in children/infants) due to the saturation of the binding process. Consequently, due to the saturation of the CBG binding and thus higher availability of unbound cortisol molecules, the fraction unbound, the fraction bound to albumin and the fraction associated with RBCs increased substantially. At the highest simulated whole blood cortisol concentrations, 45% more cortisol was associated with RBCs in neonates (12% at 820 nmol/L  $C_{\text{max}}$ ) compared to children/infants (8.3% at 180 nmol/L  $C_{\text{max}}$ ). These simulation results therefore supported the results from the exploratory analysis which showed a decreasing plasma/DBS cortisol ratio, i.e., relatively higher DBS cortisol concentrations, with increasing plasma cortisol concentrations and could partly explain the high difference in the plasma/DBS concentration ratio observed for the two age groups.

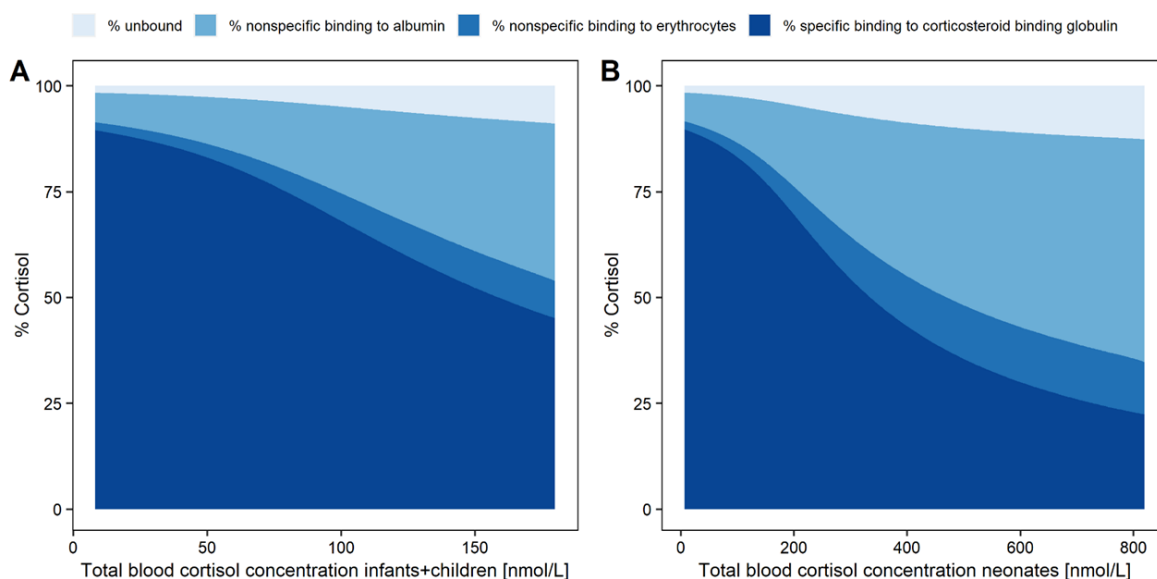


**Figure 4.5** Simulated cortisol concentration fractions (%) as unbound (pale blue), with non-specific linear binding to albumin (light blue), non-specific linear binding to red blood cells (middle blue) or specific nonlinear binding (dark blue) to corticosteroid binding globulin, over total whole blood (dried blood spot) concentration (1.8 nmol/L=LLOQ to  $C_{max}$ ) in infants and children (A) and neonates (B).

This project represented a first step to quantitatively link plasma and DBS cortisol concentrations measured in paediatric CAH patients. In future, after re-evaluation of this analysis with a richer paediatric dataset, a simulation-based regression equation could be established to enable a conversion of measured DBS cortisol concentrations into the more conventionally known plasma cortisol concentrations. Such an equation would open the opportunity for a routine use and interpretation of DBS measurements obtained during CAH monitoring in the vulnerable paediatric patient population. Furthermore, the applicability of the PK model to children older than 6 years can be assessed in future with corresponding available data. Moreover, the DBS data used in this analysis comprised venous whole blood concentrations, whereas in clinical practice either capillary or venous whole blood is obtained for DBS sampling. The comparability of capillary and venous cortisol and 17-OHP concentrations was addressed in *Paper II* (see 2.4 and 4.2).

## **4.2 Target morning dried blood spot 17 $\alpha$ -hydroxyprogesterone concentrations for paediatric congenital adrenal hyperplasia patients (Paper II)**

To derive a target morning DBS concentration range for the clinically important biomarker 17-OHP, the challenge of limited available data was met by leveraging different sources of cortisol (PK) concentrations and 17-OHP (PD) concentrations in a modelling and simulation analysis framework. A PK/PD model, linking plasma cortisol concentrations and venous DBS 17-OHP concentrations, was successfully developed, and applied in simulations using plasma cortisol data of non-CAH children. Moreover, to determine the clinical applicability of the derived target range, a Bland-Altman and Passing-Bablok regression analysis were conducted to investigate the comparability of venous and capillary 17-OHP concentrations since both venous and capillary DBS samples are usually obtained in clinical practice.

### ***Exploratory graphical analysis and PK/PD model development***

The observed concentration-time profiles of DBS 17-OHP resembled a u-shape indicating an initial decrease of 17-OHP (Figure 4.6 A). The decrease was likely due to the HC treatment-mediated inhibition of 17-OHP synthesis followed by a subsequent increase of 17-OHP due to cortisol clearance. This tendency was also visible for DBS 17-OHP versus plasma cortisol concentrations where 17-OHP concentrations decreased with increasing cortisol concentrations (Figure 4.6 B). Since plasma cortisol profiles from healthy children aged between 5 and 9 were applied in the later simulations, the young children cohort from the Alkindi<sup>®</sup> study (see 2.1.3), i.e., children of a similar age range ( $\geq 2$ -6 years), were used for the PK/PD model development. Moreover, infant data ( $\geq 28$  days-2 years) from the same study was included in the model analysis, as the DBS 17-OHP concentrations, including the concentrations at baseline, were in comparable ranges for young children and infants.

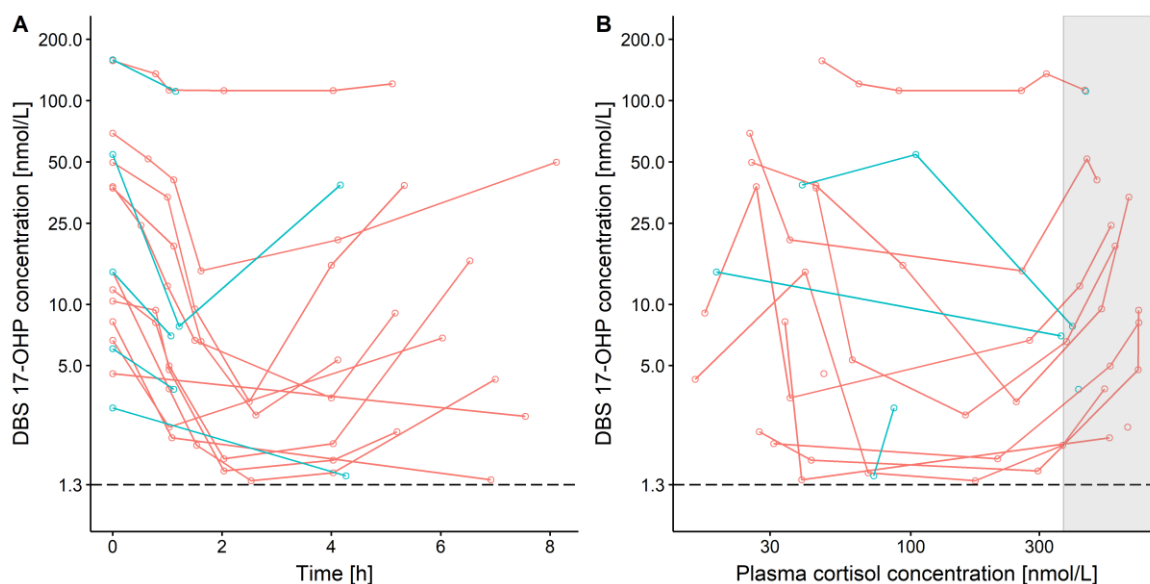


**Figure 4.6**  $17\alpha$ -hydroxyprogesterone (17-OHP) concentrations measured in venous dried blood spots (DBS) over time after first (baseline) observation, semi-log scale (A) and versus plasma cortisol concentration, log scales (B), in paediatric CAH patients receiving hydrocortisone (HC) single morning dose. Red: young children, blue: infants, dashed line: lower limit of quantification = 1.3 nmol/L, grey box: highest plasma cortisol concentrations directly after HC administration.

Based on the well-known mechanism of cortisol inhibiting 17-OHP biosynthesis via the suppression of the HPA-axis by a negative feedback mechanism [12-14] and on the findings from the exploratory graphical analysis, a so-called indirect PK/PD response model was developed.

The PK/PD model development was sequential [125,126], i.e., the individual PK parameter estimates of the paediatric subpopulation in the PK model presented in *Paper I* were directly incorporated into the modelling dataset. This approach resulted in only the PD parameters being estimated and thus overcoming the difficulty of building an overparameterised and unstable model. In Figure 4.7, the full PK/PD model scheme is shown with all PK parameters, of which the individual estimates were incorporated into the modelling dataset, highlighted in orange. Besides modelling young children and infant data combined, also the development of a PK/PD model based on young children only was tested. No significant differences were found in the estimated model parameters, their imprecisions and in the derived morning target DBS 17-OHP concentrations.

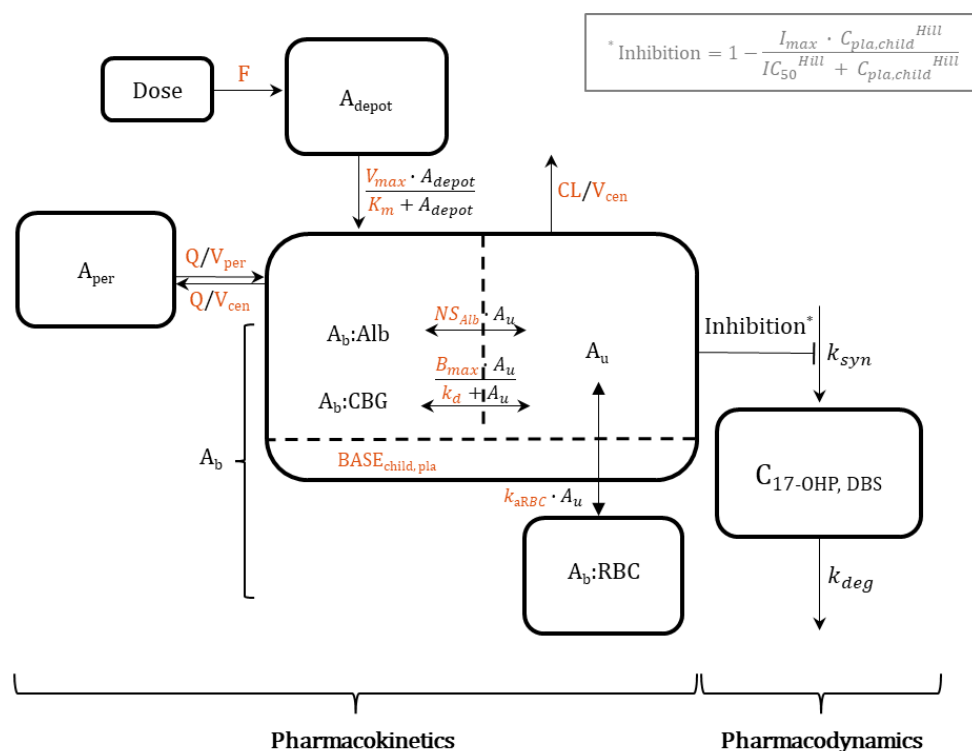


**Figure 4.7** Schematic representation of developed pharmacokinetic/pharmacodynamic (PK/PD) model. PK parameters of which the paediatric individual estimates from the previous PK model (*Paper I*) were used as part of the dataset are marked in orange.

Pharmacokinetics: Bioavailability ( $F$ ), amount in depot compartment ( $A_{depot}$ ), maximum absorption rate ( $V_{max}$ ), amount in depot compartment resulting in half of  $V_{max}$  ( $K_m$ ), amount bound ( $A_b$ ), amount bound to albumin ( $A_b:Alb$ ), amount associated with red blood cells ( $A_b:RBC$ ), unbound amount ( $A_u$ ), amount bound to corticosteroid-binding globulin ( $A_b:CBG$ ), linear non-specific parameter for albumin binding ( $NS_{Alb}$ ) and linear association constant for association with red blood cells ( $k_{aRBC}$ ), maximum binding capacity ( $B_{max}$ ), equilibrium dissociation constant ( $k_d$ ), clearance ( $CL$ ), intercompartmental clearance ( $Q$ ), central volume of distribution ( $V_{cen}$ ), peripheral volume of distribution ( $V_{per}$ ), cortisol plasma baseline of children ( $BASE_{child, pla}$ ). The dashed line divides the central compartment into the  $A_b$  and  $A_u$  subcompartments, respectively.

Pharmacodynamics:  $17\alpha$ -hydroxyprogesterone (17-OHP) concentration in dried blood spots ( $C_{17-OHP, DBS}$ ), first-order synthesis rate constant of 17-OHP ( $k_{syn}$ ), first-order degradation rate constant of 17-OHP ( $k_{deg}$ ), Hill coefficient (Hill), maximum inhibitory effect ( $I_{max}$ ), Cortisol concentration inhibiting 50% of  $I_{max}$  ( $IC_{50}$ ), paediatric plasma cortisol concentration ( $C_{pla,child}$ ).

The developed PK/PD model described a cortisol-mediated inhibition of the 17-OHP synthesis, characterised by its synthesis rate ( $k_{syn}$ ) (Figure 4.7). The inhibition term was described by an  $I_{max}$ -model [126] (Eq. 4.4.) with the paediatric plasma cortisol concentration  $C_{pla,child}$  driving the inhibition of  $k_{syn}$ , and with the maximum inhibitory effect  $I_{max}$  as well as the ‘Hill’ coefficient describing the steepness of the inhibition curve, both fixed to 1.  $k_{syn}$  was defined as the product of the estimated 17-OHP first-order degradation rate constant ( $k_{deg}$ ) and the observed DBS 17-OHP baseline concentration

( $OHP_{BASE}$ , Eq. 4.5). The 17-OHP baseline concentrations were modelled according to the B2 method, using the DBS 17-OHP baseline observations [120] (see 2.2.5).

$$I = 1 - \frac{I_{max} \cdot C_{pla,child}^{Hill}}{IC_{50}^{Hill} + C_{pla,child}^{Hill}} \quad (\text{Eq. 4.4})$$

$$k_{syn} = OHP_{BASE} \cdot k_{deg} \quad (\text{Eq. 4.5})$$

The cortisol concentration inhibiting 50% of the maximum inhibitory effect ( $IC_{50}$ ) was estimated to be 21 nmol/L with a high estimated IIV (104% CV) which could not be explained by any available covariate such as body weight, CBG or albumin due to the sparse modelling data (Table 4.2). The  $IC_{50}$  estimate was approximately half of previously reported estimate values, e.g., 40.3 nmol/L by Al-Kofahi *et al.* [100] and 48.6 nmol/L by Melin *et al.* [99]. This difference was due to the  $IC_{50}$  in this analysis representing plasma cortisol inhibiting the 17-OHP synthesis in a different matrix, i.e., in DBS and is well in line with the plasma/DBS concentration ratios observed in *Paper I* (see 4.1). Despite the sparseness of the data, as being typical for study data in young children, the model overall resulted in plausible PD parameter estimates with satisfactory precision. RSEs of the estimated model parameters were low, except for IIV on  $IC_{50}$  (53%). The RUV was estimated by an additive model on a logarithmic scale. GOF plots and the VPC indicated that the venous DBS 17-OHP observations were adequately described by the PK/PD model (Figures 4.8 and 4.9).

**Table 4.2.** Parameter estimates of developed pharmacokinetic/pharmacodynamic (PK/PD) model for cortisol (drug) and 17 $\alpha$ -hydroxyprogesterone (biomarker) concentrations in young children and infants.

Parameter	Estimate (RSE, %)
<b>Structural model</b>	
$k_{deg}$ [1/h]	1.22 (7.0)
$IC_{50}$ [nmol/L]	21.0 (27)
$I_{max}$ [-]	1*
Hill [-]	1*
<b>Interindividual variability</b>	
$\omega_{kdeg}$ , % CV	5.0*
$\omega_{IC50}$ , % CV	104 (53)
$\omega_{17-OHPBASE}$ , % CV	131*
<b>Residual variability</b>	
$\sigma_{exp}$ [% CV]	38.1 (15)

17-OHPBASE: 17 $\alpha$ -hydroxyprogesterone (17-OHP) dried blood spot concentration at baseline, Hill: Hill coefficient,  $IC_{50}$ : Cortisol concentration inhibiting 50% of the maximum inhibitory effect  $I_{max}$ ,  $k_{deg}$ : first-order degradation rate constant of 17-OHP, RSE: Relative standard error, interindividual ( $\omega$ ) and residual ( $\sigma$ ) variability (additive model on a logarithmic scale), \*: fixed parameters.

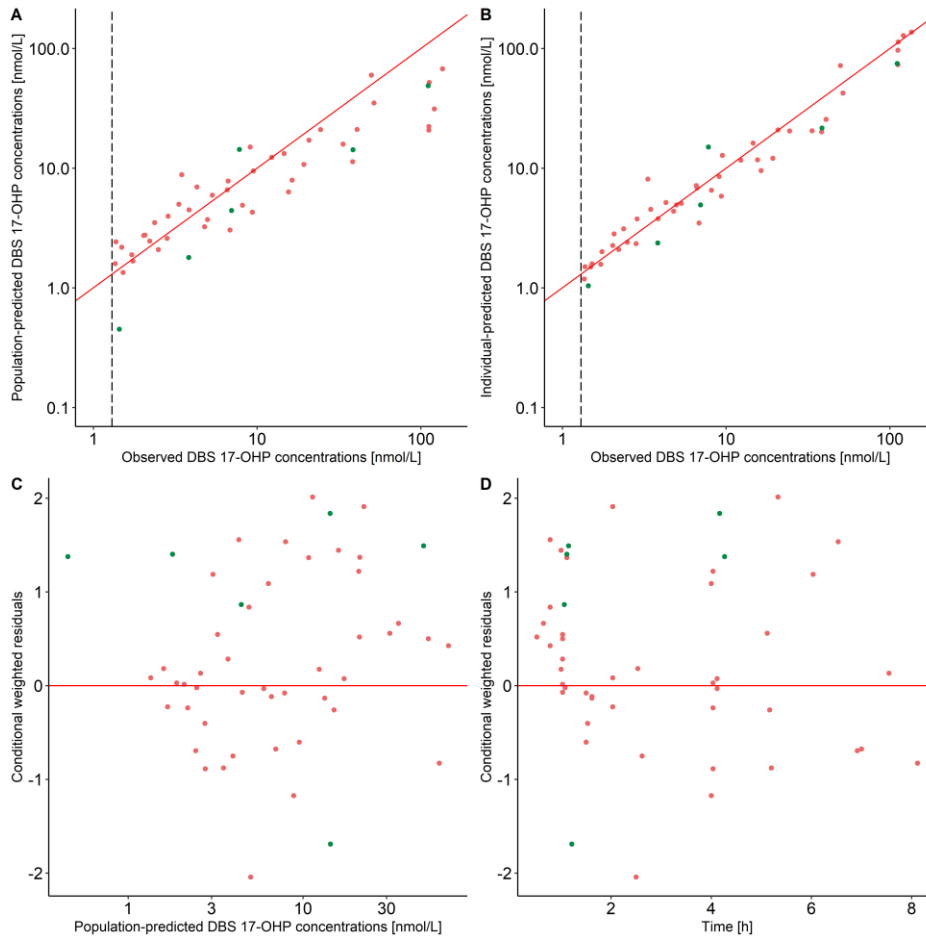


**Figure 4.8** Goodness-of-fit plots for developed pharmacokinetic/pharmacodynamic (PK/PD) model. A: Population-predicted dried blood spot (DBS) 17 $\alpha$ -hydroxyprogesterone (17-OHP) concentrations versus observed DBS 17-OHP concentrations, B: Individual DBS 17-OHP predictions versus observed DBS 17-OHP concentrations, C: Conditional weighted residuals versus population-predicted DBS 17-OHP concentrations, D: Conditional weighted residuals versus time. Red dots: young children, green dots: infants, red line: line of identity (A, B), line  $y=0$  (C, D), vertical dashed line: lower limit of quantification (LLOQ) = 1.3 nmol/L.

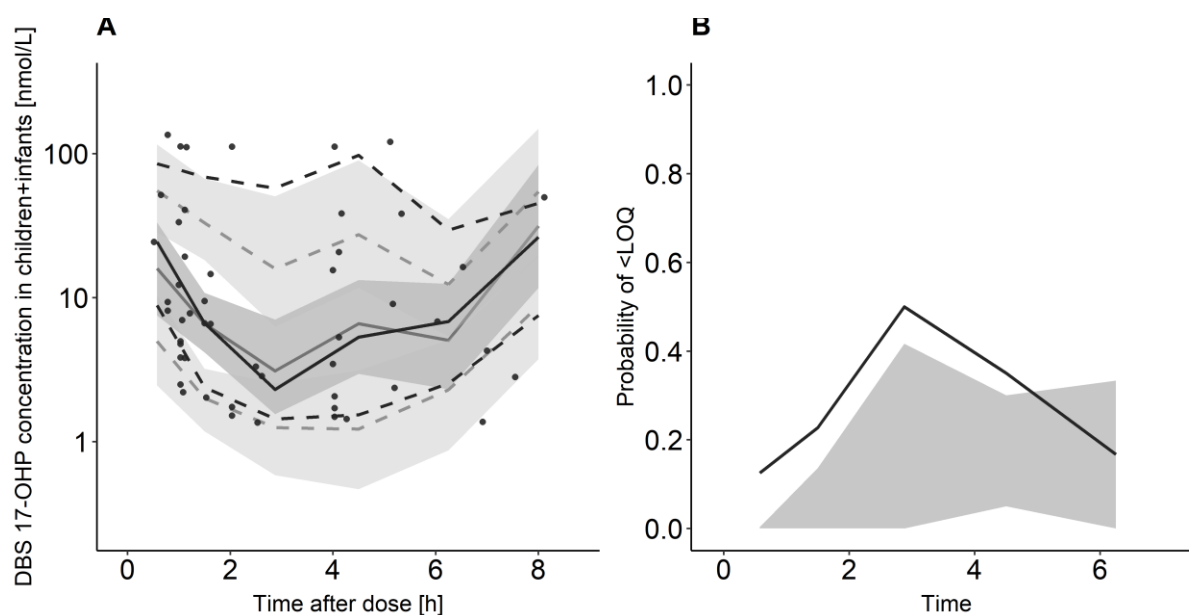


**Figure 4.9** Visual predictive check (n=1000) for developed pharmacokinetic/pharmacodynamic (PK/PD) model.

A: Circles: 17 $\alpha$ -hydroxyprogesterone (17-OHP) dried blood spot (DBS) observations, solid line: 50<sup>th</sup> percentile of observed (black) and simulated (grey) DBS 17-OHP concentrations, dashed lines: 10<sup>th</sup> and 90<sup>th</sup> percentiles of observed (black) and simulated (grey) DBS 17-OHP concentrations, shaded areas: 95 % confidence intervals for the percentiles of the simulated data. B: Black line: Observed probability of DBS 17-OHP concentrations below lower limit of quantification (LLOQ), grey area: 95 % confidence interval for simulated probability of 17-OHP concentrations below LLOQ.

#### ***Deriving target morning DBS 17-OHP concentrations in simulations***

Physiological DBS 17-OHP concentrations were simulated in stochastic simulations (n=1000), to take the high estimated IIVs of IC<sub>50</sub> and of the DBS 17-OHP baseline from the developed PK/PD model into account. Circadian cortisol concentration-time profiles from 28 healthy children (Figure 4.10) served as the PK input in the model dataset to simulate corresponding physiological DBS 17-OHP concentrations. The simulated physiological concentrations were then multiplied by the factors 3 and 5 to obtain the corresponding target concentrations (see 2.4). Considering DBS 17-OHP concentrations simulated for relevant time range of 6 to 8 a.m. (corresponding to the time before the morning dose) this resulted in a target morning DBS 17-OHP concentration range of 2.1-8.3 nmol/L, which is shown in the boxplot in Figure 4.11, depicting the interquartile range of all derived and highly variable target morning DBS 17-OHP concentrations.

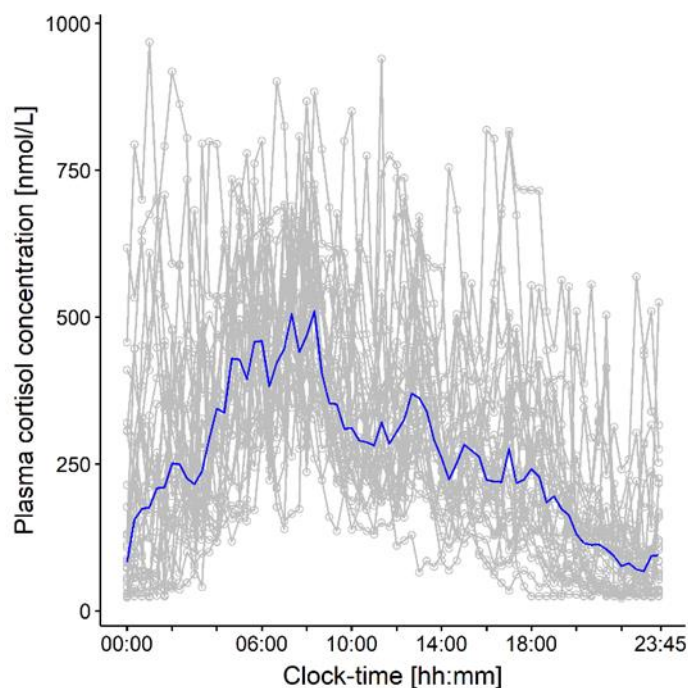


**Figure 4.10** Individual plasma cortisol concentration-time profiles (grey) and median plasma cortisol concentration-time profile (blue), obtained over 24 hours from 28 non-CAH children, aged 5-9 years.

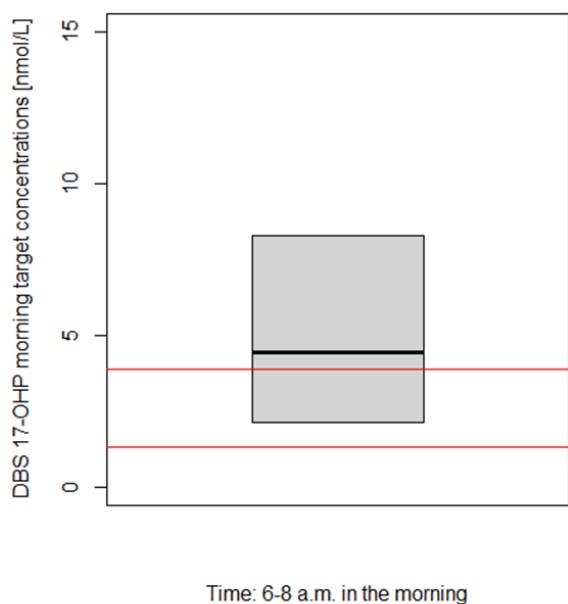


**Figure 4.11** Derived dried blood spot (DBS)  $17\alpha$ -hydroxyprogesterone (17-OHP) target morning concentration range (= model-predicted physiological range multiplied by 3 to 5). Interquartile range (grey box) and median (black line) of the derived DBS 17-OHP target morning concentrations. Red lines: Calculated expected target DBS 17-OHP concentration range in the morning.

The same simulation approach can also serve as a basis to obtain DBS 17-OHP target concentrations in other age groups e.g., neonates or older children, when corresponding data becomes available in the

future, to further inform the PK/PD model accordingly. Since the current PK/PD model did not characterise the circadian rhythm of 17-OHP, the derived target DBS 17-OHP target only apply to the morning hours, before the next HC administration. To identify circadian target profiles for 17-OHP in DBS, the PK/PD model can be expanded, e.g., with the impact of ACTH on the circadian rhythm of 17-OHP in future. Thus, this target morning range derived in this analysis has the potential to develop further and to provide guidance for monitoring young children suffering from CAH in the future. As the PK/PD model described it, there is a time lag between the HC administration and its effect on the decrease of 17-OHP. Therefore, the choice of the right sampling time point during CAH therapy monitoring is important for adequately interpreting the measured concentrations and could be assessed by pharmacometric approaches in the future. Furthermore, the haematocrit influences the spreading of the sampled blood on the DBS filter paper [75,76,135] and is therefore valuable future information as an important factor to take into account when quantifying DBS concentrations.

### ***Plausibility check of the derived target morning DBS 17-OHP concentration range***

To get an understanding of the DBS 17-OHP target morning range to be expected, the known (adult) 17-OHP target morning concentration range in plasma (12-36 nmol/L) [2] was divided by the median plasma/DBS 17-OHP morning concentration ratio of 9.29 which was observed in the young children and infants (n=18). Since the underlying plasma and DBS 17-OHP data was limited and the plasma 17-OHP target range referred to adults, this expected target range represented a simple calculation to evaluate the appropriateness of the simulation-derived results. The derived target morning DBS 17-OHP range (2.1-8.3 nmol/L) was in the same order of magnitude as the approximately expected range (1.3-3.9 nmol/L), indicated by the red horizontal lines (Figure 4.11), and was therefore judged as plausible.

### ***Investigating the agreement between capillary and venous DBS measurements***

The Bland-Altman analysis (Figure 4.12, panels A+B) did not reveal any significant bias between capillary and venous DBS concentrations (mean difference cortisol: +3.13%, 17-OHP: +3.73%). All data points, except one for cortisol and 17-OHP each, lay within the agreement range of the mean difference  $\pm 1.96 \cdot SD$ . In the Passing-Bablok regression the lines of identity lay within the CIs of the regression lines for both analytes (Figure 4.12, panels C+D), showing an agreement between the venous and capillary DBS concentrations as well. The slopes of both regression lines were sufficiently close to 1 (1 for cortisol and 0.7 for 17-OHP) and the y-intercept for cortisol was close to 0 (0.8 for cortisol and 1.7 for 17-OHP), further indicating a high comparability between capillary and venous DBS concentrations.

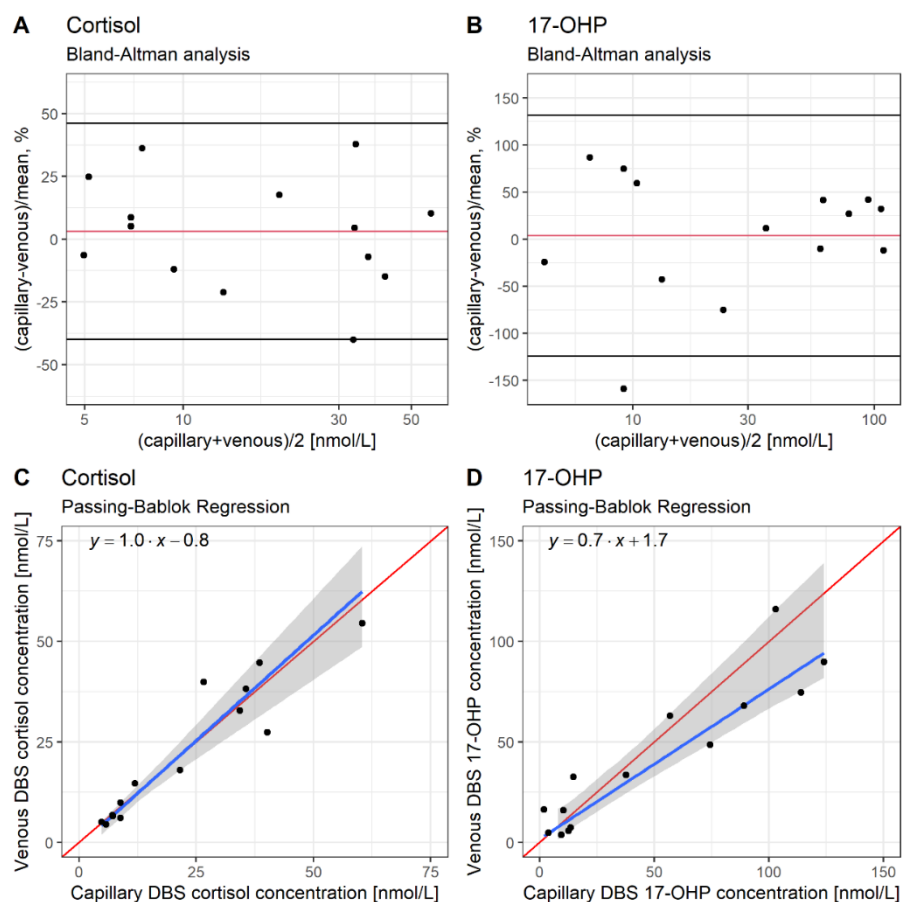


**Figure 4.12** Comparison between capillary and venous cortisol (A+C) and  $17\alpha$ -hydroxyprogesterone (17-OHP, A+D) dried blood spot (DBS) concentrations, obtained from 15 paediatric congenital adrenal hyperplasia (CAH) patients.

A+B: Bland-Altman analysis. Capillary-venous/mean of difference [%] versus mean of capillary and venous DBS cortisol and 17-OHP concentrations. Red line: Mean difference [%], black lines: Mean difference  $- 1.96 \cdot \text{SD}$  (standard deviation) and mean difference  $+ 1.96 \cdot \text{SD}$  [%].

C+D: Passing-Bablok regression. Red line: Line of identity, blue line: Regression line, grey area: 95 % confidence interval for regression line.

The findings of both the Bland-Altman and the Passing-Bablok regression analysis showed that capillary and venous DBS concentrations were indeed comparable for cortisol as well as for 17-OHP. These results not only confirmed the applicability of the derived target morning DBS 17-OHP concentration range for either capillary or venous DBS sampling. They also confirmed the applicability of the modelling and simulation results in *Paper I*, which were based on venous DBS data as well, for both kind of DBS samplings.

### **4.3 Rational dexamethasone dose in prenatal congenital adrenal hyperplasia therapy (Paper III)**

In the modelling and simulation analysis workflow described in *Paper III*, a rational suggestion for a lower Dex dose in prenatal CAH treatment was determined by simulating maternal Dex concentrations under different dosing regimens based on a developed Dex NLME model. This was achieved by leveraging published Dex PK data for modelling and simulation as well as literature data for identifying target Dex concentration thresholds.

#### ***Data selection***

Due to the lack of available PK studies in prenatal CAH therapy or studies investigating DEX concentrations in pregnant women, data from a published bioavailability study in healthy adult individuals receiving Dex perorally (see 2.1.1.2) [68] was selected as the best matching modelling dataset (see Table 2.2 in section 2.1.1.2). 15 of 24 (63%) of the study population were female. Since PK studies in female healthy volunteers are an exception, the female majority in this dataset was seen as highly advantageous for the analysis. The subjects had a median age of 32 years which was judged as a matching age for the pregnant target population. The body weight range of 60 to 90 kg well-matched the expected weight of women in their early pregnancy and was overlapping between sexes. Most importantly, all relevant individual-level data was available. The perorally administered Dex dose of 2 mg in this study was approximately four times higher than the traditional single dose used in prenatal CAH therapy for a pregnant 70 kg patient. Since linear binding was previously observed [66] within a Dex concentration range matching the 2 mg dose as well as all Dex doses to be simulated, the PK of Dex was assumed to be linear within the concentration range of interest.

The main limitation of the chosen modelling dataset was the absence of pregnant individuals. Since sexual differentiation takes place at 7 to 12 weeks post conception [137], it is important to ensure a successful suppression of the foetal HPA axis during this early stage of pregnancy. In near-term pregnant women, higher Dex clearances were described, compared to non-pregnant women, while the terminal half-life or plasma protein binding of Dex was not affected [72,73]. However, only few PK models generally exist for the first trimester of pregnancy and the PK of Dex has not been modelled yet in the early stage of pregnancy [11]. In pregnancy PBPK models, organ volumes are assumed to increase only slightly within the first trimester [138]. Therefore, it was assumed that changes of Dex PK in the early stage of pregnancy were negligible for this analysis. Thus, the predefined criteria for dataset selection (see 2.5) were fulfilled and the data was seen as adequate for the modelling analysis of this project.

**Dex PK model development**

Out of 432 Dex observations, 83 concentrations (19.2%) were below the LLOQ (=1.78 nmol/L). Since 24 of the concentrations below LLOQ were pre-dose measurements and 22 were measured at 24 hours post-dose, those 83 concentrations were discarded for analysis, leaving 349 Dex observations in the database. Similar as in previously reported Dex PK analyses, the data was best described by a two-compartment model including first-order absorption of Dex [69,70] with an estimated lag-time of 12 min and a first-order elimination process corresponding to a half-life of approximately 2.5 hours (see Table 4.3).

**Table 4.3** Parameter estimates of developed dexamethasone PK model.

Parameter	Estimate (RSE, %)
<b>Structural model</b>	
F [-]	1*
$k_a$ [h <sup>-1</sup> ]	2.95 (20.6)
$t_{lag}$ [h]	0.20 (4.10)
$V_c$ [L]	148 (8.70)
expBW, $V_c$ [-]	1*
Q [L/h]	75.5 (26.6)
expBW, Q [-]	0.75*
$V_p$ [L]	88.9 (15.9)
expBW, $V_p$ [-]	1*
CL [L/h]	40.4 (6.80)
expBW, CL [-]	0.75*
<b>Interindividual variability</b>	
$\omega_{k_a}$ , %CV	110 (19.6)
$\omega_{V_c}$ , %CV	37.4 (14.2)
$\omega_Q$ , %CV	129 (17.5)
$\omega_{V_p}$ , %CV	29.9 (61.3)
$\omega_{CL}$ , %CV	33.6 (15.3)
<b>Residual variability</b>	
$\sigma_{prop}$ , %CV	14.6 (9.1)

Bioavailability (F), absorption rate constant ( $k_a$ ), absorption lag time ( $t_{lag}$ ), central volume of distribution ( $V_c$ ), body weight (BW), allometric scaling exponent for body weight (expBW), intercompartmental clearance (Q), peripheral volume of distribution ( $V_p$ ), clearance (CL), interindividual ( $\omega$ ) and residual ( $\sigma$ ) variability (proportional residual variability), \*: fixed parameters.

All PK parameter estimates were plausible and corresponded to previous knowledge on the PK of Dex. For instance, the estimated population clearance of 40.4 L/h was in line with the area under the curve (AUC) which was reported for the chosen Dex PK data in the original publication (corresponding to clearance of 41.6 L/h) [68]. IIV was moderate to high with high variability on intercompartmental clearance (98.7% CV) and absorption rate constant (116% CV), similar to another published Dex PK

analysis [67]. RUV was implemented as a proportional model and was estimated to be low (14.6% CV). Body weight was identified as an influential covariate on the clearance and volume of distribution parameters and was implemented using theory-based allometric scaling (see 2.2.2) [5]. GOF plots and VPCs revealed an adequate prediction of the Dex observations by the Dex PK model and that standard criteria for an appropriate model were fulfilled (Figures 4.13 and 4.14).

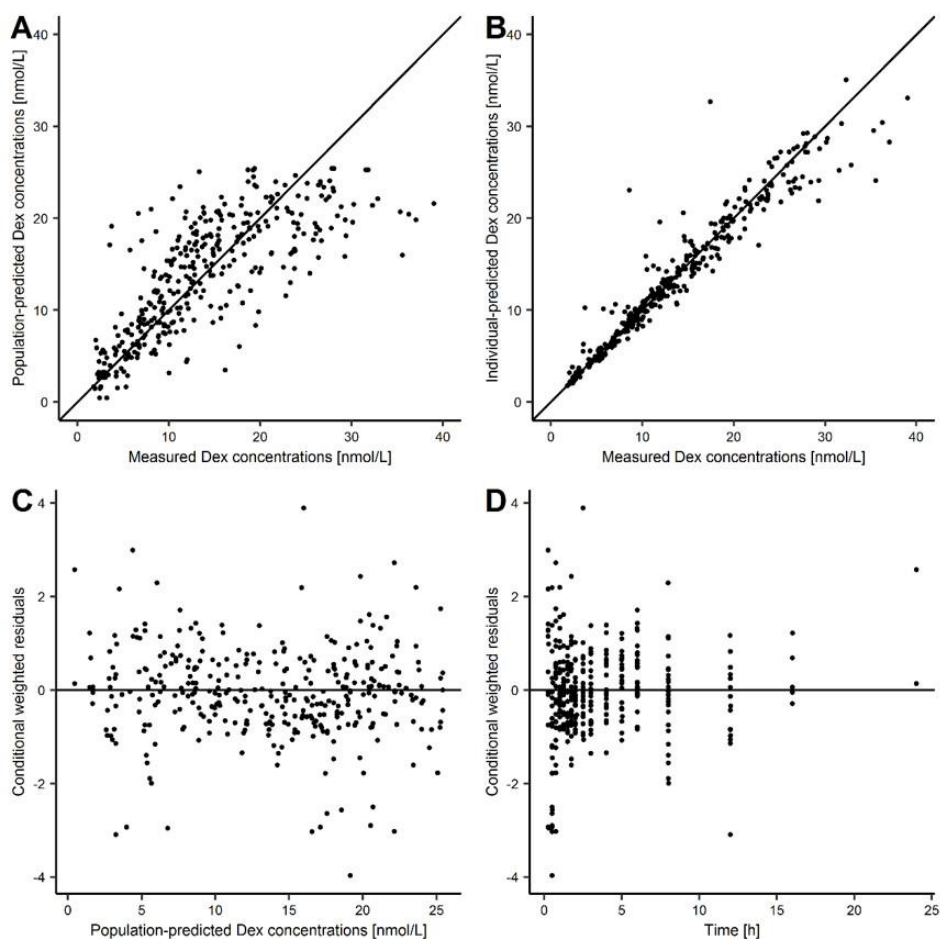


**Figure 4.13** Goodness-of-fit plots of the developed dexamethasone (Dex) pharmacokinetic model. A: Population-predicted Dex concentrations versus measured Dex concentrations, B: Individual Dex predictions versus measured Dex concentrations, C: Conditional weighted residuals (CWRES) versus population-predicted Dex concentrations, D: Conditional weighted residuals versus time. Solid line: Line of identity (A and B), CWRES=0 (C and D).

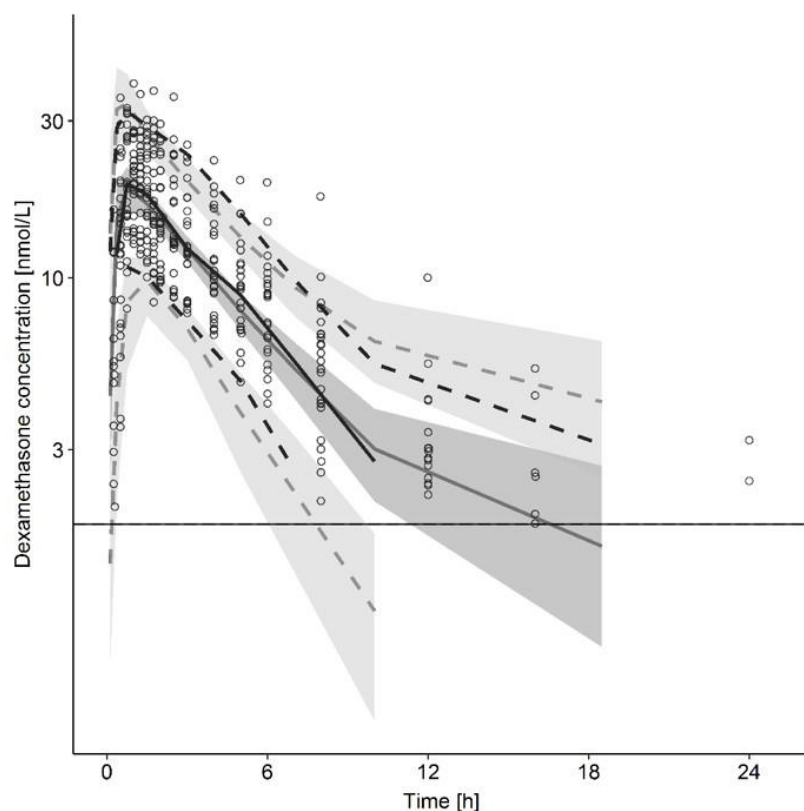


**Figure 4.14** Visual predictive check ( $n=1000$  simulations) for the dexamethasone (Dex) pharmacokinetic model. Lines: the 5<sup>th</sup> (upper dashed), 50<sup>th</sup> (solid) and 95<sup>th</sup> (lower dashed) percentiles of measured (black) and simulated (grey) Dex concentrations; grey shaded areas: 95% confidence interval around the simulated percentiles. Circles: Measured Dex concentrations. Horizontal line: Lower limit of quantification.

#### ***Identification of target Dex concentration threshold***

In order to determine a foetal target Dex concentration threshold, as a first step, literature was searched for physiological foetal cortisol concentrations which physiologically suppress the foetal HPA axis. In Goto *et al.* [137], a physiological foetal cortisol concentration of around 4 pmol/mg was measured in adrenal tissue at 8 weeks post conception, or 4 nmol/L assuming a tissue density of 1 g/cm<sup>3</sup>. Dex is reported to be between 50 and 80 times more potent than cortisol [139]. Thus, the corresponding foetal target Dex concentration was calculated to be 0.05–0.08 nmol/L. The reported ratio of 0.45 for the foetal:maternal Dex concentration [72] was then used to calculate the corresponding maternal target Dex concentration threshold to be between 0.11 and 0.18 nmol/L. Both threshold values were considered in the subsequent simulations.

#### ***Simulation of Dex dosing regimens***

The traditional Dex dosing regimen with 20  $\mu\text{g}/\text{kg}/\text{day}$  as well as dosing regimens with 5, 6, 7.5, 9 or 10  $\mu\text{g}/\text{kg}/\text{day}$ , divided into three single doses every 8 h, were simulated in stochastic simulations ( $n=1000$ ), considering the moderate to high IIVs estimated in the Dex PK model. The simulated study

population was split into two weight groups to simulate a realistic scenario of a clinical study in which pharmacies would need to compound only one dose strength per study arm. A successful suppression of the foetal HPA axis was assumed when the 10<sup>th</sup> percentiles of the simulated maternal Dex concentrations were exceeding the assumed minimum maternal target Dex thresholds at all times during steady state.

For all reduced doses of 5, 6, 7.5, 9 and 10  $\mu\text{g}/\text{kg}/\text{day}$  the 10<sup>th</sup> percentiles of the simulated profiles were above the maternal Dex thresholds of 0.05–0.08 nmol/L during steady-state, as shown for e.g., 7.5  $\mu\text{g}/\text{kg}/\text{day}$  in Figure 4.15, panel A. Compared to the traditional dose of 20  $\mu\text{g}/\text{kg}/\text{day}$ , the Dex exposure of the 7.5  $\mu\text{g}/\text{kg}/\text{day}$  dose was considerably reduced with a 63.1% lower maximum (dashed box) and a 62.7% lower minimum (grey box) Dex concentration at steady state (Figure 4.15 B).

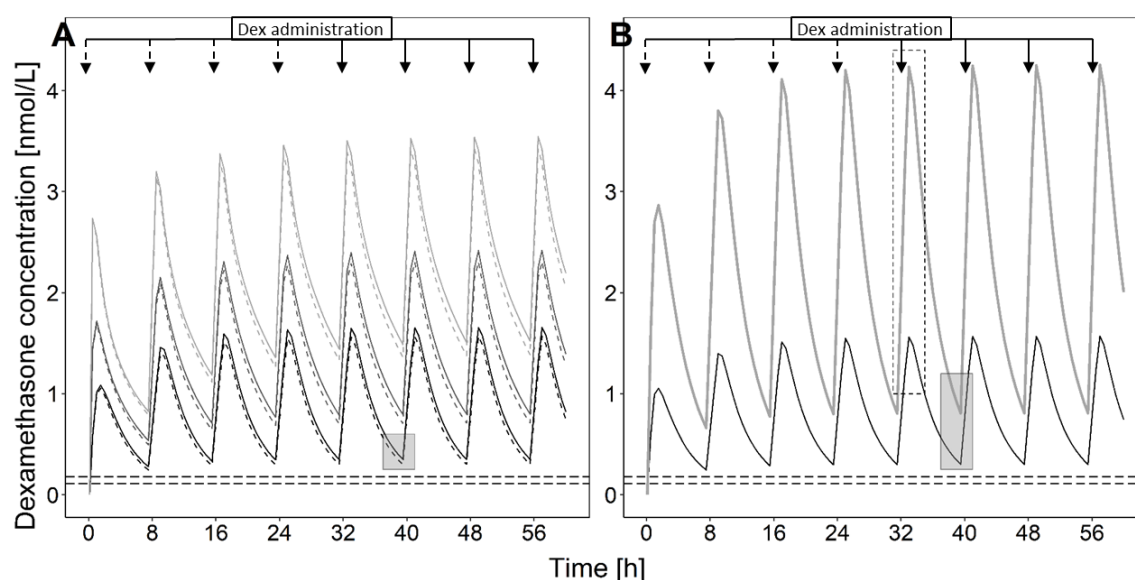


**Figure 4.15** Dexamethasone (Dex) concentration–time profiles after administration of

A: 7.5  $\mu\text{g}/\text{kg}/\text{d}$  as reduced dose for light (50–72 kg, dashed lines) and heavy (73–95 kg, solid lines) body weight groups ( $n=62$  patients per group with  $n=1000$  simulations each) with 10<sup>th</sup> percentile (black lines), median (dark grey lines) and 90<sup>th</sup> percentile (light grey lines)

B: 7.5  $\mu\text{g}/\text{kg}/\text{d}$  as reduced dose (black solid line of A) and traditional dose (20  $\mu\text{g}/\text{kg}/\text{d}$ , grey line) of 10<sup>th</sup> percentiles and light body weight group only.

Dashed horizontal lines: Dex threshold concentration if Dex is 50- (upper line) or 80-fold (lower line) more potent than cortisol, light grey filled boxes: minimum Dex concentration at steady state, dashed non-filled box: maximum Dex concentration at steady state. Arrows: Dex dose administrations before (dashed arrows) and after (solid line arrows) steady state.

Since for the foetal:maternal Dex concentration ratio only one value, which was determined in near-term pregnant women, was retrieved in literature (0.45) [72], this ratio was identified as the most critical assumption. A sensitivity analysis was therefore conducted with decreased ratios of 0.3 and 0.25 as the ‘worst-case-scenario’. When simulating the reduced dosing regimens of 5 and 6  $\mu\text{g}/\text{kg}/\text{day}$  with both lower ratios, the minimum concentrations of the 10<sup>th</sup> percentiles were not exceeding the upper maternal

target threshold (Figure 4.16). Thus, these doses were considered too low for successful suppression of the foetal HPA axis.

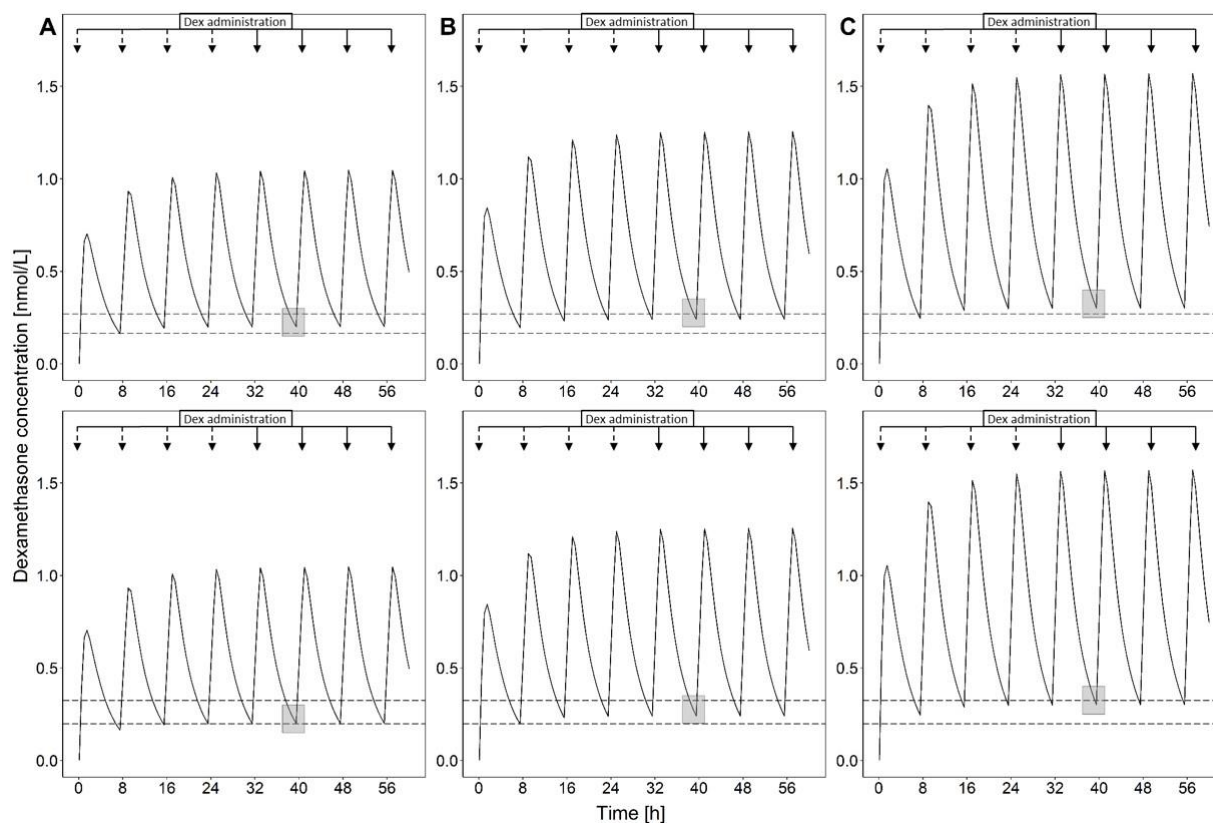


**Figure 4.16** Sensitivity analysis for foetal:maternal dexamethasone (Dex) concentration ratio. Simulated 10<sup>th</sup> percentile Dex concentration-time profiles of light (50-72 kg) body weight group (n=62 patients) after administration of reduced doses with 5 (A), 6 (B) and 7.5 (C) µg/kg/d, if foetal:maternal Dex concentration ratio = 0.3 (top) or 0.25 (bottom) instead of 0.45 (ratio retrieved from literature). Dashed horizontal lines: Dex threshold concentration if Dex is 50- (upper line) or 80-fold (lower line) more potent than cortisol, light grey boxes: Minimum Dex concentration at steady state. Arrows: Dex dose administrations before (dashed arrows) and after (solid line arrows) steady state.

The dose regimen of 7.5 µg/kg/day, i.e., about a third of the traditional dose, was selected as the lowest maternal dosage resulting in sufficient HPA axis suppression in the foetus and was thus recommended as a reduced dose to decrease the risk of adverse events and simultaneously prevent foetal female virilisation. Moreover, this suggested dose corresponds to less than 1 mg/day (for body weights up to 130 kg), which is commonly regarded as a threshold Dex dose for iatrogenic Cushing's syndrome [140], and is therefore expected to reduce the risk for GC-related adverse events in the mother. This rational dose, based on NLME modelling and simulation, should be evaluated in a prospective clinical study which has been recommended for years [38,141-143] to investigate the prevention of virilisation in female foetuses while minimising adverse effects for the treated mother and child during prenatal CAH therapy with Dex.

## 5 Conclusions and perspectives

Within this work, pharmacometric analyses were applied to elucidate PK and PD processes of plasma and DBS cortisol in paediatric CAH patients, and to re-evaluate the traditionally given Dex dose in prenatal CAH therapy, with the overall aim to contribute to an optimised CAH therapy for paediatric and foetal populations. More specifically, in *Paper I*, the relationship between plasma and DBS cortisol concentrations was quantified in a NLME PK model using paediatric CAH patient data. In *Paper II*, target morning DBS concentrations were derived for the commonly used CAH biomarker 17-OHP in simulations with a PK/PD model linking plasma cortisol and DBS 17-OHP concentrations obtained from paediatric CAH patients. Furthermore, the comparability between capillary and venous DBS concentrations was assessed for cortisol and 17-OHP. In *Paper III*, the traditional Dex dose, given in prenatal CAH therapy, as well as dosing regimens with reduced Dex doses were evaluated and compared in simulations, after developing a maternal Dex PK model and identifying minimum target Dex concentrations, in order to optimise foetal Dex exposure.

The relationship between plasma and DBS cortisol concentrations (*Paper I*) was found to be nonlinear in graphical evaluations, with a decreasing plasma/DBS ratio from 1.62 to 8.01 at increasing DBS cortisol concentrations up to 800 nmol/L. This relationship was subsequently described in a semi-mechanistic paediatric cortisol PK model, based on patient cortisol concentrations simultaneously sampled in plasma and in DBS. In addition to saturable cortisol binding to CBG and linear binding to albumin in plasma, the model was extended to characterise linear association of cortisol with RBCs in DBS. Deterministic simulations of unbound cortisol and of the cortisol binding species showed an increase of the cortisol fraction associated with RBCs (children/infants: from 1.9% to 8.3%; neonates: from 1.9% to 12%) with increasing DBS cortisol concentrations, due to the CBG binding saturation and subsequent higher availability of unbound cortisol. These results represent a first step towards understanding the relationship between plasma and DBS cortisol, which is critical for routinely applying DBS sampling in CAH monitoring and adequately interpreting DBS measurements. More paediatric plasma and DBS cortisol data is needed for future analyses to investigate whether the higher cortisol fraction associated with RBCs and thus lower plasma/DBS concentration ratios observed in neonates were due to higher cortisol concentrations or if there was an additional underlying age-effect caused by maturation processes, e.g., the maturation of CBG.

The PK/PD relationship between plasma cortisol and DBS 17-OHP concentrations was successfully characterised in an indirect response model (*Paper II*) with HC, i.e., synthetic cortisol, administered to paediatric CAH patients, inhibiting the biosynthesis of 17-OHP. The PK/PD model as well as healthy paediatric cortisol data were leveraged in stochastic simulations where a concentration range of 2.1-8.3 nmol/L was derived as target morning DBS 17-OHP concentrations in paediatric CAH patients. In future applications of this modelling and simulation approach, the PK/PD model can be extended by

characterising the circadian rhythm of cortisol and of 17-OHP under consideration of ACTH secretion, when the data becomes available. With such a PK/PD model, circadian target DBS 17-OHP concentrations can be derived to enable monitoring of 17-OHP measurements at any time during the day. Moreover, data and information on healthy cortisol profiles in neonates are needed to apply the model to derive target DBS 17-OHP concentrations in this special age group.

Since the DBS concentration data used in *Paper I* and *Paper II* came from venous DBS sampling and also capillary DBS sampling is often done in clinical practice, Bland-Altman and Passing-Bablok regression analyses were performed to compare capillary and venous DBS cortisol and 17-OHP concentrations which were collected during CAH therapy monitoring in paediatric CAH patients. The results of both analyses lead to the conclusion that capillary and venous DBS concentrations are comparable for cortisol and 17-OHP and thus the derived target morning DBS 17-OHP concentration range is applicable for both capillary and venous DBS samples. Despite DBS sampling being a highly advantageous alternative for drug therapy monitoring, especially in paediatric patients, it is still not fully established today as sampling and measurement techniques can vary between laboratories [74,144,145]. Further research and establishment of standardisation is therefore needed for DBS sampling in future to fully exploit the potential of this sampling method.

Another paediatrics-friendly sampling method which is used in CAH therapy monitoring besides DBS sampling, is the collection of saliva with mouth swabs [102,146,147]. A future characterisation of the circadian rhythm of cortisol and other biomarkers in saliva is crucial to understand which saliva target concentration profiles should be obtained when using this sampling matrix for CAH monitoring. Besides 17-OHP as the most commonly used biomarker, other biomarkers relevant for CAH monitoring are the androgens testosterone and androstenedione, progesterone, 21-deoxycortisol and cortisone (see Figure 1.2.B). Target concentrations for these biomarkers can be derived by using a pharmacometrics approach as in *Paper II*. Moreover, elucidating the impact of the competitive binding of cortisone with cortisol to, e.g., CBG on the PK of cortisol and quantitatively investigating the maturation of 11 $\beta$ -HSD1 and 11 $\beta$ -HSD2 can help developing models for simulation and evaluation of optimised HC dosing regimens for neonates and young infants. Finally, one of the most critical keys to an improved HC dosing in CAH therapy, for patients of all age groups, will be the use of sustained-release HC formulations which are currently under development to better mimic the circadian concentration-time profiles of cortisol [15,148].

In *Paper III*, a Dex dose of 7.5  $\mu\text{g}/\text{kg}/\text{day}$ , representing a third of the traditional Dex dose of 20  $\mu\text{g}/\text{kg}/\text{day}$ , was selected as a reduced rational Dex dose for prenatal CAH therapy. Maternal target Dex concentration ranges were identified from literature and a maternal Dex PK model was then developed and applied to compare simulated Dex PK profiles, following the administration of the traditional and of reduced Dex doses, to the identified minimum target Dex concentrations. Subsequently, a sensitivity analysis was performed on the foetal-to-maternal Dex concentration ratio as

the most critical model assumption. Based on all simulation results, this first evidence-based Dex dose was chosen as the dose to sufficiently suppress the foetal HPA axis and simultaneously reduce the risk of adverse effects for the treated mother and the foetus, such as postnatal hypertension and negative effects on brain development. The suggested dose needs to be evaluated in future clinical studies.

In conclusion, this work contributed to the optimisation of CAH therapy in paediatric and foetal populations. Cortisol concentrations measured in DBS were compared and quantitatively linked to cortisol in plasma and a paediatric DBS target morning concentration range was derived for the biomarker 17-OHP. Additionally, for the first time, a rational reduced Dex dose was suggested for prenatal CAH therapy, based on modelling and simulation.

## 6 Bibliography

- [1] E. Kimland, V. Odland. Off-Label Drug Use in Pediatric Patients. *Clin. Pharmacol. Ther.* 91: 796–801 (2012).
- [2] European Medicines Agency. Guidance on clinical investigation of medicinal products in the paediatric population. CPMP/ICH/2711/99 (2001). [https://www.ema.europa.eu/en/documents/scientific-guideline/e-11-clinical-investigation-medicinal-products-paediatric-population-step-5\\_en.pdf](https://www.ema.europa.eu/en/documents/scientific-guideline/e-11-clinical-investigation-medicinal-products-paediatric-population-step-5_en.pdf), last access 25 Jun 2023.
- [3] G.L. Kearns, S.M. Abdel-Rahman, S.W. Alander, D.L. Blowey, J.S. Leeder, R.E. Kauffman. Developmental Pharmacology — Drug Disposition, Action, and Therapy in Infants and Children. *N. Engl. J. Med.* 349: 1157–1167 (2003).
- [4] B.J. Anderson, N.H.G. Holford. Understanding dosing: Children are small adults, neonates are immature children. *Arch. Dis. Child.* 98: 737–744 (2013).
- [5] N.H.G. Holford. A size standard for pharmacokinetics. *Clin. Pharmacokinet.* 30: 329–332 (1996).
- [6] B.J. Anderson, N.H.G. Holford. Mechanism-based concepts of size and maturity in pharmacokinetics. *Annu. Rev. Pharmacol. Toxicol.* 48: 303–332 (2008).
- [7] R. Gore, P.K. Chugh, C.D. Tripathi, Y. Lhamo, S. Gautam. Pediatric Off-Label and Unlicensed Drug Use and Its Implications. *Curr. Clin. Pharmacol.* 12: 18–25 (2017).
- [8] S. Balan, M.A.A. Hassali, V.S.L. Mak. Two decades of off-label prescribing in children: a literature review. *World J. Pediatr.* 14: 528–540 (2018).
- [9] Regulation (EC) No 1901/2006 of the European parliament and of the council on medicinal products for paediatric use and amending Regulation (EEC) No 1768/92, Directive 2001/20/EC, Directive 2001/83/EC and Regulation (EC) No 726/2004 (2006). <https://eur-lex.europa.eu/LexUriServ/LexUriServ.do?uri=CONSLEG:2006R1901:20070126:EN:PDF>, last access 25 Jun 2023.
- [10] D.C. Campbell. Physiological changes of pregnancy. *Semin. Anesth.* 19: 149–156 (2000).
- [11] A. Dallmann, P. Mian, J. Van den Anker, K. Allegaert. Clinical Pharmacokinetic Studies in Pregnant Women and the Relevance of Pharmacometric Tools. *Curr. Pharm. Des.* 25: 483–495 (2019).
- [12] G.P. Chrousos. Stress and disorders of the stress system. *Nat. Rev. Endocrinol.* 5: 374–381 (2009).
- [13] D.P. Merke, S.R. Bornstein. Congenital adrenal hyperplasia. *Lancet* 365: 2125–2136 (2005).
- [14] H.L.C. van der Grinten, P.W. Speiser, S. Faisal Ahmed, W. Arlt, R.J. Auchus, H. Falhammar, C.E. Flück, L. Guasti, A. Huebner, B.B.M. Kortmann, N. Krone, D.P. Merke, W.L. Miller, A. Nordenström, N. Reisch, D.E. Sandberg, N.M.M.L. Stikkelbroeck, P. Touraine, A. Utari, S.A. Wudy, P.C. White. Congenital Adrenal Hyperplasia—Current Insights in Pathophysiology, Diagnostics, and Management. *Endocr. Rev.* 43: 91–159 (2022).
- [15] A.A. Nella, A. Mallappa, A.F. Perritt, V. Gounden, P. Kumar, N. Sinaii, L.-A. Daley, A. Ling, C.-Y. Liu, S.J. Soldin, D.P. Merke. A Phase 2 Study of Continuous Subcutaneous Hydrocortisone Infusion in Adults With Congenital Adrenal Hyperplasia. *J. Clin. Endocrinol. Metab.* 101: 4690–4698 (2016).
- [16] N. Nader, G.P. Chrousos, T. Kino. Interactions of the circadian CLOCK system and the HPA axis. *Trends Endocrinol. Metab.* 21: 277–286 (2010).
- [17] J.S.E. Melin. Pharmacometric approaches to assess hydrocortisone therapy in paediatric patients with adrenal insufficiency. Freie Universität Berlin. (2017).

- [18] H.J. van der Kamp, J.M. Wit. Neonatal screening for congenital adrenal hyperplasia. *Eur J Endocrinol* 151: U71–U75 (2004).
- [19] R. Podgórski, D. Aebisher, M. Stompor, D. Podgórska, A. Mazur. Congenital adrenal hyperplasia: Clinical symptoms and diagnostic methods. *Acta Biochim. Pol.* 65: 25–33 (2018).
- [20] A. Balsamo, F. Baronio, R. Ortolano, S. Menabo, L. Baldazzi, V. Di Natale, S. Vissani, A. Cassio. Congenital Adrenal Hyperplasias Presenting in the Newborn and Young Infant. *Front. Pediatr.* 8: (2020).
- [21] P.W. Speiser, W. Arlt, R.J. Auchus, L.S. Baskin, G.S. Conway, D.P. Merke, H.F.L. Meyer-Bahlburg, W.L. Miller, M. Hassan Murad, S.E. Oberfield, P.C. White. Congenital adrenal hyperplasia due to steroid 21-hydroxylase deficiency: An endocrine society\* clinical practice guideline. *J. Clin. Endocrinol. Metab.* 103: 4043–4088 (2018).
- [22] A. Oprea, N.C.G. Bonnet, O. Pollé, P.A. Lysy. Novel insights into glucocorticoid replacement therapy for pediatric and adult adrenal insufficiency. *Ther. Adv. Endocrinol. Metab.* 10: 1–27 (2019).
- [23] W.L. Miller. Fetal endocrine therapy for congenital adrenal hyperplasia should not be done. *Best Pract. Res. Clin. Endocrinol. Metab.* 29: 469–483 (2015).
- [24] M. Kamoun, M. Feki, M. Sfar, M. Abid. Congenital adrenal hyperplasia: Treatment and outcomes. *Indian J. Endocrinol. Metab.* 17: 14 (2013).
- [25] A. Dabas, P. Vats, R. Sharma, P. Singh, A. Seth, V. Jain, P. Batra, N. Gupta, R. Kumar, M. Kabra, S. Kapoor, S. Yadav. Management of Infants with Congenital Adrenal Hyperplasia. *Indian Pediatr.* 57: 159–164 (2020).
- [26] S.R. Bornstein, B. Allolio, W. Arlt, A. Barthel, A. Don-Wauchope, G.D. Hammer, E.S. Husebye, D.P. Merke, M.H. Murad, C.A. Stratakis, D.J. Torpy. Diagnosis and treatment of primary adrenal insufficiency: An endocrine society clinical practice guideline. *J. Clin. Endocrinol. Metab.* 101: 364–389 (2016).
- [27] U. Neumann, D. Burau, S. Spielmann, M.J. Whitaker, R.J. Ross, C. Kloft, O. Blankenstein. Quality of compounded hydrocortisone capsules used in the treatment of children. *Eur. J. Endocrinol.* 177: 239–242 (2017).
- [28] U. Neumann, M.J. Whitaker, S. Wiegand, H. Krude, J. Porter, M. Davies, D. Digweed, B. Voet, R.J. Ross, O. Blankenstein. Absorption and tolerability of taste-masked hydrocortisone granules in neonates, infants and children under 6 years of age with adrenal insufficiency. *Clin. Endocrinol. (Oxf)*. 88: 21–29 (2018).
- [29] D.P. Merke, D. Cho, K.A. Calis, M.F. Keil, G.P. Chrousos. Hydrocortisone Suspension and Hydrocortisone Tablets Are Not Bioequivalent In The Treatment of Children with Congenital Adrenal Hyperplasia. *J. Clin. Endocrinol. Metab.* 86: 441–445 (2001).
- [30] J. Porter, M. Withe, R.J. Ross. Immediate-release granule formulation of hydrocortisone, Alkindi<sup>®</sup>, for treatment of paediatric adrenal insufficiency (Infacort development programme). *Expert Rev. Endocrinol. Metab.* 13: 119–124 (2018).
- [31] M.J. Whitaker, S. Spielmann, D. Digweed, H. Huatan, D. Eckland, T.N. Johnson, G. Tucker, H. Krude, O. Blankenstein, R.J. Ross. Development and testing in healthy adults of oral hydrocortisone granules with taste masking for the treatment of neonates and infants with adrenal insufficiency. *J. Clin. Endocrinol. Metab.* 100: 1681–1688 (2015).
- [32] N. Karunasena, D.N. Margetson, G. Neal, M.J. Whitaker, R.J.M. Ross. Impact of food, alcohol and pH on modified-release hydrocortisone developed to treat congenital adrenal hyperplasia. *Eur. J. Endocrinol.* 176: 405–411 (2017).
- [33] A. Mallappa, N. Sinaii, P. Kumar, M.J. Whitaker, L.A. Daley, D. Digweed, D.J.A. Eckland, C. Van Ryzin, L.K. Nieman, W. Arlt, R.J. Ross, D.P. Merke. A phase 2 study of Chronocort, a modified-release formulation of hydrocortisone, in the treatment of adults with classic

- congenital adrenal hyperplasia. *J. Clin. Endocrinol. Metab.* 100: 1137–1145 (2015).
- [34] A.A. Nella, A. Mallappa, A.F. Perritt, V. Gounden, P. Kumar, N. Sinaii, L.A. Daley, A. Ling, C.Y. Liu, S.J. Soldin, D.P. Merke. A phase 2 study of continuous subcutaneous hydrocortisone infusion in adults with congenital adrenal hyperplasia. *J. Clin. Endocrinol. Metab.* 101: 4690–4698 (2016).
- [35] A. Mallappa, A.A. Nella, N. Sinaii, H. Rao, V. Gounden, A.F. Perritt, P. Kumar, A. Ling, C.-Y. Liu, S.J. Soldin, D.P. Merke. Long-term use of continuous subcutaneous hydrocortisone infusion therapy in patients with congenital adrenal hyperplasia. *Clin. Endocrinol. (Oxf)*. 89: 399–407 (2018).
- [36] M. David, M.G. Forest. Prenatal treatment of congenital adrenal hyperplasia resulting from 21-hydroxylase deficiency. *J. Pediatr.* 105: 799–803 (1984).
- [37] M.G. Forest, Y. Morel, M. David. Prenatal Treatment of Congenital Adrenal Hyperplasia. *Trends Endocrinol. Metab.* 9: 284–289 (1998).
- [38] M.G. Forest. Recent advances in the diagnosis and management of congenital adrenal hyperplasia due to 21-hydroxylase deficiency. *Hum. Reprod. Update* 10: 469–485 (2004).
- [39] M.I. New, A. Carlson, J. Obeid, I. Marshall, M.S. Cabrera, A. Goseco, K. Lin-Su, A.S. Putnam, J.Q. Wei, R.C. Wilson. Extensive personal experience: Prenatal diagnosis for congenital adrenal hyperplasia in 532 pregnancies. *J. Clin. Endocrinol. Metab.* 86: 5651–5657 (2001).
- [40] M.I. New, M. Abraham, T. Yuen, O. Lekarev. An update on prenatal diagnosis and treatment of congenital adrenal hyperplasia. *Semin. Reprod. Med.* 30: 396–399 (2012).
- [41] T. Hirvikoski, A. Nordenström, A. Wedell, M. Ritzén, S. Lajic. Prenatal dexamethasone treatment of children at risk for congenital adrenal hyperplasia: The Swedish experience and standpoint. *J. Clin. Endocrinol. Metab.* 97: 1881–1883 (2012).
- [42] H. Nowotny, U. Neumann, V. Tardy-Guidollet, S. Faisal Ahmed, F. Baronio, T. Battelino, J. Bertherat, O. Blankenstein, M. Bonomi, C. Bouvattier, A.B. De la Perrière, S. Brucker, M. Cappa, P. Chanson, H.L.C. Van der Grinten, A. Colao, M. Cools, J.H. Davies, H.G. Dorr, W.K. Fenske, E. Ghigo, R. Giordano, C.H. Gravholt, A. Huebner, E.S. Husebye, R. Igbokwe, A. Juul, F.W. Kiefer, J. Leger, R. Menassa, G. Meyer, V. Neocleous, L.A. Phylactou, J. Rohayem, G. Russo, C. Scaroni, P. Touraine, N. Unger, J. Vojtkova, D. Yeste, S. Lajic, N. Reisch. Prenatal dexamethasone treatment for classic 21-hydroxylase deficiency in Europe. *Eur. J. Endocrinol.* 168: K17–K24 (2022).
- [43] B. Khulan, A.J. Drake. Glucocorticoids as mediators of developmental programming effects. *Best Pract. Res. Clin. Endocrinol. Metab.* 26: 689–700 (2012).
- [44] T. Hirvikoski, T. Lindholm, S. Lajic, A. Nordenström. Gender role behaviour in prenatally dexamethasone-treated children at risk for congenital adrenal hyperplasia - A pilot study. *Acta Paediatr. Int. J. Paediatr.* 100: 112–119 (2011).
- [45] T. Hirvikoski, A. Nordenström, T. Lindholm, F. Lindblad, E.M. Ritzén, A. Wedell, S. Lajic. Cognitive functions in children at risk for congenital adrenal hyperplasia treated prenatally with dexamethasone. *J. Clin. Endocrinol. Metab.* 92: 542–548 (2007).
- [46] T. Hirvikoski, A. Nordenström, T. Lindholm, F. Lindblad, E.M. Ritzén, S. Lajic. Long-term follow-up of prenatally treated children at risk for congenital adrenal hyperplasia: Does dexamethasone cause behavioural problems? *Eur. J. Endocrinol.* 159: 309–316 (2008).
- [47] A. Maryniak, M. Ginalska-Malinowska, A. Bielawska, A. Ondruch. Cognitive and social function in girls with congenital adrenal hyperplasia - Influence of prenatally administered dexamethasone. *Child Neuropsychol.* 20: 60–70 (2014).
- [48] H.F.L. Meyer-Bahlburg, C. Dolezal, S.W. Baker, A.D. Carlson, J.S. Obeid, M.I. New. Cognitive and Motor Development of Children with and without Congenital Adrenal Hyperplasia after Early-Prenatal Dexamethasone. *J. Clin. Endocrinol. Metab.* 89: 610–614 (2004).

- [49] H.F.L. Meyer-Bahlburg, C. Dolezal, R. Haggerty, M. Silverman, M.I. New. Cognitive outcome of offspring from dexamethasone-treated pregnancies at risk for congenital adrenal hyperplasia due to 21-hydroxylase deficiency. *Eur. J. Endocrinol.* 167: 103–110 (2012).
- [50] P.D. Trautman, H.F.L. Meyer-Bahlburg, J. Postelnek, M.I. New. Effects of early prenatal dexamethasone on the cognitive and behavioral development of young children: Results of a pilot study. *Psychoneuroendocrinology* 20: 439–449 (1995).
- [51] L. Karlsson, M. Barbaro, E. Ewing, D. Gomez-Cabrero, S. Lajic. Epigenetic alterations associated with early prenatal dexamethasone treatment. *J. Endocr. Soc.* 3: 250–263 (2019).
- [52] A. Van't Westeinde, M. Zimmermann, V. Messina, L. Karlsson, N. Padilla, S. Lajic. First Trimester DEX Treatment Is Not Associated with Altered Brain Activity during Working Memory Performance in Adults. *J. Clin. Endocrinol. Metab.* 105: (2020).
- [53] A. Van't Westeinde, L. Karlsson, A. Nordenström, N. Padilla, S. Lajic. First-Trimester Prenatal Dexamethasone Treatment Is Associated With Alterations in Brain Structure at Adult Age. *J. Clin. Endocrinol. Metab.* 105: (2020).
- [54] E.G.W.M. Lentjes. Temperature-Dependent Cortisol Distribution among the Blood Compartments in Man. *J. Clin. Endocrinol. Metab.* 84: 682–687 (1999).
- [55] R.D. Toothaker, P.G. Welling. Effect of Dose Size on the Pharmacokinetics of Intravenous Hydrocortisone During Endogenous Hydrocortisone Suppression. *J. Pharmacokinet. Biopharm.* 10: 147–156 (1982).
- [56] H. Derendorf, H. Mollmann, J. Barth, C. Mollmann, S. Tunn, M. Krieg. Pharmacokinetics and oral bioavailability of hydrocortisone. 31: 473–6. (1991).
- [57] H. Lennernäs, S. Skrtic, G. Johannsson. Replacement therapy of oral hydrocortisone in adrenal insufficiency : the influence of gastrointestinal factors. *Expert Opin. Drug Metab. Toxicol.* 4: 749–758 (2008).
- [58] J. Melin, Z.P. Parra-Guillen, N. Hartung, W. Huisinga, R.J. Ross, M.J. Whitaker, C. Kloft. Predicting Cortisol Exposure from Paediatric Hydrocortisone Formulation Using a Semi-Mechanistic Pharmacokinetic Model Established in Healthy Adults. *Clin. Pharmacokinet.* 57: 515–527 (2018).
- [59] M. Hoshiro, H. Masaki, H. Iwase, N. Aoki. Comprehensive study of urinary cortisol metabolites in hyperthyroid and hypothyroid patients. *Clin. Endocrinol. (Oxf).* 64: 37–45 (2006).
- [60] J.W. Tomlinson, P.M. Stewart. Cortisol metabolism and the role of 11 $\beta$ -hydroxysteroid dehydrogenase. *Best Pract. Res. Clin. Endocrinol. Metab.* 15: 61–78 (2001).
- [61] S.L. Rogers, B.A. Hughes, C.A. Jones, L. Freedman, K. Smart, N. Taylor, P.M. Stewart, C.H.L. Shackleton, N.P. Krone, J. Blissett, J.W. Tomlinson. Diminished 11 $\beta$ -Hydroxysteroid dehydrogenase type 2 activity is associated with decreased weight and weight gain across the first year of life. *J. Clin. Endocrinol. Metab.* 99: 1–10 (2014).
- [62] S.A. Wudy, M.F. Hartmann, T. Remer. Sexual dimorphism in cortisol secretion starts after age 10 in healthy children: Urinary cortisol metabolite excretion rates during growth. *Am. J. Physiol. - Endocrinol. Metab.* 293: 970–976 (2007).
- [63] S.L. Rogers, B.A. Hughes, C.A. Jones, L. Freedman, K. Smart, N. Taylor, P.M. Stewart, C.H.L. Shackleton, N.P. Krone, J. Blissett, J.W. Tomlinson. Diminished 11 $\beta$ -Hydroxysteroid Dehydrogenase Type 2 Activity Is Associated With Decreased Weight and Weight Gain Across the First Year of Life. *J. Clin. Endocrinol. Metab.* 99: E821–E831 (2014).
- [64] A. Hadjian, M. Chedin, C. Cochet, E. Chambaz. Cortisol Binding to Proteins in Plasma in the Human Neonate and Infant. *Pediatr. Res.* 9: 40–45 (1975).
- [65] J.J. Bonner, H. Burt, T.N. Johnson, M.J. Whitaker, J. Porter, R.J. Ross. Development and verification of an endogenous PBPK model to inform hydrocortisone replacement dosing in children and adults with cortisol deficiency. *Eur. J. Pharm. Sci.* 165: (2021).

- [66] D.M. Cummings, G.E. Larijani, D.P. Conner, R.K. Ferguson, M.L. Rocci. Characterization of Dexamethasone Binding in Normal and Uremic Human Serum. *Ann. Pharmacother.* 24: 229–231 (1990).
- [67] D. Loew, O. Schuster, E.H. Graul. Dose-dependent pharmacokinetics of dexamethasone. *Eur. J. Clin. Pharmacol.* 30: 225–230 (1986).
- [68] C. Queckenberg, B. Wachall, V. Erlinghagen, P. Di Gion, D. Tomalik-Scharte, M. Tawab, K. Gerbeth, U. Fuhr. Pharmacokinetics, pharmacodynamics, and comparative bioavailability of single, oral 2-mg doses of dexamethasone liquid and tablet formulations: A randomized, controlled, crossover study in healthy adult volunteers. *Clin. Ther.* 33: 1831–1841 (2011).
- [69] J. Li, R. Chen, Q.Y. Yao, S.J. Liu, X.Y. Tian, C.Y. Hao, W. Lu, T.Y. Zhou. Time-dependent pharmacokinetics of dexamethasone and its efficacy in human breast cancer xenograft mice: A semi-mechanism-based pharmacokinetic/pharmacodynamic model. *Acta Pharmacol. Sin.* 39: 472–481 (2018).
- [70] G. Hochhaus, J. Barth, S. Al-Fayoumi, S. Suarez, H. Derendorf, R. Hochhaus, H. Möllmann. Pharmacokinetics and pharmacodynamics of dexamethasone sodium-m-sulfobenzoate (DS) after intravenous and intramuscular administration: A comparison with dexamethasone phosphate (DP). *J. Clin. Pharmacol.* 41: 425–434 (2001).
- [71] J.R. Seckl. Glucocorticoids, feto-placental 11 $\beta$ -hydroxysteroid dehydrogenase type 2, and the early life origins of adult disease. *Steroids* 62: 89–94 (1997).
- [72] E. Tsuei, M. Petersen, J. Ashley, W. McBride, G. Moore. Disposition of synthetic glucocorticoids. *Clin. Pharmacol. Ther.* 28: 88–98 (1980).
- [73] A.B. Ke, M.A. Milad. Evaluation of Maternal Drug Exposure Following the Administration of Antenatal Corticosteroids During Late Pregnancy Using Physiologically-Based Pharmacokinetic Modeling. *Clin. Pharmacol. Ther.* 106: 164–173 (2019).
- [74] P.M. Edelbroek, J. Van Der Heijden, L.M.L. Stolk. Dried blood spot methods in therapeutic drug monitoring: Methods, assays, and pitfalls. *Ther. Drug Monit.* 31: 327–336 (2009).
- [75] A.J. Wilhelm, J.C.G. den Burger, E.L. Swart. Therapeutic Drug Monitoring by Dried Blood Spot: Progress to Date and Future Directions. *Clin. Pharmacokinet.* 53: 961–973 (2014).
- [76] D.O. Qasrawi, J.M. Boyd, S.M.H. Sadrzadeh. Measuring steroids from dried blood spots using tandem mass spectrometry to diagnose congenital adrenal hyperplasia. *Clin. Chim. Acta* 520: 202–207 (2021).
- [77] T.A. Jacobson, J.S. Kler, Y. Bae, J. Chen, D.T. Lador, R. Iyer, D.A. Nunes, N.D. Montgomery, J.D. Pleil, W.E. Funk. A state-of-the-science review and guide for measuring environmental exposure biomarkers in dried blood spots. *J. Expo. Sci. Environ. Epidemiol.* doi: 10.1038/s41370-022-00460-7 (2022).
- [78] S.J. Moat, R.S. George, R.S. Carling. Use of Dried Blood Spot Specimens to Monitor Patients with Inherited Metabolic Disorders. *Int. J. Neonatal Screen.* 6: 1–17 (2020).
- [79] S. Lehmann, C. Delaby, J. Vialaret, J. Ducos, C. Hirtz. Current and future use of “dried blood spot” analyses in clinical chemistry. *Clin. Chem. Lab. Med.* 51: 1897–1909 (2013).
- [80] N. Grecsó, A. Zádori, I. Szécsi, Á. Baráth, Z. Galla, C. Bereczki, P. Monostori. Storage stability of five steroids and in dried blood spots for newborn screening and retrospective diagnosis of congenital adrenal hyperplasia. *PLoS One* 15: 1–10 (2020).
- [81] V.S. Lando, M.C. Batista, I.T. Nakamura, C.R. Mazi, B.B. Mendonca, V.N. Brito. Effects of long-term storage of filter paper blood samples on neonatal thyroid stimulating hormone, thyroxin and 17-alpha-hydroxyprogesterone measurements. *J. Med. Screen.* 15: 109–111 (2008).
- [82] A. Boelen, A.F.C. Ruiten, H.L. Claahsen-Van Der Grinten, E. Endert, M.T. Ackermans. Determination of a steroid profile in heel prick blood using LC-MS/MS. *Bioanalysis* 8: 375–384

- (2016).
- [83] P.J. Williams, E.I. Ette. *Pharmacometrics: The science of quantitative pharmacology*. John Wiley & Sons, Hoboken, New Jersey. (2006).
- [84] D.R. Mould, R.N. Upton. *Basic Concepts in Population Modeling, Simulation, and Model-Based Drug Development*. *CPT Pharmacometrics Syst. Pharmacol.* 1: 1–14 (2012).
- [85] J. Fiedler-Kelly, J.S. Owen. *Introduction to population pharmacokinetic/pharmacodynamic analysis with nonlinear mixed effects models*. (2014).
- [86] E.I. Ette, P.J. Williams. *Population pharmacokinetics I: Background, concepts, and models*. *Ann. Pharmacother.* 38: 1702–1706 (2004).
- [87] P.L. Bonate. *Pharmacokinetic-pharmacodynamic modeling and simulation*. Springer, New York, 2nd ed. (2011).
- [88] M. Rowland, T.N. Tozer. *Clinical pharmacokinetics and pharmacodynamics: concepts and applications*. (2011).
- [89] D.R. Mould, R.N. Upton. *Basic concepts in population modeling, simulation, and model-based drug development-part 2: introduction to pharmacokinetic modeling methods*. *CPT pharmacometrics Syst. Pharmacol.* 2: e38 (2013).
- [90] J.Y. Lee, C.E. Garnett, J.V.S. Gobburu, V.A. Bhattaram, S. Brar, J.C. Earp, P.R. Jadhav, K. Krudys, L.J. Lesko, F. Li, J. Liu, R. Madabushi, A. Marathe, N. Mehrotra, C. Tornøe, Y. Wang, H. Zhu. *Impact of pharmacometric analyses on new drug approval and labelling decisions: A review of 198 submissions between 2000 and 2008*. *Clin. Pharmacokinet.* 50: 627–635 (2011).
- [91] S.F. Marshall, R. Burghaus, V. Cosson, S. Cheung, M. Chenel, O. DellaPasqua, N. Frey, B. Hamrén, L. Harnisch, F. Ivanow, T. Kerbusch, J. Lippert, P.A. Milligan, S. Rohou, A. Staab, J.L. Steimer, C. Tornøe, S.A.G. Visser. *Good Practices in Model-Informed Drug Discovery and Development: Practice, Application, and Documentation*. *CPT Pharmacometrics Syst. Pharmacol.* 5: 93–122 (2016).
- [92] S. Marshall, R. Madabushi, E. Manolis, K. Krudys, A. Staab, K. Dykstra, S.A.G. Visser. *Model-Informed Drug Discovery and Development: Current Industry Good Practice and Regulatory Expectations and Future Perspectives*. *CPT Pharmacometrics Syst. Pharmacol.* 8: 87–96 (2019).
- [93] European Medicines Agency. *Committee for Medicinal Products for Human Use. Guideline on reporting the results of population pharmacokinetic analyses*. EMEA/CHMP/EWP/185990/06 (2007). [https://www.ema.europa.eu/en/documents/scientific-guideline/guideline-reporting-results-population-pharmacokinetic-analyses\\_en.pdf](https://www.ema.europa.eu/en/documents/scientific-guideline/guideline-reporting-results-population-pharmacokinetic-analyses_en.pdf), last access 25 Jun 2023.
- [94] U.S. Department of Health and Human Services Food and Drug Administration. *Population Pharmacokinetics Guidance for Industry*. (2022).
- [95] J.F. Standing. *Understanding and applying pharmacometric modelling and simulation in clinical practice and research*. *Br. J. Clin. Pharmacol.* 83: 247–254 (2017).
- [96] R.F.W. De Cock, C. Piana, E.H.J. Krekels, M. Danhof, K. Allegaert, C.A.J. Knibbe. *The role of population PK-PD modelling in paediatric clinical research*. *Eur. J. Clin. Pharmacol.* 67: 5–16 (2011).
- [97] I.R. Younis, R.J. Powell, A. Rostami-Hodjegan, B. Corrigan, N. Stockbridge, V. Sinha, P. Zhao, P. Jadhav, B. Flamion, J. Cook. *Utility of Model-Based Approaches for Informing Dosing Recommendations in Specific Populations: Report From the Public AAPS Workshop*. *J. Clin. Pharmacol.* 57: 105–109 (2017).
- [98] R. Michelet, J. Melin, Z.P. Parra-Guillen, U. Neumann, M.J. Whitaker, V. Stachanow, W. Huisinga, J. Porter, O. Blankenstein, R.J. Ross, C. Kloft. *Paediatric population pharmacokinetic modelling to assess hydrocortisone replacement dosing regimens in young children*. *Eur. J. Endocrinol.* 183: 357–368 (2020).
- [99] J. Melin, Z.P. Parra-Guillen, R. Michelet, T. Truong, W. Huisinga, N. Hartung, P. Hindmarsh,

- C. Kloft. Pharmacokinetic/Pharmacodynamic evaluation of hydrocortisone therapy in pediatric patients with congenital adrenal hyperplasia. *J. Clin. Endocrinol. Metab.* 105: E1729–E1740 (2020).
- [100] M. Al-Kofahi, M.A. Ahmed, M.M. Jaber, T.N. Tran, B.A. Willis, C.L. Zimmerman, M.T. Gonzalez-Bolanos, R.C. Brundage, K. Sarafoglou. An integrated PK-PD model for cortisol and the 17-hydroxyprogesterone and androstenedione biomarkers in children with congenital adrenal hyperplasia. *Br. J. Clin. Pharmacol.* 87: 1098–1110 (2021).
- [101] J.G. Lewis, B. Möpert, B.I. Shand, M.P. Doogue, S.G. Soule, C.M. Frampton, P.A. Elder. Plasma Variation of Corticosteroid-binding Globulin and Sex Hormone-binding Globulin. *Horm. Metab. Res.* 38: 241–245 (2006).
- [102] M. Debono, R.F. Harrison, M.J. Whitaker, D. Eckland, W. Arlt, B.G. Keevil, R.J. Ross. Salivary Cortisone Reflects Cortisol Exposure Under Physiological Conditions and After Hydrocortisone. *J. Clin. Endocrinol. Metab.* 101: 1469–1477 (2016).
- [103] J. Melin, N. Hartung, Z.P. Parra-Guillen, M.J. Whitaker, R.J. Ross, C. Kloft. The circadian rhythm of corticosteroid-binding globulin has little impact on cortisol exposure after hydrocortisone dosing. *Clin. Endocrinol. (Oxf.)* 91: 33–40 (2019).
- [104] M.J. Whitaker, S. Spielmann, D. Digweed, H. Huatan, D. Eckland, T.N. Johnson, G. Tucker, H. Krude, O. Blankenstein, R.J. Ross. Development and testing in healthy adults of oral hydrocortisone granules with taste masking for the treatment of neonates and infants with adrenal insufficiency. *J. Clin. Endocrinol. Metab.* 100: 1681–1688 (2015).
- [105] J.S. Barton, H.M. Gardiner, S. Cullen, P.C. Hindmarsh, C.G.D. Brook, M.A. Preece. The growth and cardiovascular effects of high dose growth hormone therapy in idiopathic short stature. *Clin. Endocrinol. (Oxf.)* 42: 619–626 (1995).
- [106] C.J. Peters, N. Hill, M.T. Dattani, E. Charmandari, D.R. Matthews, P.C. Hindmarsh. Deconvolution analysis of 24-h serum cortisol profiles informs the amount and distribution of hydrocortisone replacement therapy. *Clin. Endocrinol. (Oxf.)* 78: 347–351 (2013).
- [107] European Medicines Agency. Committee for Medicinal Products for Human Use. Guideline on bioanalytical method validation. EMEA/CHMP/EWP/192217/2009 (2012). [https://www.ema.europa.eu/en/documents/scientific-guideline/guideline-bioanalytical-method-validation\\_en.pdf](https://www.ema.europa.eu/en/documents/scientific-guideline/guideline-bioanalytical-method-validation_en.pdf), last access 25 Jun 2023.
- [108] <https://www.iconplc.com/solutions/technologies/nonmem/>, last access 25 Jun 2023.
- [109] R.J. Bauer. NONMEM Tutorial Part II: Estimation Methods and Advanced Examples. *CPT Pharmacometrics Syst. Pharmacol.* 8: 538–556 (2019).
- [110] S. Beal, L.B. Sheiner, A. Boeckmann, R.J. Bauer. NONMEM User's Guide VII. (1989-2013). (2013).
- [111] X. Liu, Y. Wang. Comparing the performance of FOCE and different expectation-maximization methods in handling complex population physiologically-based pharmacokinetic models. *J. Pharmacokinet. Pharmacodyn.* 43: 359–370 (2016).
- [112] E.L. Plan, A. Maloney, F. Mentré, M.O. Karlsson, J. Bertrand. Performance comparison of various maximum likelihood nonlinear mixed-effects estimation methods for dose-response models. *AAPS J.* 14: 420–432 (2012).
- [113] K.E. Karlsson, E.L. Plan, M.O. Karlsson. Performance of three estimation methods in repeated time-to-event modeling. *AAPS J.* 13: 83–91 (2011).
- [114] J.C. Pinheiro, D.M. Bates. Model Building for Nonlinear Mixed-Effects Models. Work. Pap. (1988).
- [115] Å.M. Johansson, S. Ueckert, E.L. Plan, A.C. Hooker, M.O. Karlsson. Evaluation of bias, precision, robustness and runtime for estimation methods in NONMEM 7. *J. Pharmacokinet. Pharmacodyn.* 41: 223–238 (2014).

- 
- [116] L. Gibiansky, E. Gibiansky, R. Bauer. Comparison of Nonmem 7.2 estimation methods and parallel processing efficiency on a target-mediated drug disposition model. *J. Pharmacokinet. Pharmacodyn.* 39: 17–35 (2012).
- [117] S.L. Beal. Ways to fit a PK model with some data below the quantification limit. *J. Pharmacokinet. Pharmacodyn.* 28: 481–504 (2001).
- [118] J.E. Ahn, M.O. Karlsson, A. Dunne, T.M. Ludden. Likelihood based approaches to handling data below the quantification limit using NONMEM VI. *J. Pharmacokinet. Pharmacodyn.* 35: 401–421 (2008).
- [119] W. Byon, C. V. Fletcher, R.C. Brundage. Impact of censoring data below an arbitrary quantification limit on structural model misspecification. *J. Pharmacokinet. Pharmacodyn.* 35: 101–116 (2008).
- [120] C. Dansirikul, H.E. Silber, M.O. Karlsson. Approaches to handling pharmacodynamic baseline responses. *J. Pharmacokinet. Pharmacodyn.* 35: 269–283 (2008).
- [121] H.T. Thai, F. Mentré, N.H.G. Holford, C. Veyrat-Follet, E. Comets. Evaluation of bootstrap methods for estimating uncertainty of parameters in nonlinear mixed-effects models: A simulation study in population pharmacokinetics. *J. Pharmacokinet. Pharmacodyn.* 41: 15–33 (2014).
- [122] A.G. Dosne, M. Bergstrand, K. Harling, M.O. Karlsson. Improving the estimation of parameter uncertainty distributions in nonlinear mixed effects models using sampling importance resampling. *J. Pharmacokinet. Pharmacodyn.* 43: 583–596 (2016).
- [123] A.G. Dosne, M. Bergstrand, M.O. Karlsson. An automated sampling importance resampling procedure for estimating parameter uncertainty. *J. Pharmacokinet. Pharmacodyn.* 44: 509–520 (2017).
- [124] M. Bergstrand, A.C. Hooker, J.E. Wallin, M.O. Karlsson. Prediction-corrected visual predictive checks for diagnosing nonlinear mixed-effects models. *AAPS J.* 13: 143–151 (2011).
- [125] L. Zhang, S.L. Beal, L.B. Sheiner. Simultaneous vs. Sequential Analysis for Population PK/PD Data I: Best-case Performance. *J. Pharmacokinet. Pharmacodyn.* 30: 387–404 (2003).
- [126] D.R. Mould, R.N. Upton. Basic concepts in population modeling, simulation, and model-based drug development: Part 3-introduction to pharmacodynamic modeling methods. *CPT Pharmacometrics Syst. Pharmacol.* 3: 1–16 (2014).
- [127] J.M. Bland, D.G. Altman. Statistical methods for assessing agreement between two methods of clinical measurement. *Lancet* 1: 307–310 (1986).
- [128] W. Bablok, H. Passing. Application of Statistical Procedures Analytical Instrument Testing. *J. Automat. Chem.* 7: 74–79 (1985).
- [129] D. Giavarina. Understanding Bland Altman analysis. *Biochem. Medica* 25: 141–151 (2015).
- [130] L. Bilic-Zulle. Lessons in biostatistics Comparison of methods : Passing and Bablok regression. *Biochem. Medica* 21: 49–52 (2011).
- [131] <https://uupharmacometrics.github.io/PsN/>, last access 25 Jun 2023.
- [132] <https://www.certara.com/software/pirana-modeling-workbench/>, last access 25 Jun 2023.
- [133] <https://www.fu-berlin.de/en/sites/high-performance-computing>, last access 25 Jun 2023.
- [134] C. de Weerth, R.H. Zijl, J.K. Buitelaar. Development of cortisol circadian rhythm in infancy. *Early Hum. Dev.* 73: 39–52 (2003).
- [135] P.M.M. De Kesel, N. Sadones, S. Capiiau, W.E. Lambert, C.P. Stove. Hemato-critical issues in quantitative analysis of dried blood spots: Challenges and solutions. *Bioanalysis* 5: 2023–2041 (2013).
- [136] E.A. Jacob. Hematological Differences in Newborn and Aging: A Review Study. *Hematol. Transfus. Int. J.* 3: 178–190 (2016).
- [137] M. Goto, K.P. Hanley, J. Marcos, P.J. Wood, S. Wright, A.D. Postle, I.T. Cameron, J.I. Mason,

- D.I. Wilson, N.A. Hanley. In humans, early cortisol biosynthesis provides a mechanism to safeguard female sexual development. *J. Clin. Invest.* 116: 953–960 (2006).
- [138] A. Dallmann, M. Pfister, J. van den Anker, T. Eissing. Physiologically Based Pharmacokinetic Modeling in Pregnancy: A Systematic Review of Published Models. *Clin. Pharmacol. Ther.* 104: 1110–1124 (2018).
- [139] S.A. Rivkees, J.D. Crawford. Dexamethasone Treatment of Virilizing Congenital Adrenal Hyperplasia: The Ability to Achieve Normal Growth. *Pediatrics* 106: 767–773 (2000).
- [140] F. Ceccato, C. Artusi, M. Barbot, L. Lizzul, S. Pinelli, G. Costantini, S. Niero, G. Antonelli, M. Plebani, C. Scaroni. Dexamethasone measurement during low-dose suppression test for suspected hypercortisolism: threshold development with and validation. *J. Endocrinol. Invest.* 43: 1105–1113 (2020).
- [141] Congenital adrenal hyperplasia due to steroid 21-hydroxylase deficiency: An endocrine society\* clinical practice guideline. (2018).
- [142] P.E. Clayton, S.E. Oberfield, E. Martin Ritzén, W.G. Sippell, P.W. Speiser, R.L. Hintz, M.O. Savage. Consensus: Consensus statement on 21-hydroxylase deficiency from The Lawson Wilkins Pediatric Endocrine Society and The European Society for Pediatric Endocrinology. *J. Clin. Endocrinol. Metab.* 87: 4048–4053 (2002).
- [143] Section on Endocrinology and Committee on Genetics Technical Report : Congenital Adrenal Hyperplasia. *Pediatrics* 106: 1511–1518 (2000).
- [144] M. Wagner, D. Tonoli, E. Varesio, G. Hopfgartner. The use of mass spectrometry to analyze dried blood spots. *Mass Spectrom. Rev.* 35: 361–438 (2016).
- [145] Y. Enderle, K. Foerster, J. Burhenne. Clinical feasibility of dried blood spots: Analytics, validation, and applications. *J. Pharm. Biomed. Anal.* 130: 231–243 (2016).
- [146] M. Gröschl, M. Rauh, H.G. Dörr. Circadian rhythm of salivary cortisol, 17 $\alpha$ -hydroxyprogesterone, and progesterone in healthy children. *Clin. Chem.* 49: 1688–1691 (2003).
- [147] M. Gröschl, M. Rauh, H.G. Dörr. Cortisol and 17-hydroxyprogesterone kinetics in saliva after oral administration of hydrocortisone in children and young adolescents with congenital adrenal hyperplasia due to 21-hydroxylase deficiency. *J. Clin. Endocrinol. Metab.* 87: 1200–1204 (2002).
- [148] D.P. Merke, A. Mallappa, W. Arlt, A. Brac De La Perriere, A. Lindén Hirschberg, A. Juul, J. Newell-Price, C.G. Perry, A. Prete, D.A. Rees, N. Reisch, N. Stikkelbroeck, P. Touraine, K. Maltby, F.P. Treasure, J. Porter, R.J. Ross. Modified-Release Hydrocortisone in Congenital Adrenal Hyperplasia. *J. Clin. Endocrinol. Metab.* 106: E2063–E2077 (2021).

## **7 Acknowledgements**

**Acknowledgements are not included in the electronic version of the dissertation for reasons of data protection.**



## 8 Publications

### Original articles

**V. Stachanow**, U. Neumann, O. Blankenstein, N. Alder-Baerens, D. Bindellini, P. Hindmarsh, R.J. Ross, M.J. Whitaker, J. Melin, W. Huisinga, R. Michelet, C. Kloft.

Model-informed target morning  $17\alpha$ -hydroxyprogesterone concentrations in dried blood spots for pediatric congenital adrenal hyperplasia patients.

Pharmaceuticals 16: 464 (2023).

doi: 10.3390/ph16030464

**V. Stachanow**, U. Neumann, O. Blankenstein, D. Bindellini, J. Melin, R.J. Ross, M.J. Whitaker, W. Huisinga, R. Michelet\*, C. Kloft\*.

Exploring dried blood spot cortisol concentrations as an alternative for monitoring pediatric adrenal insufficiency patients: A model-based analysis.

Front. Pharmacol. 13: 819590 (2022).

doi: 10.3389/fphar.2022.819590

\* shared senior authorship

**V. Stachanow**, U. Neumann, O. Blankenstein, U. Fuhr, W. Huisinga, R. Michelet, N. Reisch\*, C. Kloft\*.

Rationale of a lower dexamethasone dose in prenatal congenital adrenal hyperplasia therapy based on pharmacokinetic modelling.

Eur. J. of Endocrinol. 185: 3 (2021).

doi: 10.1530/EJE-21-0395

\* shared senior authorship

R. Michelet, J. Melin, Z.P. Parra-Guillen, U. Neumann, M.J. Whitaker, **V. Stachanow**, W. Huisinga, J. Porter, O. Blankenstein, R.J. Ross, C. Kloft.

Paediatric population pharmacokinetic modelling to assess hydrocortisone replacement dosing regimens in young children.

Eur. J. Endocrinol. 183: 357-368 (2020).

doi: 10.1530/EJE-20-0231

## Conference abstracts

U. Neumann, **V. Stachanow**, N. Reisch, O. Blankenstein, U. Fuhr, W. Huisinga, R. Michelet, C. Kloft.  
Pharmakokinetische Modellierung der Intrauterinen Dexamethasonkonzentration – Neue Option zur  
Dosierung einer pränatalen AGS-Therapie?

Gemeinsame Jahrestagung der Arbeitsgemeinschaft Pädiatrische Diabetologie (AGPD) e.V. und der  
Deutschen Gesellschaft für Kinderendokrinologie und -diabetologie (DGKED) e.V., Virtual, 23-26  
June 2021.

[https://ja-ped.de/wp-content/uploads/2021/06/JA-PED-2021\\_Abstracts-fuer-Homepage\\_FV-  
Endokrinologie.pdf](https://ja-ped.de/wp-content/uploads/2021/06/JA-PED-2021_Abstracts-fuer-Homepage_FV-Endokrinologie.pdf), (2021).

(oral presentation)

N. Reisch, **V. Stachanow**, O. Blankenstein, U. Neumann, U. Fuhr, W. Huisinga, R. Michelet, C. Kloft.  
Rationale for a reduced dexamethasone dosis in prenatal CAH therapy based on pharmacokinetic  
modelling.

23rd European Congress of Endocrinology (e-ECE), Virtual, 22-26 May 2021.

<https://www.endocrine-abstracts.org/media/12974/ece2021abstractbook.pdf>, (2021).

doi: 10.1530/endoabs.73.PEP1.3

(poster presentation)

**V. Stachanow**, J. Melin, R. Michelet, O. Blankenstein, U. Neumann, W. Huisinga, R.J. Ross, M.J.  
Whitaker, C. Kloft.

Does dried blood spot data enrich our understanding of hydrocortisone pharmacokinetics in paediatric  
patients with adrenal insufficiency?

28<sup>th</sup> Population Approach Group Europe (PAGE), Stockholm, Sweden, 11-14 June 2019.

<https://www.page-meeting.org/default.asp?abstract=9097>, (2019).

(poster presentation)

**V. Stachanow**, J. Melin, R. Michelet, O. Blankenstein, U. Neumann, W. Huisinga, R.J. Ross, M.J.  
Whitaker, C. Kloft.

Semi-mechanistic modelling of hydrocortisone pharmacokinetics in paediatric patients with adrenal  
insufficiency.

17<sup>th</sup> Congress of the European Society for Developmental Perinatal and Paediatric Pharmacology  
(ESDPPP), Basel, Switzerland, 28-30 May 2019.

<http://dx.doi.org/10.1136/archdischild-2019-esdppp.131>, (2019).

(poster presentation)

**V. Stachanow**, J. Melin, O. Blankenstein, U. Neumann, W. Huisinga, R.J. Ross, M. Whitaker, C. Kloft. Semi-mechanistic modelling of hydrocortisone pharmacokinetics in paediatric patients including dried blood spot data.

Annual Meeting of the Deutsche Pharmazeutische Gesellschaft (DPhG), Hamburg, Germany, 02-05 October 2018.

[https://www.dphg.de/fileadmin/downloads/DPhG2018\\_ConferenceBook\\_Final\\_27-09-2018.pdf](https://www.dphg.de/fileadmin/downloads/DPhG2018_ConferenceBook_Final_27-09-2018.pdf), 141, (2018).

(poster presentation)

## 9 Curriculum vitae

**According to the EU General Data Protection Regulation (GDPR) the curriculum vitae has been removed from the electronic version.**

